DRVNA INDUSTRIJA

SCIENTIFIC JOURNAL OF WOOD TECHNOLOGY

ZNANSTVENI ČASOPIS
ZA PITANJA DRVNE TEHNOLOGIJE

Juglans nigra L.

UDK 674.031.677.7
ISO: Drv. Ind.
CODEN: DRINAT
JCR: DRVNA IND
ISSN 0012-6772

2/24
VOLUME **75**

since 1913

tvin.

UDK 630*8+674 Coden: Drinat ISSN 0012-6772

DRVNA INDUSTRIJA

SCIENTIFIC JOURNAL OF WOOD TECHNOLOGY

Znanstveni časopis za pitanja drvne tehnologije

PUBLISHER AND EDITORIAL OFFICE
Izdavač i uredništvo
University of Zagreb
Faculty of Forestry and Wood Technology
Sveučilište u Zagrebu
Fakultet šumarstva i drvne tehnologije
www.sumfak.unizg.hr

CO-PUBLISHER / Suizdavač
Hrvatska komora inženjera šumarstva i drvne tehnologije

FOUNDER / Osnivač
Institut za drvnoindustrijska istraživanja, Zagreb

The journal Drvna industrija is a public scientific journal for publishing research results on structure, properties and protection of wood and wood materials, application of wood and wood materials, mechanical woodworking, hydrothermal treatment and chemical processing of wood, all aspects of wood materials and wood products production and trade in wood and wood products. The journal is published quarterly and financially supported by the Ministry of Science and Education of the Republic of Croatia

Časopis Drvna industrija javno je znanstveno glasilo za objavu rezultata istraživanja građe, svojstava i zaštite drva i drvnih materijala, primjene drva i drvnih materijala, mehaničke i hidrotermičke obrade te kemijske prerade drva, svih aspekata proizvodnje drvnih materijala i proizvoda te trgovine drvom i drvnim proizvodima.
Časopis izlazi četiri puta u godini uz financijsku potporu Ministarstva znanosti i obrazovanja Republike Hrvatske.

Contents
Sadržaj

CIRCULATION: *400 pieces*

INDEXED IN: *Science Citation Index Expanded, Scopus, CAB Abstracts, Compendex, Environment Index, Veterinary Science Database, Geobase, DOAJ, Hrčak, Sherpa Romeo*

MANUSCRIPTS ARE TO BE SUBMITTED *by the link http://journal.sdewes.org/drvind*

CONTACT WITH THE EDITORIAL *e-mail: editordi@sumfak.hr*

SUBSCRIPTION: *Annual subscription is 55 EUR. For pupils, students and retired persons the subscription is 15 EUR. Subscription shall be paid to the IBAN HR0923600001101340148 with the indication "Drvna industrija".*

PRINTED BY: *DENONA d.o.o., Getaldićeva 1, Zagreb, www.denona.hr*

DESIGN: *Bernardić Studio*

THE JOURNAL IS AVAILABLE ONLINE: *https://drvnaindustrija.com*

COVER: *Radial-sectional view of Juglans nigra L., xylotheca of Institute for Wood Science, University of Zagreb Faculty of Forestry and Wood Technology*

DRVNA INDUSTRIJA · VOL. 75, 2 · P. 149-272 · SUMMER 2024. · ZAGREB EDITORIAL COMPLETED 15. 2. 2024.

NAKLADA: *400 komada*

ČASOPIS JE REFERIRAN U: *Science Citation Index Expanded, Scopus, CAB Abstracts, Compendex, Environment Index, Veterinary Science Database, Geobase, DOAJ, Hrčak, Sherpa Romeo*

ČLANKE TREBA SLATI *putem poveznice http://journal.sdewes.org/drvind*

KONTAKT S UREDNIŠTVOM: *e-mail: editordi@sumfak.hr*

PRETPLATA: *Godišnja pretplata za pretplatnike u Hrvatskoj i inozemstvu iznosi 55 EUR. Za đake, studente i umirovljenike 15 EUR. Pretplata se plaća na IBAN HR0923600001101340148 s naznakom "Drvna industrija".*

TISAK: *DENONA d.o.o., Getaldićeva 1, Zagreb, www.denona.hr*

DESIGN: *Bernardić Studio*

ČASOPIS JE DOSTUPAN NA INTERNETU: *https://drvnaindustrija.com*

NASLOVNICA: *Radijalni presjek drva Juglans nigra L., ksiloteka Zavoda za znanost o drvu, Sveučilište u Zagrebu Fakultet šumarstva i drvne tehnologije*

DRVNA INDUSTRIJA · VOL. 75, 2 · STR. 149-272 · LJETO 2024. · ZAGREB REDAKCIJA DOVRŠENA 15. 2. 2024.

Meryem Ondaral*[1], Mustafa Usta[2], Sedat Ondaral[2]

Dimensional Stability Properties of Medium-Density Fiberboards Produced Using Silicone-Based Chemicals

Dimenzijska stabilnost srednje gustih ploča vlaknatica proizvedenih uz upotrebu kemikalija na bazi silikona

ORIGINAL SCIENTIFIC PAPER
Izvorni znanstveni rad
Received – prispjelo: 13. 9. 2022.
Accepted – prihvaćeno: 15. 11. 2023.
UDK: 539.388.8; 674.817
https://doi.org/10.5552/drvind.2024.0061

ABSTRACT • *The purpose of this study was to investigate the effects of two different silicon-based water-repellent chemicals (Dow Corning 87 and Xiameter PMX-200 1000cs) added to melamine urea formaldehyde glue (1.07 mol, 5 % melamine additive) in different proportions (0.5 %, 1.0 %, 1.5 % and 3.0 %) on the dimensional properties (swelling-shrinkage and length extension and shrinkage) of the medium density fiberboard. In the context of the study, the dimensional stability properties of the boards were measured based on the TS EN 318:2005 standard. It was observed that, when the relative humidity of the air conditioning room increased from 65 % to 85 %, the swelling decreased and the extension increased, respectively, in the thickness and length directions of the boards produced with silicon-based chemicals (compared to the control board produced without using silicone-based chemicals). On the other hand, it was determined that the shrinkage in the thickness and length direction of the boards decreased when the relative humidity of the air-conditioning room was reduced from 65 % to 30 %. Moreover, the dimensional stability properties of medium density boards produced with silicon-based chemicals increased (resistance to moisture).*

KEYWORDS: *MDF; hydrophobic; silicone-based chemical; water repellent; dimensional stability*

SAŽETAK • *Cilj ove studije bio je istražiti učinke dviju različitih vodoodbojnih kemikalija na bazi silikona (Dow Corning 87 i Xiameter PMX-200 1000cs), dodanih melamin-ureaformaldehidnom ljepilu (1,07 mol, 5 % melamina) u različitim udjelima (0,5 %, 1,0 %, 1,5 % i 3,0 %) na dimenzijska svojstva srednje gustih ploča vlaknatica (bubrenje/utezanje i promjene dimenzija po duljini). Mjerenje dimenzijske stabilnosti provedeno je prema standardu TS EN 318:2005. Utvrđeno je da se s povećanjem relativne vlažnost zraka u klimatiziranoj prostoriji sa 65 na 85 % u ploča proizvedenih uz dodatak kemikalija na bazi silikona (u usporedbi s kontrolnim pločama proizvedenima bez kemikalija na bazi silikona) bubrenje u smjeru debljine smanjilo, a istezanje u smjeru duljine povećalo. Istodobno je uočeno da se utezanje ploča u smjeru debljine i duljine smanjilo kada je relativna vlažnost zraka u klimatiziranoj prostoriji smanjena sa 65 na 30 %. Štoviše, povećala se dimenzijska stabilnost srednje gustih ploča vlaknatica proizvedenih s kemikalijama na bazi silikona (otpornost na vlagu).*

KLJUČNE RIJEČI: *MDF; hidrofoban; kemikalija na bazi silikona; vodoodbojan; dimenzijska stabilnost*

* Corresponding author
[1] Author is researcher at Karadeniz Technical University, Arsin Vocational School of Higher Education, Arsin,Turkey. https://orcid.org/0000-0001-7767-4853
[2] Authors are researchers at Karadeniz Technical University, Department of Pulp and Paper Technology, Faculty of Forestry, Kanuni Campüs, Turkey. https://orcid.org/0000-0003-2019-6584; https://orcid.org/0000-0002-8388-1944

1 INTRODUCTION
1. UVOD

Medium-density fiberboard (MDF) is a hygroscopic material like solid wood. Since it is composed of wood fibers, its dimensions (thickness and longitudinal direction) change by absorption or desorption due to changes in temperature and relative humidity of the environment (Ayrılmış and Mater, 2007; Grigsby *et al*., 2012; Dopico and Heroux, 2004; Xu and Winistorfer, 1995). The change in the dimensions of a board occurs as swelling/shrinkage in the thickness direction and as extension/shrinkage in the length direction. Changes in the dimensions of the boards are an important issue in terms of their end-use and the board storage areas. Therefore, various experiments have been conducted by focusing on different board production parameters, such as raw material preference, press conditions, different glue content, board density, and water-repellent chemicals.

The hygroscopic structure of wood is formed by the hydroxyl groups of polymers in the cell wall (Papadopoulos *et al*., 2019). It is important to ensure that these hydroxyl groups form bonds that are resistant to water and moisture and do not break easily. For this purpose, a number of studies, in which different glues and water-repellent chemicals are used and different board-forming methods are applied, have been conducted (Halligan, 1970; Mantanis and Papadopoulos, 2010a; Mantanis and Papadopoulos, 2010b). Besides the production of melamine and phenolic-containing glues, researchers have also investigated the addition of chemical substances such as water-repellent rosin and wax in order to improve the water and moisture resistance of fiber boards (Segovia *et al*., 2021; Moreno-Anguiano *et al*., 2022). As a result of these studies, water and moisture resistant boards have been produced, but completely water-resistant (unchangeable in size) boards could not be produced. However, it has been determined that long-term use of boards produced with the wax chemical causes changes (swelling- elongation) in their dimensions (Garcia *et al*., 2005; Halligan, 1970; Hsu *et al*., 1990; Press, 1990). This situation has led researchers to search for using different chemicals in board production. Various water-repellent chemicals, such as nanotechnology compounds, nanowollastonite, oils, organosilicon, and organo-silane compounds, have been tested, and boards with different levels of water-moisture resistance have been produced (De Vetter *et al*., 2011; Esmailpour *et al*., 2021; Hassani *et al*., 2019; Ibrahim *et al*., 2016; Kloeser, 2010; Mantanis and Papadopoulos, 2010a; Taghiyari *et al*., 2015; Wang *et al*., 2020).

Silicones with water-repellent properties are hydrophobic substances and have a positive effect (reduction in water and moisture absorption) on the interaction of wood-based boards with water-moisture (Donath *et al*., 2006; Ghosh, 2009; Aziz *et al*., 2021). In addition to their moisture resistance in the production of wood-based boards, they are used in a wide variety of fields such as textiles, cosmetics, wood preservation and furniture (Buyl, 2007). For the boards to remain dimensionally stable, it is necessary to add water-repellent chemicals as well as glue; the compatibility between the used water-repellent chemicals and the glue is important. In this sense, the reactive silane groups of silicon-based chemicals act as binders for both organic and inorganic components. Moreover, because of their dual reactive properties, they form bridges between inorganic and organic surfaces (cellulose- filling material) and organic polymeric matrices (e.g., rubber-thermosets), and they increase adhesion. (Materne *et al*., 2004; Kartal *et al*., 2009). These properties of silicon-based chemicals make them important in board production. In addition, their ability to bind inorganic fillers or fibers to organic glues to create or promote a stronger bond at the interface is another reason for their preference in board production. Furthermore, the chemical substances used in the production of the board do not threaten human and environmental health. In this sense, for sectors such as food industry, textile and medical applications, silicone-based chemicals that do not contain threatening elements can be safely used in production (Mai and Militz, 2004).

This study aimed to investigate the effect of Dow Corning 87 and Xiameter PMX-200 1000cs chemicals on the dimensional stability properties of medium-density fiberboard. The density of MDF boards, produced with a mixture of MUF glue and silicone-based chemicals added at different concentrations and their dimensional stability properties (swelling-shrinkage in thickness, extension-shrinkage in length direction) occurring based on the effect of the amount of chemicals, was evaluated.

2 MATERIALS AND METHODS
2. MATERIJALI I METODE

2.1 Materials
2.1. Materijali

In this study, mixed fibers produced from softwood (pine 50 %) and hardwood (beech 40 % +oak 10 %=50 %) were obtained from Çamsan Anonym Company (Sakarya, Turkey). Melamine Urea Formaldehyde (F/U: 1.07 mol 5 % melamine added) glue and ammonium chloride (glue hardener) supplied from Çamsan A.Ş. (Sakarya, Turkey) were used. Dow Corning 87 (DC) and Xiameter PMX-200 1000cs (XM) produced by Dow Corning company (Seneffe, Belgium) were used as chemicals. DC (Octyltriethoxysilane) is a liquid and white color chemical with boiling point > 35 °C and dynamic viscosity of 50 mPa·s. On the other hand, XM (Trimethylsiloxy) is a liquid and colorless chemical whose initial boiling point and boiling range are higher than 65 °C, flash point is higher than 120 °C, relative density is 0.97 and kinematic viscosity is 1000 cSt (25 °C). DC is an active (40 %) silane-based silicone glue emulsion, and its components are determined by the XRF device as given in Table 1.

Table 1 XRF elemental analysis results of DC chemical
Tablica 1. XRF rezultati elementarne analize DC kemikalije

Component *Komponenta*	**Solid content, %** *Udio suhe tvari, %*
Si	0.432
S	0.056
Cu	0.003
Plastic	99.508

The chemical name of XM is silicone and it is a linear polydimethylsiloxane. Its components are determined by XRF device as given in Table 2.

Table 2 XRF elemental analysis results of XM chemical
Tablica 2. XRF rezultati elementarne analize XM kemikalije

Component *Komponenta*	**Solid content, %** *Udio suhe tvari, %*
Si	25.665
S	0.052
Cu	0.008
K	0.052
Fe	0.004
Plastic	74.220

The properties of 5 % melamine added Melamine urea formaldehyde glue are presented in Table 3.

2.2 Methods
2.2. Metode

2.2.1 Board production
2.2.1. Proizvodnja ploča

The fibers supplied wet from the factory were laid out and dried in the laboratory, and the fiber lumps formed after drying were opened by pressing lightly on the sieve surface. After the opened fibers were dried in a drying oven (100 °C) until 7 % dryness, they became ready for use in board production. In order to create the fiber board, first, the glue, hardener and silicon chemical were mixed in a baker. Then the mixture was sprayed into the container in which the fibers were located, and the mixing process was carried out. After the fiber and glue mixture was homogeneously laid on the frame placed on the press board steel, manual pre-compression was performed with the help of a flat surface. After the other press-board steel was placed on the fiber mat and the thickness wedges were placed, the hot press was applied. In the context of the study, a total of 16 boards with 8 different board groups were produced. The amount of glue, fiber and hardener were calculated depending on the dry weights. The amount of glue was 20 % based on the amount of dry fiber, and the amount of hardener was used as 2 % based on dry glue. Silicon chemicals were applied at the content ratios of 0 %, 0.5 % - 1 %, 1.5 % and 3 % (w/w of fiber). The boards were formed by keeping the draft of the board in a single-layer press at 180 °C, under a pressure of 45-30 kg/cm^2 for 420 seconds. Boards were produced in 300 mm × 300 mm × 10 mm (length × width × thickness) dimensions. The test procedures were started after the produced boards were conditioned at room temperature (20±2 °C, 65 % relative humidity) until reaching equilibrium moisture.

2.2.2 Board tests
2.2.2. Ispitivanje ploča

2.2.2.1 Determination of dimensional change properties of boards
2.2.2.1. Određivanje dimenzijskih promjena ploča

The test of wood based-panels determination of dimensional changes associated with changes in relative humidity (TS EN 3182005) was applied to the test samples. This test is a method based on calculation of the difference between the thickness and length of the board by keeping it in an air conditioning room (20 °C, 65 % - 85 %, 65 % - 30 %) until it reaches constant weight at different relative humidity values. Test pieces were obtained by cutting them to be (300±2) mm × (50±2) mm × 10 mm (board thickness) in dimension. A total of 64 test samples were prepared by taking 8 test samples from each board group. A conditioning process consisting of three stages was applied to the board pieces separately as two sets. This process kept going until each board piece reached a constant mass. The length, thickness and mass were measured after the 2nd and 3rd conditioning process. The dimensional change in the length and thickness of the board sam-

Table 3 Properties of melamine urea formaldehyde (Çamsan Sakarya AŞ., Turkey, 2018)
Tablica 3. Svojstva melamin-ureaformaldehida (Çamsan Sakarya AŞ., Turkey, 2018.)

Glue type *Vrsta ljepila*	**Solid matter, %** *Udio suhe tvari, %*	pH	**Viscosity (flow time, 20 °C), s** *Viskoznost (vrijeme istjecanja, 20 °C), s*	**Gel time, s** *Vrijeme želiranja, s*	**Density (20 °C), g/cm^3** *Gustoća (20 °C), g/cm^3*
1,16 mol MUF	60	9.11	43	48	1258

ples at different relative humidity values was calculated with the formula below.

Change in the length of the board piece:

$$\delta I_{65,85} = \frac{I_{85} - I_{65}}{I_{65}} \cdot 100 \text{ (with using results of 1 team)}$$

$$\delta I_{65,30} = \frac{I_{30} - l_{65}}{I_{65}} \cdot 100 \text{ (with using results of 2 team)}$$

Where $\delta I_{65,85}$ is relative change in length (mm/m) for the change of relative humidity from 65 % to 85 %. $\delta I_{65,30}$ is relative change in length (mm/m) for the change of relative humidity from 30 % to 65 %. l_{85} is verified length (mm) between measuring points at 20 °C temperature and 85 % relative humidity for the effect of marking used. l_{65} is verified length (mm) between measuring points at 20 °C temperature and 65 % relative humidity for the effect of marking used. l_{30} is verified length (mm) between measuring points at 20 °C temperature and 30 % relative humidity for the effect of marking used.

Change in the thickness of the board piece:

$$\delta t_{65,85} = \frac{t_{85} - t_{65}}{t_{65}} \cdot 100 \text{ (with using results of 1team)}$$

$$\delta t_{65,30} = \frac{t_{30} - t_{65}}{t_{65}} \cdot 100 \text{ (with using results of 2 team)}$$

Where $\delta t_{65,85}$ is relative change in thickness for the change of relative humidity from 65 % to 85 %. $\delta t_{65,30}$ is relative change in thickness for the change of relative humidity from 30 % to 655 %. t_{85} is verified thickness (mm) for the effect of marking measured at 20 °C temperature and 85 % relative humidity and used when necessary. t_{65} is verified thickness (mm) for the effect of marking measured at 20 °C temperature and 65 % relative humidity and used when necessary.

t_{30} is verified thickness (mm) for the effect of marking measured at 20 °C temperature and 30 % relative humidity and used when necessary.

2.2.2.2 Determination of density values of boards
2.2.2.2. Određivanje gustoće ploča

The density values of the samples were determined based on the principles specified in the EN 323:1999 standard. Four test samples were used to determine the board density and the averages of the obtained results were taken. After measuring the weight, thickness and width of two edges of the test samples, which were conditioned and prepared in sample sizes of 50 mm × 50 mm × 10 mm, their densities were calculated with the formula below. A total of 32 test samples, four from each board, were used for the test.

$$\delta = \frac{m}{a_1 \cdot a_2 \cdot t} \cdot 10^3 (g / cm^3)$$

Where δ is density (g/cm^3), m is air dry weight (g), a_1 and a_2 are sample width (mm), t is sample thickness (mm).

2.2.2.3 X-Ray Fluorescence Spectrometer
2.2.2.3. Rendgenski fluorescentni spektrometar

The contents of DC and XM chemicals were determined using an "Energy Dispersive X-ray Fluorescence Spectrometer" (Shimadzu EDX 8000, Japan). Our samples were placed in a sample cell (30 mm diameter) with film on the bottom. The amount of substance in the sample was measured by sending X-rays on it. The measurements were automatically transferred to the computer screen connected to the device. XRF (Setaş Kimya AŞ.) measurement process was done in the laboratory.

2.2.3 Statistical analysis
2.2.3. Statistička analiza

To determine the effects of the added chemicals, the dimensional stability test of the fiberboards was carried out with SPSS 22.0 software (version 29.0.0.0) by using the One Way ANOVA test at 95 % confidence interval. The mean and standard deviation values of each group were calculated, and significant differences between the groups were determined by Duncon homogeneity test.

3 RESULTS AND DISCUSSION
3. REZULTATI I RASPRAVA

3.1 Changes in board dimensions
3.1. Promjene dimenzija ploča

3.1.1 Changes in thickness
3.1.1. Promjene debljine ploča

In Table 1, swelling-shrinkage values in the thickness direction of the boards are given depending on the chemical substance concentrations used in the study.

Figures 1A and 1B show the mean thickness (swelling/shrinkage) change values of the boards produced with the addition of DC and XM chemicals when the relative humidity was increased from 65 % to 85 % and decreased from 65 % to 30 %. In both graphs, decrease in swelling/ shrinkage values of the boards in the thickness direction compared to the control board was observed depending on the chemical ratio added. As the addition amount of DC and XM chemicals increased, the changes in the thickness direction (swelling and shrinkage) of the boards decreased compared to the control board, but this change was not directly proportional to the chemical addition rate. However, changes in the form of decrease and increase in board thickness were observed.

Among the boards produced by adding XM chemical, the lowest increase in thickness was obtained in the board in which XM was used at a rate of 1 % (4.45 %). The lowest increase in thickness in the boards produced by adding DC chemical was determined in

Table 4 Swelling-shrinkage properties in terms of thickness direction of MDF boards
Tablica 4. Debljinsko bubrenje i utezanje MDF ploča

Dimensional stability / *Dimenzijska stabilnost*							
% Cons. DC	**Density, g/cm³** *Gustoća*, g/cm³	$\delta t_{(65,85)}$	$\delta t_{(65.30)}$	**% Cons. XM**	**Density, g/cm³** *Gustoća*, g/cm³	$\delta t_{(65.85)}$	$\delta t_{(65,30)}$
0	762	5.14 (0.16)* c	-2.45 (0.08) a	0	762	5.14 (0.16)*d	-2.45 (0.08) a
0.5	760	5.16 (0.13) c	-1.85 (0.13) c	0.5	764	4.58 (0.12) b	-2.13 (0.14) b
-	-	-	-	1	757	4.45 (0.39) a	-1.94 (0.01) c
1.5	801	4.34 (0.39) a	-1.67 (0.27)d	1.5	758	4.86 (0.41) c	-2.06 (0.06) b
3	753	4.89 (0.31) b	-2.32 (0.9) b	3	761	4.70 (0.06) b	-1.93 (0.19) c

*Numbers in parentheses are standard deviations. The sample with 0 % concentration is the control board. Letters represent each homogenous subset analyzed with Duncan test.
**Brojevi u zagradama standardne su devijacije. Uzorak s 0 % koncentracije kontrolna je ploča. Slova predočuju svaki homogeni podskup analiziran Duncanovim testom.*

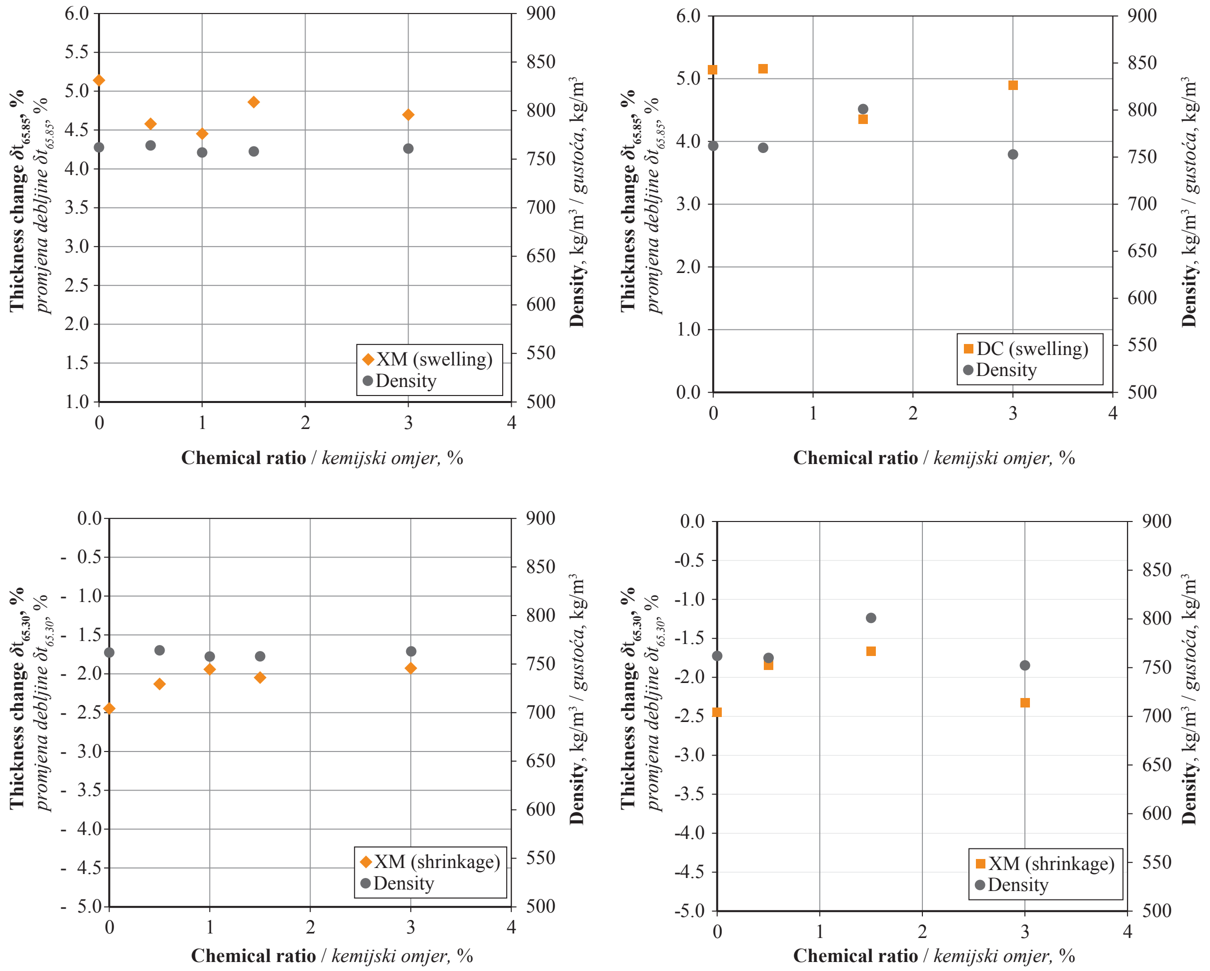

(A) (B)

Figure 1 (A) Change in thickness of the boards produced with XM chemical, (swelling/shrinkage), (B) change in thickness of the boards produced with DC chemical (swelling/ shrinkage)
Slika 1. (A) Promjena debljine ploča proizvedenih s XM kemikalijom (bubrenje/utezanje), (B) promjena debljine ploča proizvedenih s DC kemikalijom (bubrenje/utezanje)

the board produced by adding 1.5 % DC. When both chemicals were compared, it was observed that the lowest thickness increase (4.34 %) occurred in the board produced by using DC chemical at a rate of 1.5 %. The fact that the swelling and shrinkage values in the thickness direction do not decrease regularly with the increase in the amount of chemical addition is attributed to the chemical-fiber bond. In other words, the fact that the swelling and shrinkage values did not change regularly, although the amount of fiber used in the production of the boards was the same and the chemical amount added increased, was attributed to the fact that the number of bonds did not increase between chemical and fiber.

When the board density values were examined, the lowest change of thickness (swelling-shrinkage) was observed in the board with the highest density value (board produced by adding 1.5 % DC). It is known that as the board density value increases, the change in the dimensions of the boards increases when the boards receive water and moisture (Akbulut and Ayrılmış, 2008). However, in our study, the lowest swelling and shrinkage amount was determined in the thickness direction of the board produced with 1.5 % DC chemical, which is high board density (at relative humidity change). As the board density increased, more fiber-chemical bonds were formed, and because of this, less swelling occurred in the thickness direction of the board. When the test boards were compared with the control board, it was determined that there was a 13.42 % (calculated based on the swelling value of control board) decrease in the thickness value of the board to which 1 % XM was added and a 15.56 % (calculated based on the swelling value of control board) decrease in the thickness value of the board to which 1.5 % DC was added. When this comparison was made in terms of shrinkage, a 21.22 % (calculated based on the shrinkage value of control board) decrease was obtained in the board to which 3 % XM was added, and a decrease of 31.83 % (calculated based on to the shrinkage value of control board) in the board to which 1.5 % DC was added. In the boards to which DC and XM chemicals were added, less contraction (shrinkage) was obtained in the thickness direction.

Reducing the water absorption and swelling rates of the boards depends on the formation of strong bonds by the free -OH groups in the fiber and the fact that these bonds are not broken. It has been stated in studies that such strong fiber bonds can be achieved with cross-linking chemicals (Mamiński *et al*., 2020; De Vetter, 2009). The reactive silane groups in the content of silicon-based chemicals bond with the hydroxyl groups of the fiber, and although the hydrogen bonds formed are sensitive to hydrolysis, they turn into covalent bonds by heat (Xie *et al*., 2010). These covalent bonds are stable bonds. Although there are functional organic and alkoxy groups in the silane-containing chemical, these groups provide adhesion between the fiber and the polymer matrix (Goyal, 2006). Organic groups interact with the polymer, while silanol groups improve the interfacial properties by creating covalent bonds on the inorganic surface (Nurazzi *et al*., 2021). In addition, alkoxy groups react with the hydroxyl groups of the fiber under humidity conditions and form silanols (Agrawal *et al*., 2000). While the hydroxyl groups of the fiber and the reactive silane groups bond together, the free silanols form a stable Si-O-Si bond by bonding with each other. These bonds form solid polysiloxane structures because of condensation reaction occurring with the effect of heat on the fiber surface. These polysiloxane layers prevent the water absorption of the fibers close to the surface, which reduces the likelihood of bonding with the hydroxyl groups of the fiber. The presence of these polysiloxane layers explains the reduction of thickness (swelling-shrinkage) of the boards produced.

In the study, it was determined that the increase in thickness of the produced boards was greater than the decrease in thickness (well-known hysteresis phenomenon). The bond established between chemical-fiber, chemical-glue and fiber-glue is broken if the moisture value of the board is increased or decreased. If the broken bonds are re-established (bond formed between fiber and moisture) bonds with the moisture taken by the board, it will cause differences in board thickness. The increase in the thickness of boards has been attributed to the relaxation of the compressive stresses in the board, the hygroscopic swelling of the fibers, and the deterioration of the bond between fibers. In this context, it is expected that the decrease in the thickness of the boards will be less than the increase in the thickness. (Ayrılmış and Mater, 2007). Rather than the hygroscopic nature of the boards, this event is due to the deterioration of the compression caused by the press pressure during the board production. When the boards absorb or desorb moisture, their thickness changes with the broken bonds. If the boards desorb moisture again after absorbing it, they cannot reach their original dimensions. If the board gets moisture, new bonds formed between moisture with fiber, glue and chemical affect the board thickness. The fact that the free -OH groups of the fiber form bonds with water causes the board to swell. These bonds will affect the thickness of the board, but the board will not reach its original state. It is thought that the same has occurred in the boards produced in the study.

3.1.2 Changes in length
3.1.2. Promjene duljine ploča

In Table 5, extension-shrinkage values in the length direction of the boards are shown based on the chemical substance concentrations used in the study.

Figures 2A and 2B show the average length (extension/shrinkage) change values that occurred when the relative humidity value of the boards produced with the addition of DC and XM chemicals at different rates changes (65 % - 85 % or 65 % - 30 %). It was observed that, as the relative humidity increased, an elongation occurred in the length direction of boards produced with DC and XM compared to the control board. It was deter-

Table 5 Extension-shrinkage properties in length direction of MDF boards
Tablica 5. Produljenje i skupljanje MDF ploča po duljini

Dimensional stability / *Dimenzijska stabilnost*							
% Cons. DC	**Density, g/cm³** *Gustoća*, g/cm³	$\delta t_{(65,85)}$	$\delta t_{(65.30)}$	% Cons. XM	**Density, g/cm³** *Gustoća*, g/cm³	$\delta t_{(65.85)}$	$\delta t_{(65,30)}$
0	762	1.79 (0.12)*ᵃ	-2.92 (0.04)ᵃ	0	762	1.79 (0.12)ᵃ	-2.92 (0.04)ᵃ
0.5	760	2.43 (0.11)ᵇ	-2.69 (0.05)ᵇ	0.5	764	2.41 (0.02)ᶜ	-2.72 (0.09)ᵇ
-	-	-	-	1	757	2.52 (0.01)ᵈ	-2.59 (0.04)ᵈ
1.5	801	2.39 (0.19)ᵇ	-2.56 (0.02)ᶜ	1.5	758	2.19 (0.09)ᵇ	-2.69 (0.09)ᵇ
3	753	2.42 (0.19)ᵇ	-2.55 (0.01)ᶜ	3	761	2.26 (0.04)ᵇ	-1.93 (0.07)ᶜ

*Numbers in parentheses are standard deviations. The sample with 0 % concentration is the control board. Letters represent each homogenous subset analyzed with Duncan test.
**Brojevi u zagradama standardne su devijacije. Uzorak s 0 % koncentracije kontrolna je ploča. Slova predočuju svaki homogeni podskup analiziran Duncanovim testom.*

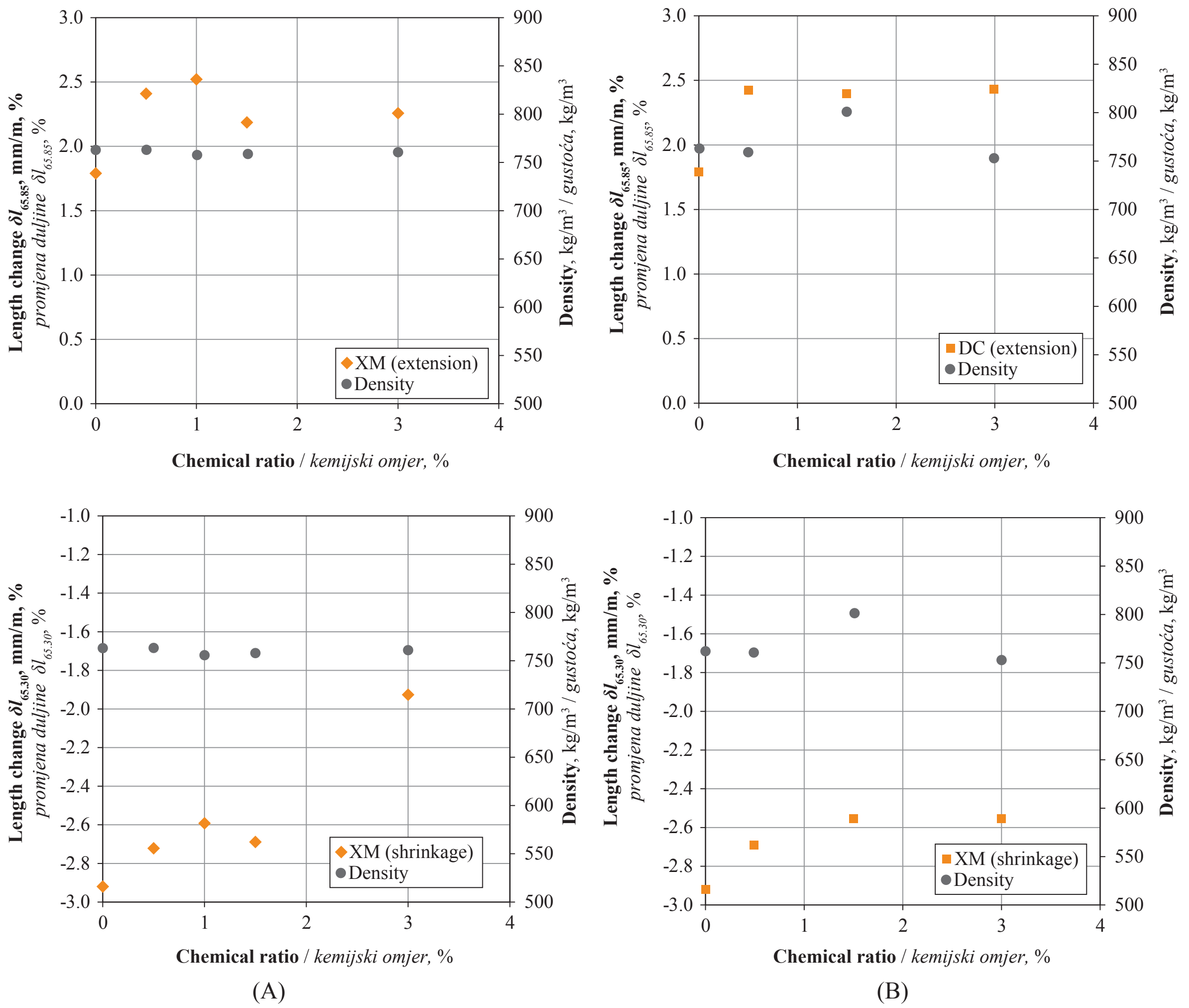

Figure 2 (A) Change in length of the boards produced with XM chemical (extension/shrinkage), (B) change in length of the boards produced with DC chemical (extension/shrinkage)
Slika 2. (A) Promjena duljine ploča proizvedenih s XM kemikalijom (produljenje/utezanje), (B) promjena duljine ploča proizvedenih s DC kemikalijom (produljenje/utezanje)

mined that the shrinkages in the length direction of the boards when the relative humidity decreased were less compared to the control group board. The lowest length shrinkage was observed in the board sample to which the XM chemical was added at a rate of 3 %.

The graph shows that the change in the density values of the boards produced using XM chemical is lower than the change in density values of the boards produced using DC. In the case of the decrease in the relative humidity, the lowest shrinkage value (-1.93 mm/m) was determined on the board produced with 3 % XM addition. On the other hand, in the case of the decrease in the relative humidity in the boards produced with DC addition, the shrinkage in the longitudinal direction decreased, and the lowest value was determined in the board produced with the 3 % DC addition (-2.55 mm/m).

The reason why the change in the direction of length is high in the boards produced with DC and XM chemicals is that, when the board absorbs moisture from the surface, the other Si-OR bonds, formed next to the Si-OH bond groups created by free OH groups and silanols in the fiber, easily hydrolyzed by moisture (Buyl, 2007). Based on this, it can be said that the bonds deteriorating in the presence of moisture cause the stress in the board to relax and increase the distance between the fibers in the length direction, and this is also effective in the length extension of the board sample.

According to Özen (1975), the work of the boards (desorption- absorption of water) in the longitudinal direction is the opposite of the work in the thickness direction. If the board loses moisture, the length change in the longitudinal direction is high. The boards absorb moisture at high relative humidity; however, they do not release all the moisture they take in when the humidity drops, while more shrinkage is seen on them. This has been attributed to the hysteresis of the boards (Ganev, 2002; Ganev *et al*., 2005). Although the extension in the length direction does not directly reflect the free expansion of the individual particles, it is a value that occurs depending on the fiber orientation and the degree of limitation of the bound expansion based on the direction of expansion of individual particles (Xu and Suchsland, 1996). In the board production performed under laboratory conditions, it is not possible to ensure homogeneous and regular distribution of fibers. In this case, the change in the dimensions of the board with the change in humidity and density is expected. This situation was also observed in the boards produced in this study.

Although silicones are chemicals that provide hydrophobic properties, diffusion of gases into silicones occurs due to their high free volume and solubility. Silicone surfaces cannot be wetted with water, but they cannot prevent the transition of oxygen and nitrogen (Colas, 2005). Based on the results obtained, it can be said that the cross-links formed because of the bonding of silane groups in silicone-based chemicals with the free OH groups of the fiber are effective on the less moisture absorption of the boards and less expansion and contraction in their dimensions.

It was determined that the changes in the thickness and length direction of the boards were not at the same rate when the boards produced with XM and DC chemicals were exposed to same climate conditions. This difference can be explained by the fact that both chemicals have different properties. DC chemical is a white colored liquid emulsified resin containing 40 % active silane, while XM chemical is an oily, transparent-colored and intense chemical containing polydimethylsiloxane groups. It was thought that the fact that the DC chemical was liquid causes it to reach the fiber and to obtain more bonding opportunities. XM chemical, on the other hand, was thought to form polysiloxane layers on the fiber surface due to its dense and oily chemical structure (Xie *et al*., 2010). There was no regular (systematic) change in the change values in the thickness (swelling-shrinkage) and length (extension-shrinkage) directions when the boards absorbed or lost moisture due to the increase in the DC and XM chemical substance ratios. It was observed that there were increases and decreases in the change values (swelling-shortening or extension-shortening) of the boards depending on the additional chemical ratios. This situation suggested that the silanes in the chemicals could not bond with all the –OH groups of the fiber and that at the same time, a bond was formed between fiber-fiber and fiber-glue. In addition, it was concluded that the increase in the amount of chemical substance added without changing the fiber amount did not increase the number of silane-fiber bonds. It is thought that the amount of silane that cannot bond with the increase in the amount of chemical substance may increase, and these silanes may remain clustered on the surface of the fiber or on the cell wall (Xie *et al*., 2010). In addition, it is seen that the –Si contents of both chemicals are different when the contents of DC and XM chemicals are examined (Table 1 and Table 2). In the study, it was observed that the –Si ratio in the DC chemical was lower than the –Si ratio in the XM chemical. The high amount of –Si in the chemical added at the same rate was interpreted as the fact that the number of bonds formed with the –OH groups of the fiber could be different. In this case, it was expected that the changes in the dimensions of the boards against humidity would be different and the results were obtained as expected. In addition, it was shown that the high plastic content of both chemicals was effective on boards to gain moisture resistance. The results revealed that the minimum change values were in the dimensions of boards produced with 1.5 % DC and 1 % - 1.5 % XM.

4 CONCLUSIONS
4. ZAKLJUČAK

In this study, the dimensional changes in the thickness (swelling/shrinkage) and length (extension/shrinkage) directions of the medium-density fiber boards produced with the mixture of Muf glue and two different silicon-based chemicals in different ratios were investigated and compared to the control board.

The results of the study are summarized below:

When the relative humidity of the environment, where the produced board samples were located, were increased from 65 % to 85 %, a slight decrease in swelling values in the thickness direction was observed compared to the control board (silicone was not added). On the other hand, it was determined that the shrinkage values of the boards decreased in the thickness direction when the relative humidity of the environment, where the boards were located, was reduced from 65 % to 30 %.

It was observed that, when the relative humidity of the environment increased for the board samples produced with DC and XM, the length extension occurred in them (65 % - 85 %). The extension values in the length direction of the board samples produced with the addition of DC at different rates were similar to each other. The lowest extension value in the length direction was determined in the board produced with 1.5 % XM. The study revealed that the shrinkage values in the length direction decreased when the relative humidity of the environment decreased (65 % - 30 %) in all board samples produced. When the effect of XM and DC chemicals on the board length extension-shrinkage was compared, it was found that the length shrinkage of the boards produced with XM (3 %) was less pronounced.

Acknowledgements – Zahvala

All authors kindly acknowledge Çamsan Sakarya A.Ş. for supplying the chemicals, glue and fiber used in board production and for all their support.

5 REFERENCES
5. LITERATURA

1. Agrawal, R.; Saxena, N. S.; Sharma, K. B.; Thomas, S.; Sreekala, M. S., 2000: Activation energy and crystallization kinetics of untreated and treated oil palm fibre reinforced phenol formaldehyde composites. Materials Science and Engineering: A, 277: 77-82. https://doi.org/10.1016/S0921-5093(99)00556-0
2. Akbulut, T.; Ayrılmış, N., 2008: Fundamental factors affecting the development of warp in MDF and particleboard. Journal of the Faculty of Forestry Istanbul University, 58 (2): 81-98 (in Turkish).
3. Ayrılmış, N.; Mater, J., 2007: Effect of panel density on dimensional stability of and high density fiberboard. Journal of Materials Science, 42: 8551-8557. https://doi.org/10.1007/s10853-007-1782-8
4. Aziz, T.; Ullah, A.; Fan, H.; Jamil, M. I.; Khan, F. U.; Ullah, R.; Iqbal, M.; Ali, A.; Ullah, B., 2021: Recent progress in silane coupling agent with its emerging applications. Journal of Polymers and the Environment, 29: 3427-3443. https://doi.org/10.1007/s10924-021-02142-1
5. Buyl, de F., 2007: Silicones in Industrial Applications, Organo-Functional Silanes, Dow Corning Europe SA, Seneffe (Belgium).
6. Colas, A., 2005: Silicones: Preparation, Properties and Performance, Dow Corning, Life Sciences.
7. De Vetter, L., 2009: Organosilicon compounds as potential wood protecting agents. PhD Thesis, Ghent University, Faculty of Bioscience Engineering, Ghent, Belgium, pp:153-172.
8. De Vetter, L.; Van den Bulcke, J.; Van Acker, J., 2011: Envelope treatment of wood based materials with concentrated organosilicons. Europe Journal of Wood Product, 69: 397-406. https://doi.org/10.1007/s00107-010-0448-4
9. Donath, S.; Militz, H.; Mai, C., 2006: Creating water repellent effects on wood by treatment with silanes. Holzforschung, 60: 40-46. https://doi.org/10.1515/HF.2006.008
10. Dopico, G. P.; Heroux, L. G., 2004: Dimensional stability of particleboard and MDF for use as substrates for lamination. In: TAPPI Decorative and Industrial Laminates Symposium.
11. EN 323:1999 Wood – Based panels – Determination of density.
12. Esmailpour, A.; Taghiyari, H. R.; Majidi, R.; Babaali, S.; Morrell, J. J.; Mohammadpanah, B., 2021: Effects of adsorption energy on air and liquid permeability of nanowollastonite-treated medium-density fiberboard. IEEE Transactions on Instrumentation and Measurement, 70, 1-8. https://doi.org/10.1109/TIM.2020.3009355
13. Ganev, S., 2002: Modeling of the hygromechanical warping of medium density fiberboard. PhD Thesis, Forestry Faculty, University of Laval, Canada, p 180.
14. Ganev, S.; Cloutier, A.; Beauregard, R.; Gendron, G., 2005: Linear Expansion and Thickness Swell of MDF as a Function of Panel Density and Sorption State. Wood and Fiber Science, 37 (2): 327-336.
15. Garcia, R. A.; Cloutier, A.; Riedl, B., 2005: Dimensional stability of MDF panels produced from fibres treated with maleated polypropylene wax. Wood Science and Technology, 39: 630-650. https://doi.org/10.1007/s00226-005-0028-7
16. Ghosh, S. C., 2009: Wood modification with functionalized polydimethylsiloxanes. PhD Thesis, University of British Columbia, Vancouver.
17. Goyal, S., 2006: Silanes: chemistry and applications. The Journal of Indian Prosthodontic Society, 6 (1): 14-18. https://doi.org/10.4103/0972-4052.25876
18. Grigsby, W.; Thumm, A.; Carpenter, J., 2012: Fundamentals of MDF Panel dimensional stability: Analysis of MDF high- density layers. Journal of Wood Chemistry and Technology, 32 (2): 149-164. https://doi.org/10.1080/02773813.2011.624667
19. Halligan, A. F., 1970: A review of the swelling in particleboard. Wood Science Technology, 4: 301-312. https://doi.org/10.1007/BF00386406
20. Hassani, V.; Taghiyari, H. R.; Schmidt, O.; Maleki, S.; Papadopoulos, A. N., 2019: Mechanical and physical properties of oriented strand lumber (OSL): The effect of fortification level of nanowollastonite on UF glue. Polymers, 11 (11): 1884. https://doi.org/10.3390/polym11111884
21. Hsu, W. E.; Melanson, R. J.; Kozak, P. J., 1990: The effect of wax type and content on waferboard properties. In: Proceedings of 24th international particleboard composites symposium. Washington State University, Pullman, WA, pp. 85-96.
22. Ibrahim, Z.; Ahmad, M.; Aziz, A. A.; Ramli, R.; Jamaludin, M. A.; Muhammed, S.; Alias, A. H., 2016: Dimensional stability properties of medium density fibreboard (MDF) from treated oil Palm (*Elaeis guineensis*) empty fruit bunches (EFB) fibres. Open Journal of Composite Materials, 6: 91-99. https://doi.org/10.4236/ojcm.2016.64009

23. Kartal, S. N.; Yoshimura, T.; Imamura, Y., 2009: Modification of wood with Si compounds to limit boron leaching from treated wood and to increase termite and decay resistance. International Biodeterioration & Biodegradation, 63: 187-190. https://doi.org/10.1016/j.ibiod.2008.08.006
24. Kloeser, L., 2010: Organofunctional silanes as formaldehyde free adhesives for fiberboards. In: Proceedings of the International Convention of Society of Wood Science and Technology and United Nations Economic Commission for Europe – Timber Committee, October 11-14, Geneva, Switzerland.
25. Mai, C.; Militz, H., 2004: Modification of wood with silicon compounds. Treatment systems based on organic silicon compounds – A Review. Wood Science and Technology, 37: 453-461. https://doi.org/10.1007/s00226-004-0225-9
26. Mamiński, M. L.; Trzepalka, A.; Auriga R.; H'Ng, P. S.; Chin, K. L., 2020: Physical and mechanical properties of thin high density fiberboard bonded with 1,3-Dimethylol-4,5-Dihydroxyethyleneurea (DMDHEU). The Journal of Adhesion, 96 (7): 679-690. https://doi.org/10.1080/00218464.2018.1500280
27. Mantanis, G. I.; Papadopoulos, A. N., 2010a: Reducing the thickness swelling of wood based panels by applying a nanotechnology compound. European Journal of Wood and Wood Products, 68: 237-239. https://doi.org/10.1007/s00107-009-0401-6
28. Mantanis, G. I.; Papadopoulos, A. N., 2010b: The sorption of water vapour of wood treated with a nanotechnology compound. Wood Science and Technology, 44 (3): 515-522. https://doi.org/10.1007/s00226-010-0326-6
29. Materne, T.; Buyl, F.; Witucki, G. L., 2004: Organosilane technology in coating applications: Rewiev and perspective. Dow Corning Corporation.
30. Moreno-Anguiano, O.; Cloutier, A.; Rutiaga-Quiñones, J. G.; Wehenkel, C.; Rosales-Serna, R.; Rebolledo, P.; Carrillo-Parra, A., 2022: Use of Agave durangensis bagasse fibers in the production of wood-based medium density fiberboard (MDF). Forests, 13 (2): 271. https://doi.org/ 10.3390/f13020271
31. Nurazzi, N. M.; Shazleen, S. S.; Aisyah, H. A.; Asyraf, M. R. M.; Sabaruddin, F. A.; Mohidem, N. A.; Norrrahim, M. N. F.; Kamarudin, S. H.; Ilyas, R. A.; Ishak, M. R.; Abdullah, N. Nor N. M., 2021: Effect of silane treatments on mechanical performance of kenaf fibre reinforced polymer composites: a review. Functional Composites and Structures, 3: 045003. https://doi.org/10.1088/2631-6331/ac351b
32. Özen, R., 1975: Lif Levhanın Fiziksel Ve Mekanik Özellikleri Ve Bunlara Tesir Eden Faktörler. İstanbul Üniversitesi Orman Fakültesi Dergisi, XXV, II.
33. Papadopoulos, N. A.; Bikiaris, D. N.; Mitropoulos, A. C.; Kyzas, G. Z., 2019: Nanomaterials and chemical modifications for enhanced key wood properties: A review. Nanomaterials, 9: 607. https://doi.org/10.3390/nano9040607
34. Press, W. A., 1990: Wax: types and applications. In: Proceedings of the NPA resin and blending seminar. National Particleboard Association, Gaithersburg, Maryland, USA, pp 29-34.
35. Segovia, F.; Blanchet, P.; Essoua, G. G. E.; 2021: Potential of the crude glycerol and citric acid mixture as a binder in medium-density fiberboard manufacturing. European Journal of Wood and Wood Products, 79 (5): 1141-1151. https://doi.org/10.1007/s00107-021-01719-w
36. Taghiyari, H. R.; Karimi, A.; Tahir, P. M., 2015: Organosilane compounds in medium density fiberboard: physical and mechanical properties. Journal of Forestry Research, 26 (2): 495-500. https://doi.org/10.1007/s11676-015-0033-0
37. ***TS EN 318:2005 Wood based panels – Determination of dimensional changes associated with changes in relative humidity.
38. Wang, Q.; Zhang, Y.; Liang, W.; Wang, J.; Chen, Y., 2020: Effect of silane treatment on mechanical properties and thermal behavior of bamboo fibers reinforced polypropylene composites. Journal of Engineered Fibers and Fabrics, 15: 1-10. https://doi.org/10.1177/1558925020958195
39. Xie, Y.; Hill, C. A. S.; Xiao, Z.; Militz, H.; Mai, C., 2010: Silane coupling agents used for natural fiber/polymer composites: A review. Composites, Part A: Applied Science and Manufacturing, 41: 806-819. https://doi.org/10.1016/j.compositesa.2010.03.005
40. Xu, W.; Winistorfer, P. M., 1995: A procedure to determine thickness swell distribution in wood composite panels. Wood and Fiber Science, 27 (2): 119-125.
41. Xu, W.; Suchsland, O., 1996: Linear expansion of wood composites: A mode. Wood and Fiber Science, 29 (3): 272-281.

Corresponding address:

Lecturer Dr. MERYEM ONDARAL, PhD
Karadeniz Technical University, Arsin Vocational School of Higher Education, Arsin, 61090 Trabzon,TURKEY,
e-mail: mondaral@ktu.edu.tr

Tatjana Kočetov Mišulić[1], Aleksandra Radujković*[1], Zdravko Popović[2], Ksenija Hiel[3]

Timber Strength Grading as Necessary Basis for Structural Design in ex-YU Region: Part 2

Ocjenjivanje drva prema čvrstoći kao nužna osnova za projektiranje konstrukcija na području bivše Jugoslavije: dio 2.

ORIGINAL SCIENTIFIC PAPER

Izvorni znanstveni rad

Received – prispjelo: 19. 4. 2023.

Accepted – prihvaćeno: 20. 9. 2023.

UDK: 674.032; 674.038; 674.06

https://doi.org/10.5552/drvind.2023.0106

ABSTRACT • *The aim of this paper is to contribute to the classification of structural timber in the ex-YU region into strength-class system through the application of experimentally obtained archive data in order to provide a realistic framework for most commonly used II grade (according to JUS) structural coniferous timber. The analysis of archive data was carried out on a sample of 150 specimens of structural size and based on the set of statistical requirements prescribed by EN standards, taking into account the change in disposition of loading in laboratory testing in the past and now. Statistical procedures prescribed by EN standards are given through calculation steps together with necessary adjustment factors that cover the size and number of specimens. The presented procedures given for structural-size specimens are also applicable to small clear specimens, so that a more comprehensive research and additional new examinations could be conducted with the available archive data simultaneously with the harmonization of the visual classification rules applied in the ex-YU region. The paper emphasises the direct dependence of the consistent application of the visual grading rules required by the relevant EN standard on strength-class system.*

KEYWORDS: *structural coniferous timber; visual grading; strength classes; statistical verification; European standards*

SAŽETAK • *Cilj ovog rada jest pridonijeti klasifikaciji konstrukcijskog drva na području bivše Jugoslavije u sustavu klasa čvrstoće primjenom eksperimentalno dobivenih arhivskih podataka kako bi se dobio realan okvir za najčešće upotrebljavano konstrukcijsko crnogorično drvo razreda II (prema JUS-u). Analiza arhivskih podataka provedena je na skupini od 150 uzoraka konstrukcijske veličine, i to na temelju skupa statističkih zahtjeva sadržanih u regulativi EU-a, pri čemu je uzeta u obzir promjena rasporeda opterećenja u laboratorijskim ispitivanjima u prošlosti i danas. Statistički postupci propisani EN normama dani su putem koraka izračuna, zajedno s potrebnim faktorima prilagodbe koji pokrivaju veličinu i broj uzoraka. Predstavljeni postupci dani za uzorke konstrukcijske veličine primjenjivi su i za male čiste uzorke, tako da bi se proširena kampanja s postojećim arhivskim podatcima i dodatnim novim ispitivanjima mogla provoditi istodobno s usklađivanjem pravila vizualne klasifikacije kon-*

* Corresponding author

[1] Authors are assistant professors at University of Novi Sad, Faculty of Technical Sciences, Department of Civil Engineering and Geodesy, Novi Sad, Serbia. https://orcid.org/0000-0003-3002-5885; https://orcid.org/0000-0003-4863-4486

[2] Author is full professor at University of Belgrade, Faculty of Forestry, Department of Wood Science and Technology Belgrade, Serbia. https://orcid.org/0000-0003-1557-4982

[3] Author is assistant professor at University of Novi Sad, Faculty of Agriculture, Department of Fruit Growing, Viticulture, Horticulture and Landscape Architecture, Novi Sad, Serbia. https://orcid.org/0009-0008-9793-7292

strukcijskog drva u bivšoj Jugoslaviji. U radu je naglašena izravna ovisnost dosljedne primjene pravila vizualnog ocjenjivanja kvalitete drva koja zahtijeva relevantna EN norma o sustavu klasa drva prema čvrstoći.

KLJUČNE RIJEČI: *konstrukcijsko crnogorično drvo; vizualno ocjenjivanje; klase čvrstoće; statistička verifikacija; europske norme*

1 INTRODUCTION
1. UVOD

The strength classification of solid timber is of key importance for the structural design and reflects on a range of modern products made of glued boards (e.g. glulam and cross-laminated timber) directly influencing their safety aspects.

In the first decade of the 21st century, countries from North and Central Europe (including Slovenia) carried out the "Gradewood" project: Grading of wood for engineering products (2007-2011), with the main goal to apply modern technologies and better practises in timber strength grading and integrate it to sawmilling process (machine grading). The results of the project significantly influenced some of the previously adopted EN standards (e.g. EN 1194:1999 with the lowest strength class GL24 withdrawn and replaced by EN 14080:2013 with the lowest strength class GL20). Within the project, the participating countries analysed commercially interesting growth areas in Europe, unifying the procedures and comparing the timber strength "quality".

However, most structural timber on EU market is still graded visually, so the optimisation of visual grading of timber in the ex-YU region and its strength classification is of greatest importance (Part 1).

Table 1 Assignment of visual graded timber to strength classes according to prEN 1912:2022
Tablica 1. Razvrstavanje vizualno ocijenjenog drva u klase čvrstoće prema prEN 1912:2022

Country/ Standard *Zemlja/Norma*	**Source** *Izvor*	**Spruce and Fir (*Picea abies* and *Abies alba*)** *Smrekovina i jelovina (Picea abies i Abies alba)*
Slovenia SIST DIN 4074-1	Slovenia	S10 → C24 S7 → C18 S7 → C16 (fir)
Germany DIN 4074-1	CNE Europe	S13(K) → C30 S10(K) → C24 S7(K) → C18
Italy UNI 11035-1	Italy	S1 → C30 S2 → C24 S3 → C18
Nordic countries INSTA 142	NNE Europe	T3 → C30 T2 → C24 T1 → C18 T0 → C14
Balkan countries JUS	SEE Europe	I → ? II → ? III → ?

Table 1 presents the assignment of spruce and fir considered as species relevant for a group of countries in the Balkan region due to traditional visual grading methods (Germany) or by geographical origin (Italy) or by practical description of structural use of particular strength classes (Sweden). The official assignment is very useful for structural engineers because some provisional explanations could be found in the regional documents (e.g. JUS grade I is sometimes assigned to series of strength classes from C30 to C50, grade II as C24-C27, while grade III as C22). That kind of "assignment" overestimates the structural timber from ex-YU regional resources and such a declarative takeover of strength classes (especially from German regulations, due to previous standards) could mislead the designers because the main timber strength characteristics are highly influenced by geographical origin and climatic conditions and should be supported with satisfactory test data.

The aim of this paper is to emphasise the necessity to assign visual grades and species into strength classes of structural timber in the region. There, according to relevant EN standards, the "framework" for strength class assignment is given using statistic and quality analysis of visually graded spruce/fir II grade (JUS). The analysis also specifies potential problems that could occur in structural design due to inconsistency in visual grading in the regional practice and formal adoption of strength classes from other countries. Realistic strength "framework" is necessary in order to improve the competitiveness and share of timber material in construction sector due to the arising awareness of green building.

2 MATERIALS AND METHODS
2. MATERIJALI I METODE

In order to get the classification framework of locally available spruce/fir for structural purposes and to demonstrate the applicability of defined EN procedures, the analysis of one regional archive data sample is given in the following section. Test results are obtained by previously used procedures in visual grading and testing (JUS).

The test was conducted on the sample of 150 specimens of coniferous (spruce/fir, Bosnia and Herzegovina source) timber in reference moisture conditions as 3-point bending test on full-size visually graded timber (II quality grade, JUS) with dimensions 3.5 cm × 12 cm × 270 cm. Test pieces were taken directly from

Table 2 Review of procedure steps for MoR analysis through expressions given in EN codes
Tablica 2. Pregled koraka postupka za analizu *MoR*-a putem izraza danih u EN kodovima

<table>
<tr><td colspan="2">MoR</td></tr>
<tr><td colspan="2">Species, grade, dimensions
Vrsta, razred, dimenzije</td></tr>
<tr><td colspan="2">Silver fir, Spruce / obična jelovina, smrekovina
Coniferous timber II grade / drvna građa od četinjača razreda II
3.5/12/270 cm; n =150</td></tr>
<tr><td colspan="2">Measurement and conversion of MoR from 3 to 4 point test – EN 408
Mjerenje i pretvorba MoR-a iz testa savijanja u 3 točke na test savijanja u 4 točke – EN 408</td></tr>
<tr><td colspan="2">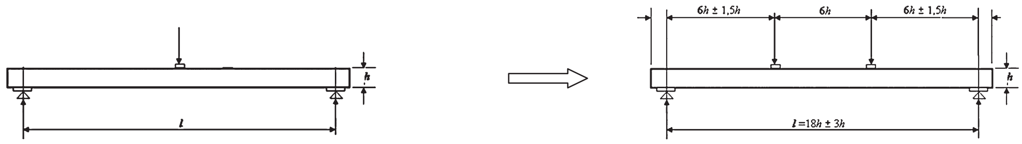

$f_{m,3P} = \frac{3Fl}{2bh^2}$ $f_{m,4P} = \frac{3Fa}{bh^2}$</td></tr>
<tr><td colspan="2">Adjustment factors – EN 384 (size and test length effects)
Faktori prilagodbe – EN 384 (visina i efektivna duljina)</td></tr>
<tr><td>$h \neq 150 \text{ mm} \rightarrow k_h = \min \begin{cases} (150/h)^{0.2} \\ 1.3 \end{cases}$</td><td>$l \neq 18h \rightarrow k_l = (48h/l_{et})^{0.2}, l_{et} = l + 5a_f$</td></tr>
<tr><td>$h = 120\text{mm} \rightarrow k_h = 1.0457$</td><td>$l = 270\text{cm}, a_f = 0 \rightarrow k_l = 1.1636$</td></tr>
<tr><td colspan="2">Characteristic values – EN 14358
Karakteristične vrijednosti – EN 14358</td></tr>
<tr><td>$m_k = \exp(\bar{y} - k_s(n) s_y)$</td><td>$k_s(n) = (6.5n + 6)/(3.7n - 3)$</td></tr>
<tr><td colspan="2">Characteristic values from subsamples – EN 384
Karakteristične vrijednosti za poduzorke – EN 384</td></tr>
<tr><td>$f_k = \min\left(1.2 f_{0.5,i,\min}; \sum_{i=1}^{ns} n_i f_{0.5,i} \Big/ n\right) \cdot k_n$</td><td>$f_{0.5,i} = m_{k,i}$; $k_n = 0.9$ for 3 subsamples</td></tr>
</table>

$f_{m,3P}$, $f_{m,4P}$ – bending strengths from 3 and 4 point tests / *čvrstoća na savijanje u 3 i 4 točke*
l – span in bending / *raspon pri savijanju*
F – loading force / *opterećenje*
a – distance between a loading position and nearest support in a bending test / *udaljenost između položaja opterećenja i najbližeg oslonca pri savijanju*
b, h – width and depth of cross section / *širina i visina presjeka*
k_h, k _ adjusting factors for size and length / *faktori prilagodbe veličine i duljine*
l_{et} – effective length / *efektivna duljina*
a_f – distance between the inner load points / *udaljenost između unutarnjih točaka opterećenja*
m_k – 5 % value of variable *m / 5 %-tna vrijednost varijable m*
$\bar{y}$ – sample mean value / *srednja vrijednost uzorka*
s_y – standard deviation / *standardna devijacija*
$k_s(n)$ – factor used to calculate characteristic properties / *faktor koji se primjenjuje za izračun karakterističnih svojstava*
n – number of test values / *broj ispitnih vrijednosti*
f_k – 5% characteristic value of strength / *5 %-tna karakteristična vrijednost čvrstoće*
$f_{0.5,i,min}$ – lowest 5 % value of all subsamples / *najniža vrijednost od 5 % svih poduzoraka*
$f_{0.5,i}$ – lowest 5 % value for each subsample / *najniža vrijednost od 5 % za svaki poduzorak*
n_i – number of specimens in a subsample / *broj uzoraka u poduzorku*
n_s _ number of subsamples / *broj poduzoraka*
k_n – factor to adjust for the number of subsamples / *faktor prilagodbe za broj poduzoraka*

production factory in order to define the real safety factor of built-in timber in low-rise wood frame buildings exported in the region. Tests were conducted until failure in edgewise position and were documented with descriptions about failure types of each specimen (e.g. zone and size of knots, slope of grains and failure in compression or tension zone, etc.). The same tests were used for the determination of bending strength (*MoR*) and bending stiffness (*MoE*), while density was determined separately.

The archive sample was considered as representative (in terms of the same origin from various areas and randomly chosen specimens) and with the possibility of division into subsamples in order to perform

Table 3 Review of procedure steps for *MoE* analysis trough expressions given in EN codes
Tablica 3. Pregled koraka postupka za analizu *MoE*-a uz pomoć izraza danih u EN kodovima

<table>
<tr><td colspan="2">MoE</td></tr>
<tr><td colspan="2">Species, grade, dimensions
Vrsta, razred, dimenzije</td></tr>
<tr><td colspan="2">Silver fir, Spruce / obična jelovina, smrekovina
Coniferous timber II grade / drvna građa od četinjača razreda II
3.5/12/270 cm; $n = 150$</td></tr>
<tr><td colspan="2">Measurement and conversion of MoE from 3 to 4 point test – EN 408
Mjerenje i pretvorba MoE-a iz testa savijanja u 3 točke na test savijanja u 4 točke – EN 408</td></tr>
<tr><td>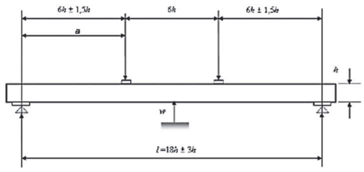
</td><td>$$E_{m,g} = \frac{3al^2 - 4a^3}{2bh^3\left(2\frac{\Delta w}{\Delta F} - \frac{6a}{5Gbh}\right)}$$
$$E_{m,g} = \frac{l^3}{2bh^3\left(2\frac{\Delta w}{\Delta F} - \frac{3l}{5Gbh}\right)}$$ for $a=l/2$</td></tr>
<tr><td colspan="2">Measurement of local MoE, EN 408
Mjerenje lokalnog MoE-a, EN 408</td></tr>
<tr><td>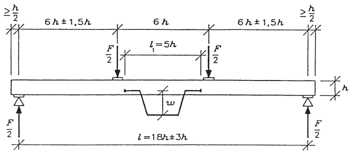
</td><td>$$E_{m,l} = \frac{3al_1^2\Delta F}{4bh^3\Delta w}$$</td></tr>
<tr><td colspan="2">Modulus of elasticity parallel to grain, EN 384
Modul elastičnosti paralelno s vlakancima, EN 384</td></tr>
<tr><td>$E_0 = E_{m,g} \cdot 1.3 - 2690\ [\mathrm{MPa}]$</td><td>$E_0 = E_{m,l}$</td></tr>
<tr><td colspan="2">Characteristic mean value – EN 14358
Karakteristična srednja vrijednost – EN 14358</td></tr>
<tr><td colspan="2">$m_{mean} = \bar{y} - k_s(n)s_y$ $k_s(n) = 0.78/n^{0.53}$</td></tr>
<tr><td colspan="2">Characteristic mean values from subsamples – EN 384
Karakteristične vrijednosti za poduzorke – EN 384</td></tr>
<tr><td colspan="2">$E_{0,mean} = \min\left(1.1\bar{E}_{i,min};\sum_{i=1}^{ns} n_i\bar{E}_i \Big/ n\right)\cdot k_n/0.95$ $\bar{E}_i = m_{mean,i}$; $k_n = 0.94$ for 3 subsamples</td></tr>
</table>

$E_{m,l}$, $E_{m,g}$ – local and global modulus of elasticity in bending / *lokalni i globalni modul elastičnosti pri savijanju*
w – displacement / *pomak*
G – shear modulus / *modul smicanja*
l_1 – gauge length for determination of modulus of elasticity / *mjerna duljina za određivanje modula elastičnosti*
E_0 – modulus of elasticity parallel to grain / *modul elastičnosti paralelno s vlakancima*
m_{mean} – population mean value of variable m / *populacijska srednja vrijednost varijable m*
$E_{0,mean}$ – mean characteristic value of E_0 / *srednja karakteristična vrijednost* E_0
$\bar{E}_i$ – mean modulus of elasticity of one subsample / *srednji modul elastičnosti jednog poduzorka*
$\bar{E}_{i,min}$ – lowest $\bar{E}_i$ of all subsamples / *najmanji* $\bar{E}_i$ *od svih poduzoraka*

more detailed statistical analyses according to relevant EN standards. Statistical analysis was performed for three observed cases:

A) Whole number of specimens A (n = 150) – one sample;
B) Three randomly divided subsamples B1, B2, B3 (n = 50);
C) Two samples on the basis of recorded types of failure of each specimen and recorded excessive defects C1 (n = 88) and C2 (n = 62).

The conducted analyses were performed in order to consider the possibility of conversion of results from JUS to EN (case A), to estimate the statistical sensitivity of the obtained results in the sample-subsample relationship (cases A and B), and to evaluate the importance of visual classification on the final outcome of the strength classes assignment in the sample (case C).

The analysis of 3 referent timber properties (*MoR*, *MoE*, density) was performed according to EN 14358 with assumed lognormal and normal distributions for characteristic 5 % fractile or mean values, respectively. Goodness-to-fit tests (KS and $\chi 2$) confirmed that both proposed theoretical distributions are acceptable, so the parametric calculation was performed. All necessary descriptive parameters (mean/characteristic values, standard deviation and coefficient of variation) are given for each case study.

Compared to the 3-point bending test, there are no shear forces in the 4-point bending test in the area between the two loading pins. In order to convert the 3-point (JUS) to 4-point bending test (EN 408), as well as to normalise the size and lengths of specimens for *MoR*, adjustment factors from EN 384 were used. For *MoE* determination (EN 408), the conversion of measured global MoE to requested E_0 - modulus of elasticity parallel to the grains (i.e. local *MoE*) was conducted according to EN 384. The expressions given in Table 2 (*MoR*) and Table 3 (*MoE*) are used in order to harmonise archive data results with the testing procedures given in EN 408.

Density was determined on a parallel sample (2x30 specimens, dimensions 3.5 cm × 2.0 cm × 2.0 cm), taken from fir and spruce planks, from which the (combined) mean value was determined according to JUS. Density was determined as an auxiliary basic indicator of strength class(es) because this grading parameter was not considered fundamental in previous standards. Density was tested on small clear specimens, due to the confirmed fact that density is not influenced by the specimen size in softwood species (Krajnc *et al.,* 2019).

3 RESULTS AND DISCUSSION
3. REZULTATI I RASPRAVA

Cases A, B, C were analysed considering 3 referent parameters (EN 338:2016) for the classification of timber: density, *MoR* and *MoE*, using expressions given in Tables 2 and 3.

Density as strength class (SC) indicator is adopted as the average value, determined from mean values from fir and spruce specimens. The moisture content of fir specimens was 11.5 % and of spruce 9.5 %, so the mean density of fir specimens adjusted to referent moisture content of 12 % was 416.6 kg/m^3 and for spruce 450.56 kg/m^3. As the archive data sample was of mixed species, the average value for further analysis was adopted as ρ=433.6 kg/m^3.

Case A is presented in Table 4 trough probability distribution functions of fitted lognormal distribution for *MoR* and fitted normal distribution for *MoE*, together with histograms of archive data for *MoR* and recalculated test data as local *MoE*. Necessary descriptive statistics and final characteristic values (adjusted and converted) are as follows: 5 % fractil for *MoR* and mean value for *MoE*. Analysis results in Case A show that the obtained characteristic value of *MoR* is 15.16 MPa, while the mean *MoE* is 10.8 GPa. Coefficients of variation (CoV) are significantly higher both for *MoR* (*CoV* =43 %) and *MoE* (*CoV*=24 %) than assumed in JCSS report (CoV_{MoR}= 25 %, CoV_{MoE}=13 %) for the determination of other mechanical properties (EN 384:2016). The higher CoV is expected for visually graded structural timber and was reported by many authors (Ridley-Ellis *et al.,* 2022; Kupniewska *et al.*, 2020; Stapel and van de Kuilen, 2014; Ranta-Maunus *et al.,* 2011; Ranta-Maunus, 2009).

Case B is analysed in Table 5, by giving the relevant statistical parameters for each subsample and taking into account the adjusting factor for the number of subsamples in characteristic value calculation. As subsamples are chosen randomly, respecting that the minimal required number of specimens (*n*>40) has to be satisfied, the *CoVs* are even higher comparing to case A. The analysis in case B indicates smaller 5 % *MoR* value (13.43 MPa) and slightly smaller value for *MoE* (10.6 GPa), compared to case A.

Case C is analysed in Table 6, where the additional visual selection of two (sub) samples was made according to the recorded "desirable" failure type in compressed/tension zone C1 (good lot - GL) and failure type due to excessive defects, and number and position of knots and/or high slope of grains C2 (low tail - LT). Relevant statistical parameters and characteristic values are given for two independent additionally graded sets of specimens. Coefficients of variation for *MoR* (CoV_{C1} =26 %, and CoV_{C2} =34 %) and *MoE* (CoV_{C1} =21 % and CoV_{C2}=22 %) show values for C1 close to those suggested by JCSS. Also, it indicates that the division of the total sample into C1 and C2 was with a reason because of insufficient quality of primary visual classification. C1 sample shows higher characteristic bending strength and stiffness properties compared to the basic sample A and remaining C2.

All analyses are summarised in Table 7 in order to get the "framework" of strength classes according to EN 338 and observed sample of II grade. The mean density value of sample(s) refers to strength class C27 (ρ_{mean}=430 kg/m^3) and is not a determining parameter for SC assignment in analysed cases - the relevant property is always the value that leads to the lowest SC based on worst characteristic criterion.

Case A shows that conversion of results regarding test arrangements and specimens size, as well as transition from previously commonly measured global modulus of elasticity to local, could be easily performed by calculation. *MoR* results indicate that SC of the observed sample is C14 ($f_{m,k}$ =14 N/mm^2, $E_{m,0,mean}$=7 kN/mm^2), while the stiffness found in tests is higher than the assigned SC value. Case B shows that statistical analyses through subsample is stricter and requires more data (min 5 subsamples with min 200 specimens in total) or better (consistent) visual grading. In Case B, the classification framework is not possible to eval-

Table 4 *MoR* / *MoE* results – CASE A
Tablica 4. Rezultati *MoR* / *MoE* – SLUČAJ A

<table>
<tr><th>MoR, MPa</th><th colspan="2">Lognormal distribution
Lognormalna distribucija</th></tr>
<tr><td rowspan="7">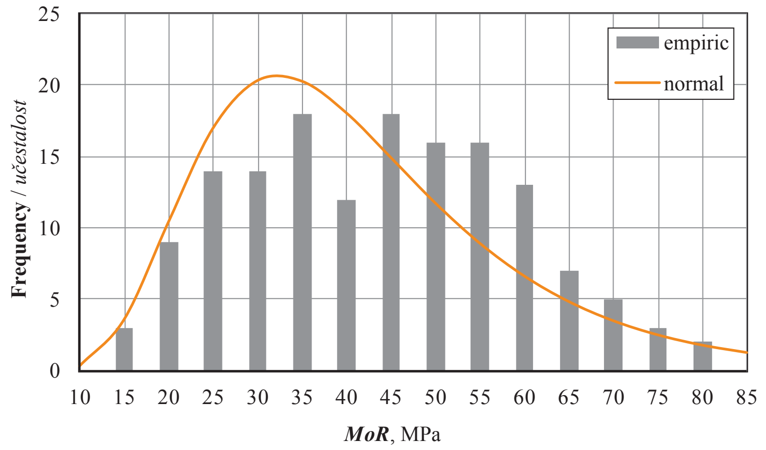
</td><td>All data</td><td>A (n=150)</td></tr>
<tr><td>$\bar{y}$</td><td>41.62</td></tr>
<tr><td>s_y</td><td>17.84</td></tr>
<tr><td>CoV</td><td>0.43</td></tr>
<tr><td>$f_{m,k}$</td><td>15.16</td></tr>
<tr><td></td><td></td></tr>
<tr><td></td><td></td></tr>
<tr><th>MoE, GPa</th><th colspan="2">Normal distribution
Normalna distribucija</th></tr>
<tr><td rowspan="7">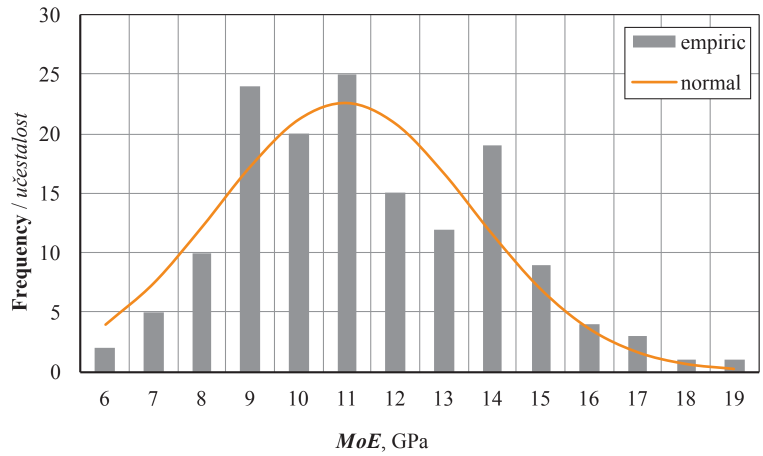
</td><td>All data</td><td>A (n=150)</td></tr>
<tr><td>$\bar{y}$</td><td>10.94</td></tr>
<tr><td>s_y</td><td>2.64</td></tr>
<tr><td>CoV</td><td>0.24</td></tr>
<tr><td>E_0</td><td>10.8</td></tr>
<tr><td></td><td></td></tr>
<tr><td></td><td></td></tr>
</table>

Table 5 *MoR* / *MoE* results – CASE B
Tablica 5. Rezultati *MoR* / *MoE* – SLUČAJ B

Lognormal distribution / *Lognormalna distribucija*				**Normal distribution** / *Normalna distribucija*			
***MoR*, MPa**	B1 (*n*=50)	B2 (*n*=50)	B3 (*n*=50)	***MoE*, GPa**	B1 (*n*=50)	B2 (*n*=50)	B3 (*n*=50)
$\bar{y}$	42.69	40.52	41.81	$\bar{y}$	10.72	10.52	11.58
s_y	21.00	16.71	16.12	s_y	2.58	2.54	2.73
CoV	0.49	0.41	0.39	*CoV*	0.241	0.242	0.236
$f_{m,k,i}$	13.52	14.98	16.29	$E_{0,i}$	10.47	10.26	11.31
$f_{m,k}$	13.43			E_0	10.57=10.6		

Table 6 *MoR* / *MoE* results – CASE C
Tablica 6. Rezultati *MoR* / *MoE*– SLUČAJ C

Lognormal distribution / *Lognormalna distribucija*			**Normal distribution / *Normalna distribucija***		
***MoR*, MPa**	C1 (GL) (*n*=88)	C2 (LT) (*n*=62)	***MoE*, GPa**	C1 (GL) (*n*=88)	C2 (LT) (*n*=62)
$\bar{y}$	50.51	28.51	$\bar{y}$	11.96	9.49
s_y	12.94	9.72	s_y	2.54	2.05
CoV	0.26	0.34	*CoV*	0.212	0.216
$f_{m,k,}$	25.60	12.18	E_0	11.78	9.31

Table 7 Summary of strength class "framework" in analysed cases
Tablica 7. Sažetak „okvira" razreda čvrstoće u analiziranim slučajevima

Spruce/fir (II) *Smrekovina/jelovina (II)*	**Relevant parameters** *Relevantni parametri*	**Cases** / *Studije slučaja*			
		A	B	C1 (GL)	C2 (LT)
MoR	$f_{m,k}$, N/mm^2	15.16	13.43	25.60	12.18
	EN 338	C14	-	C24	-
MoE	$E_{m,0,mean}$, kN/mm^2	10.8	10.6	11.8	9.3
	EN 338	C22	C22	C27	C18
Density / *gustoća*	ρ_{mean}, kg/m^3	433.6			
	EN 338	C27			
Strength class / *klasa čvrstoće*	EN 338	C14	-	C24	-

uate due to *MoR*, while *MoE* still remains high. Case C indicates that the analysed timber C1 could be classified as C24 ($f_{m,k}$ =24 N/mm^2, $E_{m,0,mean}$=11 kN/mm^2), while the remaining part of the basic sample C2 stays unclassified.

The linear regression model, Figure 1a, as a convenient method for the presentation of the interdependence of mechanical properties, was applied on the test results of the whole sample.

The coefficient of determination between *MoE* and *MoR* is R^2=0.415, which is consistent with other similar studies (Steiger and Arnold, 2009; Ranta Manus *et al.,* 2009/2011; Kupniewska *et al.,* 2020; Moore *et al.,* 2009). Although moderate and lower compared to small-size tests, the *MoE-MoR* correlation is found satisfactory and comparable for full-size tests (Krajnc *et al.,* 2019), so the structural size specimens could be used in the evaluation of the relative quality of timber.

Figure 1b) represents the EN 338 basic strength class values for $f_{m,k}$ and $E_{m,0,mean}$, following the experimental data values from the analysed cases and assigned SC values. From the diagram, it is obvious that *MoE-MoR* test points lay below the EN 338 line, so that strength is the limiting factor. Higher MoE obtained from tests than assigned strength class values in EN 338 could be considered as additional hidden safety. Due to geographical position of the region and on the basis of "Gradewood" project results (Ranta Manus *et al.,* 2011), stiffness and density were expected to be relatively higher in Southern Europe, which was confirmed by the results from Italy (Nocetti *et al.,* 2013; Negro *et al.,* 2013). The structural timber of similar mixed species is habitual in civil engineering practice. The research findings (Steiger and Arnold, 2009) show that the differences among species are less pronounced in structural size timber than in small clear specimens, which also contributes to a realistic result.

4 CONCLUSIONS
4. ZAKLJUČAK

Based on the consideration of EN standards, JUS visual grading rules and analysed cases, the following conclusions were made:

Overall, the analysed test results show that bending strength is the limiting property for SC classification of regional timber, while stiffness provides an additional safety factor.

Evaluation of II grade structural fir/spruce timber (Case A) points out that all data corresponds to C14, which is generally acceptable for the intended use in low-rise wood frame buildings (for wall studs with deformation requirements that are not too stringent).

Recommended analysis through subsamples (Case B) requires more specimens in factory production control.

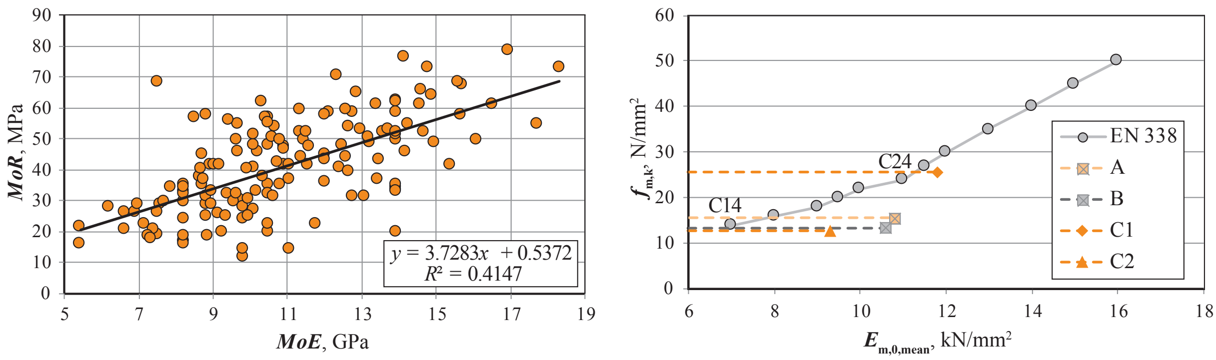

Figure 1 a) *MoE-MoR* linear regression, b) *MoR/MoE*: analysed cases vs EN 338 SC
Slika 1. a) Linearna regresija *MoE-MoR*, b) *MoR/MoE*: analizirani slučajevi u odnosu prema klasama EN 338

By additional visual grading (Case C1) of the basic sample, the strength class C24 was achieved, which is generally expected in EU countries for II grade (S10) coniferous timber, considered as high strength class for load-bearing purposes.

The rough estimation of mean strength values (case C), with the application of the global safety factor (*n*=4 for bending) according to the concept of allowable stress design, indicates that the whole sample of II grade (S10) is obtained by mixing the grade I (S13) and grade III (S7), which also highlights the need for stricter visual grading in limit state design concept.

High coefficients of variation in the analysed cases for class determining parameter - bending strength, also indicate the need for more consistent visual grading assessment, because the other strength parameters in a particular strength class are established on the basis of recommended *CoV*=0.25. Also, in the case of high(er) *CoV*s, the conversion of other mechanical properties (EN 384) could not be considered valid and reliable. That could lead to incorrect assessment (even overestimation) of the other strength properties (especially perpendicular to the grains), which could be a very sensitive problem in design calculations.

Regional coniferous timber is obviously in the range of C14 to C24 for normal structural use and it will be very helpful to introduce one SC in between, as well as to define the final structural purpose of each class. This would lead to additional benefits in the ex-YU timber trade (Part 1).

Considering the need of conversion of regional construction timber classification into EN SC system, it has been confirmed that the conversion of archive test results on structural size specimens with different loading arrangement directly leads to realistic SC of timber. The necessary additional data can also be obtained through the analysis of archive test data on small clear specimens that are widely available in the ex-YU region. In that case, the correlation of mechanical properties, determined on small and structural size specimens, should be taken into account.

Acknowledgements – Zahvala

This research has been supported by the Ministry of Science, Technological Development and Innovation through project No. 451-03-47/2023-01/200156 "Innovative scientific and artistic research from the FTS domain".

5 REFERENCES
5. LITERATURA

1. Burawska-Kupniewska, I.; Krzosek, S.; Mańkowski, P.; Grześkiewicz, M., 2020: Quality and Bending Properties of Scots Pine (*Pinus Sylvestris* L.) Sawn Timber. *Forests, 11:* 1200: 1-12. https://doi.org/10.3390/f11111200
2. Krajnc, L.; Farrelly, N.; Harte, A., 2019: Relationships between wood properties of small clear specimens and structural – sized boards in three softwood species. Holzforschung, 73 (11): 987-996. https://doi.org/10.1515/hf-2019-0039
3. Moore, J.; Mochan, S.; Brüchert, F.; Hapca, A.; Ridley-Ellis, D.; Gardiner, B.; Lee, S., 2009: Effects of genetics on the wood properties of Sitka spruce growing in the UK: bending strength and stiffness of structural timber. *Forestry,* 82 (5): 491-501. https://doi.org/10.1093/forestry/cpp018
4. Negro, F.; Cremonini, C.; Zanuttini, R., 2013: CE Marking of structural timber: the European standardization framework and its effects on Italian manufacturers. Drvna industrija, 64 (1): 55-62. https://doi.org/10.5552/drind.2013.1214
5. Nocetti, M.; Brancheriau, L.; Bacher, M.; Brunetti, M.; Crivellaro, A., 2013: Relationship between local and global modulus of elasticity in bending and its consequence on structural timber grading. European Journal of Wood and Wood Products, 71: 297-308. https://doi.org/10.1007/s00107-013-0682-7
6. Ranta-Maunus, A., 2009: Strength of European timber. Part 1: Analysis of growth areas based on existing test results. VTT Publications, 706: 1-174. ISBN 978-951-38-7337-0
7. Ranta-Maunus, A.; Denzler, J. K.; Stapel, P., 2011: Strength of European timber. Part 2: Properties of spruce and pine tested in Gradewood project. VTT Working Papers, 179: 1-115. ISBN 978-951-38-7521-3
8. Ridley-Ellis, D.; Stapel, P.; Bano, V., 2016: Strength grading of sawn timber in Europe: an explanation for engineers and researchers. European Journal of Wood and Wood Products, 74: 291-306. https://doi.org/10.1007/s00107-016-1034-1
9. Ridley-Ellis, D.; Gil-Moreno, D.; Harte, A., 2022: Strength grading of timber in the UK and Ireland in 2021. International Wood Products Journal, 13 (2): 127-136. https://doi.org/10.1080/20426445.2022.2050549
10. Stapel, P.; van de Kuilen, J. W., 2014: Efficiency of visual strength grading of timber with respect to origin, species, cross section, and grading rules: a critical evaluation of the common standards. Holzforschung, 68 (2): 203-216. https://doi.org/10.1515/hf-2013-0042
11. Steiger, R.; Arnold, M., 2009: Strength grading of Norway spruce structural timber: revisiting property relationships used in EN 338 classification system. Wood Science and Technology, 43: 259-278. https://doi.org/10.1007/s00226-008-0221-6
12. *** DIN 4074-1:2012 Strength grading of wood. Part 1: Coniferous sawn timber. German National Standard.
13. ***EN 14080:2013 Timber structures – Glued laminated timber and glues solid timber – Requirements. European Committee for Standardization, Brussels.
14. ***EN 14081-1:2016 Timber structures – Strength graded structural timber with rectangular cross section. Part 1: General requirements. European Committee for Standardization, Brussels.
15. ***EN 14358:2016 Timber structures – Calculation and verification of characteristic values. European Committee for Standardization, Brussels.
16. ***EN 1995-1-1:2004 Eurocode 5: Design of timber structures. Part 1-1: General – Common rules and rules for buildings. European Committee for Standardization, Brussels.
17. ***EN 338:2016 Structural timber – Strength classes. European Committee for Standardization, Brussels.

18. ***EN 384:2016 Structural timber – Determination of characteristic values of mechanical properties and density. European Committee for Standardization, Brussels.
19. ***EN 408:2012 Timber structures – Structural timber and glued laminated timber – Determination of some physical and mechanical properties. European Committee for Standardization, Brussels.
20. ***prEN 1912:2022 Structural timber – Strength classes – Assignment of visual grades and species. European Committee for Standardization, Brussels.
21. ***JCSS, 2006: Probabilistic model code. Part 3.5: Timber. Joint Committee on Structural Safety, 16 p.
22. ***Sweedish wood: https://www.swedishwood.com/wood-facts/about-wood/wood-grades (Accessed Jan 27, 2023).
23. ***Zbirka jugoslovenskih pravilnika i standarda za gradjevinske konstrukcije, 1995. Knjiga 4: Drvene konstrukcije. Beograd, 687 p.

Corresponding address:

Assist. Prof. ALEKSANDRA RADUJKOVIĆ
University of Novi Sad, Faculty of Technical Sciences, Department of Civil Engineering and Geodesy,
Dr Sime Miloševića 12, 2100 Novi Sad, SERBIA, e-mail: leksa@uns.ac.rs

Lin

Laboratorij za ispitivanje namještaja i opreme dječjih igrališta

laboratorij za ispitivanje namještaja i opreme dječjih igrališta osposobljen je prema normi HRN EN ISO/IEC 17025

više od 40 akreditiranih metoda u području ispitivanja namještaja, premaza i dijelova za namještaj, dječjih igrališta i opreme

usluge izvan područja akreditacije:

istraživanje konstrukcija i ergonomije namještaja

ispitivanje materijala i postupaka površinske obrade

ispitivanje zapaljivosti madraca i ojastučenog namještaja

vještačenja namještaja i stručna mišljenja

Laboratorij **je član udruge Hrvatski laboratoriji CROLAB – čiji je cilj razvoj hrvatskih laboratorija kao infrastrukture razvoja proizvodnje i gospodarstva u okviru zahtjevnog otvorenog tržišta, korištenjem zajedničkih potencijala i sinergijskih učinaka udruživanja, dok je...**

...*Fakultet šumarstva i drvne tehnologije* punopravni član udruženja INNOVAWOOD – kojemu je cilj doprinijeti poslovnim uspjesima u šumarstvu, drvnoj industriji i industriji namještaja s naglaskom na povećanje konkurentnosti europske industrije.

Istraživanje kreveta i spavanja, istraživanja dječjih kreveta, optimalne konstrukcije stolova, stolica i korpusnog namještaja, zdravog i udobnog sjedenja u školi, uredu i kod kuće neka su od brojnih istraživanja provedena u *Zavodu za namještaj i drvo u graditeljstvu*, kojima je obogaćena riznica znanja o kvaliteti namještaja.

Dobra suradnja s proizvođačima, uvoznicima i distributerima namještaja čini nas prepoznatljivima

Znanje je naš kapital

Sveučilište u Zagrebu • Fakultet šumarstva i drvne tehnologije
Laboratorij za ispitivanje namještaja i opreme dječjih igrališta
Zavod za namještaj i drvo u graditeljstvu
Svetošimunska cesta 23
10000 Zagreb, Hrvatska

Emirhan Akdemir, Osman Goktas, Mehmet Yeniocak*, Mehmet Colak[1]

Effects of Ultrasound-Assisted Varnish and Component Mixing Method on Mechanical and Physical Properties of Varnish Layer

Učinci metode miješanja laka i komponenata potpomognute ultrazvukom na mehanička i fizikalna svojstva sloja laka

ORIGINAL SCIENTIFIC PAPER
Izvorni znanstveni rad
Received – prispjelo: 25. 5. 2023.
Accepted – prihvaćeno: 29. 11. 2023.
UDK: 620.198; 674.06
https://doi.org/10.5552/drvind.2024.0115

ABSTRACT • *The aim of this study was to determine the effects of mechanical and ultrasound-assisted stirring methods for varnish + components mixing on the varnish layer coating adhesion, surface roughness and glossiness. For this purpose, polyurethane, acrylic and polyester varnish systems were applied on three different wood types, namely Scots pine (Pinus sylvestris L.), Eastern beech (Fagus orientalis L.) and Mahogany (Khaya ivorensis), with mechanical and ultrasound-assisted mixing methods. In the mechanical mixing method, 3 and 5 minutes were applied, while in the ultrasonic mixing method, beside 3- and 5- minute stirring time, 80-watt, and 120-watt ultrasonic power was applied during mixing. When research results are generally evaluated, it cannot be said that ultrasound-assisted mixing method is superior to mechanical mixing method. However, the ultrasound-assisted mixing of varnish components at 80 watts for 3 minutes can be recommended.*

KEYWORDS: *ultrasound stirring; adhesion strength; roughness; glossiness; varnish*

SAŽETAK • *Cilj ovog istraživanja bio je utvrditi učinke mehaničke i ultrazvučno potpomognute metode miješanja laka i komponenata na adheziju sloja laka te na hrapavost i sjaj površine drva. Stoga su na drvo običnog bora (Pinus sylvestris L.), kavkaske bukve (Fagus orientalis L.) i mahagonija (Khaya ivorensis) naneseni sustavi poliuretanskoga, akrilnoga i poliesterskog laka. Sustavi laka pripremljeni su metodama mehaničkog miješanja i miješanja potpomognutoga ultrazvukom. Pri mehaničkoj metodi miješanje je trajalo tri odnosno pet minuta, dok je pri ultrazvučnoj metodi uz vrijeme miješanja od tri i pet minuta tijekom miješanja primijenjena snaga ultrazvuka od 80 i 120 W. U općenitoj ocjeni rezultata istraživanja ne može se reći da metoda miješanja laka i komponenata potpomognuta ultrazvukom ima prednost pred metodom mehaničkog miješanja. Međutim, može se preporučiti miješanje komponenata laka uz pomoć ultrazvuka na 80 W tijekom tri minute.*

KLJUČNE RIJEČI: *ultrazvučno miješanje; adhezivna čvrstoća; hrapavost; sjaj; lak*

* Corresponding author
[1] Authors are researchers at Mugla Sitki Kocman University, Faculty of Technology, Department of Woodworking Industrial Engineering, Turkey. https://orcid.org/0000-0001-8174-3233; https://orcid.org/0000-0001-7459-1104; https://orcid.org/0000-0002-8757-5688; https://orcid.org/0000-0003-4780-587X

1 INTRODUCTION
1. UVOD

Despite its many advantages, wood has some disadvantages as well. Primarily, wood is a hygroscopic material. Because of these properties, wood material is affected by chemical, physical, biological, and mechanical factors (Berkel, 1972). Therefore, for long service life, wood should be protected.

Varnishing is one of the most popular protection methods that provides protective coatings and enhances the appearance of wooden surfaces, paintings, and various decorative objects. Although polyurethane, lacquer, and shellac are all types of wood finishes that are frequently referred to as varnish, the term actually refers to a particular mixture of resins, oils, and liquids. Most varnishes are a blend of resin, drying oil, drier, and volatile solvent. Varnishes may consist of a single or more than one compounds. Multi-component varnishes are applied by adding and mixing each component in the amounts determined in accordance with the company's recommendations. The performance of dry varnish coating is affected by the proper mixing of varnish liquid that is composed of all components. Although varnish manufacturers give information about how and when these mixtures should be made, this process is sometimes not ideal and causes significant and costly defects in the varnish layer in the short and long term (Baykan *et al*., 2000).

Varnish adhesion strength on wood plays an important role for effective use of the final product for different applications. In many cases, the surface coating fails due to de-bonding from the surface of the wood. There are some factors that limit the service life of varnishes applied on wood material. One of them is the cavitation that occurs in the varnish liquid during the mixing of varnish and its components. The propagation of the acoustic waves in a liquid produces the phenomenon of cavitation (Shutilov and Alferieff, 2020). Cavitation is a process whereby a liquid forms tiny vapour-filled cavities when the static pressure of the liquid falls to less than its vapour pressure. These gaps or cavities, also known as "bubbles," burst under greater pressure and can cause layer flaws. During the varnishing process in furniture and woodworking operations, applicators generally use propeller mixers to mix the varnish and its components. However, propeller mixers can cause cavitation in the liquid mixture. It is believed that cavitation can lead to adverse effects on the applied varnish layer. According to the literature, ultrasonic cavitation may accelerate the breakdown and deterioration of substances that are only partly stable when examined in terms of carbon chains (Effendi and Wulandari 2019). Simple propeller mixers create micro-cavities in the liquid, causing the layer to have a porous structure after drying and adversely affect the quality properties such as surface coating adhesion, surface hardness, scratch resistance, surface roughness and surface gloss. In the long term, other problems are encountered in the medium such as cracks caused by different elastic behaviours in different parts of the varnish surface layer applied with an inhomogeneous mixing, the film layer separated from the surface due to low coating adhesion resistance, and the accumulation of salt and dirt on rough surfaces.

Some of the factors that negatively affect the life of the varnish are also related to the "improper mixing" process that will be the cause of cavitation. Some of the problems caused by improper mixing (AkzoNobel, 2019) are as follows: Insufficient curing, subsidence in the wet layer, formation of non-homogeneous hardness areas on the surface, non-homogeneous gloss distribution on the surface, low coating adhesion resistance, crater formation due to air bubbles in the varnish and subsequent bursting, regional drying time differences, and layer formation in the form of a misty view.

Recently, ultrasonic wave technique has been introduced as one of the methods used for mixing materials and preventing cavitation. The use of the ultrasonic blender eliminates the need to access or shake hermetically sealed plastic or metallic boxes (or bottles) containing any liquids, including those with high viscosity. It is known that composite materials are broken down by the cavitation droplets and shock waves (shockwaves) produced by ultrasonic waves (Mason, 2004). Effendi and Wulandari (2019) used ultrasonic power for clearing petroleum hydrocarbon from low permeability contaminated soils. Halacinski *et al*. (1994) used ultrasound wave technique for effective mixing of various sedimented paints and viscous fluids. Zanghellini *et al*. (2021) used solvent-free ultrasonic dispersion method for nanofillers in epoxy matrix and obtained the best results by ultrasound-assisted mixing. In their study, Stephen *et al.* (2003) described a device that contains a mixing receptacle for ultrasonically spreading an additive with another coating component. Nejad *et al*. (2015) investigated dispersion quality of nanoparticles into a bio-based coating by ultrasound assisted mixing. He *et al*. (2018) used ultrasound stirring method for effective metal composite mixing. Masri *et al*. (2018) presented a comparison analysis of the esterification process using either ultrasonic cavitation or traditional mechanical stirring with a number of recently developed SO_3H-functionalized dicationic ammonium- and diazabicyclo octane (DABCO)-based acidic ionic liquids. In order to enhance the dispersion and dispersal of composite particles in the rubber matrix and the general performance of rubber goods, Cheng and Wang (2022) used ultrasound-assisted mixing. They claimed that the benefits of dispersive mixing and distribute mixing could be enhanced by ultrasonic waves, which would improve the comprehensiveness of rubber goods. All the above researchers reported that the ultrasound-assisted mixing method was beneficial.

Currently, there is limited information about the effect of varnish-component mixing by ultrasound-assisted method on the varnish layer adhesion, roughness, and glossiness of wood materials. In this study, experiment was carried out by comparing the efficiency of mechanical and ultrasound-assisted mixing methods by various time and ultrasonic power in varnish-component mixing.

2 MATERIALS AND METHODS
2. MATERIJALI I METODE

2.1 Wood materials
2.1. Drvni materijali

Three different types of wood were used in this study: Eastern beech (*Fagus Orientalis* L.), Scots pine (*Pinus sylvestris* L.), and Mahogany (*Khaya ivorensis*) as test samples. These wood varieties were chosen due to their widespread use in the wood products business. The wood samples came from Turkish lumber traders in the Turkish city of İzmir, chosen at random.

The timber was selected from sapwood, with smooth fibres, no knots, no cracks, no difference in color and density, annual rings perpendicular to the surfaces and chosen randomly. The sapwood-derived wood samples were conditioned at a temperature of 20 °C and a relative humidity of 65 % until their weights settled. Air-dried specimens from each species were cut in either the radial or tangential direction to the final size of 100 mm × 100 mm × 10 mm and then sanded by paper grit (140, and 180 grit). According to the technique outlined in TS 2470 (1976), test samples (3 wood × 3 varnish × 6 stirring method × 3 test × 10 repeat = 1620) of each wood species with an average moisture content of 12 %.

2.2 Varnishing
2.2. Nanošenje laka

The polyurethane, acrylic, and polyester fillers and topcoat varnishes used in experiments are all solvent-based and applied according to the guidelines in ASTM D 3023 (1998). The varnishes were purchased from companies located in Mugla, Turkey.

Polyurethane filler and topcoat varnishes are solvent-based varnishes that use alkyd resin-based primary components and hardeners based on isocyanate groups enriched with isocyanate prepolymers. Therefore, polyurethanes are polymers available for many technical applications requiring strong bonding force, flexibility, durability, and impact resistance. Polyurethane varnish, a popular type of coating, exhibits several mechanical properties that make it desirable for various applications. (Li *et al*., 2018; Chen *et al*., 2018). Polyurethane varnishes, due to their abrasion resistance, are mainly used for varnishing furniture and floors in rooms with high intensity of movement, such as halls and lounges.

Acrylic filler and topcoat varnishes are solvent-based varnishes that use acrylic resin-based primary components and hardeners based on isocyanate groups enriched with isocyanate prepolymers. They are durable and resistant to UV light, water, and abrasion, and they can be used for both interior and exterior applications.

Polyester filler and topcoat varnishes are solvent-based varnishes that are based on unsaturated polyester resin. They have a very high filling capacity and are suitable for application on various types of wood. The composition of varnishes and the components subjected to the mixture are provided in Table 1.

Before applying the filler varnish, all wooden test pieces were sanded with a vibrating sander using 180-grit sandpaper. The sanded test samples were varnished by spraying with three types of varnish, according to ASTM D 3023 (1998). The manufacturer's instructions for the solvent composition and hardener mixture were considered. Varnishes and components were mixed by two mixing methods, namely ultrasound-assisted stirring, and conventional mechanical stirring. Mechanical stirring was performed by a power mixer with 700 rpm. For ultrasonic stirring, an ultrasonic device was used (Kudos HP 53 kHz) with ultrasound energy (wave powers) of 80 and 120 W. In this study, two mixing times were used: 3 and 5 minutes. The varnish mixtures of polyurethane and acrylic were rested for 10 minutes before application on wood test samples (Megep, 2012). However, as polyester varnish quickly

Table 1 Varnishes and components mixing
Tablica 1. Lakovi i njihove komponente

Varnish type *Vrsta laka*	**Primer coat** / *Temeljni sloj*		**Top coat** / *Završni sloj*	
	Varnish /hardener/ accelerator *Lak / otvrđivač / ubrzivač*	**Solvent** *Otapalo*	**Varnish/hardener/ accelerator** *Lak / otvrđivač / ubrzivač*	**Solvent** *Otapalo*
Polyurethane	2/1	Polyurethane thinner (5 %)	1/1	Polyurethane thinner (5 %)
Acrylic	5/1	Acrylic thinner (40 %)	5/1	Acrylic thinner (40 %)
Polyester	1 kg/20 ml/20 ml	Monostirol (15 %)	1 kg/20 ml/20 ml	Monostirol (15 %)

Table 2 Varnish application conditions
Tablica 2. Uvjeti nanošenja laka

Type of varnish *Vrsta laka*	**Viscosity** / *Viskoznost* DIN Cup/4 mm	**Amount used, g/m²** *Količina nanosa,* g/m²	**Nozzle gap, mm** *Veličina sapnice,* mm	**Air pressure, bar** *Tlak zraka,* bar
Polyurethane	18-20	120-150 (filling) 100-120 (top)	1.8	2
Acrylic	15-18	100-120	1.8	2
Polyester	32-40	100	2.5	2

gels when mixed with its components, no resting time was made. After application every filling varnishing coat, the dried varnish layer was sanded by abrasive papers (220-320-400). Each cross layer of varnish was applied after six hours for polyurethane, three hours for acrylic and 25 minutes for polyester. Application conditions are given in Table 2.

In this study, after applying the varnish to wood samples, some mechanical properties of the applied varnish layer such as hardness and scratch resistance were also determined. The surface hardness of the varnishes was measured using a pendulum hardness device, and the average values were as follows: polyester (143.89), polyurethane (100.49), and acrylic (89.32). Meanwhile, the scratch resistance of the varnishes, in the given order, was as follows: polyurethane (0.31 N), acrylic (0.30 N), and polyester (0.24 N).

2.3 Determination of coating adhesion strength
2.3. Određivanje adhezivne čvrstoće premaza

The adhesion properties of the coated samples were evaluated in accordance with ASTM D4541 standards (2022). For the assessment of the bond strength between the varnish layer and the wood surface, Araldite 2021-1, a robust plastic steel two-component epoxy adhesive, was employed. Steel test spheres, 20 mm in diameter, were securely affixed to the sample surfaces and left for 24 h at room temperature (approximately 20 °C). Subsequently, the adhesive and coating film were meticulously removed using a cutter.

Coating adhesion strength (X) was automatically determined by pull-off tester (PosiTest AT-M Manual) in N/mm² according to Eq. 1.

$$X = 4 \cdot F / \pi \cdot d^2 \quad (1)$$

Where;
F – rupture force (Newton)
d – diameter of experiment cylinder (mm).

2.4 Surface roughness
2.4. Hrapavost površine

Surface roughness of coated test samples, which were coated by three varnish types, was measured by the Mitutoyo Surftest SJ-301 according to DIN 4768 (1990). A diamond scan needle with a width of 5 mm was used by the device to move up and down while measuring the surface roughness on the outline of the cavities and protrusion of the sample surface. The three factors measured were the greatest height of the profile (*Ry*), the average height of the ten tallest spots (*Rz*), and the mean deviation between valleys and peaks (*Ra*). Ra (mean variation) was used as the foundation for reporting the surface roughness. Readings were obtained across the grain (─|).

2.5 Surface glossiness
2.5. Sjaj površine

The gloss of the varnished samples was determined using a gloss meter (BYK Gardner, Micro-TRIGloss) according to ASTM D523-08 (2008). At 60° geometry, the gloss readings were taken both parallel (||) and perpendicular (⊥) to the wood grain. Each uniform measuring angle and orientation were recorded twice for each sample in accordance with the ISO 2813:2014 standard.

2.6 Statistical evaluation
2.6. Statistička procjena

Multiple comparisons were first subjected to an analysis of variance (ANOVA), and significant differences between average values of variables were determined using Duncan's multiple range test at P value of 0.05. This analysis was done to determine the effects of the wood species, varnish type, and stirring method on adhesion resistance, surface roughness, and surface glossiness. A total of 1620 observations (surface binding strength (540), surface roughness (540), and glossiness (540) were statistically analyzed.

3 RESULTS AND DISCUSSION
3. REZULTATI I RASPRAVA

Means of adhesion strength, surface roughness and surface gloss arithmetic and standard deviations are summarized in Table 3.

Table 4 presents data analysis and figures as well as the relationships between wood type (WT), varnish type (VT), and stirring technique (SM) and their impact on adhesion strength. All the factors and interactions had a significant impact ($p < 0.05$) on adhesion strength, surface roughness, and surface glossiness.

The results of the Duncan test for multiple comparisons and homogeneity grouping of adhesion resist-

Table 3 Means of adhesion strength, surface roughness and surface glossiness
Tablica 3. Srednje vrijednosti adhezivne čvrstoće, hrapavosti i sjaja površine

			Adhesion strength, N/mm² *Adhezivna čvrstoća,* N/mm²		**Roughness *Ra* (−|), *µ*m** *Hrapavost Ra* (−|), *µ*m		**Glossiness at 60°, GU** *Sjaj pri 60°,* JS	
Wood type *Vrsta drva*	**Varnish type** *Vrsta laka*	**Stirring method** *Metoda miješanja*	Mean	S.D	Mean	S.D	Mean	S.D
Scots pine *obični bor*	Polyurethane	Mechanic / 3	3.86	0.29	0.17	0.04	96.65	2.63
		Mechanic / 5	5.33	1.89	0.12	0.03	97.20	0.54
		Ultrasonic 80 W / 3	5.59	1.04	0.10	0.01	97.62	0.98
		Ultrasonic 80 W / 5	6.27	0.90	0.13	0.04	95.17	4.35
		Ultrasonic 120 W / 3	5.69	0.80	0.11	0.03	95.66	3.44
		Ultrasonic 120 W / 5	3.73	1.42	0.15	0.03	94.86	2.21
	Acrylic	Mechanic / 3	1.96	0.76	0.24	0.05	87.24	5.68
		Mechanic / 5	1.70	0.39	0.16	0.04	83.26	4.04
		Ultrasonic 80 W / 3	2.04	0.49	0.23	0.05	86.66	3.31
		Ultrasonic 80 W / 5	2.50	1.05	0.24	0.08	86.74	4.58
		Ultrasonic 120 W / 3	2.23	0.87	0.23	0.06	83.39	5.52
		Ultrasonic 120 W / 5	1.94	0.48	0.17	0.06	84.33	5.42
	Polyester	Mechanic / 3	4.78	0.61	0.15	0.02	68.90	1.86
		Mechanic / 5	4.29	0.44	0.15	0.03	68.73	1.89
		Ultrasonic 80 W / 3	4.25	0.48	0.10	0.01	74.66	1.71
		Ultrasonic 80 W / 5	4.38	0.38	0.11	0.01	74.45	2.31
		Ultrasonic 120 W / 3	4.26	0.61	0.13	0.01	76.32	1.35
		Ultrasonic 120 W / 5	4.69	1.51	0.13	0.02	71.05	1.84
Eastern beech *kavkaska bukva*	Polyurethane	Mechanic / 3	4.98	1.15	0.28	0.09	89.36	7.46
		Mechanic / 5	7.47	2.01	0.26	0.11	83.19	9.01
		Ultrasonic 80 W / 3	5.53	1.48	0.12	0.06	81.14	8.37
		Ultrasonic 80 W / 5	6.75	1.20	0.15	0.07	85.66	9.00
		Ultrasonic 120 W / 3	5.74	2.15	0.14	0.09	85.53	6.57
		Ultrasonic 120 W / 5	5.86	1.00	0.21	0.09	87.77	8.03
	Acrylic	Mechanic / 3	3.20	1.17	0.23	0.10	77.17	17.10
		Mechanic / 5	2.87	0.89	0.16	0.07	86.47	7.31
		Ultrasonic 80 W / 3	2.90	0.78	0.22	0.06	93.01	1.71
		Ultrasonic 80 W / 5	3.04	0.88	0.11	0.05	79.00	7.37
		Ultrasonic 120 W / 3	2.88	1.18	0.19	0.04	84.63	4.07
		Ultrasonic 120 W / 5	2.83	1.06	0.13	0.05	75.05	6.04
	Polyester	Mechanic / 3	5.00	0.85	0.14	0.02	65.79	5.55
		Mechanic / 5	4.32	0.73	0.12	0.02	64.15	7.01
		Ultrasonic 80 W / 3	5.50	0.84	0.09	0.01	65.30	4.87
		Ultrasonic 80 W / 5	4.76	0.47	0.10	0.02	64.54	6.20
		Ultrasonic 120 W / 3	4.07	0.76	0.11	0.02	65.47	6.20
		Ultrasonic 120 W / 5	4.66	0.74	0.11	0.01	59.29	7.24
Mahogany *mahagonij*	Polyurethane	Mechanic / 3	6.27	0.70	0.24	0.05	77.64	7.37
		Mechanic / 5	7.07	1.32	0.14	0.04	81.78	5.42
		Ultrasonic 80 W / 3	6.78	0.62	0.08	0.03	89.15	2.75
		Ultrasonic 80 W / 5	6.79	0.94	0.14	0.05	89.08	4.74
		Ultrasonic 120 W / 3	6.93	1.02	0.16	0.05	89.05	3.50
		Ultrasonic 120 W / 5	6.09	1.32	0.12	0.04	85.81	7.01
	Acrylic	Mechanic / 3	1.78	1.57	0.22	0.06	76.36	5.30
		Mechanic / 5	1.82	1.02	0.15	0.04	84.20	4.86
		Ultrasonic 80 W / 3	1.38	0.38	0.28	0.05	80.23	3.13
		Ultrasonic 80 W / 5	2.16	0.76	0.25	0.07	79.27	5.72
		Ultrasonic 120 W / 3	1.63	1.02	0.19	0.06	79.39	6.53
		Ultrasonic 120 W / 5	1.83	1.00	0.27	0.11	78.90	8.68
	Polyester	Mechanic / 3	5.97	1.02	0.14	0.02	67.38	2.10
		Mechanic / 5	5.53	0.88	0.14	0.02	69.09	1.39
		Ultrasonic 80 W / 3	5.62	0.67	0.19	0.28	70.76	1.81
		Ultrasonic 80 W / 5	5.45	0.69	0.10	0.01	70.37	1.58
		Ultrasonic 120 W / 3	5.77	0.49	0.13	0.03	70.91	1.27
		Ultrasonic 120 W / 5	5.62	0.80	0.12	0.02	66.81	1.60

Table 4 Interactions between factors influencing adhesion strength, surface roughness and surface glossiness
Tablica 4. Interakcije utjecajnih čimbenika na adhezivnu čvrstoću, hrapavost i sjaj površine

Statistical analysis (*p* value) (Adhesion) / *Statistička analiza (p-vrijednost) (adhezija)*						
WT	VT	SM	WT+ VT	WT+ SM	VT+ SM	WT + VT + SM
0.000*	0.000*	0.005*	0.000*	0.225*	0.000	0.033*
Statistical analysis (*p* value) (Roughness)/ *Statistička analiza (p-vrijednost) (hrapavost)*						
WT	VT	SM	WT+ VT	WT+ SM	VT+ SM	WT + VT + SM
0.102	0.000*	0.000*	0.000*	0.008*	0.000*	0.000*
Statistical analysis (*p* value) (Glossiness) / *Statistička analiza (p-vrijednost) (sjaj)*						
WT	VT	SM	WT+ VT	WT+ SM	VT+ SM	WT + VT + SM
0.000*	0.000*	0.000*	0.000*	0.023*	0.002*	0.000*

* = Significant according to $\alpha \leq 0.05$; WT – Wood Type; VT – Varnish type; SM – Stirring method / ** = značajno pri α ≤ 0,05; WT – vrsta drva; VT – vrsta laka; SM – metoda miješanja*

Table 5 Results of Duncan test for wood type, varnish type and stirring method as well as mean and standard deviation of adhesion strength, surface roughness and surface glossiness
Tablica 5. Rezultati Duncanova testa za vrstu drva, vrstu laka i metodu miješanja te za srednje vrijednosti i standardne devijacije adhezivne čvrstoće, hrapavosti i sjaja površine

	Adhesion *Adhezija,* N/mm^2		**Roughness (*Ra*)** *Hrapavost* (*Ra*), mm		**Glossiness at 60°, GU** *Sjaj pri 60°,* JS	
		Mean		Mean		Mean
Wood type *Vrsta drva*	Scots pine [b]	3.86 ± 0.12	Scots pine	0.16 ± 0.00	Scots pine [a]	84.61 ± 0.78
	Eastern beech [a]	4.57 ± 0.13	Eastern beech	0.16 ± 0.01	Eastern beech [b]	77.36 ± 0.95
	Mahogany [a]	4.69 ± 0.17	Mahogany	0.17 ± 0.01	Mahogany [b]	78.12 ± 0.64
Varnish type *Vrsta laka*	Polyurethane [a]	5.93 ± 0.12	Polyurethane [b]	0.16 ± 0.01	Polyurethane [a]	89.02 ± 0.61
	Acrylic [c]	2.26 ± 0.08	Acrylic [c]	0.20 ± 0.01	Acrylic [b]	82.52 ± 0.58
	Polyester [b]	4.94 ± 0.07	Polyester [a]	0.13 ± 0.01	Polyester [c]	68.55 ± 0.41
Stirring method *Metoda miješanja*	Mechanic / 3 [bc]	4.20 ± 0.19	Mechanic / 3 [a]	0.20 ± 0.01	Mechanic / 3 [c]	78.50 ± 1.31
	Mechanic / 5 [ab]	4.49 ± 0.24	Mechanic / 5 [b]	0.15 ± 0.01	Mechanic / 5 [bc]	79.79 ± 1.18
	Ult / 80W / 3 [abc]	4.40 ± 0.20	Ult / 80W / 3 [b]	0.16 ± 0.01	Ult / 80W / 3 [a]	82.06 ± 1.13
	Ult / 80W / 5 [a]	4.68 ± 0.20	Ult / 80W / 5 [b]	0.15 ± 0.01	Ult /80W / 5 [ab]	80.48 ± 1.12
	Ult /120W / 3 [abc]	4.36 ± 0.21	Ult / 120W / 3 [b]	0.15 ± 0.01	Ult/ 120W / 3 [ab]	81.15 ± 1.04
	Ult /120W / 5 [c]	4.14 ± 0.08	Ult / 120W / 5 [b]	0.16 ± 0.01	Ult / 120W / 5 [c]	78.21 ± 1.27

Ult: Ultrasonic / *ultrazvučno*

ance, surface roughness, and glossiness, considering different wood types, varnish coatings, and mixing methods, are presented in Table 5.

Table 5 presents the results of the Duncan test, where superscript letters (a, b, c) are commonly used to denote statistical significance. These symbols aid in ranking differences between groups based on the level of significance, typically set at $p<0.05$ or $p<0.01$.

3.1 Adhesion strength
3.1. Adhezivna čvrstoća

In certain samples, cohesive failure between the adhesive and the varnish surface occurred during the adhesion strength test procedure. The analysis did not include these samples. Surface cracks took many different shapes in the cases used in the investigation. Most of these cracks occurred between the varnish and the wood, especially in Eastern beech and mahogany wood samples. On the other hand, with Scots pine wood samples, fractures mostly occurred inside the wood layer. Test samples made of Scots pine were more likely to fracture. This result is consistent with the fact that Scots pine wood is classified as a softwood, whereas Eastern beech and mahogany wood are tougher. The accompanying photos (Figure 1) list the main fracture types that correlate to the various tree species.

The mean values of adhesion strengths are given in Table 4 and illustrated in Figure 2. The mechanical properties of varnishes used in this study vary depending on the specific formulation of the varnish and its application method. It is important to note that the performance of the varnish layer can also be influenced by factors such as the thickness of the coating, surface preparation, and environmental conditions in which it is used. The highest adhesion strength was obtained on Eastern beech / polyurethane varnish / mechanic stirring method / 5 minutes (7.47 N/mm^2). Meanwhile the lowest was observed on mahogany / acrylic varnish / ultrasound stirring method / 3 minutes (1.38 N/mm^2).

When comparing the wood species in terms of surface adhesion strength performance, the ranking was as follows: mahogany (4.69 N/mm^2), beech (4.57 N/mm^2), and pine (3.86 N/mm^2). It is important to note that this result could be influenced by the density differences among the wood species. The adhesion strength of varnish on wood surfaces has been reported to be higher in wood from angiosperm trees compared to gymnosperms (Sonmez *et al*., 2009).

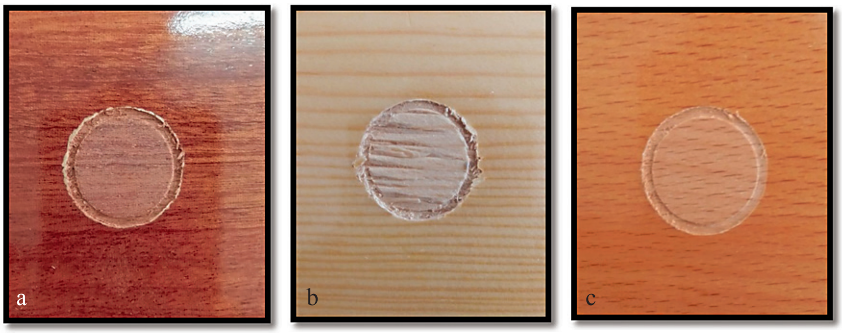

Figure 1 Most common forms of fractures on wood samples (a – Mahogany, b – Scoth Pine, c – Eastern beech)
Slika 1. Najčešći oblici lomova na uzorcima drva (a – mahagonij, b – obični bor, c – kavkaska bukva)

When varnishes were compared in terms of surface adhesion resistance strength, it was seen that they were ranked as follows: polyurethane (5.93 N/mm^2), polyester (4.94 N/mm^2) and acrylic (2.26 N/mm^2). The high adhesion strength of polyurethane varnish was consistent with previous studies (Kilic and Sogutlu, 2023; Gurleyen, 2021; Ghofrani *et al*., 2106; Sogutlu *et al*., 2016; Budakci and Sonmez, 2010). Budakci and Sonmez (2010) studied varnish adhesion properties. According to their research, polyurethane and acrylic varnishes achieved the greatest adhesion strength. The polyurethane outcomes of our study are generally consistent with their observations. The highest and the lowest surface adhesion resistance values of the varnishes obtained in our study were higher than those in the similar study (Gurleyen, 2021). This result may be due to the mixing of varnishes with their components for a standard period of time before the application of varnishes or due to the use of different materials.

The fact that the adhesion resistance of polyester varnish was lower than that of polyurethane varnish was also found in previous studies (Gurleyen, 2021; Ghofrani *et al*., 2106; Sogutlu *et al.* 2016; Budakci and Sonmez 2010. It is possible to discuss that this highest adhesion polyurethane varnish completes its polymerization reaction on the wood surface, making chemical bonding with wood, which creates a stronger adhesion on the surface (Ghofrani *et al*., 2106). In their study, Ghofrani *et al*. (2016) explained that the lower adhesion resistance of polyester varnish (pH 3.8), compared to polyurethane varnish (pH 4.5), can be attributed to the acidity levels present in their respective formulations.

When comparing the effects of the mixing method on adhesion strength, the ultrasound-assisted mixing / 80 W / 5 minutes has the best value. The lowest adhesion performance was obtained in the ultrasound-assisted mixing method / 120 W / 5 minutes. It is seen that, when the ultrasound power increases, it has a negative effect on the adhesion. Temperature has a significant impact on the efficiency of ultrasound-assisted processes (Niemczewski, 2007). Solvent vapours and dissolved gases penetrate the cavitation cavities as the solvent temperature rises. As a result, the cavitation process is less efficient and the fall increases. The other reason for this lowest value may be that the varnish liquid heats up with the extended time and starts to cure early. It is estimated that this early curing or gelling also makes it difficult for the varnish to penetrate the wood material. Viscosity, coating binder type, solid substance, pigmentation, and curing speed all have an impact on penetration, which in turn has an impact on the binding strength (Vitosyte *et al*., 2012).

The adhesion resistance values obtained in tests, where varnishes were pulled off from the wood surface, were influenced by the splitting resistance, a structural property of the wood material. When evaluating the surface adhesion resistance of varnishes on different wood types, Eastern beech and mahogany were found to belong to the top group (a), whereas Scots pine was categorized in a lower group (b). In the literature, it was reported that broadleaf wood generally exhibits higher adhesion strength compared to coniferous wood. This may result from the type of wood materials, anatomical structure, surface properties, resin content, density, cell structure, components of wood, texture, surface roughness, and moisture content. The results are consistent with the literature. It has been reported that hardwood exhibits higher adhesion resistance compared to softwood (Sonmez *et al*., 2009; Budakcı and Sonmez, 2010; Karamanoğlu and Kesik, 2021; Kretschmann, 2010). For example, Scots pine wood exhibited an adhesion resistance of 3.27, whereas ash tree displayed an adhesion resistance of 3.98 (Karamanoğlu and Kesik, 2021). One of the elements affecting the bonding between the samples and the covering would be the species anatomical structure. (Ozdemir *et al*., 2015). Sogutlu *et al*. (2016) estimated that the high adhesion strength of beech compared to pine may be due to the strong adhesion to the surface due to the homogeneous wood structure of broadleaved trees and scattered small trachea. This inference seems reasonable because the adhesion data obtained from mahogany and Eastern beech in our study are higher than that of Scots pine. The study's findings are in line with the above statement. Polyurethane varnish, followed by polyester and acrylic varnish, produced

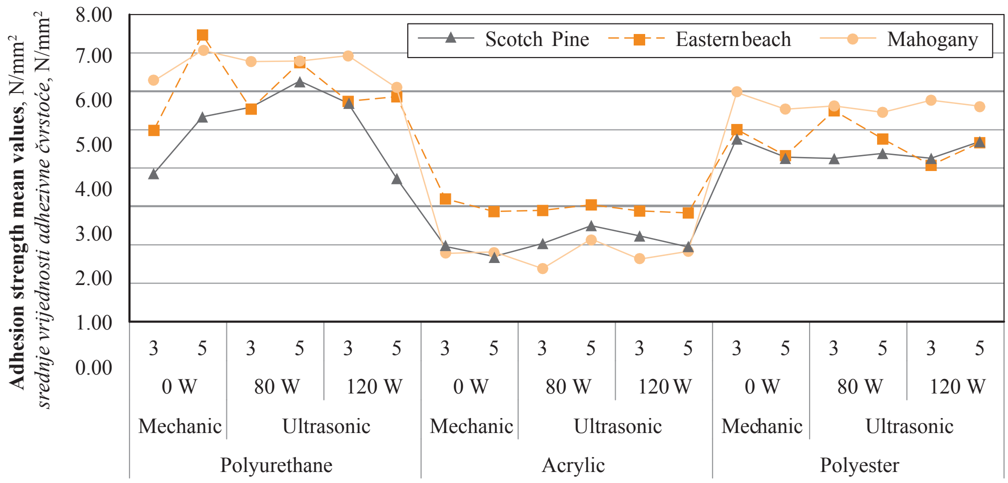

Figure 2 Surface adhesion strength
Slika 2. Adhezivna čvrstoća na površini

the strongest bonding. Similar outcomes were attained in additional trials (Sogutlu *et al*., 2016; Sonmez *et al*., 2009). Sonmez *et al*. (2009) explain this situation as "this highest adhesion two-part polyurethane varnish completes its polymerization reaction on the surface of wood which makes chemical bonding with wood, so it creates a stronger adhesion on surface". Sogutlu (2016) hypothesized that a flexible layer and a weak molecular link with the compounds in wood caused this outcome.

The ultrasound-assisted technique / 80 W / 5 minutes produced the greatest adhesion strength in our research when compared to the stirring method. However, the lowest adhesion was seen in the ultrasound-assisted method / 120 W / 5 minutes. Numerous variables can influence the success of the ultrasonic technique, as highlighted by Kim and Wang (2003). These variables include the type of substance, solid-to-liquid ratio, temperature, wave frequency, and the amount of energy or power used. It is crucial to consider these factors for achieving optimal results when using ultrasonic methods. Effendi and Wulandary (2019) outlined that the increase in ultrasound power also had a great effect on removing pollutants from the contaminated soil. Their results with high ultrasound power have served their purpose. In our study, however, it was observed that the increasing in ultrasound wave power caused an increase in temperature in the varnish and component mixture. It has been estimated that this temperature increase causes earlier curing of the varnishes with their components and negatively affects the adhesion strengths in the dry varnish layer. Kim and Wang (2003) stated that the ultrasound power should be increased as the density increases. Therefore, it is seen that 80-watt ultrasound power is suitable for the densities of the varnish types used in our study. Taking all these factors into account, the surface adhesion resistance values obtained in this study may have been influenced not only by the applied varnish and application method but also by the underlying structural properties of the wood. It should also be noted that there are many variables that determine the results. In most cases, it is not easy to determine which variable has the greatest impact.

3.2 Roughness
3.2. Hrapavost

The mean values of roughness are given in Table 4 and illustrated in Figure 3. As can be seen in Table 4, the highest surface roughness (Ra) value was obtained on Eastern beech / polyurethane varnish / mechanic stirring method / 3 minutes (0.28). The same value was obtained on mahogany / acrylic varnish / ultrasound mixing method 80 W / 3 minutes. Meanwhile the lowest (*Ra*) value was observed on mahogany / polyurethane varnish/ ultrasound 80 W / 3 minutes (0.08).

When the wood species were compared in terms of surface roughness performance, there was no statistical difference between wood types. In general, roughness values (R_a) of Eastern beech and mahogany test samples are expected to be lower than those of Scots pine. However, in our study, the sanding between the varnish layers during the varnishing of the test samples may also have influenced the lack of difference in surface roughness between wood species.

When the surface roughness is compared in terms of varnishes, there is polyester (*Ra* = 0.13), polyurethane (*Ra* = 0.16) and acrylic (*Ra* = 0.20), ranked from lowest to highest.

When the surface roughness is compared in terms of mixing methods, statistically the option with the mechanical stirring method / 3 minutes showed the lowest performance (0.20). All options with ultrasound-assisted stirring methods appear to perform better. The reason for this is our hypothesis, which suggests that ultrasound will mix the liquids more homogeneously. It is

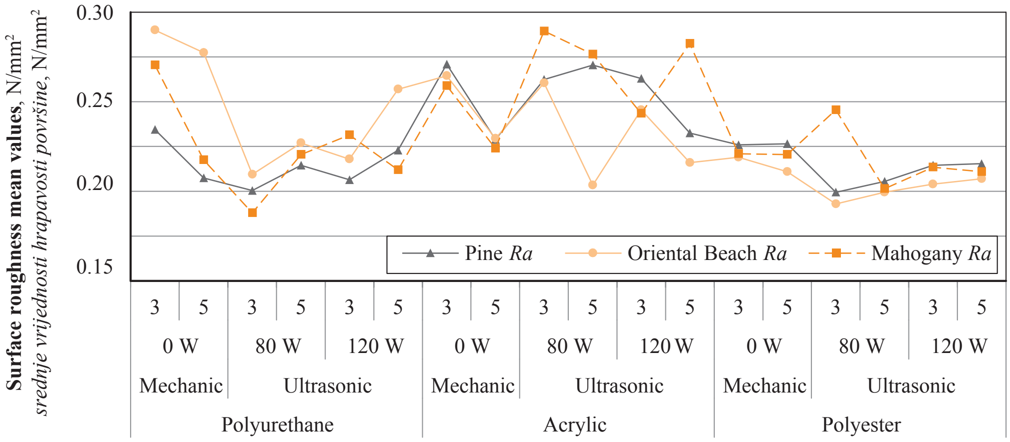

Figure 3 Mean values of roughness
Slika 3. Srednje vrijednosti hrapavosti površine

expected that components with homogeneous mixing will also have smoother surfaces. There was no statistical difference between wood species in terms of surface roughness. This result may be because the wooden test specimens were sanded very well before varnishing and because of sanding between the varnish layers one after the other during varnishing.

When the varnishes were compared in terms of surface roughness, it was seen that the best surface roughness value was obtained with polyester varnish. This may be due to the presence of filler chemicals in polyester varnish that have the ability to make a thicker layer. This may have resulted in the varnish layer being less affected by the raw wood surface roughness. When the mixing methods are compared in terms of surface roughness of the varnish layer, it is seen that ultrasound-assisted mixing performs better in general. The lowest performance was obtained with mechanical mixing for 3 minutes. This result can be interpreted as a positive contribution of ultrasound-assisted mixing, especially with 80 W. He *et al*. (2012) reported that 70 W ultrasonic power provided the best results among the 40, 70 and 100 W options for ultrasound-assisted mixing in composite metal alloys in homogeneous distribution.

3.3 Glossiness
3.3. Sjaj

The mean values of glossiness are given in Table 4 and are illustrated in Figure 4. To ascertain the glossiness for the coated samples, one measurement direction (parallel direction) was observed for the 60° measuring geometry. For coating wooden surfaces, 60° geometry is generally recommended (Salca *et al*., 2021), so the results of glossiness of this study are given based on 60°.

Considering the effects of the factors on the surface gloss, the highest gloss value was obtained on Scots pine / polyurethane varnish / ultrasound 80 W / 3 minutes (97.62). Meanwhile the lowest was observed on Eastern beech / polyester varnish / ultrasound stirring 120 W / 5 minutes (59.29).

When the wood species were compared in terms of surface glossiness performance, the ranking was Scots pine (84.61), mahogany (78.12) and Eastern beech (77.36). However, there was no statistically significant difference between mahogany and Eastern beech.

When varnishes were compared in terms of surface glossiness, it was seen that they were ranked as polyurethane (89.02), acrylic (82.52) and polyester

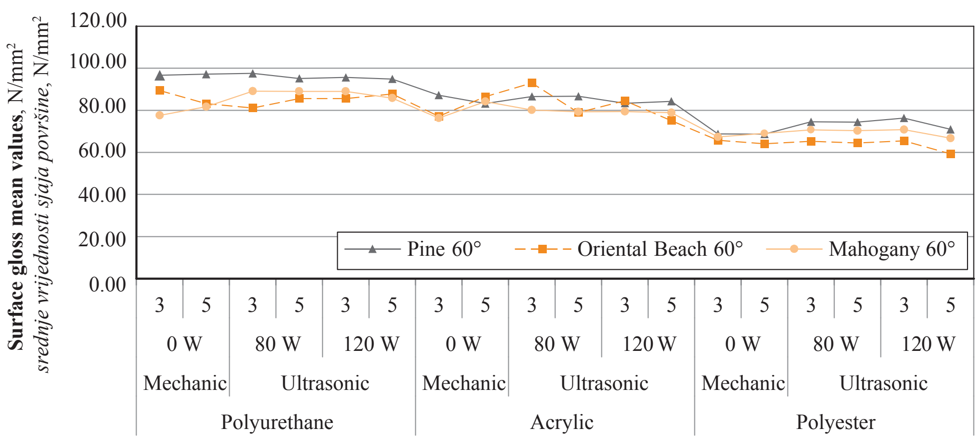

Figure 4 Mean values of surface glossiness
Slika 4. Srednje vrijednosti sjaja površine

(68.55). The high gloss values obtained from samples treated with polyurethane and acrylic varnishes, particularly on Scots pine, are consistent with the literature (Baysal *et al*., 2014; Keskin and Atar, 2008).

When comparing the effects of the mixing method on surface glossiness, the ultrasound-assisted mixing / 80 W / 3 minutes has the highest value (82.06). The lowest glossiness was observed in the ultrasound-assisted mixing / 120 W / 5 minutes (78.21).

During the study, it was observed that increasing the ultrasound wave power raised the temperature in the varnish mixture. It is estimated that this temperature increase accelerates the curing process of the varnishes and negatively affects the gloss of the dry varnish layer.

4 CONCLUSIONS
4. ZAKLJUČAK

The effects of ultrasound-assisted and mechanical mixing method in the varnish component mixture on the surface adhesion resistance, surface roughness and surface glossiness were investigated. The results of this study can be used to choose the finest varnish-component mixing technique when making furnishings. The following is a presentation of the study's particular findings:

In this study, it was determined that Eastern beech and mahogany wood species were more successful in terms of adhesion resistance than Scots pine wood. Scots pine wood, on the other hand, is superior in glossiness compared to other wood species. Meanwhile, it was determined that there was no difference between the three wood species in terms of surface roughness.

In terms of adhesion resistance performance of varnishes, the ranking was as follows: polyurethane, polyester and acrylic. Polyester achieved the best surface roughness performance, followed by polyurethane and acrylic. In terms of surface gloss performance of varnishes, polyurethane achieved the best results, followed by acrylic and polyester.

Between stirring methods, in general, the ultrasound-assisted 80-watt mixing method improved the varnish layer properties. The mixing time of 3 minutes, which is the lower version of ultrasound, was superior to the time of 5 minutes in surface adhesion and surface gloss, while the times of 3 and 5 minutes in surface roughness were in the same group.

Many variables determine the results. In most cases, it is difficult to say which one is the most influential. As a result, ultrasound-assisted / 80 watt / 3 minutes of mixing can be recommended for varnish component mixing. However, to further strengthen this opinion, for future studies, it would be beneficial to test the mechanical and ultrasonic mixing methods with the varnish component mixture applied on glass plates because the surface roughness of timber has a major impact on the binding quality. The area for mechanical bonding between the coating and the timber base grows as the surface roughness rises, and as a result, the adhesion strength also grows (Vitosyte *et al*., 2012). By applying varnish on glass plates, the effect of mixing methods can be seen more clearly by eliminating the effects of wood material properties on the adhesion, roughness, and gloss of varnishes. In addition, ultrasonic and mechanical mixing methods should also be tested with a specific and hybrid method as suggested by prior research, based on mechanical swaying alone and mechanical shaking combined with ultrasonic irradiation (Effendi and Wulandari, 2019).

Acknowledgements – Zahvala

This document was created using the results of the project "Determination of the Effects of Ultrasound-Assisted Mixing Method in Varnish-Component Mixture on Layer Quality". This project is supported by Scientific and Technological Research Council of Turkey (TÜBİTAK) (Project number: 120O793).

5 REFERENCES
5. LITERATURA

1. Baysal, E.; Dizman Tomak, E.; Ozbey, M.; Altin, E., 2014: Surface properties of impregnated and varnished Scots pine wood after accelerated weathering. Coloration Technology, 130 (2): 140-146. https://doi.org/10.1111/cote.12070
2. Baykan, İ.; Kilic, Y.; Bakır, K., 2000: Surface treatments in the furniture industry, KOSGEB small scale industry development and support administration, Ankara (in Turkish).
3. Berkel, A., 1972: Wood Technology, 2. Volume. Istanbul University publications, No: 1745/183, 246-247 (in Turkish).
4. Budakci, M.; Sonmez, A., 2010: Determining adhesion strength of some wood varnishes on different wood surfaces. Journal of The Faculty of Engineering and Architecture of Gazi University, 25 (1): 111-118.
5. Chen, J.; Yin, X.; Wang, H.; Ding, Y., 2018: Evaluation of durability and functional performance of porous polyurethane mixture in porous pavement. Journal of cleaner production, 188, 12-19. https://doi.org/10.1016/j.jclepro.2018.03.297
6. Cheng, Y.; Wang, Q., 2022: Enhancement of green tires performance through ultrasound-assisted mixing. Polymers, 14 (3): 418. https://doi.org/10.3390/polym14030418
7. Effendi, A. J.; Marita, W., 2019: The impact of ultrasonic power and time for the removal of Total Petroleum Hydrocarbon from low permeability contaminated soils. In: Proceedings of the 1st International Conference on Environmental Sciences (ICES2018). West Sumatra, Indonesia.
8. Ghofrani, M.; Mirkhandouzi, F. Z. & Ashori, A., 2016: Effects of extractives removal on the performance of clear varnish coatings on boards. Journal of Composite Materials, 50 (21): 3019-3024.
9. Gurleyen, L., 2021: Effects of artificial weathering on the color, gloss, adhesion and pendulum hardness of UV sys-

tem parquet varnish applied to Doussie (*Afzelia africana*) wood. BioResources, 16 (1): 1616-1627. https://doi.org/10.15376/biores.16.1.1616-1627
10. He, T.; He, Y.; Li, H.; Fan, Y.; Yang, Q.; He, Z., 2018: A comparative study of effect of mechanical and ultrasound agitation on the properties of pulse electrodeposited Ni-W/MWCNTs composite coatings. Journal of Alloys and Compounds, 743: 63-72. https://doi.org/10.1016/j.jallcom.2018.01.368
11. Halacinski, B.; Kotlicka, E.; Latuszek, A., 1994: Ultrasonic mixer for paints and emulsions. In: Proceedings of IEEE Ultrasonics Symposium. Cannes, France. https://doi.org/10.1016/j.jallcom.2018.01.368
12. Karamanoğlu, M.; Kesik, H. İ., 2021: Factors affecting some properties on surface of thermowood material applied with water-based varnishes modified with nanoparticles. Technology of Forest Products CERNE, 27. https://doi.org/10.1590/01047760202127012886
13. Keskin, H.; Atar, M., 2008: Impact of impregnation chemical on surface glossiness of synthetic, acrylic, polyurethane and water□based varnishes. Journal of Applied Polymer Science, 108 (5): 3361-3369. https://doi.org/10.1002/app.27981
14. Kilic K.; Sogutlu C., 2023: Varnish adhesion strength in natural aged wood material. Journal of Polytechnic, 26 (2): 847-854. https://doi.org/10.2339/politeknik.1072314
15. Kretschmann, D. E., 2010: Mechanical properties of wood. In: Wood handbook: wood as an engineering material. Chapter 5: General technical report FPL; GTR-190. Madison, WI: US Dept. of Agriculture, Forest Service, Forest Products Laboratory, pp. 1-46.
16. Kim, Y. U.; Wang, M. C., 2003: Effect of ultrasound on oil removal from soils. Ultrasonics 41 (7): 539-542. https://doi.org/10.1016/S0041-624X(03)00168-9
17. Masri, A. N.; Abdul Mutalib, M. I.; Aminuddin, N. F.; Lévêque, J.-M., 2018: Novel SO_3H-functionalized dicationic ionic liquids – A comparative study for esterification reaction by ultrasound cavitation and mechanical stirring for biodiesel production. Separation and Purification Technology, 196: 106-114. https://doi.org/10.1016/j.seppur.2017.08.061
18. Li, C. T.; Ye, X. J., 2018: The effect of hard segment structure on the operating performance and mechanical properties of polyurethane elastomers. Polyurethane Ind., 33: 41-43.
19. Nejad, M.; Cooper, P.; Landry, V.; Blanchet, P.; Koubaa, A., 2015: Studying dispersion quality of nanoparticles into a bio-based coating. Progress in Organic Coatings, 89: 246-251. https://doi.org/10.1016/j.porgcoat.2015.09.006
20. Niemczewski, B., 2007: Observations of water cavitation intensity under practical ultrasonic cleaning conditions. Ultrasonics Sonochemistry, 14: 13-18. https://doi.org/10.1016/j.ultsonch.2005.11.009
21. Ozdemir, T.; Hiziroglu, S.; Kocapınar, M., 2015: Adhesion strength of cellulosic varnish coated wood species as function of their surface roughness. Advances in Materials Science and Engineering, 2015: 525496. https://doi.org/10.1155/2015/525496
22. Salca, E. A.; Krystofiak, T.; Lis, B.; Hiziroglu, S., 2021: Glossiness evaluation of coated wood surfaces as function of varnish type and exposure to different conditions. Coatings, 11 (5): 558. https://doi.org/10.3390/coatings11050558
23. Shutliov, M.; Alferieff, R.; Beyer, T., 1990: Fundamental physics of ultrasounds. Journal of the Acoustical Society of America, 88 (6): 2906. https://doi.org/10.1121/1.399657
24. Sogutlu, C.; Nzokou, P.; Koc, I.; Tutgun, R.; Dongel, N., 2016: The effects of surface roughness on varnish adhesion strength of wood materials. Journal of Coatings Technology and Research, 13: 863-870. https://doi.org/10.1007/s11998-016-9805-5
25. Sonmez, A.; Budakci, M.; Bayram, M., 2009: Effect of wood moisture content on adhesion of varnish coatings. Scientific Research and Essays, 4 (12): 1432-1437.
26. Stephen, G.; Moore, K. R.; Malone, J.; McGarvey, C., 2003: Coating production systems and methods with ultrasonic dispersion and active cooling. US7083322B2 PATENT.
27. Vitosyte, J.; Ukvalbergiene, K.; Keturakis, G., 2012: The effects of surface roughness on adhesion strength of coated ash (*Fraxinus excelsior* L.) and birch (*Betula* L.) wood. Materials Science, 18 (4): 347-351. https://doi.org/10.5755/j01.ms.18.4.3094
28. Zanghellini, B.; Knaack, P.; Schörpf, S.; Semlitsch, K. H.; Lichtenegger, H. C.; Praher, B.; Omastova, M.; Rennhofer, H., 2021: Solvent-free ultrasonic dispersion of nanofillers in epoxy matrix. Polymers, (13) 2: 308. https://doi.org/10.3390/polym13020308
29. Shutilov, V. A.; Alferieff, M. E., 2020: Fundamental physics of ultrasound. CRC Press.
30. ***AkzoNobel, 2023: Paint defects (online). https://slideplayer.biz.tr/slide/1956766/ (in Turkish) (Accessed: May 25, 2023).
31. ***ASTM D3023:1998 Standard Practice for Determination of Resistance of Factory Applied Coatings on Wood Products to Stains and Reagents. ASTM International: West Conshohocken, PA, USA, 1998.
32. ***ASTM D4541-22:2022 Standard Test Method for Pull-Off Strength of Coatings Using Portable Adhesion Testers. ASTM International: West Conshohocken, PA, USA, 2022.
33. ***ASTM D523-08:2008 Standard test method for specular gloss. West Conshohocken, PA, USA, 2008.
34. ***DIN 4768:1990 Determination of values of surface roughness parameters Ra, Rz, Rmax using electrical contact (stylus) instruments, concepts and measuring conditions. Deutsches Institut fur Normung E.V. (DIN) Germany.
35. ***ISO 2813:2014 Paints and Varnishes – Determination of Gloss Value at 20 Degrees, 60 Degrees and 85 Degrees. International Organization for Standardization: Geneva, Switzerland.
36. ***Megep, 2012: Furniture and Interior Design. Top coat varnish. Republic of Turkey Ministry of National Education, Ankara (in Turkish).
37. ***TS 2470:1976 Wood – Sampling Methods and General Requirements for Physical and Mechanical Tests. Turkish Standard Institute, Ankara, Türkiye.

Corresponding address:

Assoc. Prof. MEHMET YENİOCAK
Mugla Sitki Kocman University, Faculty of Technology, Department of Woodworking Industrial Engineering, Mugla, TURKEY, e-mail: myeniocak@mu.edu.tr

Erwin M. Schau, Eva Prelovšek Niemelä*[1]

A Benchmark for a New Nearly Zero Energy Wooden Building in Europe

Referentna vrijednost za novu drvenu zgradu s gotovo nultom potrošnjom energije u Europi

ORIGINAL SCIENTIFIC PAPER
Izvorni znanstveni rad
Received – prispjelo: 31. 5. 2023.
Accepted – prihvaćeno: 12. 1. 2024.
UDK: 630*83
https://doi.org/10.5552/drvind.2024.0121

ABSTRACT • *To mitigate dangerous climate change, a drastic reduction of CO_2 emissions is needed by 2030. Buildings contribute significantly to emissions, with the use phase of existing buildings being responsible for the majority of energy consumption. In addition, environmental problems associated with the production of raw materials, construction, and the end of life of buildings are serious concerns that require urgent solutions. Life cycle assessment (LCA) and the EU-recommended Environmental Footprint (EF) are widely accepted tools to measure environmental impacts throughout a product life cycle. However, assessing the environmental performance of wooden buildings remains a challenge. This study presents a benchmark for an average new European wooden building fulfilling the European nearly Zero Energy Building (nZEB) requirement. The benchmark utilizes the recommended EU EF impact categories with normalization and weighting, allowing for easy and quick comparisons. The results communicate the average environmental impact per square meter of floor area over one year. This benchmark is a suitable comparison point for new wooden building designs and is used as an effective tool for architects and designers during the initial planning stages of wooden buildings. By using this benchmark, the environmental performance of the building can be improved, and the communication and interpretation of LCA results can be facilitated for customers and other relevant stakeholders.*

KEYWORDS: *benchmark; nearly zero energy building (nZEB); life cycle assessment (LCA); wood construction; environmental footprint*

SAŽETAK • *Kako bi se ublažile opasne klimatske promjene, do 2030. godine potrebno je drastično smanjiti emisiju CO_2. Tim emisijama znatno pridonose i zgrade, pri čemu je korištenje postojećim zgradama odgovorno za većinu potrošnje energije. Osim toga, ekološki problemi povezani s proizvodnjom sirovina, gradnjom i krajem životnog vijeka zgrada ozbiljni su problemi koji zahtijevaju hitna rješenja. Procjena životnog vijeka (LCA) i ekološki otisak proizvoda (EF) koji preporučuje EU široko su prihvaćeni alati za mjerenje utjecaja na okoliš tijekom njihova životnog vijeka. Međutim, procjena ekološke učinkovitosti drvenih zgrada ostaje izazov. Ovom je studijom predstavljena prosječna nova europska drvena zgrada referentne vrijednosti koja ispunjava europski zahtjev za zgradu gotovo nulte energije (nZEB). Za zgradu referentne vrijednosti primjenjuju se preporučene EU EF kategorije utjecaja s normalizacijom i ponderiranjem, što omogućuje jednostavne i brze usporedbe. Rezultati pokazuju prosječan utjecaj zgrade na okoliš po četvornome metru podne površine tijekom jedne godine. Zgrada referentne vrijednosti prikladna je točka za usporedbu drvenih zgrada novog dizajna i služi kao učinkoviti alat za arhitekte*

* Corresponding author
[1] Authors are researchers at InnoRenew CoE, Izola-Isola, Slovenia. https://orcid.org/0000-0002-1806-8658; https://orcid.org/0000-0003-2069-4428

i dizajnere tijekom početnih faza planiranja drvenih zgrada. Primjerom zgrade referentne vrijednosti može se poboljšati ekološki učinak novih zgrada a korisnicima i drugim relevantnim sudionicima olakšati komunikacija i tumačenje LCA rezultata.

KLJUČNE RIJEČI: *referentna vrijednost; zgrada gotovo nulte energije (nZEB); procjena životnog vijeka (LCA); drvena konstrukcija; ekološki otisak*

1 INTRODUCTION
1. UVOD

The Intergovernmental Panel on Climate Change (IPCC) recommends in their report *Global Warming of 1.5 °C* a drastic reduction of carbon dioxide (CO_2) emissions. This means roughly halving the CO_2 emissions from approximately 40+ billion tonnes today to 20 billion tonnes in the year 2030 and reaching zero-emission or net uptake of CO_2 by the year 2050 to hinder dangerous climate change (IPCC, 2018). Accordingly, among others, the European Commission has set tough policy goals for reducing global warming gases (GHG) like CO_2 (EU 2018/773).

In 2019, the Intergovernmental Science-Policy Platform on Biodiversity and Ecosystem Services (IPBES) published a report stating that nature, which is vital for all life on Earth, is deteriorating worldwide (Diaz *et al*., 2019). In addition, bad air quality has a negative impact on health, life quality and length of life. Alone in the European Union, 400 000 people died each year prematurely because of the polluted air they breathe (EEA, 2019).

Part of these threats to nature and people are caused by buildings through their life cycle, with the raw material extraction, production of building materials, heating and cooling of air and water in the long use phase, and waste at the end of life of the buildings. According to the European Commission, the construction industry accounts for 15 % of all greenhouse gas emissions (European Commission, 2016). During their use phase, buildings use 80 % of the cradle-to-grave energy consumption (Lavagna *et al*., 2018), which contributes significantly to air pollution and other environmental impacts stemming from energy sourcing, distribution and transformation.

While energy consumption during the use phase is predicted to decrease as efficient buildings, like zero and near-zero energy buildings (nZEB), become more common, climate change and other environmental problems from the production of raw materials, construction and end-of-life remain serious concerns that need to be solved urgently. This calls for a lifecycle-based approach, taking into account the raw material extraction and production phase which need to be controlled when the buildings are made with more material to increase energy efficiency to evaluate the potential environmental consequences of a construction.

During the trial period of the EU Environmental Footprint initiative between 2013 and 2018, a mean reference point (average benchmark) proved highly beneficial for various categories of goods (Gül *et al*., 2015; Guiton and Benetto, 2018; Schau, 2019) in aiding the comprehension of outcomes derived from the life cycle assessment of products within their respective product groups.

Bejo (2017) performed a review investigating the operational energy and energy embodied in wood constructions, compered them to other materials and concluded that wood is significantly better in terms of energy efficiency and greenhouse gas emissions (Bejo, 2017).

Sinha *et al*. (2012) investigated how sustainable development relates to green buildings. They concluded that advance in the field of "green" buildings requires LCA analysis which should be applied to all product stages, from primary processing and use to disposal, and call for a multidisciplinary approach that involves scientists from engineering, material science, forestry, environmental science, architecture, marketing, and business (Sinha *et al*., 2012).

Menezes *et al*. (2019) reviewed 43 papers that integrated benchmark techniques with LCA results to improve communication and found that benchmark techniques for product oriented LCAs work best if combined with another harmonization strategy like product category rules as done for the EU Product Environmental Footprint (PEF). Ferrari *et al*. (2019) developed a sustainability benchmark for a building material (ceramic tiles) and integrated life cycle costing (LCC), LCA and Social LCA (S-LCA), which gives companies in this product group the possibility to integrate sustainability perspectives into their strategies and operation. Aschenback *et al*. (2018) created an LCA model of Life Cycle Inventory (LCI) data from 12 prefab timber house manufacturers focusing on the A1-A5 modules (Figure 4). The manufacturing of building materials (module A1) accounted for the highest impacts, while approximately 30 % of the Global Warming Potential (GWP) and Acidification Potential (AP) impacts were attributed to the prefabrication of building elements, their transportation, and processes at the construction site (A4-A5).

Lützkendorf *et al*. (2012) described a benchmark for buildings used in Germany. This system was built on the established criteria and sustainability performance of office buildings and then developed further for residential buildings with the support of the German Building Ministry. The benchmark covers large residential multi-family buildings with 6-100 flats of existing representative building types (Lützkendorf *et al*., 2012). Hollberg *et al*. (2019) investigated how top-down and bottom-up benchmarks can help designers and constructors in the early phase to evaluate if a building is „climate-friendly" and how the environmental performance can be improved. Spirinckx *et al*. (2019) gave recommendations on benchmarks for office buildings. Based on an EU Product Environmental Footprint of two office buildings, testing of benchmarks and classes of performance were performed. The results focused on the methodological aspects rather than on absolute values.

The potential (historical) environmental impact of current residences in Europe were presented by Lavagna *et al*. (2018) through their LCA study on typical dwellings. This publication is based on a comprehensive report by Baldassarri *et al*. (2017), that focuses on existing buildings in the EU and provides an average environmental footprint of a building in four different geographical zones based on the *Basket of Products* approach (cf. Notarnicola *et al*., 2017; European Commission, 2012). However, a considerable share of the buildings assessed were older than 70 years (Lavagna *et al*., 2018).

With the revised Energy Performance in Buildings Directive 2018/844 (EU, 2018), the European Union has introduced a stricter policy for buildings use of energy. Therefore, it is expected that the environmental impacts of buildings in Europe are decreasing in light of the actions taken to reduce the climate change.

Therefore, to summarize, we believe that a benchmark for to-be-constructed buildings is needed. It could be useful in the early planning phase of new buildings when changes and environmental optimization can still be done for a reasonable cost (Fabricky, 1991). In this work, an environmental benchmark for a near-zero energy wooden residential building (nZEB) is provided for new buildings built after 2020.

2 DATA AND METHOD
2. PODATCI I METODE

2.1 Background data for a typical (European average) wooden single-family house
2.1. Dosadašnji podatci za tipičnu (prosječnu europsku) drvenu obiteljsku kuću

To design a European average reference building, the following elements have to be considered: 1) the market situation in Europe regarding wooden houses (Currently, Scandinavia, Germany and the UK are the largest markets for building with wood.); 2) climate conditions, which are important for the level of insulation of the house and the energy used for heating in the use phase; and 3) the different levels of the energy requirement which is different in each country.

Based on market-based statistics from Eurostat (2019a), supplemented with national data where necessary (SSB, 2019), Table 1 contains apparent consumption of wood-based residential housing by country in Europe. The apparent consumption (Sala *et al.*, 2019) is what is consumed in each country and calculated based on production value plus import minus export (EUR). The apparent consumption is used for weighting the climate data and energy requirement data of the countries investigated to come to an average wooden residential building.

The diverse climates across European countries result in varying heating demands for residential buildings. Our assessment of country-level climatic conditions relies on the utilization of heating degree days (hdd), which is used as a metric for quantifying the annual heating requirements (Eurostat, 2019b; Enova, 2019) and correlates extremely well with the use of energy, like fuel wood, for heating (Petrović, 2021). According to Table 1, the (apparent consumption of wood-based residential housing weighted) average of heating degree days for European countries stands at 3500 hdd. To better reflect climate change in the analysis, we have utilized a 10-year dataset for climate conditions instead of the conventional 30-year span. This decision was motivated by two factors: Firstly, acquiring prefabricated building statistics spanning 30 years proved challenging (for data weighting). Secondly, and more significantly, climate patterns are shifting towards warmer conditions, leading to an observable decrease in heating degree days. For instance, the reference climate in Germany, during the period of 2008-2017, experienced 3000 heating degree days, which is 500 heating degree days fewer (i.e., warmer) compared to the reference data from 20 years ago (3500 hdd).

Each country set its own requirement for a nearly Zero Energy Building (nZEB), such that this is influenced not only by the climate but also by political ambitions. In this study, the maximum allowed energy use for new buildings (nZEB) in different countries is shown in Table 1 (European Commission, 2016; BPIE, 2015; D'Agostino *et al*., 2019; Kurnitski and Ahmed, 2018; NRW ÖkoZentrum, 2019; Schau *et al*., 2022).

The weighted average maximum energy allowed (nearly zero energy building) is 67.5 kWh/(m^2 year).

2.2 Design of a typical European (average) wooden single-family building
2.2. Projekt tipične europske (prosječne) drvene obiteljske kuće

Using the average climatic conditions (derived from Table 1, encompassing 3500 degrees heating days, akin to the approximate climate in regions such

Table 1 Apparent consumption (million EUR) of prefabricated wooden buildings, heat demand expressed as heating degree days, and maximum energy use for new buildings (nZEB) from 2021 in different countries
Tablica 1. Prividna potrošnja (u milijunima eura) montažnih drvenih zgrada, potražnja topline izražena kao stupanj dana grijanja i maksimalna potrošnja energije za nove zgrade (nZEB) od 2021. u različitim državama

Country *Država*	**Consumption**[1], million EUR *Potrošnja*[1], milijuni EUR	**Heat demand**[2] heating degree days/year *Potreba za toplinom*[2], *stupanj dana grijanja/godina*	**Max energy use, kWh/(m²·year)]**[3] *Maksimalna potrošnja energije, kWh/(m²·godina)*
Austria	583	3482	160.0
Belgium	56	2697	45.0
Bulgaria	5	2494	40.0
Croatia	11	2281	37.0
Cyprus*	1	691	100.0
Czechia	27	3309	57.5
Denmark	121	3244	20.0
Estonia	23	4224	75.0
Finland	414	5466	130.0
France	231	2380	52.5
Germany	1 658	3053	48.3
Greece	2	1546	57.5
Hungary	10	2668	61.0
Ireland	42	2821	45.0
Italy	615	1875	57.5
Latvia	5	4046	95.0
Lithuania	65	3854	77.5
Luxemburg	7	2906	57.5
Malta*	0.1	468	40.0
Netherlands	150	2721	57.5
Norway	544	4113	97.5
Poland	4	3370	67.5
Portugal	14	1201	57.5
Romania	30	2924	155.0
Slovakia	10	3173	43.0
Slovenia	25	2785	47.5
Spain	143	1742	57.5
Sweden	1 126	5221	52.5
United Kingdom	1 226	3033	44.0

*Cyprus and Malta are the only countries in the table where the need for cooling in summer (expressed as cooling degree days - cdd) are higher than the need for heating in winter. E.g. Cyprus had 710 cdd and Malta 618 cdd, while e.g. Greece had 343 cdd and Spain 243 cdd (Eurostat, 2019b). The focus of this article is on heating (Quintana-Gallardo *et al*., 2022). / *Cipar i Malta jedine su zemlje u tablici u kojima su potrebe za hlađenjem ljeti (izražene kao stupnjevi dana hlađenja – cdd) veće od potreba za grijanjem zimi. Cipar je, primjerice, imao 710 cdd, a Malta 618 cdd, dok je npr. Grčka imala 343 cdd, a Španjolska 243 cdd (Eurostat, 2019b). Fokus ovog članka je na grijanju (Quintana-Gallardo et al., 2022).*; [1](sources: Eurostat, 2019a; SSB, 2019); [2](sources: Eurostat, 2019b; Enova, 2019) (average per year in the period 2008-2017); [3](sources: European Commission, 2016; BPIE 2015; D'Agostino *et al*., 2019; Kurnitski and Ahmed, 2018; NRW ÖkoZentrum, 2019; Schau *et al*., 2022).

as Austria, South Germany, Slovenia, and Italy near the Alps) and energy demands (average maximum nZEB requirement), the initial stages of designing a wooden detached house were made as a reference model. The architectural layout of the house was based on prevalent blueprints and structures commonly offered by prefabricated wooden house construction companies in Austria and Slovenia. The benchmark dwelling encompasses three bedrooms, a living room, a cabinet, a toilet, a utility room, a staircase, and a bathroom, encompassing a total area of 100 m². The external dimensions of the house are 9.6 m × 6.7 m, with a maximum height of 7.72 m. The house boasts a sloping roof with an inclination of 35° and a 1.0 m overhang. The wooden windows (featuring triple glazing) and doors have a U_w value of 0.8 W/m²K. The foundation of the house is made of 25 cm thick concrete slab. The walls are constructed using 8/16 cm wooden profiles, with stone wool insulation filling the gaps and an additional 10 cm layer of stone wool on the outer side, covered with a finishing plaster. The roof structure also consists of 8/16 cm wooden profiles, with mineral wool insulation in-between and an additional 10 cm layer on top. The roof covering is comprised of corrugated fibre cement roof tiles. The interior floors are adorned with parquet flooring on a floating screed, while ceramic tiles are employed in the sanitary areas. Figure 1 shows the east façade of the building. Figure 2 shows a section draw-

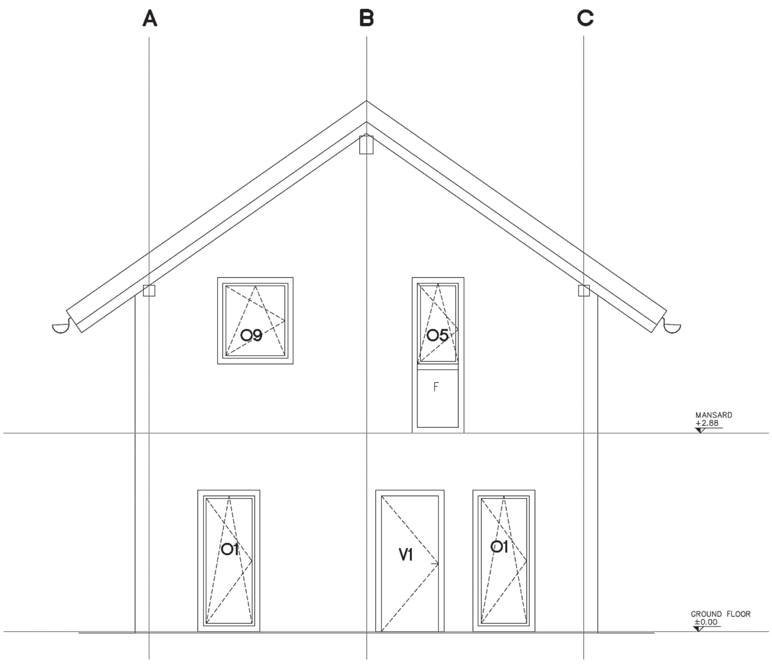

Figure 1 Drawing of east façade of benchmark house
Slika 1. Nacrt istočne fasade referentne kuće

ing of the house, while Figure 3 shows a schematic floor plan of the house. Further illustrations of the building can be found in Schau *et al*. (2022).

Once initial sketches were completed, a thorough assessment of the structural integrity of the edifice was conducted, resulting in necessary updates to the drawings. The composition of each building component was meticulously determined, and the U-values for the external enclosure were calculated using various online resources. Subsequently, an estimation of the house energy consumption was performed using a simplified building energy calculation method, specifically the Preliminary Passive House Planning tool (in German: *Passivhaus Vorprojektierung* - PHVP) (Feist *et al*., 2002), which is well-suited for the preliminary design stage. Given the building streamlined and compact design, with a deliberate avoidance of windows on the northern facade, the projected energy consumption (heat energy demand) was determined to be 26.9 kWh/m^{2}a. This value adheres to the nZEB requirement outlined in Table 1 for all countries, except Denmark, which imposes more stringent standards. Table 3 summarizes the single-family house with the main components and characteristics.

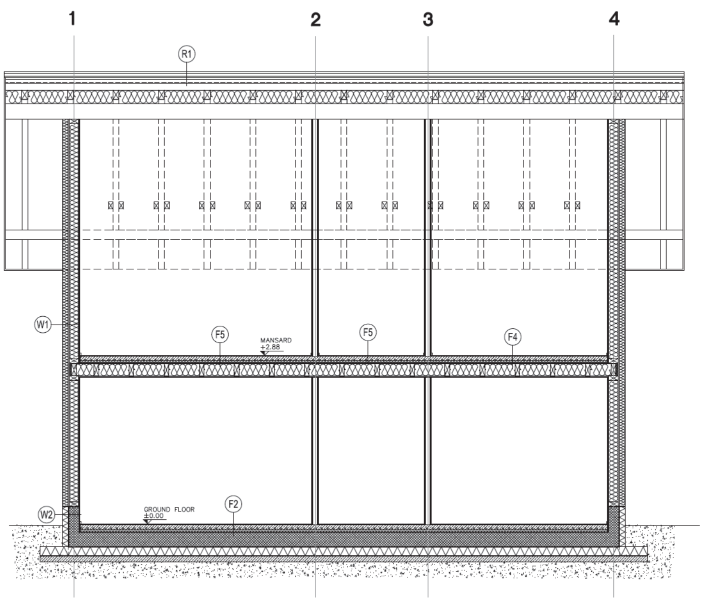

Figure 2 Drawing of section A – B of benchmark house
Slika 2. Prikaz presjeka A – B referentne kuće

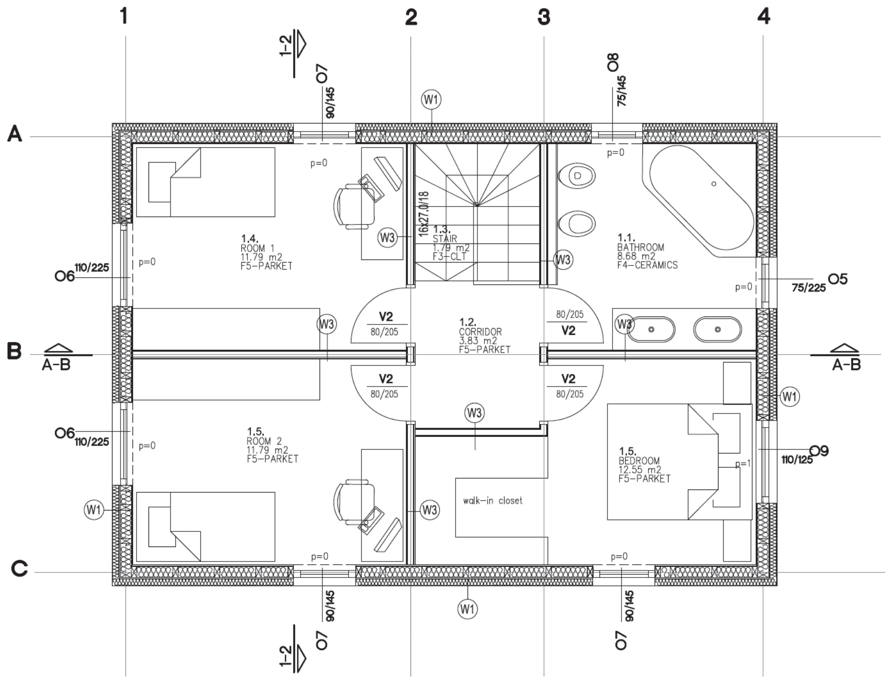

Figure 3 Drawing of the 1st floor of benchmark house
Slika 3. Prikaz prvog kata referentne kuće

3 LIFE CYCLE ASSESSMENT OF A TYPICAL (EUROPEAN AVERAGE) WOODEN SINGLE-FAMILY HOUSE
3. PROCJENA ŽIVOTNOG VIJEKA TIPIČNE (PROSJEČNE EUROPSKE) DRVENE OBITELJSKE KUĆE

3.1 Goal and scope
3.1. Cilj i opseg

The goal of conducting a life cycle assessment (LCA) for an average wooden single-family dwelling is to establish a benchmark that can serve as a reference point for the design of new wooden houses that aim to achieve near-zero energy consumption. This benchmark is intended to assist architects and designers in the early planning stages, when modification is still possible, to enhance the environmental performance of wooden buildings. Additionally, the LCA aims to facilitate the interpretation and communication of LCA outcomes to customers and other stakeholders involved in wooden construction. This is particularly valuable when comparing the environmental impact of various materials or building components, such as the facade.

The functional unit, which serves as the standard reference unit in LCAs, is defined as a single-family house with a projected lifespan of 100 years. This is a long time, but numerous existing wooden buildings that are centuries old (Hill *et al.*, 2022 for some examples) show that a 100-year service life is no problem with regular maintenance. Although our specific dwelling encompasses a living area of 100 m^2, the results are presented per square meter per year in accordance with the EN 15978:2011 and EN 15804:2012 standards, allowing for straightforward comparisons with LCA results from other building designs.

The system boundaries are cradle to grave, starting with the production of the raw materials, like seedling production (i.e. cultivation of plant seeds in a nursery) for trees and forest management for the wood products. The system ends with the final waste treatment of the waste from the deconstructed house, e.g. incinerated. In the case of landfill, the management of the landfill is included in the system boundaries (Module C: End of life). The system is divided into modules based on the EN 15978:2011 and EN 15804:2012 standards (Figure 4 and the Results section 4).

3.2 Life cycle inventory
3.2. Popis stavki koje se uzimaju u obzir pri procjeni životnog vijeka

The house only exists as a model, and therefore, only scenarios - (also for A1 to A3 modules) have been developed. The Modules A1-A3 are the best developed, where detailed drawings of the house have been used to calculate the life cycle inventory. The construction phase (A4-A5) has been calculated based on assumptions in Baldassarri *et al.* (2017) and Lavagna *et al.* (2018). The use stage is based on regular maintenance intervals of 30 and 50 years, resulting in one and two rounds of maintenance, following Baldassari *et al.* (2017) and Lavagna *et al.* (2018).

For the end-of-life and recycling of waste materials (Module C and D), a rather conservative approach is followed, including the transportation to the waste treatment centre (50 km), the treatment at the sorting

Table 2 Summary description of detached house
Tablica 2. Sažeti opis samostojeće kuće

Building typology *Tipologija zgrade*	**Detached house** *Samostojeća kuća*	**Insulation** *Izolacija*	**Mineral wool (10 + 16 cm)** *Mineralna vuna* (10 + 16 cm)
Number of floors *broj katova*	2	External walls finishes *završne obrade vanjskih zidova*	Plaster *gips*
Lifetime of the building, years / *životni vijek zgrade,* godine	100	Windows *prozori*	Wood frame, triple glassed *drveni okvir, trostruko staklo*
Climate *klima*	Moderate (average European) / *umjerena (prosječna europska)*	Roof insulation *izolacija krova*	Pitched, mineral wool (16 + 10 cm) / *nagib, mineralna vuna (16 + 10* cm*)*
Heating degree days *stupanj dana grijanja*	3500	Bottom floor insulation *izolacija donjeg kata*	(hard + soft) mineral wool (4 + 20 cm) *(tvrda + meka) mineralna vuna (4 + 20* cm*)*
Year of construction *godina gradnje*	After 2020 *nakon 2020.*	Roof finishes *izolacija krova*	Cement tiles *cementne pločice*
Model dwelling size, m^2 *veličina modela stana,* m^2	100	Internal walls *unutarnji zidovi*	Wood frame *drveni okvir*
Number of inhabitants *broj stanara*	Typically 2 – 4 (2.36*) *obično 2 – 4 (2,36*)*	Internal walls finishes *završne obrade unutarnjih zidova*	Plasterboard *gipsane ploče*
Internal height, m *unutarnja visina,* m	2.5	Flooring *podovi*	Ceramic tiles and wood *keramičke pločice i drvo*
Window-to-wall ratio *odnos prozora i zida*	0.21	U-value walls, W/(m²K) *U-vrijednosti zidova,* W/(m²K)	0.154**
Construction technology *tehnologija gradnje*	Light, dry assembly *lagana, suha montaža*	U-value roof *U-vrijednost krova*	0.132
Foundations *temelji*	Reinforced concrete *ojačani beton*	U-value windows *U-vrijednost prozora*	0.8 ***
Load bearing elements *nosivi elementi*	Timber frame *drveni okvir*	U-value bottom floor *U-vrijednost donjeg kata*	0.175
Floors (structure) *podovi (struktura)*	Timber frame + board *drveni okvir + ploča*	Heating energy consumption, kWh/(m^2·year) *potrošnja energije za grijanje,* kWh/(m^2·godina)	29.7
Stairs *stubišta*	Timber frame *drveni okvir*	Heating systems *sustavi grijanja*	Boiler and electricity *bojler i struja*
External walls *vanjski zidovi*	Timber frame *drveni okvir*		

*Statistical value based on dwelling size (100 m^2 and average floor occupancy in Europe) / *statistička vrijednost na temelju veličine stana (100* m^2 *i prosječna veličina poda u Europi)*
**Weighted average of the U-value for the walls / *ponderirani prosjek U-vrijednosti za zidove*
***Assumed U-Values; glass 0.7 and frame 1.0 as in PHVP 2.0 (Feist *et al.* 2002) / *pretpostavljene U-vrijednosti; staklo 0,7 i okvir 1,0 kao u PHVP 2.0* (Feist *et al*., 2002.)

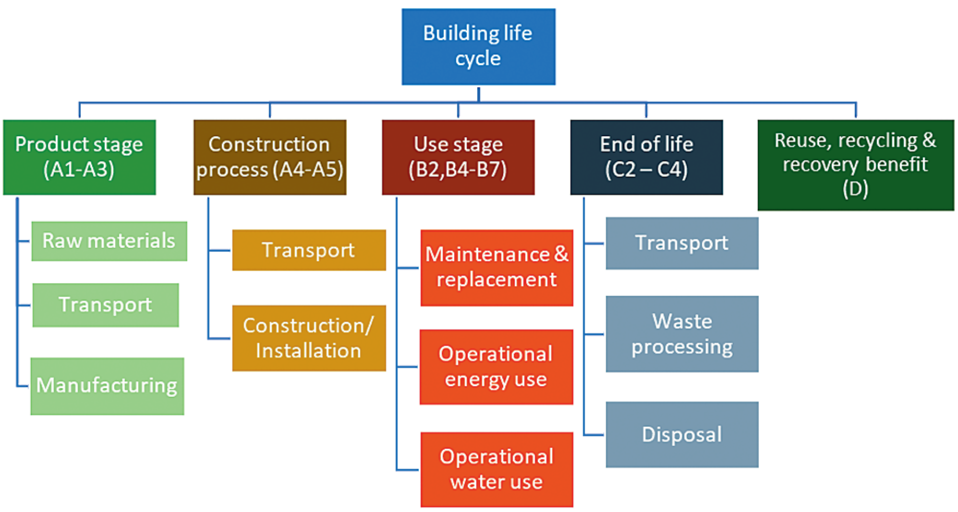

Figure 4 System divided into modules based on EN 15978:2011 and EN 15804:2012 standards
Slika 4. Sustav podijeljen na module prema standardima EN 15978:2011 i EN 15804:2012.

plant (machines for handling, electricity demand, emissions from handling) and any impacts of landfill disposal (residual inert masses), as well as impacts and benefits associated with recycling operations, according to Baldassarri *et al*. (2017) and Lavagna *et al.* (2018). After treatment, the sorted materials can be landfilled, incinerated or recycled (Lavagna *et al.*, 2018). In Module D, the benefits from the materials that are considered recycled (avoided production) and energy recovery (incineration with energy production) are reported.

Building services appliances like boilers, pipes, and ducts are excluded from the analysis.

The impact categories chosen are from the EU-recommended Environmental Footprint (EF) method, with 16 impact indicators. Version 2.0 (as available in SimaPro, Pre Consultants, 2019) was applied, with the following adjustment: The climate change indicator is further subdivided into three sub-indicators – fossil, biogenic and land use/transformation (see Results section). To better assess the different life cycle stages from a climate change perspective and to best fit the Ecoinvent database as implemented in SimaPro, we changed the climate change sub-indicator biogenic to -1 for the uptake of CO_2 (air raw) and the emissions of $CO_{2,biogenic}$ to +1 (which are both set to 0 in the EF method). This is in line with EN 15804:A2 (2019). For even more transparency on the climate change indicator, we also included two additional indicators; 1) *climate change, biogenic, emissions* (where biogenic CO, CO_2 and methane emissions are calculated and 2) *climate change, biogenic, uptake* (where biogenic CO_2 uptake, mainly by the growing tree in the sustainable managed forest is calculated. However, these changes and additions do not impact the results from cradle to grave, nor are they considered for the normalization and weighting.

Also, as the three toxicity impact categories directly taken over from the International Reference Life Cycle Data System (ILCD) impact categories are not considered stable, and newer background data for these are underway, we limit our results to the 13 other impact indicators.

Data collection, which is the starting point for the life cycle inventory, was based on the detailed architectural drawings of the house (see Figures 1-3). Table 2 shows an example of data collection for one element of the house, the external walls (W1), while Table 3 shows the external walls with ceramics in bathrooms (W1’). The full material lists can be found in Supplementary Material (SM) 2.

In the supplementary material, Table SM1 shows the complete area calculation based on the architectural drawings, and Table SM2 shows the calculations of all the material quantities.

Table 3 First example of data collection for external walls (W1)
Tablica 3. Prvi primjer prikupljanja podataka za vanjske zidove (W1)

W1 – exterior walls (dimension) / *W1 – vanjski zidovi (dimenzije)*	**Quantity** *Količina*	**Unit** *Jedinica*
Gypsum plasterboards (1.25 cm) / *gips-kartonske ploče (1,25 cm)*	131.32	m^2
OSB plate (1.2 cm) / *OSB ploče (1,2 cm)*	131.32	m^2
Stone wool between the load-bearing construction profiles (16 cm) *kamena vuna između nosivih građevnih profila (16 cm)*	21.01	m^3
Load-bearing construction profiles (8/16 cm) / *nosivi građevni profili (8/16 cm)*	5.25	m^3
Gypsum fibreboard (1.5 cm) / *gips-vlaknaste ploče (1,5 cm)*	131.32	m^2
Stone wool (10 cm) / *kamena vuna (10 cm)*	13.13	m^3
Reinforcing mortar, mesh and finishing plaster (0.6 cm) *ojačani mort, mrežica i završna žbuka (0,6 cm)*	131.32	m^2

Table 4 Second example of data collection for external walls with ceramics in bathrooms (W1‘)
Tablica 4. Drugi primjer prikupljanja podataka za vanjske zidove s keramikom u kupaonicama (W1‘)

W1‘ – exterior walls – ceramics in bathrooms (dimension) *W1’ – vanjski zidovi – keramika u kupaonicama (dimenzije)*	**Quantity** *Količina*	**Unit** *Jedinica*
Ceramic plates (1 cm) / *keramičke pločice (1 cm)*	10.73	m^2
Glue for ceramic plates (0.5 cm) / *ljepilo za keramičke pločice (0,5 cm)*	10.73	m^2
Hydro-isolating layer (0.3 cm) / *hidroizolacijski sloj (0,3 cm)*	10.73	m^2
Gypsum plasterboards (1.25 cm) / *gips-kartonske ploče (1,25 cm)*	10.73	m^2
OSB plate (1.2 cm) / *OSB ploče (1,2 cm)*	10.73	m^2
Stone wool between load bearing construction profiles (16 cm) *kamena vuna između nosivih građevnih profila (16 cm)*	1.72	m^3
Load bearing construction profiles (8/16 cm) / *nosivi građevni profili (8/16 cm)*	0.43	m^3
Gypsum fibreboard (1.5 cm) / *gips-vlaknaste ploče (1,5 cm)*	10.73	m^2
Stone wool (10 cm) / *kamena vuna (10 cm)*	1.07	m^3
Reinforcing mortar, mesh and finishing plaster (0.6 cm) *ojačani mort, mrežica i završna žbuka (0,6 cm)*	10.73	m^2

Table 5 Material quantities used for construction and maintenance (own data, c.f. supplementary materials) in addition to waste handling scenario (Baldassari *et al*., 2017; Lavagna *et al*., 2018)
Tablica 5. Količine materijala upotrijebljene za izgradnju i održavanje (vlastiti podatci, c.f. dodatak) uz scenarij rukovanja otpadom (Baldassari *et al*., 2017.; Lavagna *et al*., 2018.)

Material *Materijal*	**Quantities for construction** *Količine za gradnju,* kg	**Quantities for maintenance** *Količine za održavanje,* kg	**Waste handling scenario** *Scenarij postupanja s otpadom*		
			% to landfill *Postotak za odlagalište*	**% to incineration** *Postotak za spaljivanje*	**% to recycling** *Postotak za recikliranje*
Concrete / *beton*	57621	0	40		60
Gypsum / *gips*	9922	17186	85		15
Wood / *drvo*	12707	5354	35	34	31
Sawnwood / *piljeno drvo*	7419	821			
Window frame, wood *prozorski okvir, drvo*	1681	3122			
OSB	1502	0			
Fibreboard / *ploča vlaknatica*	423	987			
Glued laminated timber *lamelirana drvna građa*	1258	0			
Door, inner, wood *unutarnja vrata, drvo*	356	356			
Door, outer, wood-glass *vanjska vrata, drvo-staklo*	67	67			
Insulation, stone wool *izolacija, kamena vuna*	4355	10161	100		
Cement / *cement*	4342	2466	38.8		61.2
Gravel / *šljunak*	5858	0	40		60
Ceramic / *keramika*	1439	1923	40		60
Glass /*staklo*	1019	1892	90		10
Plastic / *plastika*	660	806	90		10
Steel / *čelik*	1286	41			100
Insulation, polystyrene *izolacija, stiropor*	288	673	100		
Glue / *ljepilo*	395	547	91.6	1.9	6.5
Bitumen / *bitumen*	591	0	50	50	
Copper / *bakar*	23	23			100
Aluminium / *aluminij*	12	0			100

Table 4 shows an overview of the materials used for construction and maintenance of the benchmark house in addition to the waste handling scenario applied for each of the different material groups. Based on common practice, we assumed that over the course of the building's 100-year lifetime, a maintenance interval of 30 years will necessitate two maintenance events. A 50-year maintenance interval will require only one. For some materials, typically the foundation and well protected structural component, no replacements during the 100-year service life is foreseen. Weathering exposed building components, like windows with frames of wood and glass sheets, are expected to be changed after 30 and 60 years and therefore, the quantities for the maintenance might be higher than that of the initial construction.

The life cycle inventory data and modelling follow closely the data and life cycle inventory modelling for the environmental impact of housing in Europe; *Consumer Footprint – Basket of Products indicator on Housing* (Baldassarri *et al*., 2017; Lavagna *et al*., 2018), where the Ecoinvent database v 3.2. was used. We use Ecoinvent version 3.5 (Ecoinvent Centre, 2018) with allocation, cut off by classification, as implemented in SimaPro v 9.0 (Pré Consultants, 2019) for the background data. Transport of materials for maintenance is assumed to be over a distance of 100 km and with a Euro 6 lorry (16 – 32 metric ton), while transport of waste is assumed to be over a distance of 50 km. Regarding energy for heating and warm water, we assumed a mix consisting of 25 % natural gas, 25 % biomass (e.g. wood pellets), 25 % electricity (e.g. heat pumps) and 25 % district heating (other than natural gas). This differs from a typical house, which usually relies on one or two energy sources. However, the use of four different energy sources is applicable for our model of an average wooden house used as a benchmark in this study. Heating with oil, a method still in use today, was not included in our considerations. This is due to its phase-out in several countries, such as Germany and Norway. Consequently, it is believed to hold minor relevance for new buildings.

4 RESULTS
4. REZULTATI

The findings highlighted in Table 5 provide a comprehensive overview of the assessment results, shedding light on the various stages that significantly contribute to the environmental impact of the house. Notably, the operational stage (Module B6 and B7) emerges as a dominant factor due to the substantial energy consumption required for heating and water usage. It is during this use-phase that the house's environmental footprint is most pronounced.

However, it is crucial to recognize that the impact categories related to land use and resource utilization, particularly minerals and metals, are primarily influenced by the earlier product stages (modules A1-A3 Production). This implies that decisions made during the production phase, such as the extraction and processing of raw materials, have lasting consequences on the overall environmental performance of the house.

In addition, maintenance activities (B2 and B4-B5) also have a significant influence on the environmental footprint results. The extensive utilization of materials over the 100-year maintenance period leads to notable impacts in terms of land use and resource consumption. Specifically, the management and transformation of land for obtaining wood products, sourced from forest management areas, contribute to the overall land use impacts observed.

Also, the *climate change* impact category is dominated by the operational use phase (especially the heating demand in Module B6) caused by fossil fuel and electricity for heating. For *climate change – biogenic*, the end-of-life (C2-C4) waste treatment with landfill and incineration are most important. The production phase (A1-A3) provides a considerable negative contribution to *climate change – biogenic*. We can see from the additional impact categories *biogenic, emissions* and *biogenic, uptake* that this is caused by the uptake of CO_2 from the atmosphere, mainly in the production of wood in the forest. These two additional impact categories reveal that in the Use phase, biogenic energy sources are used for heating and warm water (with CO_2 uptake when growing and release when incinerated, e.g. wood pellets). For the so-called recycling benefit in Module D, this is not a benefit for *climate change – biogenic* as recycled wood from the building is assumed to replace other wood that would have taken up CO_2 from the atmosphere. *Climate change – land use* and *land transformation*, are of minor importance for the benchmark house compared to the other climate change impact categories.

These findings underscore the importance of considering the entire life cycle of the house when assessing its environmental impact. By comprehensively evaluating the operational stage, product stages, and maintenance activities, a more holistic understanding of the house's sustainability performance can be obtained. This knowledge can inform decision-making processes and guide efforts toward reducing the environmental burdens associated with each stage, ultimately fostering the development of more environmentally responsible and resource-efficient housing solutions.

To come to the normalized results shown in Table 7, the characterized results are divided by the reference unit, that is, the impact for each impact category is di-

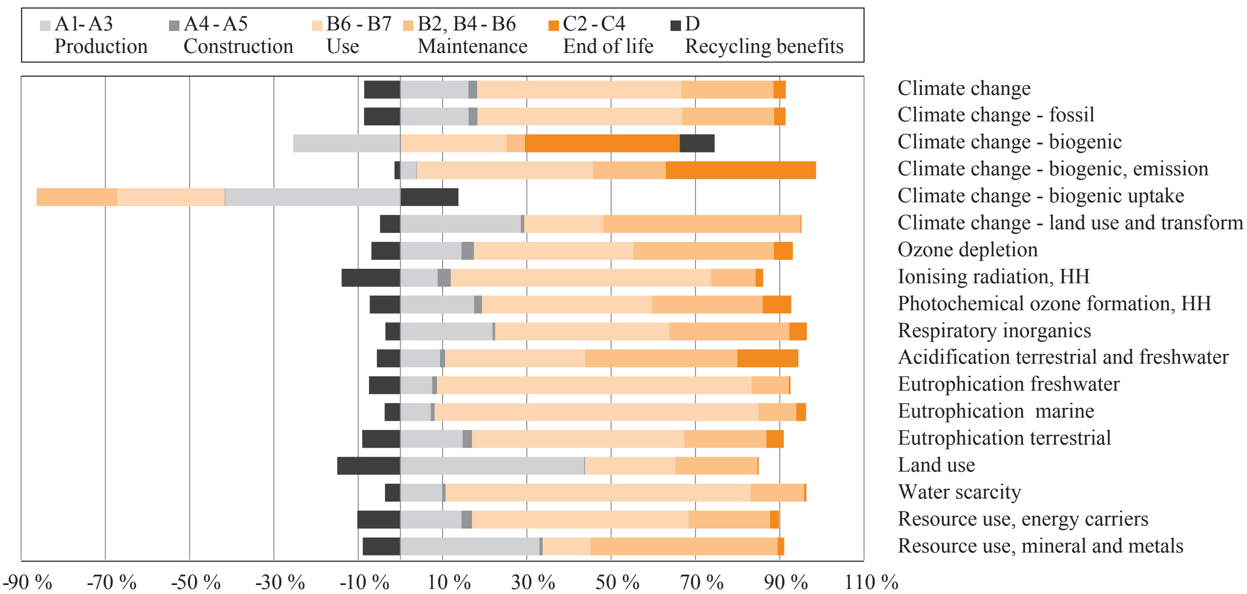

Figure 5 Characterized results showing contribution of different life cycles for impact indicators and sub-indicators investigated
Slika 5. Obrađeni rezultati koji pokazuju djelovanje različitih životnih ciklusa na ispitane pokazatelje utjecaja i podindikatore

Table 6 Characterized results (per m^2 and year) broken down to different stages/modules
Tablica 6. Obrađeni rezultati (po m^2 i godini) raščlanjeni na različite faze/module

Impact category *Utjecajne kategorije*	**Unit** *Jedinica*	**A1 - A3** **Production** *Proizvodnja*	**A4 - A5** **Construction** *Gradnja*	**B6-B7** **Use** *Uporaba*	**B2, B4-B6** **Maintenance** *Održavanje*	**C2 - C4** **End of life** *Kraj životnog vijeka*	**D** **Recycling benefits** *Prednosti recikliranja*	**Total** *Ukupno*
Climate change / *klimatske promjene*	kg CO_2 eq	2.99E+00	3.90E-01	8.98E+00	4.06E+00	5.36E-01	-1.59E+00	1.54E+01
Climate change – fossil *klimatske promjene – fosilne sirovine*	kg CO_2 eq	2.97E+00	3.88E-01	8.89E+00	4.00E+00	5.00E-01	-1.58E+00	1.52E+01
Climate change – biogenic (adapted) *klimatske promjene – biogene sirovine (prilagođene)*	kg CO_2 eq	-3.96E+00	6.66E-03	3.91E+00	6.76E-01	5.71E+00	1.29E+00	7.64E+00
Climate change - biogenic, emission *klimatske promjene – biogene sirovine, emisije*	kg CO_2 eq	6.05E-01	2.30E-02	6.70E+00	2.77E+00	5.72E+00	-2.22E-01	1.56E+01
Climate change - biogenic, uptake *klimatske promjene – biogene sirovine, apsorpcija*	kg CO_2 eq	-4.56E+00	-1.64E-02	-2.79E+00	-2.09E+00	-4.02E-03	1.51E+00	-7.96E+00
Climate change - land use and land, transformation *klimatske promjene – zemljišta i iskorištavanje zemljišta, transformacija*	kg CO_2 eq	1.92E-02	5.54E-04	1.26E-02	3.14E-02	1.90E-04	-3.25E-03	6.07E-02
Ozone depletion / *oštećenje ozonskog omotača*	kg CFC11 eq	2.60E-07	5.31E-08	6.79E-07	5.98E-07	8.10E-08	-1.23E-07	1.55E-06
Ionising radiation, HH / *ionizirajuće zračenje, HH*	kBq U^{235} eq	1.42E-01	5.04E-02	9.89E-01	1.69E-01	2.90E-02	-2.23E-01	1.16E+00
Photochemical ozone formation, HH *fotokemijsko stvaranje ozona, HH*	kg NMVOC eq	1.24E-02	1.34E-03	2.87E-02	1.87E-02	4.84E-03	-5.17E-03	6.08E-02
Respiratory inorganics *respiratorni anorganski utjecaji*	disease inc.	5.35E-07	1.60E-08	1.01E-06	6.96E-07	1.03E-07	-8.69E-08	2.27E-06
Acidification terrestrial and freshwater *zakiseljavanje kopna i slatkih voda*	mol H^+ eq	1.95E-02	2.52E-03	6.87E-02	7.50E-02	3.00E-02	-1.16E-02	1.84E-01
Eutrophication freshwater / *eutrofikacija slatke vode*	kg P eq	1.95E-04	2.94E-05	1.93E-03	2.28E-04	1.15E-05	-1.92E-04	2.20E-03
Eutrophication marine / *eutrofikacija mora*	kg N eq	3.23E-03	4.38E-04	3.45E-02	4.00E-03	1.06E-03	-1.68E-03	4.15E-02
Eutrophication terrestrial / *eutrofikacija kopna*	mol N eq	4.34E-02	6.67E-03	1.48E-01	5.74E-02	1.20E-02	-2.66E-02	2.41E-01
Land use / *upotreba zemljišta*	Pt	7.97E+02	4.07E+00	3.90E+02	3.57E+02	5.68E+00	-2.74E+02	1.28E+03
Water scarcity / *nestašica vode*	m^3 depriv.	1.06E+00	8.24E-02	7.69E+00	1.35E+00	6.02E-02	-3.89E-01	9.86E+00
Resource use, energy carriers *iskorištavanje resursa, nositelji energije*	MJ	4.13E+01	7.11E+00	1.46E+02	5.52E+01	6.05E+00	-2.91E+01	2.27E+02
Resource use, mineral and metals *iskorištavanje resursa, minerali i metali*	kg Sb eq	3.19E-05	7.82E-07	1.09E-05	4.29E-05	1.53E-06	-8.64E-06	7.95E-05

Table 7 Normalized results – Global 2010 (unitless per m² and year) broken down to different stages/modules
Tablica 7. Normalizirani rezultati – globalno u 2010. (bez jedinica po m² i godini) raščlanjeni na različite faze/module

Impact category *Utjecajne kategorije*	**A1 - A3** **Production** *Proizvodnja*	**A4 - A5** **Construction** *Gradnja*	**B6-B7** **Use** *Uporaba*	**B2, B4-B6** **Maintenance** *Održavanje*	**C2 - C4** **End of life** *Kraj životnog vijeka*	**D** **Recycling benefits** *Prednosti recikliranja*	**Total** *Ukupno*
Climate change *klimatske promjene*	3.86E-04	5.02E-05	1.16E-03	5.23E-04	6.91E-05	-2.05E-04	1.98E-03
Ozone depletion *oštećenje ozonskog omotača*	1.11E-05	2.27E-06	2.91E-05	2.56E-05	3.47E-06	-5.28E-06	6.63E-05
Ionising radiation, HH *ionizirajuće zračenje, HH*	3.36E-05	1.19E-05	2.34E-04	4.01E-05	6.87E-06	-5.29E-05	2.74E-04
Photochemical ozone formation, HH *fotokemijsko stvaranje ozona, HH*	3.06E-04	3.30E-05	7.06E-04	4.59E-04	1.19E-04	-1.27E-04	1.50E-03
Respiratory inorganics *respiratorni anorganski utjecaji*	8.41E-04	2.52E-05	1.59E-03	1.09E-03	1.62E-04	-1.37E-04	3.57E-03
Acidification terrestrial and freshwater *zakiseljavanje kopna i slatkih voda*	3.51E-04	4.54E-05	1.24E-03	1.35E-03	5.40E-04	-2.08E-04	3.32E-03
Eutrophication freshwater *eutrofikacija slatke vode*	7.63E-05	1.15E-05	7.56E-04	8.93E-05	4.50E-06	-7.53E-05	8.62E-04
Eutrophication marine *eutrofikacija mora*	1.14E-04	1.55E-05	1.22E-03	1.41E-04	3.75E-05	-5.94E-05	1.47E-03
Eutrophication terrestrial *eutrofikacija kopna*	2.45E-04	3.77E-05	8.36E-04	3.24E-04	6.79E-05	-1.50E-04	1.36E-03
Land use / *upotreba zemljišta*	5.97E-04	3.05E-06	2.93E-04	2.67E-04	4.25E-06	-2.05E-04	9.59E-04
Water scarcity / *nestašica vode*	9.23E-05	7.18E-06	6.71E-04	1.18E-04	5.25E-06	-3.39E-05	8.59E-04
Resource use, energy carriers *iskorištavanje resursa, nositelji energije*	6.33E-04	1.09E-04	2.24E-03	8.45E-04	9.27E-05	-4.46E-04	3.48E-03
Resource use, mineral and metals *iskorištavanje resursa, minerali i metali*	5.51E-04	1.35E-05	1.89E-04	7.42E-04	2.64E-05	-1.49E-04	1.37E-03

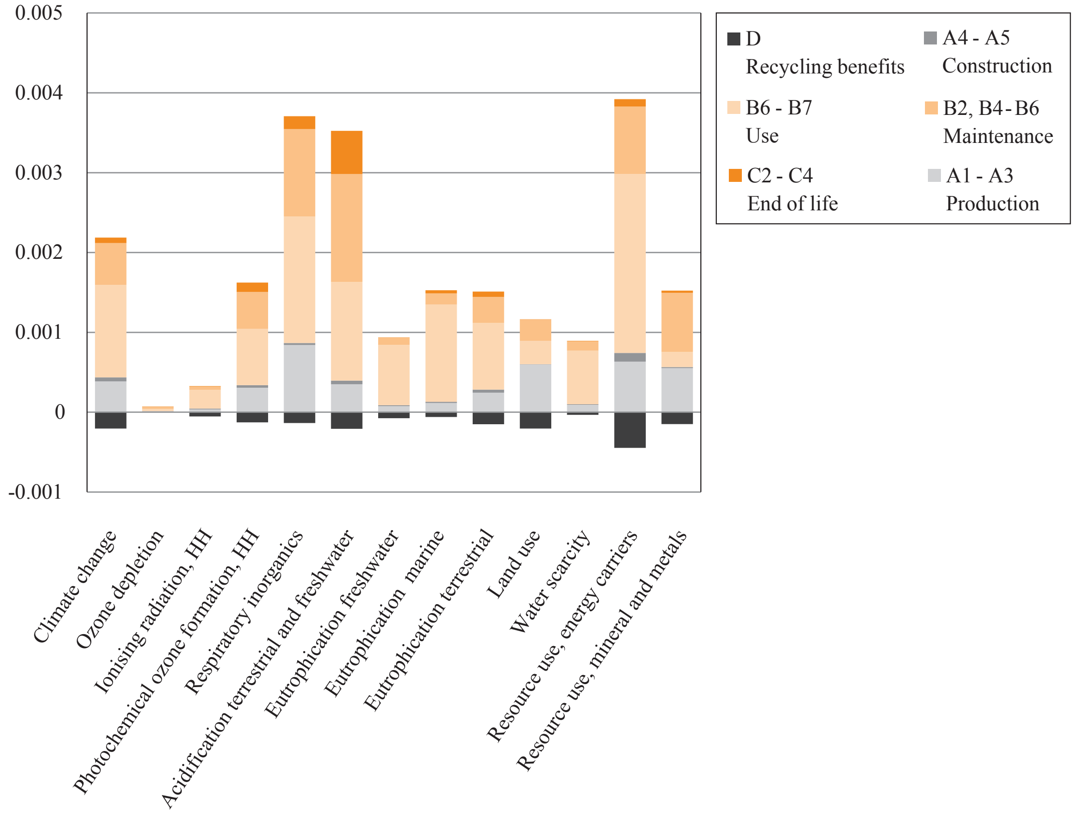

Figure 6 Normalized results Global 2010 (unitless, per m² and year)
Slika 6. Globalni normalizirani rezultati u 2010. (bez jedinica, po m² i godini)

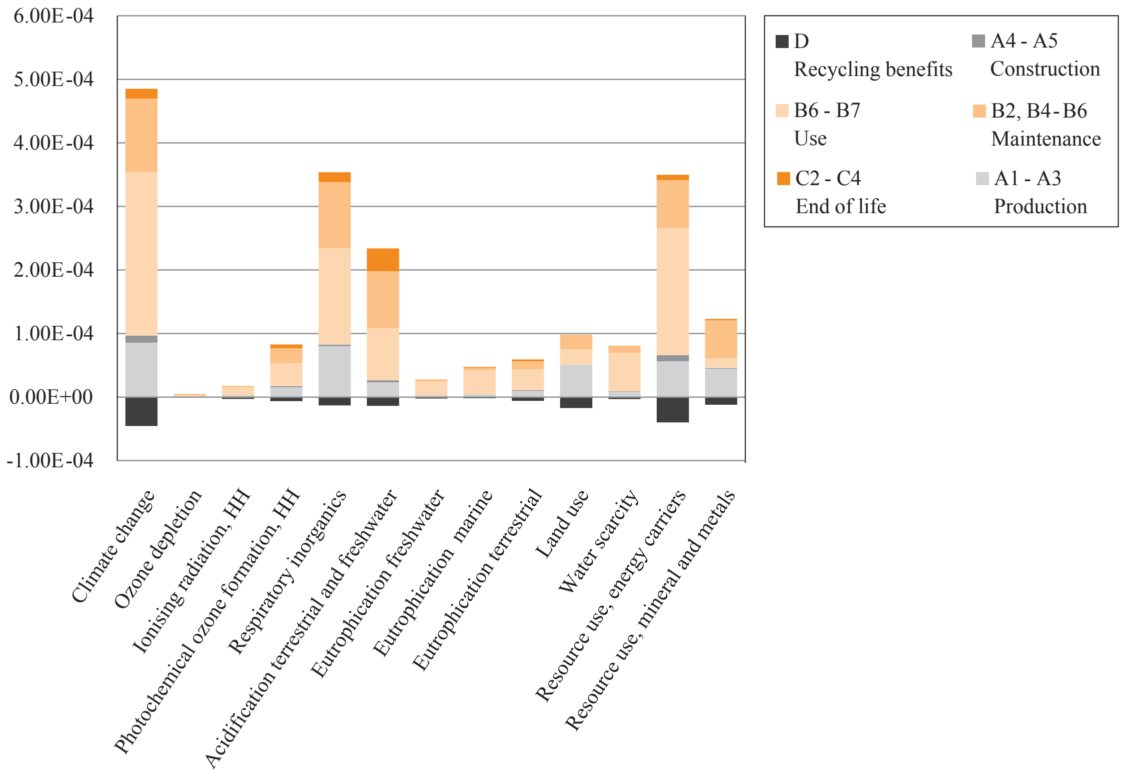

Figure 7 Weighted results (weighting points per m² and year)
Slika 7. Ponderirani rezultati (ponderi, po m² i godini)

Table 8 Weighted results and total (weighting points per m^2 and year)
Tablica 8. Ponderirani i ukupni rezultati (ponderi, po m^2 i godini)

Impact category *Utjecajne kategorije* — **Units: pt** *Jedinice: bod*	**A1 - A3 Production** *Proizvodnja*	**A4 - A5 Construction** *Gradnja*	**B6-B7 Use** *Uporaba*	**B2, B4-B6 Maintenance** *Održavanje*	**C2 - C4 End of life** *Kraj životnog vijeka*	**D Recycling benefits** *Prednosti recikliranja*	**Total** *Ukupno*
Climate change *klimatske promjene*	8.56E-05	1.11E-05	2.57E-04	1.16E-04	1.53E-05	-4.55E-05	4.40E-04
Ozone depletion *oštećenje ozonskog omotača*	7.52E-07	1.53E-07	1.96E-06	1.73E-06	2.34E-07	-3.57E-07	4.47E-06
Ionising radiation, HH *ionizirajuće zračenje, HH*	1.80E-06	6.42E-07	1.26E-05	2.16E-06	3.69E-07	-2.84E-06	1.47E-05
Photochemical ozone formation, HH *fotokemijsko stvaranje ozona, HH*	1.56E-05	1.68E-06	3.60E-05	2.34E-05	6.08E-06	-6.49E-06	7.63E-05
Respiratory inorganics *respiratorni anorganski utjecaji*	8.02E-05	2.40E-06	1.51E-04	1.04E-04	1.55E-05	-1.30E-05	3.41E-04
Acidification terrestrial and freshwater *zakiseljavanje kopna i slatkih voda*	2.33E-05	3.02E-06	8.21E-05	8.97E-05	3.59E-05	-1.38E-05	2.20E-04
Eutrophication freshwater *eutrofikacija slatke vode*	2.25E-06	3.40E-07	2.23E-05	2.63E-06	1.33E-07	-2.22E-06	2.54E-05
Eutrophication marine *eutrofikacija mora*	3.56E-06	4.84E-07	3.80E-05	4.41E-06	1.17E-06	-1.85E-06	4.58E-05
Eutrophication terrestrial *eutrofikacija kopna*	9.58E-06	1.47E-06	3.27E-05	1.27E-05	2.66E-06	-5.88E-06	5.32E-05
Land use / *upotreba zemljišta*	5.03E-05	2.57E-07	2.46E-05	2.25E-05	3.58E-07	-1.73E-05	8.08E-05
Water scarcity / *nestašica vode*	8.33E-06	6.49E-07	6.06E-05	1.06E-05	4.74E-07	-3.06E-06	7.76E-05
Resource use, energy carriers *iskorištavanje resursa, nositelji energije*	5.64E-05	9.71E-06	2.00E-04	7.54E-05	8.27E-06	-3.98E-05	3.10E-04
Resource use, mineral and metals *iskorištavanje resursa, minerali i metali*	4.45E-05	1.09E-06	1.53E-05	6.00E-05	2.13E-06	-1.21E-05	1.11E-04
Total / *ukupno*	3.82E-04	3.30E-05	9.34E-04	5.26E-04	8.86E-05	-1.64E-04	1.80E-03

vided by the average world inhabitants in the year 2010 (Fazio *et al*., 2018; Pre Consultants, 2019). The normalized results show that the respiratory inorganics impact category, closely followed by resource use, energy carriers and acidification terrestrial and freshwater are the dominant impact categories before weighting. The ozone depletion impact category is of minor importance.

The weighted results in Table 8 and Figure 7 show that the impact category climate change is most important, followed by resource use, energy and respiratory inorganics. The impact category ozone depletion is less relevant, as expected also in the weighted results.

5 DISCUSSION
5. RASPRAVA

This study presents the outcomes of a comprehensive life cycle assessment (LCA) conducted on a typical residential wooden building in Europe.

Despite incorporating design improvements, such as enhanced insulation and reduced windows areas towards the north, the results underscore the continued significance of the Use phase, particularly in relation to heating, as a primary contributor to the investigated environmental impact categories. It is within this stage that considerable environmental effects are observed.

Among the various impact categories examined, climate change emerges as the most prominent and influential. This finding highlights the substantial role played by the residential building sector in contributing to climate-altering greenhouse gas emissions and emphasizes the urgent need for sustainable solutions to mitigate these effects. However, three further impact categories, namely respiratory inorganics (particulate matter), resource use - energy carriers and acidification terrestrial and freshwater are also important.

By comprehensively assessing the cradle-to-grave life cycle of the average wooden residential building, this study provides valuable insights into the environmental implications associated with its construction and use. The findings underscore the importance of continually improving building designs and technologies to minimize the environmental impact of the use phase, particularly in terms of energy consumption for heating. Furthermore, the focus on climate change as the key impact category serves as a reminder of the pressing global challenges and the imperative to adopt eco-friendly practices in the construction and operation of residential buildings.

The Modules A4-A5 Construction phase is of minor importance compared to the whole life cycle but relies on assumptions based on literature ((Baldassarri *et al*., 2017; Lavagna *et al*., 2018). Waste handling at end of life has little impact on the total contribution. This is partially achieved by reuse and material recycling of some of the waste material from the demolition of the house. In practice, waste handling will occur decades or years into the future, and it is difficult to develop realistic future waste scenarios. However, waste handling is modelled based on the present situation. The connected recycling benefits (Module D) compensate to a certain degree some of the environmental impacts. Reuse and material recycling are believed to increase a lot in line with the EU circular economy policy, but as this is a long-lived house with a modelled 100-year lifetime, the positive effects are something to wait for decades, so that a conservative approach was followed.

6 CONCLUSION
6. ZAKLJUČAK

In making the assessment, the recommended Environmental Footprint (EF) indicators were used as prescribed by the European Union to explore the entire cradle-to-grave life cycle of the wooden single-family house, encompassing Modules A1 to D. The aim was to establish the house as a benchmark for evaluating environmental performance.

Despite design improvements, the Use phase, particularly heating, remained a significant contributor to the environmental impact categories examined. Climate change emerged as the most prominent impact category, underscoring the urgent need for sustainable practices in the construction and operation of residential buildings. Other important impact categories included respiratory inorganics (particulate matter), resource use, energy carriers, and acidification terrestrial and freshwater.

The study highlights the importance of continually improving building designs and technologies to minimize the environmental impact of the Use phase. It also emphasizes the global challenges associated with climate change and the necessity of adopting eco-friendly practices in the residential building sector.

The Construction phase had a minor impact compared to the overall life cycle, and waste handling at the end of life had little influence on the total contribution. Assumptions based on literature and current waste handling practices were made, but future waste scenarios are uncertain. However, the potential benefits of reuse and material recycling in line with the EU circular economy policy were acknowledged, although their effects may take decades to be fully realized.

Overall, this study sheds light on the environmental considerations of residential wooden buildings and underscores the importance of sustainable approaches throughout their life cycle. It serves as a reminder of the need for continuous improvement and the adoption of environmentally sound practices in the construction and use of buildings to mitigate climate change and minimize overall environmental impacts.

Future studies should apply the new EU Environmental Footprint method v.3, including the new toxicity impact indicators, such that these can be included, as this was not yet implemented in the software used at the time of our impact assessment calculations. Also, a better estimation of both the actual heating demand and the heat source mix for future buildings should be determined. Different scenarios for waste handling, and especially recycling rates, should be investigated as these might lower the total environmental burden.

The results could be used to compare to existing housing but mainly to design more environmentally sound single-family houses and establish and compare the reference houses in specific countries. Other building types, like multi-family houses and other buildings made of wood, could be investigated based on the same life cycle assessment concept and calculations.

Acknowledgements – Zahvala

The authors gratefully acknowledge funding from the Horizon 2020 Framework Programme of the European Union; H2020 WIDESPREAD-2-Teaming (#739574) and the Republic of Slovenia. The authors also thank Aarne Johannes Niemelä, Tatiana Abaurre Alencar Gavric and Iztok Šušteršič for valuable comments on an earlier version of this manuscript. E. M. S. also thanks COST Action CA20139 *Holistic design of taller timber buildings* (HELEN) members for fruitful discussions around the service life of buildings and motivation to publish these results.

5 REFERENCES
5. LITERATURA

1. Achenbach, H.; Wenker, J. L.; Rüter, S., 2018: Life cycle assessment of product- and construction stage of prefabricated timber houses: a sector representative approach for Germany according to EN 15804, EN 15978 and EN 16485. European Journal of Wood and Wood Products, 76 (2): 711-729. https://doi.org/10.1007/s00107-017-1236-1
2. Baldassarri, C.; Allacker, K.; Reale, F.; Castellani, V.; Sala, S., 2017: Consumer footprint: basket of products indicator on housing, EUR 28765 EN. Publications Office of the European Union, Luxembourg. https://doi.org/10.2760/05316
3. Bejo, L., 2017: Operational vs. embodied energy: a case for wood construction. Drvna industrija, 68 (2): 163-172. https://doi.org/10.5552/drind.2017.1423
4. D'Agostino, D.; Mazzarella, L., 2019: What is a Nearly zero energy building? Overview, implementation and comparison of definitions. Journal of Building Engineering, 21: 200-212. https://doi.org/10.1016/j.jobe.2018.10.019
5. Díaz, S.; Settele, J.; Brondízio, E.; Ngo, H.; Guèze, M.; Agard Arneth, J.; Balvanera, P.; Brauman, K.; Butchart, S.; Chan, K.; Garibaldi, L.; Ichii, K.; Liu, J.; Subrmanian, S.; Midgley, G.; Miloslavich, P.; Molnár, Z.; Obura, D.; Pfaff, A.; Polasky, S.; Purvis, A.; Jona Razzaq, C. Z., 2019: Summary for policymakers of the global assessment report on biodiversity and ecosystem services of the Intergovernmental Science – Policy Platform on Biodiversity and Ecosystem Services assessment (online). https://www.ipbes.net/news/ipbes-global-assessment-summary-policymakers-pdf (Accessed Mar. 28, 2019).
6. Fabrycky, W., 1991: Life Cycle Costs and Economics. Prentice Hall, N. J.
7. Fazio, S.; Castellani, V.; Sala, S.; Schau, E. M.; Secchi, M.; Zampori, L., 2018: Supporting information to the characterisation factors of recommended EF Life Cycle Impact Assessment methods, EUR 28888 EN, European Commission, Ispra. https://doi.org/10.2760/671368
8. Feist, W.; Baffia, E.; Schnieders, J.; Pfluger, R., 2002: Energiebilanzverfahren für die Passivhaus Vorprojektierung 2002 (PHVP02). Darmstadt (online). https://passivehouse.com/05_service/02_tools/02_tools.htm (Accessed Jul. 7, 2019).
9. Ferrari, A. M.; Volpi, L.; Pini, M.; Siligardi, C.; García-Muiña, F. E.; Settembre-Blundo, D., 2019: Building a sustainability benchmarking framework of ceramic tiles based on life cycle sustainability assessment (LCSA). Resources, 8 (1): 11. https://doi.org/10.3390/resources8010011
10. Guiton, M.; Benetto, E., 2018: Special session on product environmental footprint. In: Designing Sustainable Technologies, Products and Policies. Cham: Springer, pp. 515520. https://doi.org/10.1007/978-3-319-66981-6
11. Gül, S.; Spielmann, M.; Lehmann, A.; Eggers, D.; Bach, V.; Finkbeiner, M., 2015: Benchmarking and environmental performance classes in life cycle assessment – development of a procedure for non-leather shoes in the context of the Product Environmental Footprint. The International Journal of Life Cycle Assessment, 20: 1640-1648. https://doi.org/10.1007/s11367-015-0975-7
12. Hill, C.; Kymäläinen, M.; Rautkari, L., 2022: Review of the use of solid wood as an external cladding material in the built environment. Journal of Materials Science, 57: 9031-9076. https://doi.org/10.1007/s10853-022-07211-x
13. Hollberg, A.; Lützkendorf, T.; Habert, G., 2019: Top-down or bottom-up? – How environmental benchmarks can support the design process. Building and Environment, 153: 148-157. https://doi.org/10.1016/j.buildenv.2019.02.026
14. Kurnitski, J.; Ahmed, K., 2018: NERO – Cost reduction of new Nearly – Zero Energy Wooden buildings in Northern Climate Conditions – D1.2: Summary report on nZEB requirements.
15. Lavagna, M.; Baldassarri, C.; Campioli, A.; Giorgi, S.; Dalla, A.; Castellani, V.; Sala, S., 2018: Benchmarks for environmental impact of housing in Europe: Definition of archetypes and LCA of the residential building stock. Building and Environment, 145: 260-275. https://doi.org/10.1016/j.buildenv.2018.09.008
16. Lützkendorf, T.; Kohler, N.; König, H., 2012: Integrated life cycle assessment – benchmarks and uncertainty. In: LCA Construction 2012, RILEM Publications, Nantes 10 – 12 July Bagneux, France, pp. 28-36.
17. Menezes, B.; Marcelo, G.; Soares, S. R., 2019: Use of benchmarking techniques to improve communication in life cycle assessment: A general review. Journal of Cleaner Production, 213: 143-157. https://doi.org/10.1016/j.jclepro.2018.12.147

18. Notarnicola, B.; Tassielli, G.; Renzulli, P. A.; Castellani, V.; Sala, S., 2017: Environmental impacts of food consumption in Europe. Journal of Cleaner Production, 140: 753-765. https://doi.org/10.1016/j.jclepro.2016.06.080
19. Petrović, S., 2021: The influence of heating degree days on fuelwood consumption in households in selected countries of central and southeastern Europe. Drvna industrija, 72 (4): 403-410. https://doi.org/10.5552/drvind.2021.2111
20. Sala, S.; Benini, L.; Beylot, A.; Castellani, V.; Cerutti, A.; Corrado, S.; Crenna, E.; Diaconu, E.; Sanyé-Mengual, E.; Secchi, M.; Sinkko, T.; Pant, R., 2019: Consumption and Consumer Footprint: methodology and results. Indicators and Assessment of the Environmental Impact of EU Consumption. Luxembourg: Publications Office of the European Union. https://doi.org/10.2760/98570
21. Schau, E. M., 2019: Product Environmental Footprint (PEF) Category Rules (PEFCR) for Intermediate Paper Products – Overview and Discussion of Important Choices Made in the Development. In: Proceedings of the 1st International Conference on Circular Packaging. Pulp and Paper Institute, Ljubljana, pp. 175-184. https://doi.org/10.5281/zenodo.3430522
22. Schau, E. M.; Niemelä, E. P.; Niemelä, A. J.; Alencar Gavric, T. A.; Šušteršič, I., 2022: Life cycle assessment benchmark for wooden buildings in Europe. In: Towards a Sustainable Future – Life Cycle Management. Springer, Cham. https://doi.org/10.1007/978-3-030-77127-0_13
23. Sinha, A.; Gupta, R.; Kutnar, A., 2013: Sustainable development and green buildings. Drvna industrija, 64 (1): 45-53. https://doi.org/10.5552/drind.2013.1205
24. Spirinckx, C.; Thuring, M.; Damen, L.; Allacker, K.; Ramon, D.; Mirabella, N.; Röck, M.; Passer, A., 2019: Testing of PEF method to assess the environmental footprint of buildings – results of PEF4Buildings project. IOP Conference Series: Earth and Environmental Science, 297: https://doi.org/012033. 10.1088/1755-1315/297/1/012033
25. Quintana-Gallardo, A.; Schau, E. M.; Niemela, E. P.; Burnard, M. D., 2022: Comparing the environmental impacts of wooden buildings in Spain, Slovenia and Germany. Journal of Cleaner Production, 329: 129587331. https://doi.org/10.1016/j.jclepro.2021.129587
26. ***BPIE, 2015: Nearly Zero Energy Building (online). Brussels: Buildings Performance Institute Europe (BPIE). http://bpie.eu/publication/nzeb-definitions-across-europe-2015/ (Accessed Mar. 28, 2019).
27. ***Ecoinvent Centre, 2018, Ecoinvent Life Cycle Inventory Database, v 3.5.
28. ***EEA, 2019 Cutting air pollution in Europe would prevent early deaths, improve productivity and curb climate change (online). https://www.eea.europa.eu/highlights/cutting-air-pollution-in-europe (Accessed Feb. 4, 2019).
29. ***EN 15804A2:2019 Sustainability of construction works – Environmental product declarations – Core rules for the product category of construction products. CEN: Brussels.
30. ***Enova, 2019: Graddagstall (in Norwegian: Degree heating days): Oslo (online). https://www.enova.no/om-enova/drift/graddagstall/ (Accessed Jun. 6, 2019).
31. ***European Commission, 2012: Life cycle indicators for resources, products and waste. Ispra, Italy: European Commission, Joint Research Centre, Institute for Environment and Sustainability. https://doi.org/10.2788/4262
32. ***European Commission, 2018: A Clean Planet for all. A European strategic long-term vision for a prosperous, modern, competitive and climate neutral economy. COM 2018/773. Brussels, 28 Nov 2018.
33. ***European Commission, 2016: Commission recommendation (EU) 2016/1318 of 29 July 2016 on guidelines for the promotion of nearly zero-energy buildings and best practices to ensure that, by 2020, all new buildings are nearly zero-energy buildings. Official Journal of the European Communities. https://doi.org/10.1680/aarots.20511.0006
34. ***Eurostat, 2019a: Sold production, exports and imports by PRODCOM list (NACE Rev. 2) – annual data [DS-066341] – Prefabricated buildings of wood.
35. ***Eurostat, 2019b: Cooling and heating degree days by country – annual data [nrg_chdd_a].
36. ***IPCC, 2018: Summary for Policymakers. In: Global Warming of 1.5 °C. An IPCC Special Report on the impacts of global warming of 1.5 °C above pre-industrial levels and related global greenhouse gas emission pathways, in the context of strengthening the global response to the threat of climate change, sustainable development and efforts to eradicate poverty.
37. ***NRW ÖkoZentrum, 2019: Gesetzentwurf der Bundesregierung (online) (in German). Draft bill from the German government) http://www.oekozentrum-nrw.de/fileadmin/Medienablage/PDF-Dokumente/190528_GEG-Entwurf.pdf (Accessed May 5, 2019).
38. ***Pré Consultants, 2019, SimaPro Analyst, v. 9.0.
39. ***SSB, 2019: ProdCom 10455: Solgt produksjon av varer for store foretak i industri (in Norwegian: Sold production of goods in the manufacturing industry). Oslo, Statistics Norway.

Corresponding address:

EVA PRELOVŠEK NIEMELÄ

InnoRenew CoE, Livade 6a, Izola-Izola, SLOVENIA, e-mail: eva.prelovsek@innorenew.eu

SUPPLEMENT – DODATAK

Table SM1 Calculation of areas based on architectural drawings
Tablica SM1. Izračun površina na temelju arhitektonskih nacrta

W1 – exterior walls / *Vanjski zidovi*					
	L, m	*h*, m	*A*_full wall, m²	*A*_openings, m²	*A*_total, m²
W1_A	9.63	4.78	46.03	2.69	36.89
W1_C	9.63	4.78	46.03	8.45	37.58
W1_1	6.70	5.85	39.20	8.66	30.53
W1_4	6.70	5.85	39.20	8.60	26.33
W1_Total					131.32

W1‘ – exterior walls – ceramics in bathrooms / *Vanjski zidovi – keramika u kupaonicama*					
	L, m	*h*, m	*A*_full wall, m²	*A*_openings, m²	*A*_total, m²
W1‘_gf_A	1.04	2.00	2.08	0.30	1.78
W1‘_1f_A	2.88	2.00	5.76	1.09	4.67
W1‘_1f_4	2.98	2.00	5.96	1.69	4.27
W1‘_Total					10.73

W2 – exterior walls – ground floor bottom / *Vanjski zidovi – prizemlje dolje*					
	L, m	*h*, m	*A*_full wall, m²	*A*_openings, m²	*A*_total, m²
W2_A	9.63	0.69	6.64	0.00	6.64
W2_C	9.63	0.69	6.64	0.00	6.64
W2_1	6.70	0.69	4.62	0.00	4.62
W2_4	6.70	0.69	4.62	0.00	4.62
W2_Total					22.54

W3 – inner walls / *Unutarnji zidovi*					
	L, m	*h*, m	*A*_full wall, m²	*A*_openings, m²	*A*_total, m²
W3_gf_A’	1.06	2.67	2.83	1.44	1.40
W3_gf_B	5.06	2.67	13.51	3.28	10.23
W3_gf_2	5.14	2.67	13.72	0.00	13.72
W3_gf_3.1	1.70	0.67	1.14	0.00	1.14
W3_gf_3.2	4.39	2.67	11.72	1.64	10.08
W3_gf_3’	1.83	0.67	1.23	0.00	1.23
W3_1f_B.1	3.96	4.16	16.47	0.00	16.47
W3_1f_B.2	3.02	2.16	6.52	0.00	6.52
W3_1f_B’	1.93	3.77	7.28	0.00	7.28
W3_1f_2	6.09	3.40	20.71	3.28	17.43
W3_1f_3	4.23	3.40	10.32	3.28	7.04
W3_Total					92.54

W3‘ – inner walls – ceramics in bathrooms / *Unutarnji zidovi – keramika u kupaonicama*					
	L, m	*h*, m	*A*_full wall, m²	*A*_openings, m²	*A*_total, m²
W3‘_gf_3	1.7	2.00	3.40	0.00	3.40
W3‘ gf_3’	1.83	2.00	3.66	0.00	3.66
W3‘_1f_B.2	3.02	2.00	6.04	0.00	6.04
W3‘_1f_3	2.03	2.00	4.06	0.00	4.06
W3‘_Total					17.16

R1 – roof / *Krov*					
	L, m	*h*, m	*A*_full wall, m²	*A*_openings, m²	*A*_total, m²
R1	11.61	5.31	61.65	0.00	61.65
R2	11.61	5.31	61.65	0	61.65
R1_Total					123.30

Table SM1 continuation
Tablica SM1. nastavak

F – ground floor / *Prizemlje*					
					*A*_total, m^2
F1					19.17
F1/A					1.53
F2					34.20
F3					3.58

F – 1st floor / *Prvi kat*					
					*A*_total, m^2
F4					9.54
F5					41.78

Windows / *Prozori*			
	b, m	*h*, m	*A*, m^2
O1	0.9	2.05	1.85
O2	1.72	1.25	2.15
O3	2.58	2.05	5.29
O4	0.6	0.5	0.30
O5	0.75	2.25	1.69
O6	1.1	2.25	2.48
O7	0.9	1.45	1.31
O8	0.75	1.45	1.09
O9	1.1	1.25	1.38

Doors / *Vrata*			
	b, m	*h*, m	*A*, m^2
V1	0.9	2.05	1.85
V2	0.8	2.05	1.64
V3	0.7	2.05	1.44

Table SM2 Calculation of material quantities
Tablica SM2. Proračun količina materijala

	W1 – exterior walls / *Vanjski zidovi*	**Quantity** *Količina*	**Unit** *Jedinica*	**Volume, m³** *Volumen,* m³	**Density, kg/m³** *Gustoća,* kg/m³	**Mass, kg** *Masa,* kg
1	gypsum plasterboards – 1.25 cm	131.32	m^2	1.642	900	1477.4
2	OSB plate – 1.2 cm	131.32	m^2	1.576	650	1024.3
3	stone wool between the load bearing construction profiles – 16 cm	21.01	m^3	21.012	40	840.5
4	load bearing construction profiles – 8/16 cm	5.25	m^3	5.253	420	2206.2
5	gypsum fibreboard – 1.5 cm	131.32	m^2	1.970	1200	2363.8
6	stone wool – 10 cm	13.13	m^3	13.132	80	1050.6
7	reinforcing mortar, mesh and finishing plaster – 0.6 cm	131.32	m^2	0.788	1900	1497.1

	W1' – exterior walls – ceramics in bathrooms / *Vanjski zidovi – keramika u kupaonicama*	**Quantity** *Količina*	**Unit** *Jedinica*	**Volume, m³** *Volumen,* m³	**Density, kg/m³** *Gustoća,* kg/m³	**Mass, kg** *Masa,* kg
1	ceramic plates – 1 cm	10.73	m^2	0.107	1850	198.4
2	glue for ceramic plates – 0.5 cm	10.73	m^2			53.6
3	hydro-isolating layer – 0.3 cm	10.73	m^2	0.032	1400	45.0
4	gypsum plasterboards – 1.25 cm	10.73	m^2	0.134	900	120.7
5	OSB plate – 1.2 cm	10.73	m^2	0.129	650	83.7
6	stone wool between the load bearing construction profiles – 16 cm	1.72	m^3	1.716	40	68.6
7	load bearing construction profiles – 8/16 cm	0.43	m^3	0.429	420	180.2
8	gypsum fibreboard – 1.5 cm	10.73	m^2	0.161	1200	193.1
9	stone wool – 10 cm	1.07	m^3	1.073	80	85.8
10	reinforcing mortar, mesh and finishing plaster – 0.6 cm	10.73	m^2	0.064	1900	122.3

	W2 – exterior walls – ground floor bottom / *Vanjski zidovi – prizemlje dolje*	**Quantity** *Količina*	**Unit** *Jedinica*	**Volume, m³** *Volumen,* m³	**Density, kg/m³** *Gustoća,* kg/m³	**Mass, kg** *Masa,* kg
1	gypsum plasterboards – 1.25 cm	22.54	m^2	0.282	900	253.5
2	reinforced concrete – 16 cm	3.61	m^3	3.606	2400	8653.6
3	Hydro isolation: polymer-bitumen, one layer Like ORION FC 160 – 0.4 cm	22.54	m^2	0.090	1400	126.2
4	XPS insulation – 12 cm	2.70	m^3	2.704	35	94.6
5	reinforcing mortar, mesh and finishing plaster – 0.6 cm	22.54	m^2	0.135	1900	256.9

	W3 – inner walls / *Unutarnji zidovi*	**Quantity** *Količina*	**Unit** *Jedinica*	**Volume, m³** *Volumen,* m³	**Density, kg/m³** *Gustoća, ,* kg/m³	**Mass, kg** *Masa,* kg
1	gypsum plasterboards – 1.25 cm*2 = 2.5 cm	92.54	m^2	2.313	900	2082.1
2	load bearing construction profiles – 6/10 cm – 10 cm	1.85	m^3	1.851	420	777.3
3	stone wool like Knauf Insulation DP-5 Venti (between wooden construction) – 10 cm	9.25	m^3	9.254	30	277.6
4	gypsum plasterboards- 1.25 cm*2 = 2.5 cm	92.54	m^2	2.313	900	2082.1

Table SM2 continuation
Tablica SM2. nastavak

	W3' – inner walls – ceramics in bathrooms / *Unutarnji zidovi – keramika u kupaonicama*	**Quantity** *Količina*	**Unit** *Jedinica*	**Volume, m³** *Volumen,* m³	**Density, kg/m³** *Gustoća,* kg/m³	**Mass, kg** *Masa,* kg
1	gypsum plasterboards – 1.25 cm*2 = 2.5 cm	17.16	m^2	0.429	900	386.1
2	load bearing construction profiles – 6/10 cm - 10 cm	0.34	m^3	0.343	420	144.1
3	stone wool like Knauf Insulation DP-5 Venti (between wooden construction) – 10 cm	1.72	m^3	1.716	30	51.5
4	gypsum plasterboards – 1.25 cm*2 = 2.5 cm	17.16	m^2	0.429	900	386.1
5	hydro-isolating layer – 0.3 cm	17.16	m^2	0.051	1400	72.1
6	glue for ceramic plates – 0.5 cm	17.16	m^2			85.8
7	ceramic plates – 1 cm	17.16	m^2	0.172	1850	317.5

	R1 – roof / *Krov*	**Quantity** *Količina*	**Unit** *Jedinica*	**Volume, m³** *Volumen,* m³	**Density, kg/m³** *Gustoća,* kg/m³	**Mass, kg** *Masa,* kg
1	wooden boards – 2 cm	123.30	m^2	2.466	420	1035.7
2	wooden laths 3x4 cm – 3 cm	0.59	m^3	0.592	420	248.6
3	reinforced ALU foil – 0.2 cm	123.30	m^2			12.3
4	mineral wool between the load bearing construction profiles – 16 cm	12.33	m^3	12.330	35	431.5
5	load bearing construction profiles (rafters) 8/16 cm – 16 cm	1.98	m^3	1.978	420	830.6
6	additional structural wooden beams	2.42	m^3	2.424	420	1018.2
7	stone wool like Rockwool Roofrock – 10 cm	12.33	m^3	12.330	80	986.4
8	roof foil like Tyvek, Eternit Meteo or similar – 0.2 cm	123.30	m^2			12.3
9	wooden laths 5x5 cm – 5 cm	0.92	m^3	0.925	420	388.39
10	wooden laths in opposite direction 3x5 cm – 3 cm	0.33	m^3	0.333	420	139.82
11	roof cover: wave fiber cement roof tiles – 0,5 cm	123.30	m^2			2465.96

	F1 – ground floor – ceramics / *Prizemlje – keramika*	**Quantity** *Količina*	**Unit** *Jedinica*	**Volume, m³** *Volumen,* m³	**Density, kg/m³** *Gustoća,* kg/m³	**Mass, kg** *Masa,* kg
1	ceramic plates – 1 cm	19.17	m^2	0.192	1850	354.6
2	glue for ceramic plates – 0.5 cm	19.17	m^2			95.9
3	concrete screed C20/25 with floor heating pipes – 7.6 cm	1.46	m^3	1.457	2250	3278.1
4	PE foil – 0.2mm	19.17	m^2			1.9
5	hard mineral wool acoustic insulation – 4 cm	0.77	m^3	0.767	80	61.3
6	reinforced concrete – 25 cm	4.79	m^3	4.793	2400	11502.0
7	XPS insulation – 15cm	2.88	m^3	2.876	35	100.6
8	Hydro isolation: polymer-bitumen, one layer, like ORION FC 160 – 0.4 cm	19.17	m^2	0.077	1400	107.4
9	bottom concrete – 10 cm	1.92	m^3	1.917	2400	4600.8

Table SM2 continuation
Tablica SM2. nastavak

	F1/A – ground floor – ceramics in bathrooms (1 cm height) / *Prizemlje – keramika u kupaonicama (visina – 1 cm)*	**Quantity** *Količina*	**Unit** *Jedinica*	**Volume, m³** *Volumen,* m³	**Density, kg/m³** *Gustoća,* kg/m³	**Mass, kg** *Masa,* kg
1	ceramic plates – 1 cm	1.53	m^2	0.015	1850	28.3
2	glue for ceramic plates – 0.5 cm	1.53	m^2			7.7
3	thin hydro-isolating layer based on hydraulic binders and elastomer additives – 0,3 cm	1.53	m^2	0.005	1400	6.4
4	concrete screed C20/25 with floor heating pipes – 7.6 cm	0.12	m^3	0.116	2250	261.6
5	PE foil – 0.2 mm	1.53	m^2			0.2
6	hard mineral wool acoustic insulation – 3 cm	0.05	m^3	0.046	80	3.7
7	reinforced concrete – 25 cm	0.38	m^3	0.383	2400	918.0
8	XPS insulation – 15cm	0.23	m^3	0.230	35	8.0
9	Hydro isolation: polymer-bitumen, one layer, like ORION FC 160 – 0.4 cm	1.53	m^2	0.006	1400	8.6
10	bottom concrete – 10 cm	0.15	m^3	0.153	2400	367.2

	F2 – ground floor – parquet / *Prizemlje – parket*	**Quantity** *Količina*	**Unit** *Jedinica*	**Volume, m³** *Volumen,* m³	**Density, kg/m³** *Gustoća,* kg/m³	**Mass, kg** *Masa,* kg
1	parquet – 1.1 cm	34.2	m^2	0.376	700	263.3
2	glue – 0.3 cm	34.2	m^2			51.3
3	concrete screed C20/25 with floor heating pipes – 7.6 cm	2.60	m^3	2.599	2250	5848.2
4	PE foil – 0.2mm	34.2	m^2			3.4
5	hard mineral wool acoustic insulation – 4 cm	1.37	m^3	1.368	80	109.4
6	reinforced concrete – 25 cm	8.55	m^2	2.138	2400	5130.0
7	XPS insulation – 15cm	5.13	m^3	5.130	35	179.6
8	Hydro isolation: polymer-bitumen, one layer, like ORION FC 160 – 0.4 cm	34.2	m^2	0.137	1400	191.5
9	bottom concrete – 10 cm	3.42	m^3	3.420	2400	8208.0

	F3 – stair – CLT / *Stepenice CLT*:	**Quantity** *Količina*	**Unit** *Jedinica*	**Volume, m³** *Volumen,* m³	**Density, kg/m³** *Gustoća,* kg/m³	**Mass, kg** *Masa,* kg
1	CLT plates, coated – 10 cm	0.36	m^3	0.358	480	171.8

	F4 – 1st floor – ceramics (1 cm height) / *Prvi kat – keramika (visina – 1 cm)*	**Quantity** *Količina*	**Unit** *Jedinica*	**Volume, m³** *Volumen,* m³	**Density, kg/m³** *Gustoća,* kg/m³	**Mass, kg** *Masa,* kg
1	ceramic plates – 1 cm	9.54	m^2	0.095	1850	176.5
2	glue for ceramic plates – 0.5 cm	9.54	m^2			38.2
3	thin hydro-isolating layer based on hydraulic binders and elastomer additives – 0.3 cm	9.54	m^2	0.029	1400	40.1
4	concrete screed C20/25 with floor heating pipes – 7.6 cm	0.73	m^3	0.725	2250	1631.3
5	PE foil – 0.2 mm	9.54	m^2			1.0
6	hard mineral wool acoustic insulation – 3 cm	0.29	m^3	0.286	80	22.9

Table SM2 continuation
Tablica SM2. nastavak

7	OSB plates – 1.5 cm	9.54	m^2	0.143	650	93.015
8	load bearing construction profiles 20x12 cm – 20 cm	0.54	m^3	0.544	420.00	228.39
9	mineral wool between the load bearing construction profiles – 20 cm	1.43	m^3	1.431	30.00	42.93
10	wooden laths 3/2 cm – 2 cm	0.02	m^3	0.017	420.00	7.21
11	gypsum plasterboards – 1.25 cm	9.54	m^2	0.119	900	107.33

	F5 – 1st floor – parquet / *Prvi kat – parket*	**Quantity** *Količina*	**Unit** *Jedinica*	**Volume, m^3** *Volumen,* m^3	**Density, kg/m^3** *Gustoća,* kg/m^3	**Mass, kg** *Masa,* kg
1	parquet – 1.1 cm	41.78	m^2	0.460	700	321.7
2	glue – 0.3 cm	41.78	m^2			62.7
3	concrete screed C20/25 with floor heating pipes – 7.6 cm	3.18	m^3	3.175	2250	7144.4
4	PE foil – 0.2 mm	41.78	m^2			4.2
5	hard mineral wool acoustic insulation – 4 cm	1.67	m^3	1.671	80	133.7
6	OSB plates – 1.5 cm	41.78	m^2	0.627	650	407.355
7	load bearing construction profiles 20x12 cm – 20 cm	2.38	m^3	2.381	420	1000.21
8	mineral wool between the load bearing construction profiles – 20 cm	6.27	m^3	6.267	30	188.01
9	wooden laths 3/2 cm – 2 cm	0.08	m^3	0.075	420	31.59
10	gypsum plasterboards – 1.25 cm	41.78	m^2	0.522	900	470.03

	Windows (wooden frames) – triple glazed (thickness 92 μm) / *Prozori (drvene okvirnice) – tri sloja premaznog materijala (debljina 92 μm)*	**Quantity** *Količina*	**Unit** *Jedinica*
1	O1 – 90x205 cm	4	pcs
2	O2 – 172x125 cm	1	pcs
3	O3 – 258x205 cm	1	pcs
4	O4 – 60x50 cm	1	pcs
5	O5 – 75x225 cm	1	pcs
6	O6 – 110x225 cm	2	pcs
7	O7 – 90x145 cm	3	pcs
8	O8 – 75x145 cm	1	pcs
9	O9 – 110x125 cm	1	pcs

	Doors / *Vrata*	**Quantity** *Količina*	**Unit** *Jedinica*
1	V1 – 90x205 cm	1	pcs
2	V2 – 80/205 cm	7	pcs
3	V3 – 70x205 cm	1	pcs

Mehmet Ali Kapçak[1], Hilmi Toker[1], Çağlar Altay*[2], Emir Özdemir[1], Ergün Baysal[1]

Some Physical and Mechanical Characteristics of Waste Olive Oil Heat-Treated Oriental Beech Wood

Neka fizička i mehanička svojstva kavkaske bukovine pregrijane u otpadnome maslinovu ulju

ORIGINAL SCIENTIFIC PAPER
Izvorni znanstveni rad
Received – prispjelo: 19. 6. 2023.
Accepted – prihvaćeno: 25. 1. 2024.
UDK: 630*84; 674.4
https://doi.org/10.5552/drvind.2024.0134

ABSTRACT • *This study set out to look into some of the mechanical and physical characteristics of oil-heated oriental beech wood. Waste olive oil was used for oil-heat treatment. Heat treatment of the oil was done at 200 °C and 230 °C for 2 hours and 4 hours, respectively. After oil-heat treatment, physical traits including oven-dry density and water absorption levels, as well as mechanical traits like compression strength parallel to the grain (CSPG), were determined. Oven dry density of wood increased significantly after being heated in oil. Compared to the control groups, waste olive oil heat-treated (WOHT) oriental beech showed lower levels of water absorption. At 200 °C for 4 h, CSPG of waste olive oil heat-treated wood were at their highest, and then they steadily fell as the temperature and treatment time rose.*

KEYWORDS: *waste oil heat-treatment; physical properties; mechanical properties; waste olive oil; oriental beech*

SAŽETAK • *Cilj ovog istraživanja bio je ispitati neka mehanička i fizička svojstva uljem pregrijane bukovine. Za toplinsku je obradu korišteno otpadno maslinovo ulje. Toplinska obrada u ulju provedena je na 200 i 230 °C tijekom dva i četiri sata. Nakon toplinske obrade uljem utvrđena su fizička svojstva bukovine: gustoća apsolutno suhog drva i upijanje vode, kao i mehaničko svojstvo čvrstoće na tlak paralelno s vlakancima (CSPG). Gustoća apsolutno suhog drva znatno se povećala nakon toplinske obrade u ulju. U usporedbi s kontrolnim uzorcima, kavkaska bukovina pregrijana u maslinovu ulju (WOHT) pokazala je nižu razinu upijanja vode. Najveća čvrstoća na tlak paralelno s vlakancima zabilježena je u bukovine pregrijane u otpadnome maslinovu ulju na 200 °C tijekom četiri sata, a zatim se postupno smanjivala kako su se temperatura i vrijeme toplinske obrade povećavali.*

KLJUČNE RIJEČI: *toplinska obrada otpadnim uljem; fizička svojstva; mehanička svojstva; otpadno maslinovo ulje; kavkaska bukva*

* Corresponding author
[1] Authors are researchers at Muğla Sıtkı Koçman University, Technology Faculty, Muğla, Turkey. https://orcid.org/0000-0002-6890-3201; https://orcid.org/0000-0002-4109-458X; https://orcid.org/0000-0001-7218-0010; https://orcid.org/0000-0002-6299-2725
[2] Author is researcher at Aydın Adnan Menderes University, Vocational School of Aydın, Aydın, Turkey. https://orcid.org/0000-0003-1286-8600

1 INTRODUCTION
1. UVOD

Wood has been used in residential building since the beginning of time, due to its very good qualities such as thermal insulation and transportation, high specific strength and easy workability (Su, 1997). However, wood is adversely affected by environmental factors such as biological creatures, fire, light, and water compared to many other materials (Kiguchi and Evans, 1998). Therefore, it is important to treat wood so as to extend its useful life and enhance some of its qualities necessary for its use (Srinivas and Pandey, 2012). Wood modification refers to improving the quality of wood through biological, chemical, or physical processes (Hill, 2007; Esteves and Pereira, 2009; Thybring, 2013). Heat treatment is an alternative approach to wood modification. Heat-treated wood has new characteristics including increased dimensional stability and greater decay resistance, while its resistance is noticeably reduced (Türkoğlu *et al.,* 2015). Heat-treated wood performs better than untreated wood in terms of aesthetic quality (effective and uniform color change) and performance in accordance with technical standards (much less shrinkage and swelling, enhanced strength to fungus) (Vukas *et al.,* 2010; Türkoğlu *et al.,* 2015). Recent research has shown that heating wood with oil is a great replacement for it. Due to their non-toxicity and being environmentally friendly, plant oils have long been used to protect wood from mold and fungal degradation as well as to drop the accessibility of moisture to the wood (Yingprasert *et al.,* 2015). Without the use of any long-lasting, dangerous chemicals, hot oil heat-treatment can improve the dimensional stability and toughness of wood, especially of plantation wood that develops quickly (Cheng *et al.,* 2014). Additionally, compared to the wood heated in other gaseous atmospheres, oil heat-treated wood has slightly better mechanical characteristics (Rapp and Sailer, 2001). One of these techniques, oil-heat treatment (OHT), was developed and first used for garden furniture in Germany in the 2000s. This technique involves adding plant oils, such as sunflower oil, rapeseed or linseed to a closed tank at a specific temperature for a predetermined amount of time (Kesik *et al.,* 2015). As oil is used as the heating medium, the process is thought to be more ecologically sustainable, eco-friendly, cost-effective, and heat treatment using oil (OHT) is seen as a slightly different approach to wood modification. Linseed, rapeseed, palm, soybean, and coconut oils are industrial vegetable oils used for heat treatment (Welzbacher and Rapp, 2005; Wang and Cooper, 2005). By combining the beneficial effects of heat with oil, a process known as "oil heat treatment" or "oleothermal treatment" can enhance the quality of wood. Researchers from all over the world have conducted a great deal of research on oil heat treating wood (Lee *et al.,* 2018). Wang *et al*. (2014) investigated the density of wood treated with hot air and hot oil from *Paulownia tomentosa* and wood from *Pinus koraiensis*. Mostly because oil was absorbed during treatment, wood from both species that had been heat-treated with oil showed noticeably higher density than wood heated with air. Var *et al.* (2021) sought to ascertain the density values of red pine treated with hot-cold bio-oil. The findings showed that the density of test samples rose by 40.38 % to 78.85 %. Mastouri *et al.* (2021) used silicone and rapeseed oil to study the water absorption rates of eastern cotton (*Populus deltoides*) wood for 4 h at 190 °C. According to the findings, heat treatment with silicon has a greater potential to enhance water-related properties of wood than heat treatment with rapeseed oil. According to Lee *et al*. (2018), heat-induced changes to the chemical composition of wood cell wall components result in changes of wood strength after oil heat treatment. Hemicellulose, cellulose, and lignin, the three main components of the cell wall, each contribute in a unique way to the characteristics of wood strength. They stated that other factors, besides an oxygen-free environment, contribute to the comparatively good mechanical characteristics of wood during oil heat treatment. In addition, more oil uptake than provided by other heat treatment techniques also improves the wood mechanical strength. Linseed oil considerably reduced the compression strength of coastal pine when samples were heated to 200 °C for 6 hours, according to Taşdelen *et al*. (2019). In contrast to vacuum heat treatment alone, other linseed oil treatments typically yielded excellent strength values, notably for 180 °C. Bak and Németh (2012) treated Poplar (*Populus × euramericana* Pannónia) and Robinia (*Robinia pseudoacacia* L.) woods by heating sunflower, rapeseed, and linseed oils to 160 °C and 200 °C for 2 h, 4 h, and 6 h, respectively. It is interesting to note that oil heat treatment of poplar wood increased the compression strength by 15 % to 25 %. In addition, when treated at 160 °C, black locust wood compression strength increased by 5 % to 15 %; however, when treated at 200 °C, it started to decline by 5 % to 10 %.

The physical and mechanical characteristics of wood that had been heat-treated with oil were explored from a variety of angles in earlier investigations. There has not been much research on the use of oils, particularly olive oil as heating oil. In order to better understand the properties of oriental beech that had been heated using waste olive oil, this study looked at its oven-dry density, water absorption (WA), and compressive strength parallel to the grain. In addition, one of the aims of the study is to enhance physical and mechanical characteristics of oriental beech with an organic material by contributing to recycling with the use of waste olive oil.

2 MATERIALS AND METHODS
2. MATERIJALI I METODE

2.1 Materials
2.1. Materijali

Wasted olive oil used for fried potatoes was used for the oil heat treatment. Wood samples were prepared from oriental beech wood.

2.2 Methods
2.2. Metode

2.2.1 Preparation of wood samples
2.2.1. Priprema uzoraka drva

Wood samples were prepared according to TS ISO 3129:2021 standard. Oriental beech (*Fagus orientalis* L.) samples were cut into rectangles with radial, tangential, and longitudinal dimensions of 20 mm × 20 mm × 20 mm, 20 mm × 20 mm × 20 mm, and 20 mm × 20 mm × 30 mm, respectively, for the oven-dry density, *WA*, and *CSPG* test samples. One hundred fifty wood samples overall, each made of ten wood samples, were prepared as control and test samples for this investigation.

2.2.2 Treatment process
2.2.2. Postupak toplinske obrade

The samples were dried in an oven at 103 ± 2 °C until they reached a consistent weight in preparation for oil heat treatment (m_1). The samples were then processed in a high temperature oven before being submerged in the oil bath at room temperature. When the oil bath reached 200 °C and 230 °C, the treatment times were 2 h and 4 h, respectively. After being removed from the oil bath, the samples were covered in aluminium foil and allowed to cool.

The weight percentage gain (WPG) of samples after the treatment were calculated by Eq. 1:

$$WPG = \frac{m_2 - m_1}{m_1} \cdot 100\ (\%) \tag{1}$$

Where:
m_1 – mass before oil heat treatment,
m_2 – mass after oil heat treatment.

An electric furnace was used to heat the air (KD 200 model drying cabinet.). The temperature was raised from ambient to the desired temperatures of 200 °C and 230 °C for 2 and 4 h, respectively. Wood samples were conditioned at 20 °C and 65 % relative humidity for two weeks before *CSPG*, oven-dry density, and *WA* tests.

2.2.3 Oven-dry density test
2.2.3. Ispitivanje gustoće apsolutno suhog drva

Oven-dry density of samples was measured in accordance with the TS ISO 13061-2 2472 (TS ISO, 2021) standard. Test samples were required to be dried at (103±2) °C until they reached a consistent weight. The samples were then allowed to cool before being weighed on an analytical balance with an accuracy of 0.01 g; their diameters were measured with a delicate calliper with an accuracy of 0.01 mm, and their volumes estimated using the stereo metric method. The oven-dry density (δ_o), oven-dry weight (M_o), and oven-dry volume (V_o) were then determined using Eq. 2:

$$\delta_0 = \frac{M_0}{V_0}\ (\text{g/cm}^3) \tag{2}$$

Where:
M_o – Oven-dry weight of specimen (g)
V_o – Oven-dry volume of specimen (cm³)

2.2.4 Water absorption test
2.2.4. Ispitivanje upijanja vode

In a room environment, wood samples were kept in distilled water for 2, 8, 24, 48, 72, 96, 120, 144, and 168 h. After each soaking interval, samples were removed from the water, patted dry with spotting paper, and then weighed. As a result, each specimen's *WA* was calculated using Eq. 3:

$$WA = \frac{M_f - M_{oi}}{M_{oi}} \cdot 100\ (\%) \tag{3}$$

Where:
WA – Water absorption (%),
M_f – Weight of specimen after water absorption (g),
M_{oi} – Oven-dry weight of specimen after impregnation (g).

2.2.5 Compression strength parallel to grain (CSPG)
2.2.5. Čvrstoća na tlak paralelno s vlakancima

According to the TSE 2595:1977 standard, the compression strength parallel to the grain test was carried out using a universal test machine with a 4000 kp capacity and a 6 mm/min loading period. The universal test device was produced by MATEŞ Electronic company located in Ankara province of Turkey.

2.2.6 Statistical evaluation
2.2.6. Statistička procjena

After the test results were acquired, the SPSS computer assessed the variance analysis and Duncan test, which was covered at a 95 % confidence level. Homogeneity groups (HG) were subjected to statistical analyses, where different letters denote statistical significance.

3 RESULTS AND DISCUSSION
3. REZULTATI I RASPRAVA

3.1 *WPG* of WOHT oriental beech wood
3.1. Povećanje mase kavkaske bukovine pregrijane u otpadnome maslinovu ulju

WPG of WOHT oriental beech wood is given in Table 1. *WPG* of WOHT oriental beech ranged from 39

Table 1 Weight percent gain (*WPG*) of waste olive oil heat-treated (WOHT) oriental beech
Tablica 1. Povećanje mase (*WPG*) kavkaske bukovine pregrijane u otpadnome maslinovu ulju (WOHT)

Treatment type *Vrsta tretmana*	**Temperature, °C** *Temperatura, °C*	**Duration, h** *Trajanje,* h	***WPG***, %	Standard deviation *Standardna devijacija*
Control kontrolni uzorak	-	-	-	-
WOHT	200	2	39	4.85
WOHT	200	4	44	6.60
WOHT	230	2	54	7.75
WOHT	230	4	60	7.30

Table 2 Oven-dry density values of waste olive oil heat-treated (WOHT) oriental beech
Tablica 2. Vrijednosti gustoće apsolutno suhe kavkaske bukovine pregrijane u otpadnome maslinovu ulju (WOHT)

Treatment type* *Vrsta tretmana**	**Temperature, °C** *Temperatura, °C*	**Duration, h** *Trajanje,* h	**Mean** *Srednja vrijednost*	**Standard deviation** *Standardna devijacija*	**Homogeneity group** *Homogene grupe*	**Compared to control, %** *Usporedba s kontrolnim uzorkom, %*
Control *kontrolni uzorak*	-	-	0.658	0.03	A	-
WOHT	200	2	0.941	0.03	B	+43.0
WOHT	200	4	1.041	0.03	B	+55.2
WOHT	230	2	1.030	0.04	B	+56.5
WOHT	230	4	1.025	0.04	B	+55.7

*Ten samples were used for each treatment group. / *Za svaki tretman korišteno je deset uzoraka.*

% to 60 %. Higher duration and temperatures resulted in higher *WPG* of WOHT oriental beech.

3.2 Oven-dry wood density
3.2. Gustoća apsolutno suhog drva

The oven-dry density values of the waste olive oil heat-treated (WOHT) oriental beech are given in Table 2.

WOHT oriental beech has significantly higher oven dry density values, increasing from 43 % to 56.5 %. For WOHT oriental beech, the oven-dry density values increased from 0.941 g/cm^3 to 1.041 g/cm^3. WOHT oriental beech oven-dry density values increased at 200 °C for 2 h and 4 h, while they dropped at 230 °C for the same amount of time. There was a statistical difference in oven-dry density values between control and WOHT oriental beech. It might be the result of the treatment oil intake (Suri *et al.,* 2022). Okon *et al.* (2018) found that the density of *Cunninghamia lanceolata* wood heated with oil increased to 75 % during the first stage of the treatment due to oil uptake, but then decreased as the temperature and treatment time increased. They clarified that the decrease in density is caused by the pyrolysis and degradation of the cell wall polymers during oil heat treatment. In our investigation, treatments carried out at 230 °C for 2 h and 4 h resulted in lower oven-dry density values for WOHT oriental beech. According to Dubey *et al.* (2016), the density of *Pinus radiata* wood after oil heat treatment was noticeably enhanced to a level of about 80 % greater than that of the untreated control group. Our findings generally agree well with those of these researchers.

3.3 Water absorption levels
3.3. Razine upijanja vode

Water absorption (*WA*) levels of the waste olive oil heat-treated (WOHT) oriental beech are presented in Table 3 and Figure 1.

According to the findings, *WA* levels were greater in the early stages of *WA*, particularly within 2 h, 8 h,

Table 3 Water absorption levels of waste olive oil heat-treated (WOHT) oriental beech
Tablica 3. Razine upijanja vode kavkaske bukovine pregrijane u otpadnome maslinovu ulju (WOHT)

Treatment type* *Vrsta tretmana**	**Temperature, °C** *Temperatura, °C*	**Duration, h** *Trajanje,* h	**Water absorption levels** / *Razine upijanja vode, %*																	
			After 2 h	H.G**	After 8 h	H.G	After 24 h	H.G	After 48 h	H.G	After 72 h	H.G	After 96 h	H.G	After 120 h	H.G	After 144 h	H.G	After 168 h	H.G
Control *kontrolni uzorak*	-	-	34.23	B	54.80	C	64.91	C	68.59	C	77.80	C	80.73	C	82.02	C	83.42	C	83.82	C
WOHT	200	2	6.70	A	15.01	B	22.85	B	26.15	B	31.02	B	32.86	B	33.93	B	35.22	B	35.30	B
WOHT	200	4	4.59	A	8.52	AB	13.42	A	16.99	AB	20.35	AB	23.21	AB	24.68	AB	26.20	AB	27.18	AB
WOHT	230	2	3.59	A	7.91	AB	13.92	A	17.56	AB	22.36	AB	24.88	AB	26.42	AB	28.41	AB	28.93	AB
WOHT	230	4	2.33	A	5.05	A	8.79	A	11.23	A	14.05	A	16.72	A	18.08	A	20.41	A	21.81	A

*Ten samples were used for each treatment group. / *Za svaki tretman korišteno je deset uzoraka.*
**Homogeneity group / *Homogene grupe*

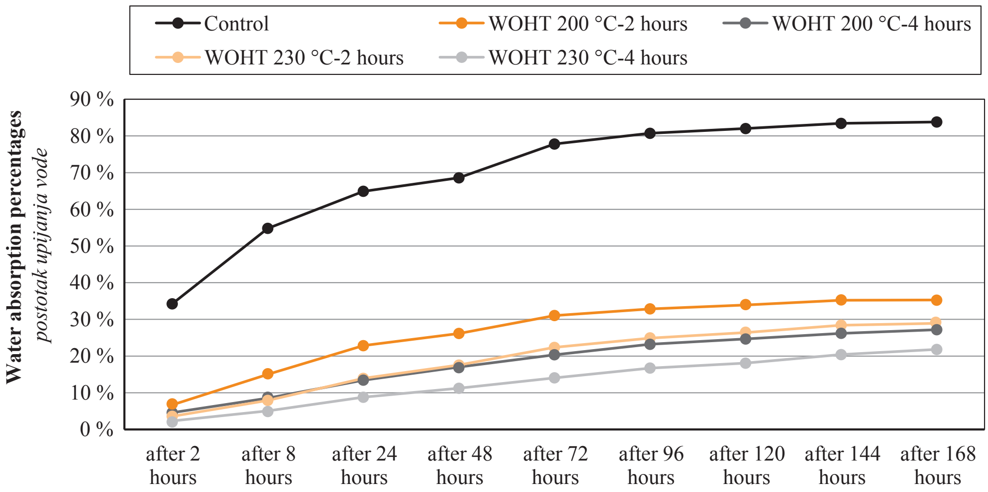

Figure 1 Water absorption percentages of oriental beech samples
Slika 1. Postotak upijanja vode uzoraka kavkaske bukovine

and 24 h, which is in line with the previous data (Alma, 1991; Hafızoğlu *et al*., 1994; Yıldız, 1994). These outcomes could be the consequence of *WA* being injected into wood empty hollow at the beginning of wetting and those spaces being smaller with time (Yalınkılıç *et al.*, 1995). In comparison to WOHT oriental beech, the water absorption (*WA*) levels of control samples were higher throughout both the initial and subsequent leaching periods. It might be because waste olive oil molecules can permeate into the water-swollen cell wall and stop or hinder the ability of treated wood samples to absorb water. The usage of waste olive oil has a water-repellent and bulking effect, which contributes significantly to the reduction of *WA*. According to a claim, the mass loss resulting from the breakdown of hemicellulose, the component of the cell wall that is most hydrophilic, after the thermal treatment of wood is the cause for the reduction in hygroscopicity of the material (Bourgois and Guyonnet, 1988). Some authors explained how vegetable oils can improve wood water repellency, while reducing water absorption. Vegetable oils produce a mechanical barrier function that prevents water from entering wood without forming any chemical bonds (Panov *et al*., 2010), and they also make wood water-repellent by permeating the tracheid lumen and parenchyma cells (Ulvcrona *et al.*, 2006). Plant oil that fills the cell lumen is stored on the exterior and partially on the interior surfaces of the wood, increasing the hydrophobicity of the surface. As a result, water absorption level is decreased because water enters wood pores through capillary action (Koski, 2008). Wang and Cooper (2005) found that soybean oil can bond in wood after analyzing the samples lowering water absorption rates after being heated with palm, soybean, and wax oils. The quality of the oil, the quantity absorbed, and the rate at which the oil is leached from the wood, all affect the success of oil treatments. It has been claimed that heat treatments under various atmospheric conditions, such as oil, steam, air, nitrogen, and vacuum have improved several wood qualities (Hakkou *et al*., 2005; Tjeerdsma and Militz, 2005; Welzbacher *et al*., 2008; Surini *et al*., 2012; Dubey *et al*., 2012; Boonstra *et al*., 2007a). Oriental beech that had been heated using waste olive oil (WOHT) had less WA than the control. These data show that lower values of *WA* were obtained (21.81 %) when the treatment temperature was 230 ºC for 4 hours, and the maximum *WA* was found in the control samples (83.82 %) after 168 hours of *WA*, indicating that a 62.01 % reduction had taken place. Our findings demonstrated that, for the total duration ranging from 2 to 168 hours, *WA* of control samples maintained a higher trend than oil heat-treated samples. A statistical difference between the control and WOHT oriental beech was seen in every period. According to Dubey *et al*., (2012), higher temperatures caused some chemical changes that had an impact on dimensional stability, and hydrophobic oils in the lumens prevented the walls from absorbing water. Hygroscopicity and water absorption in wood treated with oil heat decreased, according to several studies (Hofland and Tjeerdsma, 2005; Hyvonen *et al*., 2005). Some dry oils, like flaxseed oil, have molecules that are too big to pass through cell membranes, according to other studies. However, according to their claims, such oils mostly remained in the cell lumens and seeped into the wood to form a water-repellent outer layer (Olsson *et al.*, 2001; Hill, 2007; Wang, 2007). According to Hyvonen *et al.*, (2005) and Hofland and Tjeerdsma (2005), wood heated with tall oil and rapeseed oil reduced the intake of water. Linseed oil-heated aspen wood levels in *WA* were investigated by Bazyar (2012). He discovered that, whereas the WA levels in control samples were 99.99 %, they were only 22.9 % in aspen wood that had been heated in linseed oil. Our results are in good agreement with the above findings. According to our

Table 4 *CSPG* levels of waste olive oil heat-treated (WOHT) oriental beech
Tablica 4. *CSPG* razine za kavkasku bukovinu pregrijanu u otpadnome maslinovu ulju (WOHT)

Treatment type* Vrsta tretmana*	**Temperature** *Temperatura* °C	**Duration** *Trajanje* h	***CSPG*** N/mm²	**Standard deviation** *Standardna devijacija*	**Homogeneity group** *Homogene grupe*	**Compared to control** *Usporedba s kontrolnim uzorkom* %
Control *kontrolni uzorak*	-	-	56.01	7.40	A	-
WOHT	200	2	57.11	6.56	A	+1.96
WOHT	200	4	59.62	8.49	A	+6.44
WOHT	230	2	55.73	7.08	A	-0.49
WOHT	230	4	54.03	5.84	A	-3.53

*Ten samples were used for each treatment group. / *Za svaki tretman korišteno je deset uzoraka.*

investigation, the water absorption levels of the control samples climbed to 83.82 % after 168 hours of *WA*, whereas it changed from 21.81 to 35.30 % for WOHT oriental beech.

3.4 Compression strength parallel to grain (*CSPG*)
3.4. Čvrstoća na tlak paralelno s vlakancima (*CSPG*)

The compression strength parallel to the grain (*CSPG*) values of the waste olive oil heat-treated (WOHT) oriental beech is presented in Table 4.

In our study, the greatest *CSPG* for WOHT oriental beech was 59.62 N/mm² at 200 °C for 4 h, while the *CSPG* value of the control was 56.01 N/mm²; the values for WOHT oriental beech were modified from 54.03 to 59.62 N/mm². The *CSPG* values between the control group and WOHT oriental beech showed no statistical differences at 95 % confidence levels. In comparison to the control, WOHT oriental beech had higher *CSPG* values for 2 and 4 hours at 200 °C. Oil is thought to fill the lumen, thicken the cell wall, and improve the lateral stability of the wood (Tomak *et al.,* 2011). Cheng *et al*. (2014) discovered that, after oil heat treatment, the *CSPG* for poplar wood increased primarily because of the high oil uptake, which thickened the fibers and improved their longitudinal strength. According to Suri *et al.* (2022), samples heated in oil exhibited significantly higher axial compressive strength than samples heated in air, with *Pinus koraiensis* exhibiting a bigger rise in compressive strength than *Paulownia tomentosa*. The increase in axial compressive strength following oil heat treatment may be attributed to several factors, including the higher density of samples that had undergone oil heat treatment, as well as the oil thickening and filling of cell wall lumens. According to Hao *et al.* (2021), as the temperature of the oil heat treatment increases, the compressive strength parallel to grain initially rises before falling. The compressive strength parallel to grain of the oil heat-treated samples is lower than that of the untreated samples at temperatures up to 200 °C. In our investigation, WOHT oriental beech heated at 230 °C for 2 hours and 4 hours exhibited lower *CSPG* values than WOHT oriental beech heated at 200 °C for 2 hours, 4 hours, and the control group. As a result, our results are in line with the previous research.

4 CONCLUSIONS
4. ZAKLJUČAK

Oven-dry density, water absorption (*WA*) levels, and compression strength parallel to the grain (*CSPG*) of WOHT wood were studied.

The WOHT oriental beech had higher oven-dry density than the control group. Our findings demonstrated that WOHT oriental beech oven-dry densities were lowered at 230 °C for 2 h and 4 h. For all *WA* periods, the *WA* of WOHT wood was lower than that of the control group. The *CSPG* values of WOHT oriental beech heated at 200 °C for 2 h and 4 h were greater than those of the control group. However, WOHT oriental beech *CSPG* levels decreased during 2 h and 4 h treatments at 230 °C.

In summary, the mechanical and physical characteristics of WOHT oriental beech wood have been generally improved. They lead to increased oven dry density values as well as reduced *WA* levels. Moreover, except for at 230 °C for 2 h and 4 h, *CSPG* values of oriental beech at 200 °C for 2 h and 4 h were higher than those of the control group. Thus, WOHT oriental beech may be a substitute structural material for exterior and interior application, depending on the level of mechanical and physical requirements.

Acknowledgements – Zahvala

This study was based on Mehmet Ali Kapçak's Engineering Project Study titled "Determination of physical, mechanical, weathering characteristics, decay resistance, and combustion properties of oriental beech wood heat-treated with waste olive oil". The aforementioned project was funded by TÜBİTAK under project application number: 1919B012204654, as part of the 2209-A University student's research projects.

5 REFERENCES
5. LITERATURA

1. Alma, H., 1991: Çeşitli ağaç türlerinde su alınımının ve çalışmanın azaltılması. Yüksek Lisans Tezi, Karadeniz Teknik Üniversitesi, Trabzon, Turkey, 104 (in Turkish).
2. Aytin, A.; Korkut, S.; Ünsal, O.; Çakıcıer, N., 2015: The effects of heat treatment with the ThermoWood® method on the equilibrium moisture content and dimensional stability of wild cherry wood. BioResources, 10 (2): 2083-2093. https://doi.org/10.15376/biores.10.2.2083-2093
3. Bak, M.; Németh, R., 2012: Changes in swelling properties and moisture uptake rate of oil-heat-treated poplar (*Populus× euramericana* cv. Pannonia) wood. BioResources, 7 (7): 5128-5137. https://doi.org/10.15376/biores.7.7.5128-5137
4. Bal, B. C.; Bektaş, İ., 2013: The effects of heat treatment on some mechanical properties of juvenile wood and mature wood of *Eucalyptus grandis*. Drying Technology, 31 (4): 479-485. https://doi.org/10.1080/07373937.2012.742910
5. Bazyar, B., 2012: Decay resistance and physical properties of oil heat treated aspen wood. BioResources, 7 (1): 696-705. https://doi.org/10.15376/biores.7.7.696-705
6. Boonstra, M. J.; Van Acker, J.; Tjeerdsma, B. F.; Kegel, E. V., 2007a: Strength properties of thermally modified softwoods and its relation to polymeric structural wood constituents. Annals of Forest Research, 64 (7): 679-690. https://doi.org/10.1051/forest:2007048
7. Boonstra, M. J.; Van Acker, J.; Kegel, E.; Stevens, M., 2007b: Optimisation of a two-stage heat treatment process: durability aspects. Wood Science and Technology, 41 (1): 31-57. https://doi.org/10.1007/s00226-006-0087-4
8. Bourgois, J.; Guyonnet, R., 1988: Characterization and analysis of torrefied wood. Wood Science and Technology, 22 (2): 143-155. https://doi.org/10.1007/BF00355850
9. Cheng, D.; Chen, L.; Jiang, S.; Zhang, Q., 2014: Oil uptake percentage in oil-heat-treated wood, its determination by soxhlet extraction and its effects on wood compression strength parallel to the grain. BioResources, 9 (1): 120-131. https://doi.org/10.15376/biores.9.1.120-131
10. Dubey, M. K.; Pang, S.; Walker, J., 2012: Changes in chemistry, color, dimensional stability and fungal resistance of *Pinus radiata* D. Don wood with oil heat-treatment. Holzforschung, 65 (1): 49-57. https://doi.org/10.1515/HF.2011.117
11. Dubey, M. K.; Pang, S.; Chauhan, S.; Walker, J., 2016: Dimensional stability, fungal resistance and mechanical properties of radiata pine after combined thermo-mechanical compression and oil heat-treatment. Holzforschung, 70 (8): 793-800. https://doi.org/10.1515/hf-2015-0174
12. Esteves, B.; Pereira, H., 2009: Wood modification by heat treatment: A review. BioResources, 4 (1): 370-404. https://doi.org/10.15376/biores.4.1.370-404
13. Esteves, B.; Velez Marques, A.; Domingos, I.; Pereira, H., 2008: Heat-induced colour changes of pine (*Pinus pinaster*) and eucalypt (*Eucalyptus globulus*) wood. Wood Science and Technology, 42 (5): 369-384. https://doi.org/10.1007/s00226-007-0157-2
14. Forsman, S., 2008: Heat treated wood – The concept house development. MSc Thesis, Luleå University of Technology Sweden, p.107.
15. Guller, B., 2012: Effects of heat treatment on density, dimensional stability and color of *Pinus nigra* wood. African Journal of Biotechnology, 11 (9): 2204-2209. https://doi.org/10.5897/ajb11.3052
16. Hafızoğlu, H.; Yalınkılıç, M. K.; Yıldız, Ü. C.; Baysal, E.; Demirci, Z.; Peker, H., 1994: Türkiye bor kaynaklarının odun koruma (emprenye) endüstrisinde değerlendirilebilme imkanları. Tübitak Projesi, Proje No: TOAG-875, Turkiye, 392s (in Turkish).
17. Hakkou, M.; Pétrissans, M.; Zoulalian, A.; Gérardin, P., 2005: Investigation of wood wettability changes during heat treatment on the basis of chemical analysis. Polymer Degradation and Stability, 89 (1): 1-5. https://doi.org/10.1016/j.polymdegradstab.2004.10.017
18. Hao, X.; Wang, Q.; Wang, Y.; Han, X.; Yuan, C.; Cao, Y.; Lou, Z.; Li, Y., 2021: The effect of oil heat treatment on biological, mechanical and physical properties of bamboo. Journal of Wood Science, 67 (1): 1-14. https://doi.org/10.1186/s10086-021-01959-7
19. Hill, C. A., 2007: Wood modification: chemical, thermal and other processes. John Wiley & Sons, p. 264.
20. Hofland, A.; Tjeerdsma, B. F., 2005: Wood protection by chemical modification. ECOTAN 3rd Report, Part, 3.
21. Hyvonen, A.; Piltonen, P.; Nelo, M.; Niinimaki, J., 2005: Wood protection of tomorrow – Potential of modified crude tall oil formulations in wood protection. In: Proceedings of the Seventh Finnish Conference of Environmental Sciences. Jyväskylä, Finland.
22. Kesik, H.; Vurdu, H.; Çağatay, K.; Özkan, Ö.; Öncel, M., 2015: Yağlı ısıl işlem görmüş sarıçam odunlarında koruyucu katmanın yapışma ve sertlik özellikleri. Kastamonu Universitesi Orman Fakültesi Dergisi, 15 (2): 261-266 (in Turkish). https://doi.org/10.17475/kuofd.34547
23. Kiguchi, M.; Evans, P. D., 1998: Photostabilisation of wood surfaces using a grafted benzophenone UV absorber. Polymer Degradation and Stability, 61 (1): 33-45. https://doi.org/10.1016/S0141-3910(97)00124-9
24. Koski, A., 2008: Applicability of crude tall oil for wood protection. Acta Universitatis Ouluensis C Technica 293, Oulu.
25. Lee, S. H.; Ashaari, Z.; Lum, W. C.; Halip, J. A.; Ang, A. F.; Tan, L. P.; Chin, K. T.; Tahir, P. M., 2018: Thermal treatment of wood using vegetable oils: A review. Construction and Buildings Materials, 181: 408-419. https://doi.org/10.1016/j.conbuildmat.2018.06.058
26. Mastouri, A.; Efhamisisi, D.; Shirmohammadli, Y.; Oladi, R., 2021: Physicochemical properties of thermally treated poplar wood in silicone and rapeseed oils: A comparative study. Journal of Building Engineering, 43: 102511. https://10.1016/j.jobe.2021.102511
27. Okon, K. E.; Lin, F.; Lin, X.; Chen, C.; Chen, Y.; Huang, B., 2018: Modification of Chinese fir (*Cunninghamia lanceolata* L.) wood by silicone oil heat treatment with micro-wave pretreatment. European Journal of Wood and Wood Products, 76 (1): 221-228. https://doi.org/10.1007/s00107-017-1165-z
28. Olsson, T.; Megnis, M.; Varna, J.; Lindberg, H., 2001: Measurement of the uptake of linseed oil in pine by the use of an X-ray microdensitometry technique. Journal of Wood Science, 47 (4): 275-281. https://doi.org/10.1007/BF00766713
29. Panov, D.; Terziev, N.; Daniel, G., 2010: Using plant oils as hydrophobic substances for wood protection. In: Proceedings of 41st Annual Meeting of the International Research Group on Wood Protection, Biarritz, France, 9-13 May 2010. IRG Secretariat.
30. Pelit, H.; Yorulmaz, R., 2019: Influence of densification on mechanical properties of thermally pretreated spruce and poplar wood. BioResources, 14 (4): 9739-9754. https://doi.org/10.15376/biores.14.4.9739-9754

31. Rapp, A. O.; Sailer, M., 2001: Oil-heat-treatment of wood-process and properties. In: Proceedings of International Conference: Wood in Construction Industry – Tradition and Future. Zagreb, Croatia.
32. Srinivas, K.; Pandey, K. K., 2012: Effect of heat treatment on color changes, dimensional stability and mechanical properties of wood. Journal of Wood Chemistry and Technology, 32 (4): 304-316. https://doi.org/10.1080/02773813.2012.674170
33. Suri, I. F.; Purusatama, B. D.; Kim, J. H.; Yang, G. U.; Prasetia, D.; Kwon, G. J.; Hidayat, W.; Lee, S. H.; Febrianto, F.; Kim, N. H., 2022: Comparison of physical and mechanical properties of *Paulownia tomentosa* and *Pinus koraiensis* wood heat-treated in oil and air. European Journal of Wood and Wood Products, 80 (6): 1389-1399. https://doi.org/10.1007/s00107-022-01840-4
34. Su, W. Y., 1997: Development of fire retardant wood composites using boron compound and their evaluation methods. Master Thesis, Kyoto University Kyoto, Japan, p. 126.
35. Surini, T.; Charrier, F.; Malvestio, J.; Charrier, B.; Moubarik, A.; Castéra, P.; Grelier, S., 2012: Physical properties and termite durability of maritime pine *Pinus pinaster* Ait., heat-treated under vacuum pressure. Wood Science and Technology, 46 (1): 487-501. https://doi.org/10.1007/s00226- 011- 0421-3
36. Taşdelen, M.; Can, A.; Sivrikaya, H., 2019: Some physical and mechanical properties of maritime pine and poplar exposed to oil-heat treatment. Turkish Journal of Forest Science, 20 (3): 254-260. https://doi.org/10.18182/tjf.566647
37. Thybring, E. E., 2013: The decay resistance of modified wood influenced by moisture exclusion and swelling reduction. International Biodeterioration & Biodegration, 82: 87-95. https://doi.org/10.1016/j.ibiod.2013.02.004
38. Tjeerdsma, B. F.; Militz, H., 2005: Chemical changes in hydrothermal treated wood: FTIR analysis of combined hydrothermal and dry heat-treated wood. Holz als Roh-und Werkstoff, 63 (2): 102-111. https://doi.org/10.1007/s00107-004- 0532-8
39. Türkoğlu, T.; Toker, H.; Baysal, E.; Kart, Ş.; Yüksel, M.; Ergün, M. E., 2015: Some surface properties of heat treated and natural weathered oriental beech. Wood Research, 60 (6): 881-890. http://www.woodresearch.sk/intro.php
40. Tomak, E. D.; Viitanen, H.; Yildiz, U. C.; Hughes, M., 2011: The combined effects of boron and oil heat treatment on the properties of beech and Scots pine wood. Part 2: Water absorption, compression strength, color changes and decay resistance. Journal of Materials Science, 46: 608-615. https://doi. org/10.1007/s10853-010-4860-2
41. Ulvcrona, T.; Lindberg, H.; Bergsten, U., 2006: Impregnation of Norway spruce (*Picea abies* L. Karst.) wood by hydrophobic oil and dispersion patterns in different tissues. Forestry, 79 (1): 123-134. https://doi.org/10.1093/forestry/cpi064
42. Ünsal, O.; Ayrılmış, N., 2005: Variations in compression strength and surface roughness of heat-treated Turkish river red gum (*Eucalyptus camaldulensis*) wood. Journal of Wood Science, 51 (4): 405-409. https://doi.org/10.1007/s10086-004-0655-x
43. Var, A. A.; Yalçın, M.; Yalçın, O. U.; Demir, M., 2021: Effects of hot-cold oil treatment on biological resistance and physical properties of *brutia pine* sapwood. Maderas-Ciencia y Tecnologia, 23 (42): 1-12. http://dx.doi.org/10.4067/s0718-221x2021000100442
44. Vukas, N.; Horman, I.; Hajdarević, S., 2010: Heat treated wood. In: Proceedings of 14th International Research / Expert Conference "Trends in the Development of Machinery and Associated Technology", TMT 2010, 11-18 September, Mediterranean Cruise.
45. Wang, X. H.; Fei, B. H.; Liu, J. L., 2014: Efect of vacuum heat treatment temperature on physical and mechanical properties of *Eucalyptus pellita* wood. Wood and Fiber Science, 46 (3): 368-375. https://wfs.swst.org/index.php/wfs/article/view/1042
46. Wang, J., 2007: Initiating evaluation of thermal-oil treatment for post-MPB lodgepole pine. Forintek Canada Corp., Vancouver, BC, Canada.
47. Wang, J. Y.; Cooper, P. A., 2005: Effect of oil type, temperature and time on moisture properties of hot oil-treated wood. Holz als Roh-und Werkstoff, 63 (6): 417-422. https://doi.org/10.1007/s00107-005-0033-4
48. Welzbacher, C.; Rapp, A., 2005: Durability of different heat treated materials from industrial processes in ground contact. The International Research Group on Wood Preservation. Document no. 05-40312. In: Proceedings of 36th Annual Meeting, Bangalore, India.
49. Welzbacher, C. R.; Wehsener, J.; Rapp, A. O.; Haller, P., 2008. Thermo-mechanical densification combined with thermal modification of Norway spruce (*Picea abies* Karst) in industrial scale – Dimensional stability and durability aspects. Holz als Roh-und Werkstoff, 66 (1): 39-49. https://doi.org/10.1007/s00107-007-0198-0
50. Yalınkılıç, M. K.; Baysal, E.; Demirci, Z., 1995: Borlu bileşiklerle emprenye edilmiş Duglas odunundan borun yıkanma oranları ve çeşitli su itici maddelerle yıkanmanın önlenmesi. Atatürk Üniversitesi, Çevre Sempozyumu Eylül 1995 (s. 501-511) (in Turkish).
51. Yıldız, Ü. C., 1994: Bazı hızlı büyüyen ağaç türlerinden hazırlanan odun-polimer kompozitlerinin fiziksel ve mekanik özellikleri. Doktora Tezi, Karadeniz Teknik Üniversitesi, Fen Bilimleri Enstitüsü, Trabzon, Türkiye, 307s. (in Turkish).
52. Yingprasert, W.; Matan, N.; Chaowana, P., 2015: Fungal resistance and physico-mechanical properties of cinnamon oil and clove oil-treated rubberwood particleboards. Journal of Tropical Forest Science, 27 (1): 69-79.
53. ***Finnish Thermowood Association, 2003: Thermowood handbook, Helsinki, Finland, pp.66.
54. ***TS ISO 13061-2:2021 Physical and mechanical properties of wood – Test methods for small clear wood samples. Part 2: Determination of density for physical and mechanical tests.
55. ***TS ISO 3129:2021 Wood – Sampling methods and general requirements for physical and mechanical testing of small clear wood samples.
56. ***TS 2595:1977 Wood-determination of ultimate stress in compression parallel to grain. Turkish Standardization Institute.

Corresponding address:

ÇAĞLAR ALTAY

Aydın Adnan Menderes University, Aydın Vocational School, Aydın, TURKEY, e-mail: caglar.altay@adu.edu.tr

Zafer Kaya[*1], Sait Dundar Sofuoglu[2]

Use of Spinning Rollers for Surface Densification of Wood

Uporaba rotirajućih valjaka za ugušćivanje površine drva

ORIGINAL SCIENTIFIC PAPER
Izvorni znanstveni rad
Received – prispjelo: 4. 7. 2023.
Accepted – prihvaćeno: 12. 1. 2024.
UDK: 630*82; 674.02
https://doi.org/10.5552/drvind.2024.0139

ABSTRACT • *In this study, softwood cedar of Lebanon (Cedrus libani A.Rich.) and hardwood black poplar (Populus nigra L.), turned into cylinders by turning, were subjected to a surface densification process. Densification was carried out on the lathe using the spinning roller designed and manufactured for this purpose. Hardness, brightness and roughness (R_z) measurements were carried out on undensified and densified regions of the cylindrical solid wood materials. An increase in hardness and brightness and a decrease in roughness values occurred under all densification conditions. The highest surface hardness values occurred in cedar of Lebanon at 0.081 mm/rev feed, 200 rpm spindle speed, and 1 mm densification depth. On densified wood surfaces, as the feed from the densification parameters increases, the hardness decreases, and as the densification depth increases, the hardness increases-. The effect of surface densification parameters on the gloss and roughness results of the samples shows no linear effect in terms of experimental parameters. In both species, lower spring back was obtained at low depth of densification.*

KEYWORDS: *surface densification; spinning roller; roughness; glossiness; hardness*

SAŽETAK • *U ovom su istraživanju cilindrični uzorci drva libanonskog cedra (Cedrus libani A.Rich.) i srži drva crne topole (Populus nigra L.) bili podvrgnuti procesu ugušćivanja površine. Postupak je obavljen na tokarskom stroju uz pomoć posebno dizajniranoga i proizvedenoga rotirajućeg valjka. Mjerenja tvrdoće, svjetline i hrapavosti (R_z) površine provedena su na neugušćenim i ugušćenim dijelovima cilindričnih uzoraka drva. Povećanje vrijednosti tvrdoće i svjetline te smanjenje vrijednosti hrapavosti dogodilo se pri svim uvjetima ugušćivanja. Najveće vrijednosti površinske tvrdoće zabilježene su na uzorku drva libanonskog cedra pri posmičnoj brzini 0,081 mm/okr., frekvenciji vrtnje vretena 200 min^{-1} i dubini ugušćivanja 1 mm. Na ugušćenim se površinama drva s povećanjem posmične brzine tvrdoća smanjivala, a s povećanjem dubine ugušćivanja tvrdoća se povećavala. Utjecaj parametara ugušćivanja površine na sjaj i hrapavost uzoraka ne pokazuje linearni odnos u sklopu eksperimentalnih parametara. Za obje vrste drva dobiven je manji elastični povrat pri manjoj dubini ugušćivanja.*

KLJUČNE RIJEČI: *ugušćivanje površine; rotirajući valjak; hrapavost; sjaj; tvrdoća*

[*] Corresponding author
[1] Author is researcher at Zafer Kaya (Kutahya Dumlupinar University, Simav Vocational School, Simav, Kutahya, Turkey. https://orcid.org/0000-0002-5489-3997
[2] Author is researcher at Sait Dundar Sofuoglu (Kutahya Dumlupinar University, Simav Technical Faculty, Department of Wood Works Industrial Engineering, Simav, Kutahya, Turkey. https://orcid.org/0000-0002-1847-6985

1 INTRODUCTION
1. UVOD

It is known that properties such as durability, hardness, and strength are generally insufficient for wood, especially in wood materials with a low density. When these properties are demanded, the use of high-density wood material or densified wood can become an alternative to other materials (Sandberg *et al*., 2021). Density is a factor affecting the mechanical properties of wood material (Blomberg and Persson, 2004). In recent years, when environmental awareness has increased, new environmentally friendly densification methods have started to be used (Senol and Budakci, 2016; Korkut and Kocaefe, 2009) such as densification using temperature and pressure in an open system known as thermo-mechanical (TM) (Sofuoglu, 2022; Sofuoglu *et al*., 2022; Salca *et al*., 2021; Tosun and Sofuoglu, 2021) and densification using temperature, pressure and steam in a closed system called thermo-hygro-mechanical (THM) (Parvis Navi, 2012). In addition to these, there is densification made by temperature and pressure after pre-softening with steam, which is called Viscoelastic-Thermal-Compression (VTC). There are also methods such as densification using temperature, pressure and vibration, called Thermo-Vibro-Mechanical (TVM) (Senol, 2018; Bekhta *et al*., 2017; Senol and Budakci, 2016).

There are studies in the literature on density analysis and various mechanical properties in densified and heat-treated wood materials (Croitoru *et al*., 2018; Burgos and Rolleri, 2012). Mechanical properties including the modulus of elasticity (MoE), modulus of rupture (MoR) (Wehsener *et al*., 2023), hardness, and surface hardness (Gao *et al*., 2019), and Janka hardness (Pertuzzatti *et al*., 2018) increased with densification. Surface hardness increased with densification (Senol and Budakci, 2019; Laskowska, 2017). The hardness values in the radial and tangential directions of the densified samples increased depending on the compression rate in the cell walls (Budakci *et al*., 2016). The surface wettability showed that surface-densified wood has good wetting protection (Rautkari *et al*., 2010). Research has been done to determine and minimize the amount of spring back and set recovery (Scharf *et al*., 2023; Neyses *et al*., 2020; Kariz *et al*., 2017). The following results were obtained in the study carried out to determine the surface properties of the surfaces obtained by applying top surface treatments. Surface roughness decreased, and surface brightness increased in densified samples. The surface brightness and hardness values increased with the increase of densification and densification ratio (Sofuoglu, 2022).

Turned wood materials are used for tool handles, wooden toys, stair railings, furniture pieces, etc. As the density increases in wood materials, porosity decreases, and smoother surfaces are obtained. Surface roughness is an important parameter in determining the economic value of wooden materials and has an important place in the success of upper surface quality. Especially when low-density wood materials are used, the mechanical properties can be improved by densification (Sogutlu, 2005). Smooth surfaces obtained by turning processes performed in accordance with the standard technique increase the success of varnishing and painting processes. Thus, more economical production can be made by using less materials and labor in surface treatments (Gurleyen, 1998). Although cylindrical wood materials have a wide area of use, scientific studies on surface densification have not been found in the literature as a result of research. It is believed that, when cylindrical, turned wood materials improve their properties by surface densification process, their areas of use increase and they can be used for a longer time without losing their surface properties. Thus, natural wood materials, which are depleted day by day, can be used more optimally.

In accordance with this purpose, in this study, surface densification was carried out using various densification parameters of cylindrical wood material. It is aimed to obtain the most suitable densification conditions in cylindrical materials by determining the high hardness and brightness and low roughness values, which are important for the use after densification.

2 MATERIALS AND METHODS
2. MATERIJALI I METODE

In the present study, cedar of Lebanon (*Cedrus libani* A.Rich.) (softwood) and black poplar (*Populus nigra* L.) (hardwood) were used (Table 1). These species are commonly grown and used in Turkey (Doğu *et al*., 2001).

The density of wood species at 12 % moisture content was determined according to ISO 13061 (ISO 13061-2:2014) standards. They were conditioned at temperatures of ~ (20±2) °C and (65±5) % relative humidity (*RH*) to moisture content (*MC*) of about 12 % (ISO 13061-1:2014).

The experimental specimens were cut from the log prismatically with a size of 2 cm × 2 cm × 32 cm. The remaining 5 cm of the test sample on the lathe chuck side was left as a 2 cm × 2 cm square. It was connected to the four-legged lathe chuck from this square section. It was connected between the chuck and the tailstock on a universal lathe and machined until it reached an average diameter of 1.9 cm. After the turning process, channels with a depth and width of 4 mm were made using a grooving tool to create 5 cm long sections. 5 cylindrical sections were made on the experimental specimens. The

Table 1 Basic properties of the studied wood species
Tablica 1. Osnovna svojstva istraživanih vrsta drva

Wood species *Vrsta drva*	**Density, kg/m³** *Gustoća,* kg/m³	**Number of rings per cm** *Broj godova po* cm	**Moisture content** *Sadržaj vode*	**Age of trees** *Starost drva*	**Region** *Regija*
Black poplar *drvo crne topole*	340	0.78	12 %	12	Bahcekoy, Istanbul, Turkey
Cedar of Lebanon *drvo libanonskog cedra*	520	1.77	12 %	75	Simav/Kutahya Turkey

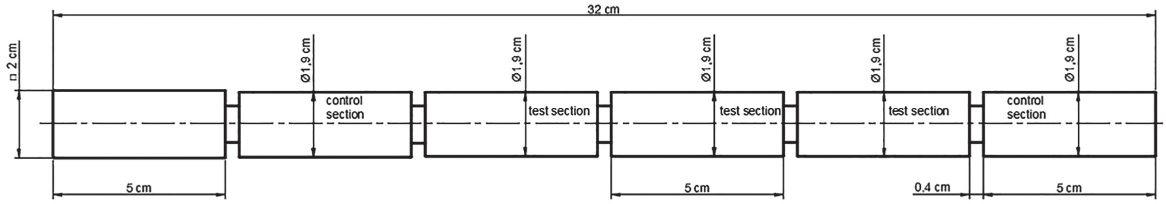

Figure 1 Technical drawing of test specimen
Slika 1. Tehnički crtež ispitnog uzorka

experimental parameters were applied to 3 of them, and the remaining 2 sections left at the end and at the tip of the sample were determined as control sections. A structure was obtained on the test specimen in which different test parameters would be created in each section. After all cylindrical turning and grooving operations, the surfaces were smoothed with 400-grit sandpaper. Each experiment parameter was performed 3 times in such a way that it was in a different part of another experiment specimen and their averages were taken. A total of 12 test specimens were used to complete the experiments (Figure 1).

The cylinder axis of the densification apparatus and the tall stock axis were aligned for the densification process. The apparatus was connected to the tool post section of the lathe. The measurement was reset when the densification cylinder started to rotate as soon as it contacted the test specimen. In order to keep bending to a minimum, low densification depths such as 0.5 mm and 1 mm, which are experimental parameters, were preferred. Experience obtained from other similar studies using the densification apparatus have also shown that the bending problem on the specimens in the experiments can be ignored for these densification depths.

2.1 Densification apparatus
2.1. Oprema za ugušćivanje

The assembly technical drawing of the spinning roller, which has been specially designed and manufactured for surface densification is shown in Figure 2. The surface densification process on a universal lathe, the shape of the specimen, the direction of densification and the details of the spinning roller set are presented in Figure 3. The densification parameters and levels are shown in Table 2. Among the process parameters, feed is the distance taken by the densification apparatus in mm for each revolution of the specimen. Spindle speed is the number of revolutions per minute of the test specimen. Experimental process of the study is presented in Figure 4.

Table 2 Process parameters used in turning of black poplar and cedar of Lebanon
Tablica 2. Parametri procesa tokarenja drva crne topole i libanonskog cedra

Parameter / *Parametar*	**Coded levels** *Oznake razina*		
	Level 1	Level 2	Level 3
Feed, mm/rev *posmična brzina,* mm/okr.	0.081	0.121	0.202
Spindle speed, rpm *brzina vretena,* okr./min	200	400	
Dept of densification, mm *dubina ugušćivanja,* mm	0.5	1	

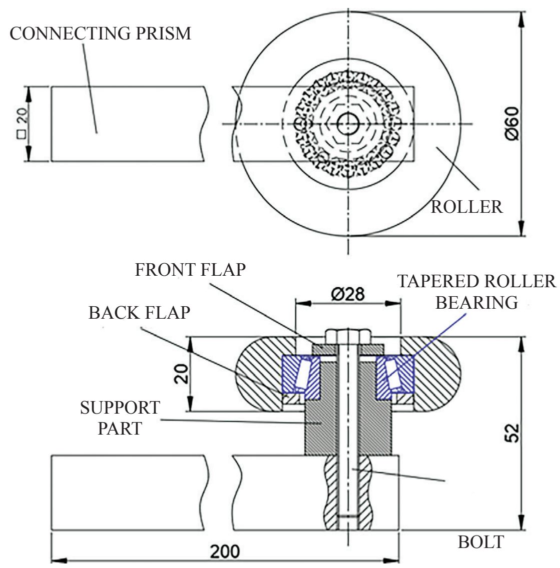

Figure 2 Technical drawing of spinning roller assembly
Slika 2. Tehnički crtež sklopa rotirajućeg valjka

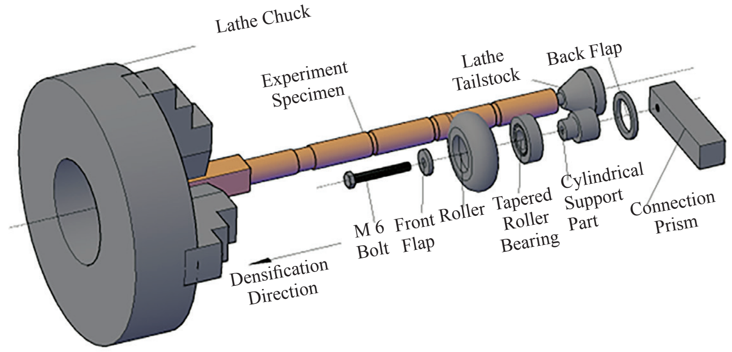

Figure 3 Densification system elements and details of assembly structure
Slika 3. Elementi sustava za ugušćivanje s detaljima

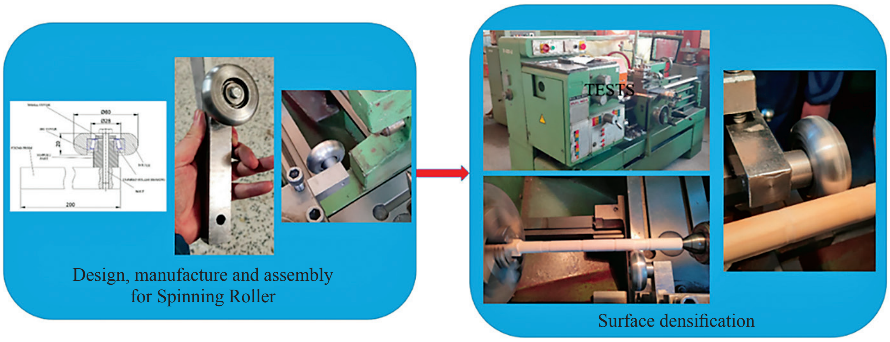

Figure 4 Schematic representation of experimental design
Slika 4. Shematski prikaz postavke eksperimenta

2.2 Determining surface glossiness, hardness and roughness
2.2. Određivanje sjaja, tvrdoće i hrapavosti površine

In the study, glossmeter (BYK Gardner brand Micro-TRI-gloss µ) was used for gloss measurements at 60°. Measurements were made according to the principles specified in EN ISO 2813:2014. The surface hardness was measured using a Shore D hardness tester (Tronic PD800). Surface roughness measurements were taken parallel to the grain at three separate points on each specimen according to ISO 468:2009 using a surface roughness tester (Time TR200, Time Group Inc., China). The measuring parameter (R_z) is described in ISO 468. The stylus probe speed was set to 10 mm/min, the diameter of the measurement needle was 4 µm, and the needle tip was 90°.

In the experimental specimen, 3 repeated hardness, roughness and brightness measurements were taken in the direction parallel to the fibers on the section where the experimental parameter was applied, and their averages were used. The same measurements were repeated for the control sections located at the tip and end of the experimental specimen, and were used for comparison with the sections where the test parameters were applied.

2.3 Determining compression ratio and spring-back
2.3. Određivanje stupnja ugušćenja i elastičnog povrata

In the study, the instantaneous compression ratio and instantaneous spring-back were evaluated depending on the densification parameters. The diameters of the test specimens were measured from 4 different points before the surface densification process and the average of the measurements was taken (D_{start}). The same measurement process was performed after the densification parameters were applied and the average diameters were determined by completing the process (D_{end}). Two surface densification depths of 0.5 mm and 1 mm were used in the study. Theoretical diameters are obtained when the densification depths are subtracted from the initial diameters of the test specimens ($D_{teor.}$). In addition to the surface densification depths, the average theoretical % compression ratio, the average experimental % compression ratio, and the average spring-back were found to depend on the feed and spindle speed. The theoretical % compression ratio (*Teo.C.R.*, %) was calculated with Eq. 1. Here x refers to the densification depths, and the results were obtained by taking 0.5 mm and 1 mm. Experimental % compression ratio (*Exp.C.R.*, %) was calculated using Eq. 2. In this equation, the average diameters before the experiment (D_{start}) and after the experiment (D_{end}) were used. In Eq. 3, the spring-back was calculated by taking the percentage of the difference between the average diameters after the experiment (D_{end}) and the theoretical diameters ($D_{teor.}$) were found.

$$Teo.C.R.(\%) = \frac{(D_{start} - (D_{start} - x))}{(D_{start} - x)} \cdot 100 \quad (1)$$

$$Exp.C.R.(\%) = \frac{(D_{start} - D_{end})}{(D_{start})} \cdot 100 \quad (2)$$

$$Spring-back\left(\%\right)=\frac{\left(D_{end}-D_{teor.}\right)}{\left(D_{teor.}\right)}\cdot 100 \qquad (3)$$

3 RESULTS AND DISCUSSION
3. REZULTATI I RASPRAVA

Hardness, brightness, and roughness parameter values measured on densified surfaces are given in Tables 3, 4 and 5.

3.1 Evaluation of glossiness, hardness and surface roughness
3.1. Analiza sjaja, tvrdoće i hrapavosti površine

In both wood species, under all surface densification conditions, an increase in brightness values occurs as densification increases. Senol and Budakci (2016) and Sofuoglu (2022) showed that an increase in brightness values occurred after TVM and TM densification processes in solid wood materials. The highest brightness values are very close to each other in the black poplar, but they were formed under the 4th and 8th process number surface densification conditions, while in cedar of Lebanon the highest brightness value was obtained under the 5th process number surface densification conditions. When comparing the brightness values between the wood types in Table 3 and 4, it can be seen that higher brightness values were obtained in the black poplar after all the surface densification processes.

In both wood species, hardness values increased with densification in all surface densification conditions. Similar results were found in some other studies (Sofuoglu, 2022; Schwarzkopf, 2021; Laskowska, 2017; Budakci *et al.*, 2016; Senol and Budakci, 2016; Rautkari *et al.*, 2009). The highest hardness values are very close to each other in the black poplar, but they

Table 3 Hardness and glossiness values obtained according to surface densification conditions for black poplar
Tablica 3. Vrijednosti tvrdoće i sjaja za površinski ugušćeno drvo crne topole pri različitim uvjetima

Process number *Broj procesa*	**Feed, mm/rev** *Posmična brzina,* mm/okr.	**Spindle speed, rpm** *Frekvencija vrtnje vretena,* okr./min	**Densification depth, mm** *Dubina ugušćivanja,* mm	**Hardness, Shore D** *Tvrdoća,* Shore D		**Glossiness, GU** *Sjaj,* JS	
				Control *Kontrolni uzorak*	**Densified** *Ugušćeno*	**Control** *Kontrolni uzorak*	**Densified** *Ugušćeno*
1	0.081	200	0.5	39.50	41.25	2.97	3.33
2	0.081	200	1	44.50	51.75	2.50	2.70
3	0.081	400	0.5	40.40	45.40	2.70	2.93
4	0.081	400	1	40.90	48.40	2.83	3.63
5	0.121	200	0.5	39.50	43.25	2.97	3.43
6	0.121	200	1	44.50	51.50	2.73	2.93
7	0.121	400	0.5	40.40	43.80	2.70	3.00
8	0.121	400	1	40.90	41.86	2.83	3.67
9	0.202	200	0.5	39.50	40.75	2.97	3.27
10	0.202	200	1	44.50	48.75	2.73	3.13
11	0.202	400	0.5	40.40	43.20	2.70	2.80
12	0.202	400	1	40.90	41.00	2.83	3.33

Table 4 Hardness and glossiness values obtained according to surface densification conditions for cedar of Lebanon
Tablica 4. Vrijednosti tvrdoće i sjaja za površinski ugušćeno drvo libanonskog cedra pri različitim uvjetima

Process number *Broj procesa*	**Feed, mm/rev** *Posmična brzina,* mm/okr.	**Spindle speed, rpm** *Frekvencija vrtnje vretena,* okr./min	**Densification depth, mm** *Dubina ugušćivanja,* mm	**Hardness, Shore D** *Tvrdoća,* Shore D		**Glossiness, GU** *Sjaj,* JS	
				Control *Kontrolni uzorak*	**Densified** *Ugušćeno*	**Control** *Kontrolni uzorak*	**Densified** *Ugušćeno*
1	0.081	200	0.5	52.08	66.00	2.13	2.80
2	0.081	200	1	56.17	59.50	2.03	2.43
3	0.081	400	0.5	54.33	61.88	1.97	2.65
4	0.081	400	1	55.67	60.17	1.98	2.73
5	0.121	200	0.5	52.08	59.00	2.13	2.87
6	0.121	200	1	53.38	54.86	2.03	2.43
7	0.121	400	0.5	54.33	58.33	1.97	2.55
8	0.121	400	1	56.29	62.86	1.98	2.70
9	0.202	200	0.5	52.08	56.22	2.13	2.52
10	0.202	200	1	53.38	55.67	2.03	2.28
11	0.202	400	0.5	53.78	56.63	1.97	1.98
12	0.202	400	1	56.29	62.13	1.98	2.53

Table 5 Surface roughness values (R_z) obtained according to surface densification conditions for black poplar and cedar of Lebanon
Tablica 5. Vrijednosti hrapavosti površine (R_z) za površinski ugušćeno drvo crne topole i libanonskog cedra pri različitim uvjetima

Process number *Broj procesa*	**Feed, mm/rev** *Posmična brzina,* mm/okr.	**Spindle speed, rpm** *Brzina vretena,* okr./min	**Densification depth, mm** *Dubina ugušćivanja,* mm	**Black poplar surface roughness, µm** *Hrapavost površine drva crne topole,* µm		**Cedar of Lebanon surface roughness, µm** *Hrapavost površine drva libanonskog cedra,* µm	
				Control *Kontrolni uzorak*	**Densified** *Ugušćeno*	**Control** *Kontrolni uzorak*	**Densified** *Ugušćeno*
1	0.081	200	0.5	8.188	6.850	7.353	5.572
2	0.081	200	1	7.315	6.367	6.473	6.131
3	0.081	400	0.5	7.199	6.217	6.485	4.240
4	0.081	400	1	7.166	4.731	6.823	6.620
5	0.121	200	0.5	8.188	6.632	7.353	5.033
6	0.121	200	1	7.315	7.157	6.473	4.800
7	0.121	400	0.5	7.199	6.607	6.485	5.455
8	0.121	400	1	7.971	7.245	6.823	6.332
9	0.202	200	0.5	8.188	7.424	7.353	5.235
10	0.202	200	1	7.315	5.810	6.473	4.343
11	0.202	400	0.5	7.772	7.447	6.485	5.518
12	0.202	400	1	7.166	7.043	6.823	5.793

were formed under the 2nd and 6th process number surface densification conditions. And in the cedar of Lebanon, it was obtained under the 1st process number surface densification conditions.

When the hardness values for both wood types were compared after surface densification, the hardness values of cedar of Lebanon were higher than those of the black poplar wood under all surface densification conditions. Although the hardness value of the cedar of Lebanon was higher in the 6th process number surface densification condition, a value close to this was obtained in the black poplar. In both wood species, a decrease in roughness occurred with densification under all surface densification conditions. It was found in the literature that smoother surfaces are obtained in solid wood and wood-derived materials with increased density (Sofuoglu and Tosun 2023; Ayrilmis *et al*., 2019; Pinkowski *et al*., 2019; Zhong *et al*., 2013; Malkocoglu and Ozdemir, 2006). In general, wood species studied showed lower surface roughness values after densification (Bekhta *et al*., 2014). Pelit and Arısut (2022) and Sofuoglu *et al*. (2022) also found in their studies that a decrease in surface roughness values occurred in the densified wood materials (the data obtained in the study seem compatible with the literature). In Tables 6, 7 and 8, hardness, brightness and R_z values obtained in average roughness measurements show normal distribution at 95 % confidence level, since the P value is higher than 0.05 (P = 0.076 for hardness, P = 0.685 for brightness, P = 0.662 for R_z). According to the results of variance analysis, for hardness at 95 % confidence level, the feed (0.05<P = 0.127), spindle speed (0.05<P = 0.871), and depth of densification (0.05<P=0.204) did not make a statistically significant difference, while wood species (0.05>P=0,000) was found to make a statistically significant difference (Table 6).

Figure 5 shows the interaction of wood species, feed, spindle speed and depth of densification in terms of hardness in the main effect plot. Generally higher hardness values were obtained with the cedar of Lebanon. Although there is no significant difference between the groups, it is possible to say that, when the graph is examined in terms of the spindle speed, the values close to each other in terms of hardness were obtained at the spindle speed of 200 and 400 rpm. After

Table 6 Results of analysis of variance for hardness
Tablica 6. Rezultati analize varijance za tvrdoću

Source / *Izvor*	**DF**	**Adj SS**	**Adj MS**	***F* Value**	***P* Value**
Wood species (black poplar and cedar of Lebanon) *vrsta drva (crna topola i libanonski cedar)*	1	1237.54	1237.54	99.80	0.000
Feed, mm/rev / *posmična brzina,* mm/okr.	2	57.51	28.76	2.32	0.127
Spindle speed, rpm / *brzina vretena,* okr./min	1	0.34	0.34	0.03	0.871
Depth of densification, mm / *dubina ugušćivanja,* mm	1	21.55	21.55	1.74	0.204
Error / *pogreška*	18	223.20	12.40		
Total / *ukupno*	23	1540.13			

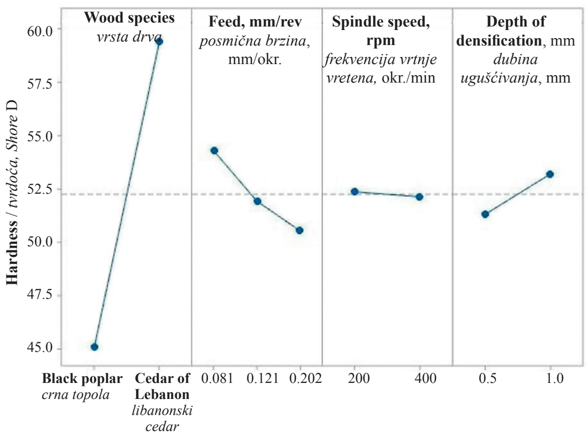

Figure 5 Main effects plot in terms of hardness of wood species, feed, spindle speed and depth of surface densification
Slika 5. Dijagram glavnih utjecaja tvrdoće drva, posmične brzine, frekvencije vrtnje vretena i dubine ugušćivanja površine na hrapavost

the surface densification process, the hardness on the wood surfaces decreases as the feed increases and increases as the densification depth increases. When evaluated in general, high surface hardness values occur in cedar of Lebanon at 0.081 feed, 200 spindle speed and 1 mm densification depth. The interaction graph in Figure 6 shows that the hardness decreases as the feed increases in the surface densification process for both wood species. As the spindle speed increases, hardness decreases in the black poplar, while an increase occurs in the cedar of Lebanon. While the depth of densification increased, the amount of hardness increased in the black poplar, but there was not much change in the cedar of Lebanon. The interactions of feed and spindle speed, feed and depth of densification, and spindle speed and depth of densification were close to each other in terms of hardness.

According to the results of the analysis of variance for brightness at a 95 % confidence level, feed ($0.05<P=0.315$), spindle speed ($0.05<P=0.793$), and depth of surface densification ($0.05<P=0.804$) did not make a statistically significant difference, while wood species ($0.05>P=0.000$) made a statistically significant difference (Table 7).

When evaluated in general, high surface brightness occurred in black poplar at 0.121 feed, 400 spindle speed, and 1 mm surface densification depth (Figure 7). The brightness value increases as the spindle speed and depth of surface densification are increased. The brightness value increases as the feed is increased, but when it is increased to 0.202 mm/rev, there is a decrease, with the lowest brightness value occurring in this feed. The interaction graphs in Figure 8 show that higher brightness is obtained in the black poplar wood. In cedar of Lebanon, the brightness did not change as the feed increased, but when it was increased to 0.202, the brightness also decreased. On the other hand, as the depth of surface densification increases, the brightness tends to decrease at 200 rpm, while it increases at 400 rpm.

According to the results of the analysis of variance for R_z at 95 % confidence level, feed ($0.05<P=0.730$), spindle speed ($0.05<P=0.644$), and depth of surface densification ($0.05<P=0.972$) did not

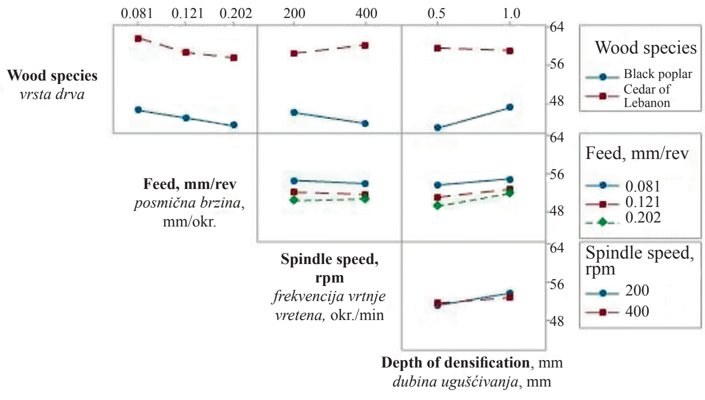

Figure 6 Interaction of wood species, feed, spindle speed and depth of surface densification in terms of hardness
Slika 6. Međusobno djelovanje vrste drva, posmične brzine, frekvencije vrtnje vretena i dubine ugušćivanja na tvrdoću

Table 7 Results of analysis of variance for glossiness
Tablica 7. Rezultati analize varijance za sjaj

Source / *Izvor*	**DF**	**Adj SS**	**Adj MS**	***F* Value**	***P* Value**
Wood species (black poplar and cedar of Lebanon) *vrsta drva (crna topola i libanonski cedar)*	1	2.45760	2.45760	28.94	0.000
Feed, mm/rev / *posmična brzina,* mm/okr.	2	0.20923	0.10462	1.23	0.315
Spindle speed, rpm / *frekvencija vrtnje vretena,* okr./min	1	0.00602	0.00602	0.07	0.793
Depth of densification, mm / *dubina ugušćivanja,* mm	1	0.00540	0.00540	0.06	0.804
Error / *pogreška*	18	1.52853	0.08492		
Total / *ukupno*	23	4.20678			

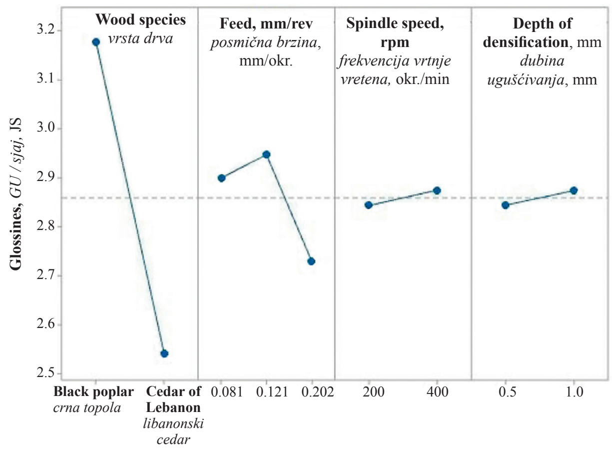

Figure 7 Main effects plot in terms of glossiness of wood species, feed, spindle speed and depth of surface densification
Slika 7. Dijagram glavnih utjecaja tvrdoće drva, posmične brzine, frekvencije vrtnje vretena i dubine ugušćivanja površine na sjaj

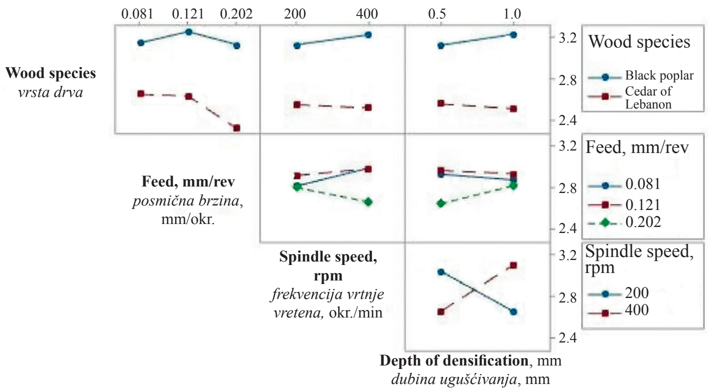

Figure 8 Interaction of wood species, feed, spindle speed and depth of surface densification in terms of brightness
Slika 8. Međusobno djelovanje vrste drva, posmične brzine, frekvencije vrtnje vretena i dubine ugušćivanja na sjaj

make a statistically significant difference, while wood species (0.05>P=0.002) made a statistically significant difference (Table 8).

When evaluated in general, according to the results of the main effect graph, low R_z value is obtained in cedar of Lebanon, 0.081 feed, 200 spindle speed and 0.5 mm surface densification depth. The brightness value increases as the spindle speed, and depth of surface densification are increased. However, with the increase in depth of surface densification, very low R_z values or close to each other have been obtained. In addition, as the feed is increased, the roughness value increases, and when it is increased to 0.202 mm/rev, a decrease occurs (Figure 9). Figure 10 shows that there is no difference between 0.081 and 0.121 feed in terms of R_z for cedar of Lebanon wood. When the feed value increased to 0.202, the roughness value decreased and the lowest R_z values were obtained at 0.202 feed for this wood species. In addition, a linear decrease occurred with increasing the feed value in cedar of Lebanon for R_z. Both wood species showed different responses in terms of spindle speed and depth of surface densification. In terms of R_z, with the increase in spindle speed and depth of surface densification, the R_z value decreased in Black poplar, while an increase occurred in cedar of Lebanon. The reason for this differ-

Table 8 Results of analysis of variance for R_z
Tablica 8. Rezultati analize varijance za parametar hrapavosti R_z

Source / *Izvor*	DF	Adj SS	Adj MS	***F*** **Value**	***P*** **Value**
Wood species (black poplar and cedar of Lebanon) *vrsta drva (crna topola i libanonski cedar)*	1	8.7097	8.70974	12.87	0.002
Feed, mm/rev / *posmična brzina,* mm/okr.	2	0.4329	0.21644	0.32	0.730
Spindle speed, rpm / *frekvencija vrtnje vretena,* okr./min	1	0.1495	0.14947	0.22	0.644
Depth of densification, mm / *dubina ugušćivanja,* mm	1	0.0008	0.00084	0.00	0.972
Error / *pogreška*	18	12.1794	0.67663		
Total / *ukupno*		21.4723			

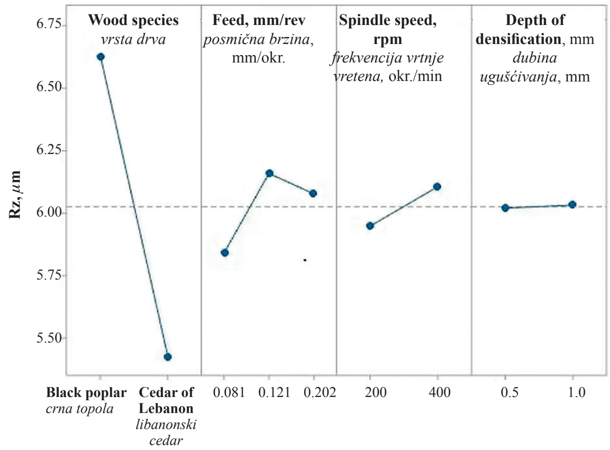

Figure 9 Main effects plot in terms of R_z of wood species, feed, spindle speed and depth of surface densification
Slika 9. Dijagram glavnih utjecaja tvrdoće drva, posmične brzine, frekvencije vrtnje vretena i dubine ugušćivanja površine na parametar hrapavosti R_z

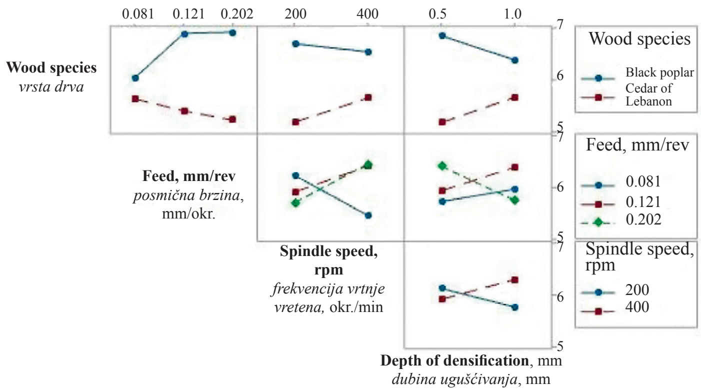

Figure 10 Interaction of wood species, feed, spindle speed and depth of surface densification in terms of R_z
Slika 10. Međusobno djelovanje vrste drva, posmične brzine, frekvencije vrtnje vretena i dubine ugušćivanja na parametar hrapavosti R_z

ence may be the fact that wood species have different anatomical structures. In the interaction between spindle speed and depth of surface densification, as the depth increases at 200 rpm, the roughness values (R_z) decrease, and this value increases at 400 rpm.

3.2 Evaluation of compression ratio and spring-back
3.2. Analiza stupnja ugušćenja i elastičnog povrata

The average % compression ratio and average % spring-back determined depending on the experimental parameters for the two wood species are given in Table 9.

Considering the feed parameter for both wood species, the most successful densification was obtained at the lowest feed (0.081 mm/rotate). Slow feed resulted in better densification of the porous wood. In terms of spindle speed, black poplar could be better densified at low rpm. Cedar of Lebanon could be better densified at high speed. Spindle speed is not seen as a direct determining factor in terms of densification among wood species. It is seen that more successful densification was obtained with high spindle speed for cedar of Lebanon. Dept of densification has been identified as the most drastic experimental parameter for densification success for both wood species. Surface densification increased with the increase of depth of densification from 0.5 mm to 1 mm for both wood species. In both species, lower spring back rate was obtained at low dept of densification.

4 CONCLUSIONS
4. ZAKLJUČAK

In this study, black poplar (*Populus nigra* L.) and cedar of Lebanon (*Cedrus libani* A. Rich.) were surface densified in their cylindrical shape. The results of the study show as follows:

- In both wood species, under all surface densification conditions, an increase in brightness and hardness values occurs with surface densification.
- After all the surface densification processes, higher gloss values were obtained in black poplar than in cedar of Lebanon.

Table 9 Average compression ratio and average spring-back for each experimental parameter
Tablica 9. Srednji stupanja ugušćenja i srednji elastični povrat za svaki parametar eksperimenta

Process parameter *Parametar procesa*		**Average diameter D_{start}, mm** *Srednji promjer D_{start}, mm*	**Theoretical diameter $D_{teor.}$, mm** *Teorijski promjer $D_{teor.}$, mm*	**Densified average diameter D_{end}, mm** *Srednji promjer nakon ugušćivanja $D_{teor.}$, mm*	**Average theoretical compression ratio, %** *Srednji teorijski stupanja ugušćenja, %*	**Average experimental compression ratio, %** *Srednji eksperimentalni stupanj ugušćenja, %*	**Average spring-back, %** *Srednji elastični povrat, %*
	Black poplar / *Drvo crne topole*						
Feed, mm/rev *posmična brzina,* mm/okr.	0.081	18.62	17.87	18.19	4.01	2.27	1.82
	0.121	18.59	17.84	18.25	4.01	1.83	2.28
	0.202	18.51	17.76	18.21	4.03	1.61	2.53
Spindle speed, rpm *frekvencija vrtnje vretena,* okr./min	200	18.46	17.71	18.02	4.03	2.37	1.74
	400	18.68	17.93	18.41	4.00	1.44	2.68
Densification depth, mm / *dubina ugušćivanja,* mm	0.5	18.26	17.76	18.04	2.74	1.21	1.57
	1	18.88	17.88	18.39	5.30	2.60	2.85
	Cedar of Lebanon / *Drvo libanonskog cedra*						
Feed, mm/rev *posmična brzina,* mm/okr.	0.081	18.29	17.54	18.00	4.16	1.61	2.68
	0.121	18.28	17.53	18.09	4.16	1.03	3.28
	0.202	18.24	17.49	18.09	4.17	0.83	3.50
Spindle speed, rpm *frekvencija vrtnje vretena,* okr./min	200	17.75	17.00	17.58	4.33	0.96	3.55
	400	18.79	18.04	18.54	3.99	1.35	2.76
Densification depth, mm / *dubina ugušćivanja,* mm	0.5	18.83	18.33	18.66	2.66	0.88	1.82
	1	17.71	16.71	17.45	5.67	1.44	4.49

- The hardness values of the cedar of Lebanon were higher than those of the black poplar in all surface densification conditions.
- In both wood species, a decrease in roughness values (Rz) occurs after surface densification under all surface densification conditions.
- When the two wood species were compared, smoother surfaces were obtained before and after surface densification due to the higher average density of the cedar of Lebanon wood material.
- The hardness of surface-densified wood surfaces decreased as the feed rate increased and increased as the surface densification depth increased.
- The most successful densification was obtained at the lowest feed.
- Spindle speed was not found to be a significant factor in terms of surface densification.

It is seen that the use of spinning rollers in the surface densification of cylindrical materials creates surface densification on the surfaces. The obtained results show that the properties of wood material are improved by surface densification. The results also show that this method is applicable to the surface densification of cylindrical wood materials.

Optimal parameters can be applied by evaluating the optimum points and results (hardness, brightness, and roughness) according to the data obtained in the surface densification of cylindrical solid wood material using a spinning roller.

5 REFERENCES
5. LITERATURA

1. Ayrilmis, N.; Kariz, M.; Kwon, J. H. and Kuzman, M. K., 2019: Surface roughness and wettability of surface densified heat-treated Norway spruce (*Picea abies* L. Karst.). Drvna industrija, 70 (4): 377-382. https://doi.org/10.5552/drvind.2019.1852
2. Bekhta, P.; Proszyk, S.; Krystofiak, T.; Mamonova, M.; Pinkowski, G.; Lis, B., 2014: Effect of thermomechanical densification on surface roughness of wood veneers. Wood Material Science and Engineering, 9 (4): 233-245. https://doi.org/10.1080/17480272.2014.923042
3. Bekhta, P.; Proszyk, S.; Krystofiak, T.; Sedliacik, J.; Novak, I.; Mamonova, M., 2017: Effects of short-term thermomechanical densification on the structure and properties of wood veneers. Wood Material Science and Engineering, 12 (1): 40-54. https://doi.org/10.1080/17480272.2015.1009488
4. Blomberg, J.; Persson, B., 2004: Plastic deformation in small clear pieces of Scots pine (*Pinus sylvestris*) during densification with the CaLignum process. Journal of Wood Science, 50 (4): 307-314. https://doi.org/10.1007/s10086-003-0566-2
5. Budakci, M.; Pelit, H.; Sonmez, A.; Korkmaz, M., 2016: The effects of densification and heat post-treatment on hardness and morphological properties of wood materials. BioResources, 11 (3): 7822-7838. https://doi.org/10.15376/biores.11.3.7822-7838

6. Burgos, F.; Rolleri, A., 2012: Effect of Hydro- and Hygro-Thermal Treatments on Some Wood Properties of Pinus Radiata and Pseudotsuga Menziesii. Drvna industrija, 63 (3): 211-215. https://doi.org/10.5552/drind.2012.1133
7. Croitoru, C.; Spirchez, C.; Lunguleasa, A.; Cristea, D.; Roata, I. C.; Pop, M. A.; Bedo, T.; Stanciu, E. M., Pascu, A., 2018: Surface properties of thermally treated composite wood panels. Applied Surface Science, 438, 114-126. https://doi.org/10.1016/j.apsusc.2017.08.19:
8. Dogu, D.; Koc, H.; As, N.; Atik, C.; Aksu, B.; Erdinler, S., 2001: Basic identification information of trees of industrial importance growing in Turkey and general evaluation for use. Journal of the Faculty of Forestry Istanbul University, 51 (2): 69-84.
9. Gao, Z.; Huang, R.; Chang, J.; Li, R.; Wu, Y., 2019: Effects of pressurized superheated-steam heat treatment on set recovery and mechanical properties of surface-compressed wood. BioResources, 14 (1): 1718-1730. https://doi.org/10.15376/biores.14.1.1718-1730
10. Gurleyen, L., 1998: Comparison of surface smoothness in the materials of solid wood using ın the furniture. MSc Thesis, Gazi University Institute of Science and Technology, Ankara, Turkey.
11. ***ISO 468:2009 Surface roughness – Parameters, their values and general rules for specifying requirements. International Organization for Standardization, Geneva, Switzerland.
12. ***ISO 2813:2014 Paints and varnishes – Determination of gloss value at 20 degrees, 60 degrees and 85 degrees. International Organization for Standardization, Geneva, Switzerland.
13. ***ISO 13061-1:2014 Physical and mechanical properties of wood Test methods for small clear wood specimens. Part 1: Determination of moisture content for physical and mechanical tests. International Organization for Standardization, Geneva, Switzerland.
14. Kariz, M.; Kuzman, M. K.; Sernek, M.; Hughes, M.; Rautkari, L.; Kamke, F. A.; Kutnar, A., 2017: Influence of temperature of thermal treatment on surface densification of spruce. European Journal of Wood and Wood Products, 75 (1): 113-123. https://doi.org/10.1007/s00107-016-1052-z
15. Kaya, Z.; Sofuoğlu, S. D., 2023: Use of spinning roller in cylindrical densification; spring back in black poplar, larch and cedar of Lebanon after densification. Bilge International Journal of Science and Technology Research, 7 (2): 117-127. https://doi.org/10.30516/bilgesci.1278745
16. Kaya, Z.; Sofuoğlu, S. D., 2023: Use of spinning roller in cylindrical densification; change in hardness, brightness and surface roughness in solid wood (Larch) after densification. Furniture and Wooden Material Research Journal, 6 (1): 14-25. https:/doi.org/10.33725/mamad.1260723
17. Korkut, S.; Kocaefe, D., 2009: Effect of heat treatment on wood properties. Duzce University, Faculty of Forestry, Journal of Forestry, 5 (2): 11-34.
18. Laskowska, A., 2017: The influence of process parameters on the density profile and hardness of surface-densified birch wood (*Betula pendula* Roth). BioResources, 12 (3): 6011-6023. https://doi.org/10.15376/biores.12.3.6011-6023
19. Malkocoglu, A.; Ozdemir, T., 2006: The machining properties of some hardwoods and softwoods naturally grown in Eastern Black Sea Region of Turkey. Journal of Materials Processing Technology, 173 (3): 315-320. https://doi.org/10.1016/j.jmatprotec.2005.09.031
20. Neyses, B.; Karlsson, O.; Sandberg, D., 2020: The effect of ionic liquid and superbase pre-treatment on the spring-back, set-recovery and Brinell hardness of surface-densified Scots pine. Holzforschung, 74 (3): 303-312. https://doi.org/10.1515/hf-2019-0158
21. Parvis Navi, D. S., 2012: Thermo-Hydro-Mechanical Wood Processing. EPFL Press. https://doi.org/10.1520/mnl10496m
22. Pelit, H.; Arısut, U., 2022: Roughness, wettability and morphological properties of impregnated and densified wood materials. BioResources, 18 (1): 429-446. https://doi.org/10.15376/biores.18.1.429-446
23. Pertuzzatti, A.; Missio, A. L.; de Cademartori, P. H. G.; Santini, E. J.; Haselein, C. R.; Berger, C.; Gatto, D. A.; Tondi, G., 2018: Effect of process parameters in the thermomechanical densification of pinus elliottii and eucalyptus grandis fast-growing wood. BioResources, 13 (1): 1576-1590. https://doi.org/10.15376/biores.13.1.1576-1590
24. Pinkowski, G.; Szymanski, W.; Krauss, A.; Stefanowski, S., 2019: Effect of sharpness angle and feeding speed on the surface roughness during milling of various wood species. BioResources, 13 (3): 6952-6962. https://doi.org/10.15376/biores.13.3.6952-6962
25. Rautkari, L.; Properzi, M.; Pichelin, F.; Hughes, M., 2009: Surface modification of wood using friction. Wood Science and Technology, 43 (3-4): 291-299. https://doi.org/10.1007/s00226-008-0227-0
26. Rautkari, L.; Properzi, M.; Pichelin, F.; Hughes, M., 2010: Properties and set-recovery of surface densified Norway spruce and European beech. Wood Science and Technology, 44 (4): 679-691. https://doi.org/10.1007/s00226-009-0291-0
27. Salca, E.; Brasov, U. T.; Bekhta, P., 2021: Effects of thermo-mechanical densification applied to veneers of fast-growing species to produce value-added plywood panels. Cutting-edge Research in Agricultural Sciences, 9: 161-177. https://doi.org/10.9734/bpi/cras/v9/8628D
28. Sandberg, D.; Kutnar, A.; Karlsson, O.; Jones, D., 2021: Wood modification technologies: principles, sustainability and the need for innovation. CRC Press.
29. Scharf, A.; Lemoine, A.; Neyses, B.; Sandberg, D., 2023: The effect of the growth ring orientation on spring-back and set-recovery in surface-densified. Holzforschung, 77 (6): 394-406. https://doi.org/10.1515/hf-2023-0004
30. Schwarzkopf, M., 2021: Densified wood impregnated with phenol resin for reduced set-recovery. Wood Material Science and Engineering, 16 (1): 35-41. https://doi.org/10.1080/17480272.2020.1729236
31. Senol, S., 2018: Determination of physical, mechanical and technological properties of some Thermo-Vibro-Mechanical (TVM) treated wood materials. PhD Thesis, Duzce University, Duzce, Turkey.
32. Senol, S.; Budakci, M., 2019: Effect of Thermo-Vibro-Mechanic® densification process on the gloss and hardness values of some wood materials. BioResources, 14 (4): 9611-9627. https://doi.org/10.15376/biores.14.4.9611-9627
33. Senol, S.; Budakci, M., 2016: Mechanıcal wood modıfıcatıon methods. Mugla Journal of Science and Technology, 2 (2): 53-59. https://doi.org/10.22531/muglajsci.283619
34. Sofuoglu, S. D., 2022: Effect of thermo-mechanical densification on brightness and hardness in wood. Turkish Journal of Engineering Research and Education, 1 (1): 15-19.
35. Sofuoglu, S. D.; Tosun, M., 2023: Determination of processing characteristics of wood materials densified by

compressing. Maderas, Ciencia y Tecnología, 25: 1-16. http://dx.doi.org/10.4067/s0718-221x2023000100427
36. Sofuoglu, S. D.; Tosun, M.; Atilgan, A., 2022: Determination of the machining characteristics of Uludağ fir (*Abies nordmanniana* Mattf.) densified by compressing. Wood Material Science and Engineering, 18 (3): 841-851. https://doi.org/10.1080/17480272.2022.2080586
37. Sogutlu, C., 2005: Bazı faktörlerin zımparalanmış ağaç malzeme yüzey pürüzlülüğüne etkisi', G.Ü. Teknik Eğitim Fakültesi Politeknik Dergisi, 8 (4): 345-350.
38. Tosun, M.; Sofuoglu, S. D., 2021: Studies on the densification of wood material by compression. Journal of Furniture and Wood Materials Research, 4 (1): 91-102. https://doi.org/10.33725/mamad.911947
39. Wehsener, J.; Bremer, M.; Haller, P.; Fischer, S., 2023: Bending tests of delignified and densified poplar. Wood Material Science and Engineering, 18 (1): 42-50. https://doi.org/10.1080/17480272.2022.2134049
40. Zhong, Z. W.; Hiziroglu, S.; Chan, C. T. M., 2013: Measurement of the surface roughness of wood based materials used in furniture manufacture. Measurement, 46 (4): 1482-1487. https://doi.org/10.1016/j.measurement.2012.11.041

Corresponding address:

Dr. ZAFER KAYA
Kutahya Dumlupinar University, Simav Vocational School, 43500, Simav, Kutahya, TURKEY,
e-mail: zafer.kaya@dpu.edu.tr

Petr Zatloukal*[1], Tadeáš Doskočil[1], Jan Tippner[1]

Acoustic Properties of Wood-Based and Non-Wood-Based Materials for Piano-Case Making

Akustična svojstva drvnih i nedrvnih materijala za izradu kućišta klavira

ORIGINAL SCIENTIFIC PAPER
Izvorni znanstveni rad
Received – prispjelo: 7. 7. 2023.
Accepted – prihvaćeno: 16. 2. 2024.
UDK: 630*83; 674.817; 780.616.433
https://doi.org/10.5552/drvind.2024.0141

ABSTRACT • *This article presents the possibilities of substituting expensive and scarce wood materials in the construction of piano cases, especially the front panels of upright pianos. Three-layer blockboard, multi-layer plywood, medium-density fibreboard (MDF), and Purenit were selected for the study. These materials were long-time climatised at 20 °C and 50 % relative air humidity. Their frequencies, damping coefficient and relative amplitude were measured. The density* ρ, *sound velocity v, dynamic modulus of elasticity E´, sound impedance* Z_n *and Acoustic Conversion Efficiency (ACE) were calculated. With the materials used to make the front panels of an upright piano, a subjective assessment of the instrument's acoustic response was made. The presence of front panels of any type was found to have a negative effect on the sound except at low frequencies. With panels fitted, the best acoustic properties were achieved by blockboard, followed by plywood, MDF and Purenit panels in that order; this was affirmed by the subjective assessment. The best acoustic performance was achieved by blockboard and plywood. Taking both price and performance into consideration, MDF presented the best compromise. Purenit was ruled out due to its high damping properties.*

KEYWORDS: *composites; acoustic; non-destructive-test; piano case*

SAŽETAK • *U ovom su članku prikazane mogućnosti zamjene skupih i rijetkih drvenih materijala za izradu kućišta klavira, posebice prednjih ploča uspravnih klavira. Za istraživanje su odabrane stolarska ploča, furnirska ploča, srednje gusta ploča vlaknatica (MDF) i purenit ploča. Ti su materijali dugotrajno klimatizirani pri temperaturi 20 °C i 50 %-tnoj relativnoj vlažnosti zraka. Mjerene su njihove frekvencije, koeficijent prigušenja i relativna amplituda. Izračunane su gustoća* ρ, *brzina zvuka v, dinamički modul elastičnosti E´, zvučna impedancija* Z_n *i učinkovitost akustične pretvorbe (ACE). Napravljena je subjektivna procjena akustičkog odziva instrumenta za materijale upotrijebljene za izradu prednjih ploča uspravnog klavira. Utvrđeno je da prednje ploče uspravnih klavira izrađene od bilo koje vrste odabranih ploča imaju negativan utjecaj na zvuk, osim na niskim frekvencijama. Prema subjektivnoj procjeni, najbolja akustična svojstva pokazala je stolarska ploča, zatim furnirska ploča te MDF i purenit ploča. Najbolja akustična svojstva imaju stolarska i furnirska ploča. Uzimajući u obzir cijenu i performanse, MDF je najbolji kompromis. Purenit je isključen zbog jakog prigušivanja zvuka.*

KLJUČNE RIJEČI: *kompoziti; akustičan; nedestruktivno ispitivanje; kućište klavira*

* Corresponding author
[1] Authors are researchers at Mendel University in Brno, Faculty of Forestry and Wood Technology, Department of Wood Science and Technology, Brno, Czech Republic. https://orcid.org/0000-0001-5898-5496; https://orcid.org/0000-0001-8532-3690

1 INTRODUCTION
1. UVOD

Wood has been used to produce musical instruments since ancient times because of its availability and workability, especially by hand before power tools were available. Some wood species are more suitable for producing musical instruments than others. For example, European spruce (*Picea abies*) is suitable for making pianos and violin soundboards due to its superb resonance properties (Bucur, 2006). Curly maple (*Acer* sp.) is used for various musical instrument parts, especially guitar back plates, bridges, ribs and necks (Bucur, 2006). The choice often depends on the culture and t region of production. Wood species used for xylophones, a very common subject of research, are black mulberry (*Morus nigra*) (Čulík *et al.*, 2015), padouk (*Pterocarpus soyauxii*) (Straže *et al.*, 2015) and vène (*Pterocarpus erinaceus* Poir) (Traoré *et al.*, 2010).

Bucur (2016) describes three groups of composites – composites with synthetic and natural fibres, nanocomposites, and ceramic-based composites. Fibres are often mentioned as a way of improving musical instrument stability. Synthetic composites include carbon and graphite fibre (Bucur, 2016), used as reinforcing elements in a polymer matrix, usually resin (Bucur, 2016).

The first attempt to replace wood in musical instruments with composite involved plywood (Besnainou, 1998), a panel built up of sheets of wood veneer. Plywood panels contain an odd number of layers – the grain orientations of which alternate at right angles – held together with urea-formaldehyde glue (Ross, 2010). Plywood may be used for small harp soundboards, for example (Waltham and Yoshikawa, 2018; Gunji *et al.*, 2012). In terms of sustainability and environmental friendliness, the tendency is to decrease emissions of formaldehyde from urea-formaldehyde glues (Bilgin and Colakoglu, 2021; Kawalerczyk *et al.*, 2020; Demir *et al.*, 2018).

Medium-density fibreboard (MDF) belongs to a group of fibreboards made from wood fibres using either a wet or dry process. MDF is made by the dry process, in which glue and other additives are applied to the fibres that are pressed and trimmed to standard formats (Ross, 2010). MDF panels are often used in musical instrument construction due to their low price and easy workability. Due to disintegration, MDF has a higher ratio of absorption coefficient than resonance wood, making it suitable for loudspeaker boxes (Sali *et al.*, 2004). Compressing wood before making MDF panels negatively affects dimensional stability (Ayrilmis, 2008). Exposing manufactured MDF panels to heat treatment at 225 °C for 30 minutes decreases surface roughness, thus decreasing wettability and the adhesive bonding strength between the veneer sheet and panel surface (Ayrilmis and Winandy, 2009). Recently, a lot of research has focused on the ecological nature of production. Special attention has been paid to the use of waste in the production of MDF boards (Olgun *et al.*, 2023; Moezzipour and Moezzipour, 2021; Ahmadi *et al.*, 2019) or use of alternative glues instead of Urea-Formaldehyde resins (Savov and Antov, 2020; Sepahvand *et al.*, 2018).

Blockboard is a material made from softwood strip-core with a veneer facing. The central core is made of 25 mm wide strips with vertically arranged growth rings that are interlocked (Böhm *et al.*, 2012). There may be three layers (strip-core and two veneers) or five layers (two strip-cores divided by one veneer and faced with two more). The elements are held together with urea-formaldehyde glue. In this study, a three-layer blockboard was used.

Purenit is a material obtained by recycling polyurethane foams and vehicle interior elements. The colour, structure, and processing parameters of purenit are similar to the properties of particleboards. Purenit is a highly compressed material based on polyurethane rigid foam, commonly used for thermal insulation. It is resistant to moisture and has dimensional stability (Majewski and Smardzewski, 2013). As its acoustic properties have not been tested before, Purenit board was selected as the last material in this study.

Composites made from carbon fibre/epoxy with a balsa core used as a drum shell may be used as a substitute for wood because of their comparable acoustic parameters (Damodaran *et al.*, 2015b).

Some research has been conducted into fibre-reinforced wood (Ono and Isomura, 2004; Ibáñez-Arnal *et al.*, 2019; Ono *et al.*, 2002) as a material for guitar (Ono and Isomura, 2004) and violin soundboards, and the results were evaluated by listeners (Duerinck *et al.*, 2020). These composites may be a good alternative to wood but require further study.

Experiments on natural fibre composites are based on the assumption that natural fibre has a structure similar to wood (Bucur, 2016). The inner part of bark lime or flax (*Linum usitatissimum*) (Bucur, 2016) is often used. The acoustic properties of musical instruments reinforced with natural fibre have been studied – e.g., (Liu *et al.*, 2021; Sun, 2018; Phillips and Lessard, 2009; Daoud *et al.*, 2017). A flax fibre-resin composite may be a good alternative to wood because of its better properties under varying humidity and temperature conditions, its lower variability than that of wood, etc. (Bucur, 2016).

Wollastonite ceramic-based composite has wood-like properties such as good machinability, high sound velocity, and high damping capacity. This material is successfully used in the production of musical instruments (Shimazu *et al.*, 2006).

Petung bamboo (*Dendrocalamus asper*) is a good alternative material for guitar top plates because its fre-

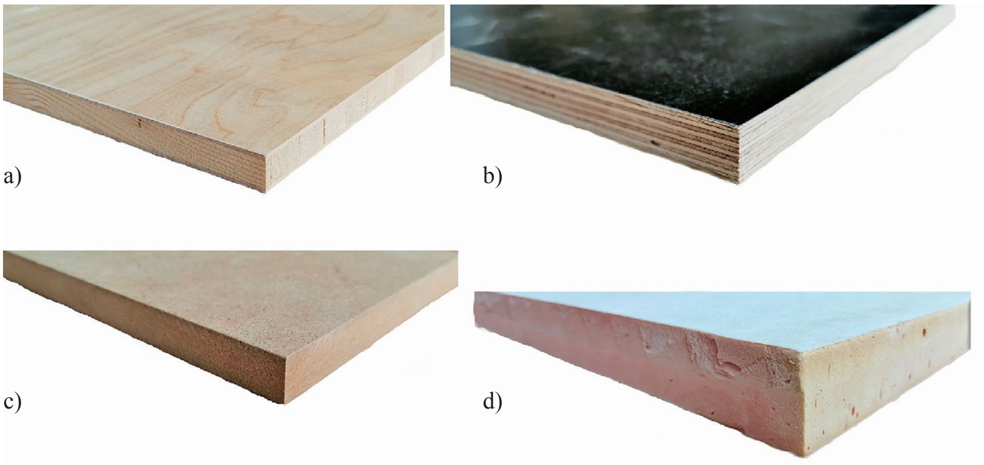

Figure 1 Samples of raw material for making piano panels: a) three-layer blockboard, b) multi-layer plywood, c) medium-density fibreboard (MDF), d) purenit
Slika 1. Uzorci materijala za izradu ploča klavira: a) stolarska ploča, b) furnirska ploča, c) srednje gusta ploča vlaknatica (MDF), d) purenit

quency response function is a fifth that of spruce (Kusumaningtyas *et al.*, 2016).

The main aim of this study was to identify composites which could be used as a substitute for wood in the production of musical instruments, in particular the construction of piano cases.

2 MATERIALS AND METHODS
2. MATERIJALI I METODE

Four materials were selected for testing – MDF, multi-layer plywood (Multiplex) made from beech (*Fagus sylvatica*, L.) veneers, three-layer blockboard whose core was made from pine (*Pinus* sp.) and face from birch (*Betula pendula*, Roth) veneers and Purenit (Figure 1). Specimens of the dimensions of the front panels of an upright piano were made. Dimensions of specimens were 1400 mm × 435 mm for the upper panel and 1310 mm × 500 mm for the lower panel. The thickness of material was 18 mm for blockboard and MDF panels, 16.5 mm for multiplex, and 21.6 mm for purenit.

The upright piano used in the tests was a P 125 M1 from a Czech manufacturer - Petrof Company. The panel specimens were climatised at 20 °C and 50 % relative air humidity for approximately two months, then weighed and placed on soft polyurethane foam pads in an anechoic chamber. The chamber was lined with triangular sound absorption wedges 1,000 mm long, with base dimensions of about 240 mm × 240 mm. The dimensions of the inner space were 8.6 mm × 7.1 mm × 6.6 m. The chamber structure was a concrete

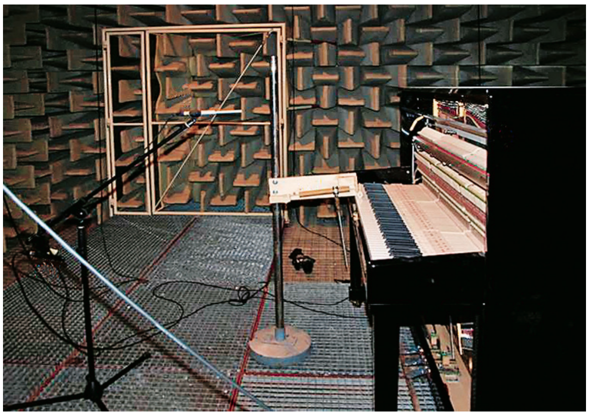

Figure 2 Measuring in anechoic chamber
Slika 2. Mjerenje u anehoičnoj komori

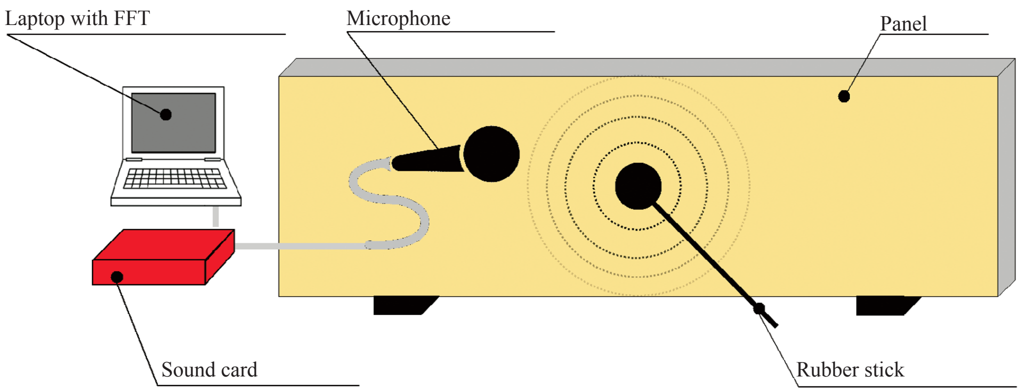

Figure 3 Scheme for measuring acoustic properties
Slika 3. Shema za mjerenje akustičnih svojstava

monolith mounted on springs to absorb vibrations from the surroundings (Figure 2).

Three measurements of acoustic parameters were taken. In the first test, the panels were struck by rubber stick (a small mallet with rubber head) and the resulting vibrations were captured with a condenser microphone (Behringer ECM 8000), connected to an external FireWire sound card Edirol FA101 (Roland, 192 kHz). The position of the struck was selected in the middle of the panels. The measurements were performed as free-free according to (Bucur, 2017). The FFT analyser application (Fakopp Enterprise Bt.) was used for a fast Fourier analysis (Figure 3).

Ten strokes were recorded and edited using a sound editor for the next analysis. The frequencies, amplitudes, and damping coefficient were captured - the five readings were statistically and visually evaluated, based on the sound curves obtained by FFT. Values of frequencies of dominant modes (peaks in the spectrum significantly higher than noise level) were processed in real-time. These points were acoustically evaluated. Acoustic parameters were calculated according to Eq. 1 to 7.

The damping coefficient was derived from logarithmic decrement using Eq.1 (Ghofrani *et al.*, 2016):

$$\tan\delta = \frac{\lambda}{\pi} \tag{1}$$

Logarithmic decrement λ is derived as a ratio of the amplitudes of two successive peaks using Eq. 2 (Lamarque *et al.*, 2000):

$$\lambda = \frac{1}{n} ln \frac{x(t)}{x(t+nT)} \tag{2}$$

The parameters describing the acoustic response of materials used in this work were obtained as follows.

Density (Eq. 3) (Glass and Zelinka, 2021):

$$\rho = \frac{m}{V} \tag{3}$$

Where: ρ is density ($kg \cdot m^{-3}$), m mass (kg) and V volume (m^{-3})

Sound velocity was calculated from the measured frequency and length of the specimen using Eq. 4 (Kretschmann, 2010):

$$v = f_n \cdot \left(\frac{2 \cdot L_{spec}}{n}\right) \tag{4}$$

Where: v is sound velocity ($m \cdot s^{-1}$), L_{spec} is length of specimen (cm), n is mode number of resonance and f_n is measured frequency (Hz)

Dynamic modulus of elasticity calculated using longitudinal waves (without taking into account Poisson´s ratio) (Eq. 5) (Niemz and Mannes, 2012):

$$E' = \rho \cdot v^2 \tag{5}$$

Where: E' is dynamic modulus of elasticity (MPa), ρ is density ($kg \cdot m^{-3}$), v is sound velocity ($m \cdot s^{-1}$)

Characteristic sound impedance for any direction (Eq. 6):

$$Z_n = \rho \cdot v \tag{6}$$

Where: Z_n is sound impedance ($kg.m^{-2}.s^{-1}$), ρ is density ($kg.m^{-3}$), v is sound velocity ($m.s^{-1}$)

Acoustic conversion efficiency (ACE) (Eq. 7) (Baar *et al.*, 2016):

$$ACE = \frac{\sqrt{\frac{E'}{\rho^3}}}{\tan\delta} \tag{7}$$

Where: *ACE* is Acoustic Conversion Efficiency ($m^{-4} \cdot kg^{-1} \cdot s^{-1}$), E' is dynamic modulus of elasticity (MPa), ρ is density ($kg \cdot m^{-3}$), and *tan δ* is damping coefficient.

In the second test, the acoustic response of the upright piano was measured while fitted with panels of the materials under investigation. Two microphones

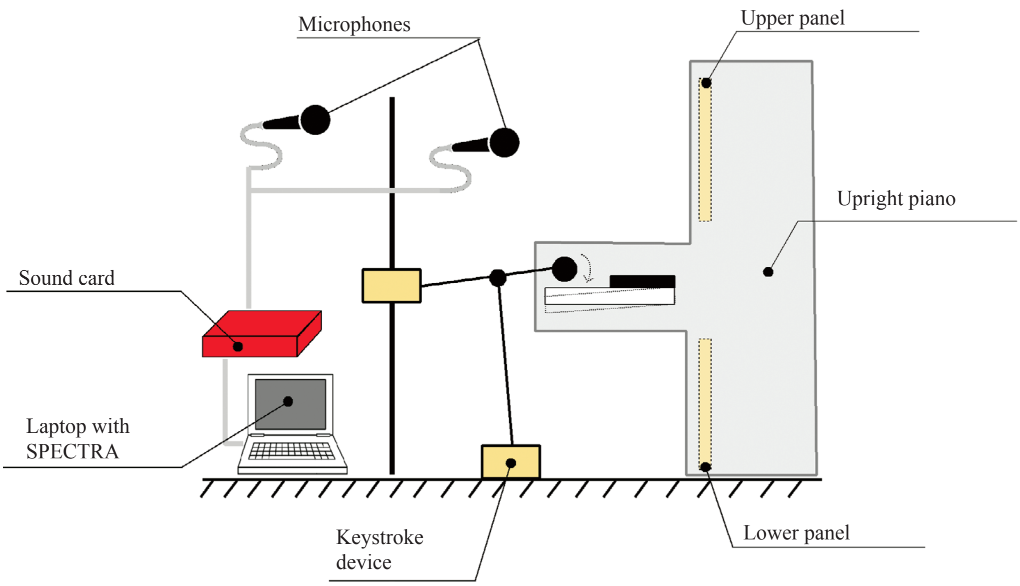

Figure 4 Second test: recording C in each octave
Slika 4. Drugi test: snimanje tona C u svakoj oktavi

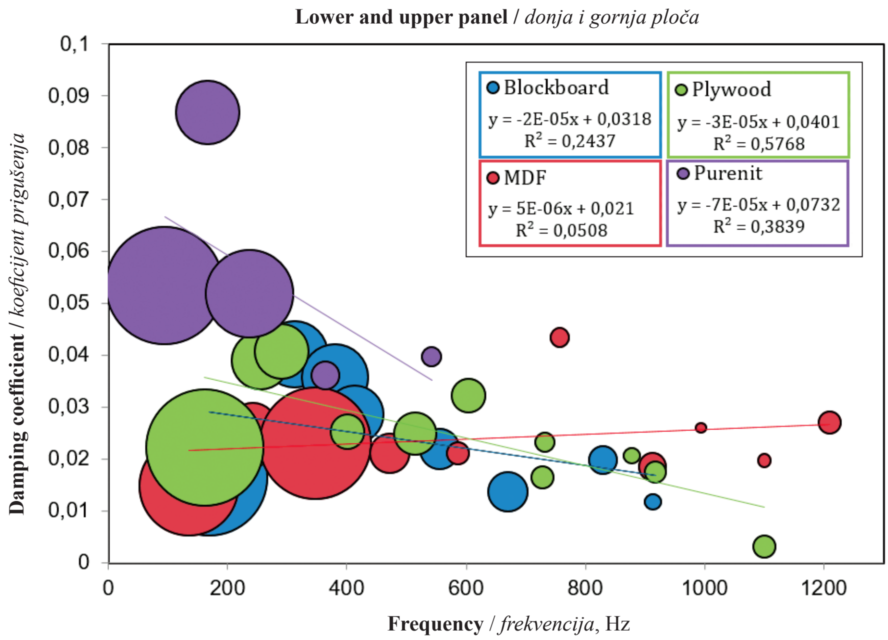

Figure 5 Damping coefficient by frequency for both panels. The area of circles represents relative amplitude.
Slika 5. Koeficijent prigušenja prema frekvenciji za ploče (površine krugova predočuju relativnu amplitudu)

were mounted in front of the piano, the first at approximately the position of the player's head and the second approximately one metre behind the player. A simple device for generating a standard keystroke was built. Eight reference keys on the piano (C in each octave) were selected and a keystroke generated. This procedure was performed with front panels of the test materials, and without panels. All repetitions were recorded and evaluated using SpectraPLUS-SC (Pioneer Hill Software LLC) software (Figure 4).

The third test was a subjective evaluation of the piano fitted with the panels under study. Pieces of music were played on the piano by three experienced players; first without panels, and then after the panels of each material were quickly changed. A committee was set up to assess the sound quality, consisting of intoners, technologists, and employees of the Petrof development department. The committee assessed the sound of the piano without knowing which type of panel was mounted. Members of the committee assessed the quality of the sound on a scale from 1 to 10, where 1 meant the best and 10 the worst result. They also assessed the influence on sound quality of the distance and position of the instrument from the listener.

3 RESULTS AND DISCUSSION
3. REZULTATI I RASPRAVA

An analysis of the frequencies, amplitudes and damping, using an FFT analyser, is shown in Figure 5 for the lower and upper panels of the piano. The values of both panels were averaged because the difference between panels is only in dimensions and support points. The damping coefficient and frequency with relative amplitude of all materials are captured in the graphs. The relative amplitude is indicated by the size of the circles in the plot.

Several points are apparent from the graphs. The data are highly variable, yet some differences are apparent. One difference is between wood-based materi-

Table 1 Comparison of physical and acoustic properties of measured materials
Tablica 1. Usporedba fizikalnih i akustičnih svojstava istraživanih materijala

	Density, kg/m³ *Gustoća,* kg/m³	**Frequency, Hz** *Frekvencija,* Hz	**Sound velocity, m/s** *Brzina zvuka,* m/s	**Dynamic modulus, MPa** *Dinamički modul,* MPa	**Impedance, (kg/m²·s) × 10⁻⁵** *Impedancija,* (kg/m²·s) × 10⁻⁵	***ACE*, m⁻⁴·kg⁻¹·s⁻¹**	**Damping coefficient** *Koeficijent prigušenja*
Plywood *furnirska ploča*	746.0	1,300.5	3,636.2	9,863.7	27.13	206.1	0.0235
Blockboard *stolarska ploča*	640.5	1,389.0	3,883.6	9,661.2	24.88	257.1	0.0234
MDF	859.3	872.5	2,439.5	5,114.1	20.96	103.7	0.0273
Purenit	653.6	400.0	1118.4	817.6	7.31	62.5	0.0536

Table 2 C notes and their frequencies on a standard range piano keyboard
Tablica 2. Tonovi C i njihove frekvencije na klavirskoj tipkovnici standardnog raspona

Note / *Tonovi*	C_1	C	c^1	c^2	c^3	c^4	c^5	c^6
Frequency, Hz *Frekvencije,* Hz	32.7	65.4	130.8	261.6	523.2	1046.4	2092.8	4185.6

als and Purenit boards, whose decrement of damping has higher values. Despite a relatively low regression coefficient, a lower damping coefficient with increasing frequency is noticeable. On average, Purenit achieved the highest damping values (0.0432 and 0.064 for the lower and upper panel, respectively). In the case of the lower panel, plywood and blockboard had almost the same damping coefficient (0.022), while MDF was higher (0.027). In the case of the upper panel, a downward trend was found for wood-based panels – 0.031, 0.024 and 0.019 for plywood, blockboard and MDF, respectively.

Based on the longitudinal frequency, dimensions and weight of the specimens, sound velocity, dynamic modulus of elasticity, characteristic impedance and ACE can be calculated.

Blockboard and plywood have structures closer to natural wood than the other materials and therefore have better acoustic properties, such as *ACE* and sound velocity. Due to the disintegration of wood fibres in MDF panels, this material shows higher damping values than blockboard or plywood. Purenit panels, as expected, gave the lowest frequency, sound velocity impedance and *ACE* due to the different non-wood structure and homogeneity of this material.

Ono and Okuda (2007) and Ono *et al.* (2002) reported acoustic parameters of carbon-fibre reinforced polyurethane foam. This material is closer to the purenit panels. They state that the frequency along the fibres is between 1,433 and 1,860 Hz. Values are higher than those in this article probably because of highly conductive carbon fibres content. Q_r^{-1} factor, which is an alternative to damping coefficient, measured about 0.014. This value is close to resonance spruce damping.

Ghofrani *et al.* (2016) reported damping coefficient between 0.039 – 0.068 for plywood with a rubber core. Due to the damping of rubber core, these values are almost 3 times higher than those of standard plywood.

Bucur (2016) reported the acoustic properties for spruce. He determined the value of longitudinal frequency of 1,405 Hz, which is very close to the measured frequency for the blockboard. The value of damping in longitudinal direction measured 0.009, which is about 2.5× lower than for blockboard. This fact is due to the presence of glue and veneers, which violate the consistency of the grown wood.

Fibreboards are often used as an absorption material. It depends on the density of the material and surface structure (Sharma *et al.*, 2020; Damodaran *et al.*, 2015a). To improve damping parameters, Liu *et al.* (2019) uses the composite made from MDF face and rubber core. They achieved a sound velocity of 594.4 m.s^{-1}, which is much lower compared to our results. The damping coefficient was measured at 0.138, which

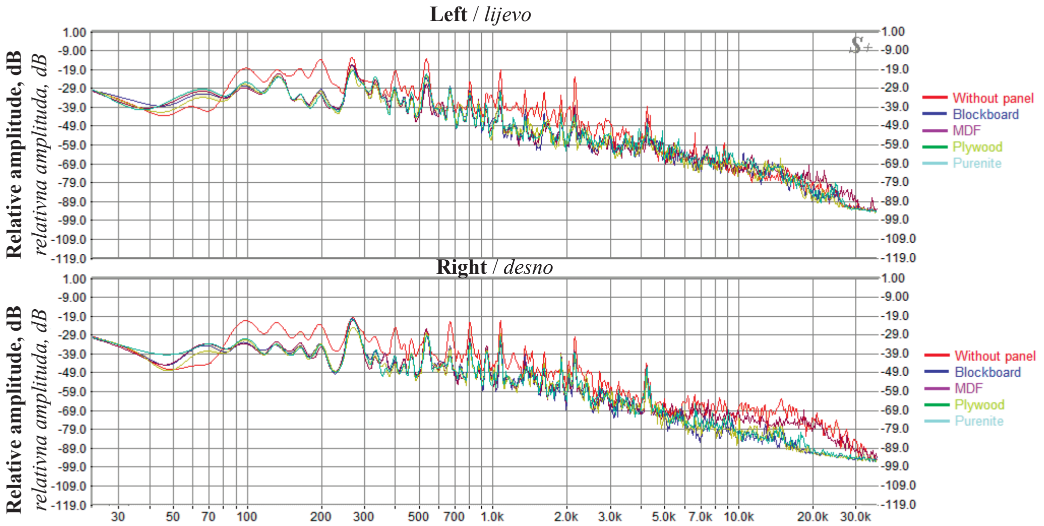

Figure 6 SpectraPLUS-SC output (scale 8000 pts). Red line without panel; blue line blockboard; purple line MDF; green line plywood; light blue line purenit. Top plot: microphone closer to the piano; bottom plot: microphone 1 m behind. Curves represent maximum amplitudes for each note sounded

Slika 6. Izlaz SpectraPLUS-SC (skala 8000 bodova). Crvena linija – bez ploče; plava linija – stolarska ploča; ljubičasta linija – MDF; zelena linija – furnirska ploča; svjetloplava linija – purenit. Gornji graf: mikrofon bliže klaviru; donji graf: mikrofon 1 m iza klavira. Krivulje predočuju maksimalne amplitude za svaki ton.

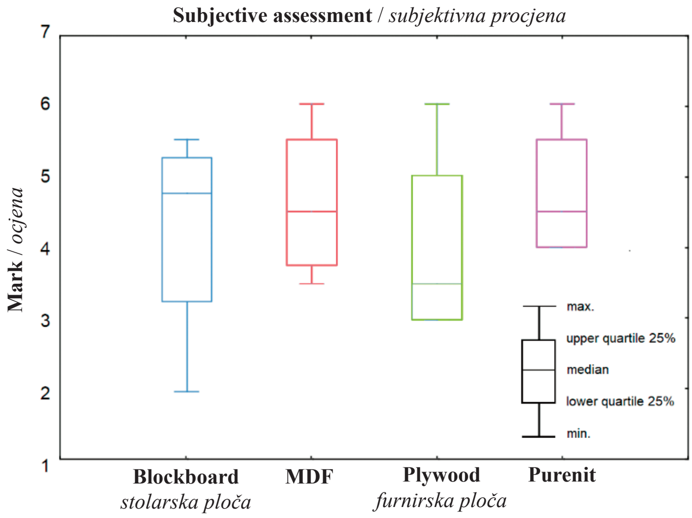

Figure 7 Subjective assessment of test materials
Slika 7. Subjektivna procjena ispitnih materijala

is about 5 times higher than our results. Rubber core makes the material very absorbent.

The second part of this study deals with the acoustic response of the musical instrument. A note C in each octave was generated sequentially one by one with a device designed to make the same stroke repeatedly. Their frequencies are given below.

Outputs from Spectra software are given in Figure 6. The plots represent the maximum amplitude at all described tones.

As can be seen, the red line falls above all others, indicating that the front panels of the piano absorb the sound in most frequencies. The exception is an area of low frequency, which the panels amplify. The amplitudes of other materials overlap considerably; therefore it is not possible to find a statistically significant difference between materials in the case of amplitudes with this measuring equipment.

The last part of the study is a subjective assessment of the piano when fitted with different panels. The best assessment was given for multi-layer plywood, the worst for Purenit, though the results found by ANOVA testing were not statistically significant. The committee found that the presence of panels decreased the acoustic radiation of the instrument. The highest decrement of damping was subjectively registered for the Purenit panel (Figure 7).

When a good acoustic response is required, piano manufacturers choose a high-quality resonance spruce wood (*Picea abies*), in other situations a compromise is struck that takes into consideration the price, availability, workability and acoustic properties of materials. Good acoustic properties of resonance spruce are well known (Zatloukal *et al.*, 2021; Endo *et al.*, 2016). Therefore, four composite materials were selected for testing in this study (three wood-based and one non-wood-based), and the acoustic response of a piano fitted with front panels made of these materials was assessed using straightforward methods. The results show that it is very hard to assess these materials either with simple measuring apparatus or by subjective judgement. The timbre of the sound and its character formed by many small nuances of higher harmonic tones is experimentally almost undetectable in all respects. Therefore, a subjective assessment is very often used, especially with violins – the wealth of research involving the legendary Stradivarius violin (Torres *et al.*, 2020; Invernizzi *et al.*, 2016; Grissino-Mayer *et al.*, 2004) serves as a good example. The fact is that players, when choosing an instrument, select the one that sounds best to them from a range of similar models. Several measurable parameters can support the basic assessment. For the suitability of the different types of material for the front panel of a piano case, the density, frequency response, sound propagation velocity, dynamic Young's modulus, characteristic impedance, and radiation ratio were also added.

In terms of these sound propagation properties, it can be said that the best performance was achieved by blockboard, followed by plywood, MDF, and last by Purenit panels. The subjective assessment made in this work confirmed this ranking.

Blockboard and plywood have a structure closer to natural wood than the other materials. Average resonance spruce achieves a longitudinal sound velocity of 5,600 $m.s^{-1}$ (Bucur, 2006), longitudinal frequency of 6400 Hz (Zatloukal *et al.*, 2021), dynamic Young's modulus of 11000 MPa (Endo *et al.*, 2016), radiation ratio of 12.3 $m^{-4}\cdot kg^{-1}\cdot s^{-1}$ (Zatloukal *et al.*, 2021), and characteristic impedance of 5.7 $(kg/m^2\cdot s)\times 10^{-5}$ (Zatloukal *et al.*, 2021) at an average density of 480 kg/m^3. The comparison of our results with the parameters of

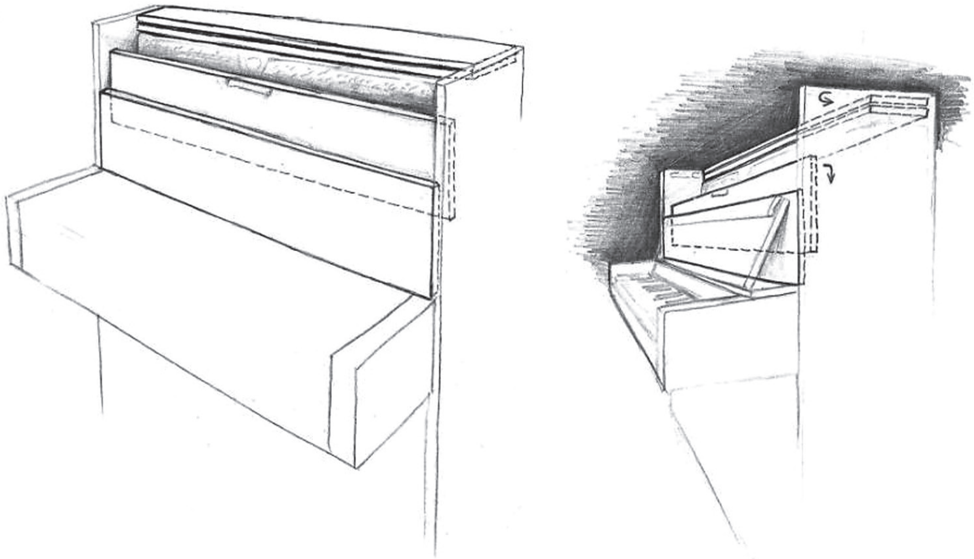

Figure 8 Suggestion of an openable upper panel for better acoustics (F. Šulc)
Slika 8. Prijedlog gornje ploče koja se može otvarati radi bolje akustike (F. Šulc)

resonance spruce, clearly show that these properties were not achieved by the tested materials. MDF panels are used rather than sound absorption panels (Sali *et al.*, 2004; Kang *et al.*, 2005; Lee *et al.*, 2014). Purenit, primarily used as a thermal insulation material, was not expected to have good results of acoustic response.

When considering price and performance, MDF becomes attractive as a material for piano panels because it is less than half the price of plywood and a third that of blockboard, at the time of writing. Despite the measured acoustic properties, the presence of front panels of any type was found to have a negative effect on the acoustics of the piano. Some piano designers acknowledge this and solve the issue by perforating the front panel (this should improve the aesthetics of the instrument as well). Better acoustic performance can be achieved by opening the top board, but this is sometimes impractical. Some manufacturers use an ellipse-shaped constriction in the front panel to improve acoustics (August Förster 125 and Rönisch 132); the panels may be openable in the manner of Venetian blinds; or the front panels may be made thinner than usual (e.g., Zeitter Winkelmann model 36930). A piano with a visible action may make listening more attractive, as used, for example, in the experimental self-playing Edelweiss U49 model. Fig. 8 suggests how to open the front panel and thus decrease damping. A similar solution can be found in the Petrof AP 136. Another example of an openable panel can be found in Feurich Model 123, which has a small window on the front. The problem of piano panels is very complex. Many professional piano players prefer damping panels instead because the sound that comes from an open piano may be too loud. If a quieter sound is desired, then materials with higher damping properties may be considered.

4 CONCLUSIONS
4. ZAKLJUČAK

Four types of front panels for upright piano were vibro-acoustically tested.

Having front panels at all was found to have a negative influence except at low frequencies.

Based on the acoustic parameters, blockboard achieved the best result with a longitudinal frequency of 1,389.0 Hz, sound velocity of 3,883.6 m/s, *ACE* 257.1 $m^{-4}\cdot kg^{-1}\cdot s^{-1}$, and damping coefficient of 0.0234.

Pywood achieved good acoustic with longitudinal frequency 1,300.5 Hz, sound velocity 3,636.2 m/s, *ACE* 206.1 $m^{-4}\cdot kg^{-1}\cdot s^{-1}$, and damping coefficient 0.0235.

MDF panel had the worse acoustic properties with a frequency of 872.5 Hz, sound velocity of 2,439.5 m/s *ACE* 103.7 $m^{-4}\cdot kg^{-1}\cdot s^{-1}$, and damping coefficient 0.0273.

Purenit panels achieved the worst acoustic properties, which was also unanimously confirmed by the committee. The measured frequency was 400.0 Hz, sound velocity 1,118.4 m/s, *ACE* 62.5 $m^{-4}\cdot kg^{-1}\cdot s^{-1}$, and damping coefficient 0.0536 This material was found inappropriate for the construction of the piano.

However, when considering the price-performance ratio, the MDF panels should be a good compromise for making the front panel of the cheaper piano.

Further research could aim to research other materials such as carbon-fibre composites, fibre-reinforced wood, or resonance spruce boards. Various shapes and structural designs of front panels might be acoustically tested.

Acknowledgements – Zahvala

This research was supported by the Czech piano maker Petrof, spol. s r.o. The authors are grateful to the company for donating the material for making the samples, for the kind loan of the upright piano for testing the front panels, and for providing the anechoic chamber space.

5 REFERENCES
5. LITERATURA

1. Ahmadi, M.; Moezzipour, B.; Moezzipour, A., 2019: Thermal stability of wood fibers produced from recycled medium density fiberboards. Drvna industrija, 70 (2): 149-155. https://doi.org/10.5552/drvind.2019.1833
2. Ayrilmis, N., 2008: Effect of compression wood on dimensional stability of medium density fiberboard. Silva Fennica, 42 (2): 257. https://doi.org/10.14214/sf.257
3. Ayrilmis, N.; Winandy, J. E., 2009: Effects of post heat-treatment on surface characteristics and adhesive bonding performance of medium density fiberboard. Materials and Manufacturing Processes, 24 (5): 594-599. https://doi.org/10.1080/10426910902748032
4. Baar, J.; Tippner, J.; Gryc, V., 2016: Wood anatomy and acoustic properties of selected tropical hardwoods. IAWA Journal, 37 (1): 69-83. https://doi.org/10.1163/22941932-20160121
5. Besnainou, C., 1998: Composite materials for musical instruments: The maturity. The Journal of the Acoustical Society of America, 103 (5): 2872-2873. https://doi.org/10.1121/1.421525
6. Bilgin, U.; Colakoglu, G., 2021: Effect of using urea formaldehyde modified with extracts in plywood on formaldehyde emission. Drvna industrija, 72 (3): 237-244. https://doi.org/10.5552/drvind.2021.2005
7. Böhm, M.; Salem, M. Z.; Srba, J., 2012: Formaldehyde emission monitoring from a variety of solid wood, plywood, blockboard and flooring products manufactured for building and furnishing materials. Journal of Hazardous Materials, 221: 68-79. https://doi.org/10.1016/j.jhazmat.2012.04.013
8. Bucur, V., 2006: Acoustics of wood. Springer Series in Wood Science, Berlin/Heidelberg. https://doi.org/10.1007/3-540-30594-7
9. Bucur, V., 2016: Handbook of materials for string musical instruments. Springer Cham. https://doi.org/10.1007/978-3-319-32080-9
10. Bucur, V., 2017: The Acoustic of wood, eBook. CRC press, Boca Raton. https://doi.org/10.1201/9780203710128
11. Čulík, M.; Danihelová, A.; Danihelová, Z., 2015: Evaluation of properties of black mulberry wood for xylophone bars. Akustika, 23 (1): 2-5.
12. Damodaran, A.; Lessard, L.; Suresh Babu, A., 2015a: An overview of fibre-reinforced composites for musical instrument soundboards. Acoustics Australia, 43: 117-122. https://doi.org/10.1007/s40857-015-0008-5
13. Damodaran, A.; Mansour, H.; Lessard, L.; Scavone, G.; Babu, A. S., 2015b: Application of composite materials to the chenda, an Indian percussion instrument. Applied Acoustics, 88: 1-5. https://doi.org/10.1016/j.apacoust.2014.07.013
14. Daoud, H.; El Mahi, A.; Rebiere, J. L.; Taktak, M.; Haddar, M., 2017: Characterization of the vibrational behaviour of flax fibre reinforced composites with an interleaved natural viscoelastic layer. Applied Acoustics, 128: 22-31. https://doi.org/10.1016/j.apacoust.2016.12.005
15. Demir, A.; Aydin, I.; Ozturk, H., 2018: Formaldehyde release from plywood manufactured with two types of urea formaldehyde resins after fire retardant treatment of veneers. Drvna industrija, 69 (2): 193-199. https://doi.org/10.5552/drind.2018.1734
16. Duerinck, T.; Verberkmoes, G.; Fritz, C.; Leman, M.; Nijs, L.; Kersemans, M.; Van Paepegem, W., 2020: Listener evaluations of violins made from composites. The Journal of the Acoustical Society of America, 147 (4): 2647-2655. https://doi.org/10.1121/10.0001159
17. Endo, K.; Obataya, E.; Zeniya, N.; Matsuo, M., 2016: Effects of heating humidity on the physical properties of hydrothermally treated spruce wood. Wood Science and Technology, 50 (6): 1161-1179. https://doi.org/10.1007/s00226-016-0822-4
18. Ghofrani, M.; Ashori, A.; Rezvani, M. H.; Ghamsari, F. A., 2016: Acoustical properties of plywood/waste tire rubber composite panels. Measurement, 94: 382-387. https://doi.org/10.1016/j.measurement.2016.08.020
19. Glass, S.; Zelinka, S., 2021: Moisture relations and physical properties of wood. Chapter 4 in FPL-GTR-282, pp. 4-1.
20. Grissino-Mayer, H. D.; Sheppard, P. R.; Cleaveland, M. K., 2004: A dendroarchaeological re-examination of the "Messiah" violin and other instruments attributed to Antonio Stradivari. Journal of Archaeological Science, 31 (2): 167-174. https://doi.org/10.1016/s0305-4403(03)00107-9
21. Gunji, T.; Obataya, E.; Aoyama, K., 2012: Vibrational properties of harp soundboard with respect to its multilayered structure. Journal of Wood Science, 58 (4): 322-326. https://doi.org/10.1007/s10086-012-1253-y
22. Ibáñez-Arnal, M.; Doménech-Ballester, L.; Sánchez-López, F., 2019: A study of the dynamic response of Carbon Fiber Reinforced Epoxy (CFRE) prepregs for musical instrument manufacturing. Applied Sciences, 9 (21): 4615. https://doi.org/10.3390/app9214615
23. Invernizzi, C.; Daveri, A.; Rovetta, T.; Vagnini, M.; Licchelli, M.; Cacciatori, F.; Malagodi, M., 2016: A multi-analytical non-invasive approach to violin materials: The case of Antonio Stradivari "Hellier"(1679). Microchemical Journal, 124: 743-750. https://doi.org/10.1016/j.microc.2015.10.016
24. Kang, C. W.; Park, H. J.; Jeong, I. S.; Kim, G. C., 2005: Measurement of the sound absorption coefficient of fiberboard by two microphone method. Journal of The Korean Wood Science and Technology, 33 (5): 45-49.
25. Kawalerczyk, J.; Dziurka, D.; Mirski, R.; Szentner, K., 2020: Properties of plywood produced with urea-formaldehyde adhesive modified with nanocellulose and microcellulose. Drvna industrija, 71 (1): 61-67. https://doi.org/10.5552/drvind.2020.1919
26. Kretschmann, D. E., 2010: Mechanical properties of wood. Environments, (5): 34.
27. Kusumaningtyas, I.; Yordaniansyah, H.; Purwanto, T. A., 2016: Acoustical properties of petung bamboo for the top plate of guitars. Applied Acoustics, 112: 123-130. https://doi.org/10.1016/j.apacoust.2016.05.016
28. Lamarque, C. H.; Pernot, S.; Cuer, A., 2000: Damping identification in multi-degree-of-freedom systems via a wavelet-logarithmic decrement. Part 1: Theory. Journal Of Sound and Vibration, 235 (3): 261-374. https://doi.org/10.1006/jsvi.1999.2928
29. Lee, M.; Park, S. B.; Byeon, H. S., 2014: Sound absorption and physical properties of carbonized fiberboards with three different densities. Journal of the Korean Wood Science and Technology, 42 (5): 555-562. https://doi.org/10.5658/wood.2014.42.5.555
30. Liu, M.; Peng, L.; Fan, Z.; Wang, D., 2019: Sound insulation and mechanical properties of wood damping composites. Wood Research, 64 (4): 743-758. https://doi.org/10.1016/j.compstruct.2021.114392

31. Liu, T.; Butaud, P.; Placet, V.; Ouisse, M., 2021: Damping behavior of plant fiber composites: A review. Composite Structures, 275: 114392. https://doi.org/10.1016/j.compstruct.2021.114392
32. Majewski, A.; Smardzewski, J., 2013: Thin purenit honeycomb panels. In: Proceedings of the XXVIth International Conference Research for Furniture Industry September, pp. 63-72.
33. Moezzipour, B.; Moezzipour, A., 2021: Thermal behavior of insulation fiberboards made from mdf and paper wastes. Drvna industrija, 72 (3): 245-254. https://doi.org/10.5552/drvind.2021.2019
34. Niemz, P.; Mannes, D., 2012: Non-destructive testing of wood and wood-based materials. Journal of Cultural Heritage, 13 (3): 26-34. https://doi.org/10.1016/j.culher.2012.04.001
35. Olgun, Ç.; Ateş, S.; Uzer, E., 2023: Effects of Medium Density Fiberboards (MDF) Recycling Methods on Fiber Dimensions and Some Reconstructed Board Properties. Drvna industrija, 74 (1): 61-69. https://doi.org/10.5552/drvind.2023.0037
36. Ono, T.; Isomura, D., 2004: Acoustic characteristics of carbon fiber-reinforced synthetic wood for musical instrument soundboards. Acoustical Science and Technology, 25 (6): 475-477. https://doi.org/10.1250/ast.25.475
37. Ono, T.; Miyakoshi, S.; Watanabe, U., 2002: Acoustic characteristics of unidirectionally fiber-reinforced polyurethane foam composites for musical instrument soundboards. Acoustical Science and Technology, 23 (3): 135-142. https://doi.org/10.1250/ast.23.135
38. Ono, T.; Okuda, A., 2007: Acoustic characteristics of guitars with a top board of carbon fiber-reinforced composites. Acoustical Science and Technology, 28 (6): 442-443. https://www.jstage.jst.go.jp/article/ast/28/6/28_6_442/_pdf
39. Phillips, S.; Lessard, L., 2009: Flax fibers in musical instrument soundboards. In Proceedings of ICCM-17 Conference.
40. Ross, R. J., 2010: Wood handbook: wood as an engineering material. USDA Forest Service, Forest Products Laboratory, General Technical Report FPL-GTR-190, pp. 509.
41. Sali, S.; Znidaric, U.; Kopac, J., 2004: An analysis of the acoustic properties of composite materials. Strojniski Vvestnik – Journal of Mechanical Engineering, 50 (12): 580-593.
42. Savov, V.; Antov, P., 2020: Engineering the properties of eco-friendly medium density fibreboards bonded with lignosulfonate adhesive. Drvna industrija, 71 (2): 157-162. https://doi.org/10.5552/drvind.2020.1968
43. Sepahvand, S.; Doosthosseini, K.; Pirayesh, H.; Maryan, B. K., 2018: Supplementation of natural tannins as an alternative to formaldehyde in urea and melamine formaldehyde resins used in MDF production. Drvna industrija, 69 (3): 215-221. https://doi.org/10.5552/drind.2018.1726
44. Sharma, S. K.; Shukla, S. R.; Sethy, A. K., 2020: Acoustical behaviour of natural fibres-based composite boards as sound-absorbing materials. Journal of the Indian Academy of Wood Science, 17: 66-72. https://doi.org/10.1007/s13196-020-00255-z
45. Shimazu, T.; Miura, M.; Kuno, H.; Isu, N.; Ota, K.; Ishida, E. H., 2006: Synthesis of novel high damping ceramic-polymer composites and its application as ceramic musical instruments. Key Engineering Materials, 319: 173-180. https://doi.org/10.4028/www.scientific.net/kem.319.173
46. Straže, A.; Mitkovski, B.; Tippner, J.; Čufar, K.; Gorišek, Ž., 2015: Structural and acoustic properties of African padouk (Pterocarpus soyauxii) wood for xylophones. European Journal of Wood and Wood Products, 73 (2): 235-243. https://doi.org/10.1007/s00107-015-0878-0
47. Sun, Z., 2018: Progress in the research and applications of natural fiber-reinforced polymer matrix composites. Science and Engineering of Composite Materials, 25 (5): 835-846. https://doi.org/10.1515/secm-2016-0072
48. Torres, J. A.; Soto, C. A.; Torres-Torres, D., 2020: Exploring design variations of the Titian Stradivari violin using a finite element model. The Journal of the Acoustical Society of America, 148 (3): 1496-1506. https://doi.org/10.1121/10.0001952
49. Traoré, B.; Brancheriau, L.; Perré, P.; Stevanovic, T.; Diouf, P., 2010: Acoustic quality of vène wood (*Pterocarpus erinaceus* Poir.) for xylophone instrument manufacture in Mali. Annals of Forest Science, 67 (8): 815. https://doi.org/10.1051/forest/2010054
50. Waltham, C.; Yoshikawa, S., 2018: Construction of wooden musical instruments. Springer Handbook of Systematic Musicology, pp. 63-79. https://doi.org/10.1007/978-3-662-55004-5_4
51. Zatloukal, P.; Suchomelová, P.; Dömény, J.; Doskočil, T.; Manzo, G.; Tippner, J., 2021: Possibilities of Decreasing Hygroscopicity of Resonance Wood Used in Piano Soundboards Using Thermal Treatment. Applied Sciences, 11 (2): 475. https://doi.org/10.3390/app11020475

Corresponding address:

PETR ZATLOUKAL

Mendel University in Brno, Zemědělská 3, Brno, CZECH REPUBLIC, e-mail: xzatlou6@mendelu.cz

İlkay Atar*, Fatih Mengeloğlu[1]

The Effect of Type of Reinforcement, Type of Glue and Reinforcement Place on Mechanical and Physical Properties of LVL

Utjecaj vrste ojačanja, vrste ljepila i mjesta ojačanja na mehanička i fizička svojstva LVL-a

ORIGINAL SCIENTIFIC PAPER
Izvorni znanstveni rad
Received – prispjelo: 24. 7. 2023.
Accepted – prihvaćeno: 15. 1. 2024.
UDK: 630*83; 674.06
https://doi.org/10.5552/drvind.2024.0144

ABSTRACT • *This study investigated the effect of the reinforcement type, glue type, and reinforcement placement on the mechanical and physical properties of LVL. In the study, the glues used were phenol- formaldehyde (FF), epoxy (EX), and polyurethane (PU), while reinforcement materials used were glass fiber, basalt, jute, and cotton fabric. The following three reinforcement combinations were applied: the first was on the bottom surface, the second was on the first adhesive line at the bottom, and the third was on both the bottom and the first adhesive line at the bottom. As part of the study, researchers manufactured 9-layer laminated veneer lumber (LVL) using alder veneers for the surface, and poplar veneers for the middle layers. They produced a total of 39 different combinations of LVL. The mechanical and physical properties of the produced samples were determined. According to the test results, bending strength (BS), modulus of elasticity (MOE), oven-dry specific gravity, and equilibrium moisture content of samples were higher with FF than with other glues. While the samples with EX glue provided the lowest values in water absorption and thickness swelling tests, glass fiber-reinforced samples provided the highest mechanical values. In addition, the samples having reinforcement on the bottom surface provided higher BS and MOE values.*

KEYWORDS: *reinforced LVL; glass fiber; basalt; epoxy; phenol formaldehyde*

SAŽETAK • *U ovom je radu istraživan utjecaj vrste ojačanja, vrste ljepila i položaja ojačanja na mehanička i fizička svojstva LVL-a (lamelirane drvne građe). U istraživanju je rabljeno fenol-formaldehidno (FF), epoksidno (EX) i poliuretansko (PU) ljepilo, dok su materijali za ojačanje bili staklena vlakna, bazalt, juta i pamučna tkanina. Primijenjene su tri kombinacije ojačanja: (1) u donjoj površini, (2) u prvoj liniji lijepljenog spoja od donje površine te (3) u donjoj površini i u prvoj liniji lijepljenog spoja od donje površine. Kao dio studije istraživači su proizveli lameliranu drvnu građu (LVL) od devet slojeva koristeći se furnirima drva johe za površinske slojeve i drva topole za srednje slojeve. Proizvedeno je ukupno 39 različitih kombinacija LVL-a te su određena mehanička i fizička svojstva proizvedenih uzoraka. Prema rezultatima ispitivanja, vrijednosti čvrstoće na savijanje (BS), modula elastičnosti (MOE), gustoće u apsolutno suhom stanju i ravnotežnog sadržaja vode uzoraka s FF ljepilom*

* Corresponding author
[1] Authors are researchers at Kahramanmaras Sutcu Imam University, Faculty of Forestry, Department of Forest Industry Enginering, Kahramanmaras, Turkey. https://orcid.org/0000-0001-9527-1791; https://orcid.org/000- 0002-2614-3662

imale su veće vrijednosti nego u uzoraka izrađenih s ostalim ljepilima. Uzorci s EX ljepilom pokazali su najmanje vrijednosti upijanja vode i debljinskog bubrenja, a uzorci ojačani staklenim vlaknima imali su najbolja mehanička svojstva. Osim toga, uzorci s ojačanjem na donjoj površini imali su veće vrijednosti čvrstoće na savijanje i veći modul elastičnosti.

KLJUČNE RIJEČI: *ojačana lamelirana drvna građa; staklena vlakna; bazalt; epoksid; fenol- formaldehid*

1 INTRODUCTION
1. UVOD

Solid wood has been used in both indoor and outdoor applications from the past to the present. The advantages of solid wood are low price, renewability, easy processing, and good shock resistance. However, solid wood also has some disadvantages such as biodegradability, anisotropic, low dimensional stability, and low mechanical properties (Bozkurt and Erdin, 1997). For this reason, it is challenging to produce large-size carrier elements from a single piece of solid wood. To overcome this problem, engineered wood materials such as oriented strand board (OSB), cross-laminated timber (CLT), plywood, and laminated veneer lumber (LVL) have been developed.

LVL is one of the most essential engineered wood materials. Due to its superior properties, LVL is preferred for many applications, such as scaffold planks, headers, joists, beams, rafters, and truss chords (Çolak *et al*., 2007). They are manufactured using low-density, fast-growing, and economically inexpensive tree species, such as poplar, alder Douglas fir, and spruce. LVL produced from these tree species has low mechanical properties. In order to increase the mechanical properties of wood-based composites, researchers focused on reinforcement studies.

Many researchers have studied fiber reinforcement of LVLs, mainly synthetic glass fiber and carbon fiber (Laufenberg *et al*., 1984). Bal (2014) produced LVL reinforced with phenol formaldehyde adhesive by placing glass fiber between the poplar veneers. With the reinforcement, the increase in impact bending strength and specific impact bending strength was reported. The shear strength of reinforced laminated veneer lumber was significantly greater than that of laminated veneer lumber, and the percentage increase was 213 %. There was also an improvement in physical properties, such as volumetric swelling, tangential swelling, and water absorption. Liu *et al*. (2019) manufactured plywood for construction formwork in different combinations using poplar, eucalyptus veneers, and carbon fiber as reinforcement. Generally, the veneers are bonded with phenol formaldehyde adhesive in plywood production, while carbon fiber is bonded with epoxy.

Plywood reinforcing material is essential for its performance. The reinforcement on the surface increases the longitudinal modulus of elasticity (*MOE*) and modulus of rupture (*MOR*) of the plywood. With the reinforcement of the surface, the ultimate load capacity increases while causing delamination failure. Auriga *et al*. (2020) investigated the effect of using carbon fiber reinforcement in parallel and cross structures. Melamine-urea formaldehyde resin was used as an adhesive, and the reinforcements were placed on the outer and internal glue lines. The results displayed that the place of reinforcement was effective on *MOR* and *MOE* and increased the *MOR* and *MOE* values. Studies show that the use of fiber reinforcements in laminated wood materials is vital in improving mechanical and physical properties. Yildirim *et al*. (2020) used 4 layers of 5 mm thick slats obtained by sawing method from poplar wood. Laminated wood composite materials were produced using 100 g/m^2 (Type 1) and 200 g/m^2 (Type 2) GFRP as reinforcement, polyvinyl acid, Polyurethane and double- layer Epoxy resin as glue. The investigation revealed that Type 2 plain woven fabric is stronger than Type 1 plain woven fabric, epoxy glue is stronger than polyurethane and polyvinyl acetate glue, and parallel loading to the glue line produces better performance than perpendicular loading to the glue line. Zor and Kartal (2020) fiber-reinforced finger corner joints were used to create control samples of the pine, beech, and oak species. The glues utilized were Teknobont 200 epoxy and polyvinyl (PVAc). The experimental samples were tested under diagonal loads, keeping in mind the critical loads that can influence their application. Speranzini and Tralascia (2010) reinforced solid wood and LVL with natural fibers such as basalt, flax, and hemp, and synthetic fibers such as glass fiber and carbon fiber. The four-point bending test results showed that the values of the samples with natural reinforcement were lower than those with the synthetic reinforcements, but their strength values were higher than those without reinforcement. Moezzipour *et al*. (2017) investigated the effect of kenaf and date palm fiber reinforcement on the mechanical and physical properties of horn beam plywood bonded with urea-formaldehyde. The study determined that kenaf fiber performed better than date palm fiber. Jorda *et al*. (2020) produced three-dimensional molded plywood reinforced with flax fibers using epoxy glue. The study showed increased load capacity and stiffness of the reinforced plywood with the reinforcement. Valdes *et al*. (2020) produced a three- and five-layer Cross Laminated Timber (CLT) reinforced with flax fabrics bonded with epoxy. As a result of the study,

Figure 1 Produced test samples
Slika 1. Proizvedeni ispitni uzorci

the load capacity and stiffness of the three-layer CLTs increased significantly with the reinforcement, while in the five-layer CLTs, it was negligible.

In the literature, some studies focus on natural and synthetic fibers and the most used glues preferred in the laminated wood sector. However, no study examines the interaction of natural and synthetic reinforcement materials, water-based and non-water-based adhesives, and the reinforcement placed together. This study investigated the changes in the mechanical and physical properties of LVLs produced by using four different types of natural and synthetic reinforcements, three types of glue, and reinforcement at three locations.

2 MATERIALS AND METHODS
2. MATERIJALI I METODE

2.1 Materials
2.1. Materijali

The study used poplar and alder rotary-peeled veneers as raw wood material. The rotary-peeled veneer thickness of poplar was 2.2 mm, while alder was 1.5 mm. The width and length of the veneer for both species was 50 cm. The veneers were dried to 8-10 % moisture content before production. Phenol formaldehyde (FF) resin Polifen 47 (Polisan, Turkey), epoxy (E) resin LR300/LH300 (Dostkimya, Turkey), and polyurethane (PU) resin PUR 501 (Kleiberit,Germany) were used as adhesives. Glass fiber, basalt, jute, and cotton woven fabrics with a density of 200 g/m^2 were used as reinforcement material. Reinforcement materials were also in 50 cm ×50 cm dimensions.

2.2 LVL production
2.2. Proizvodnja LVL-a

Nine-layer LVLs were produced in 39 different combinations using three different glues, four different reinforcing materials, and three different reinforcement materials in place of use. Test examples are presented in Figure 1. LVLs had alder veneer in the outer and poplar veneer in the middle layers. The placement of reinforcement materials in LVL and the production plan are presented in Figure 2 and Table 1, respectively. The adhesive application per glue line was set to 200 g/m^2. The hydraulic hot press was set at 140 °C for phenol formaldehyde, 110 ºC for other glues, and 10 kg/cm^2 press pressure with 1 mm/min + 3 min press time.

2.3 Physical and mechanical characterization of LVLs
2.3. Fizička i mehanička karakterizacija LVL-ova

The physical properties, oven-dry density, density profile, equilibrium moisture content, thickness swelling, and water absorption tests were carried out. In addition, the images of the test samples were taken with a Canon EOS 70D (EF 100 mm f/2.8L Macro IS

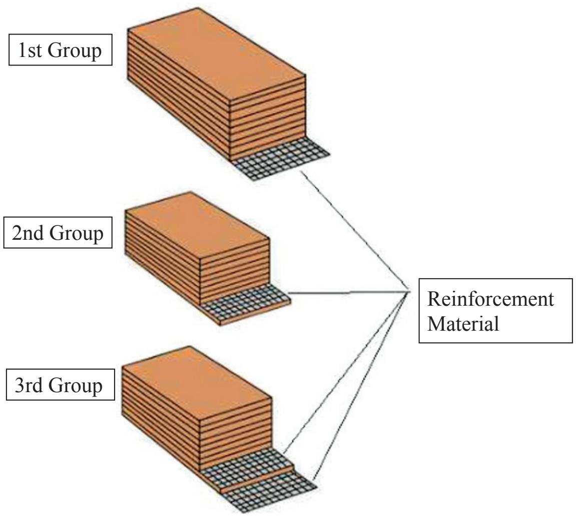

Figure 2 Reinforcement place of use
Slika 2. Položaj ojačanja

Table 1 Production plan
Tablica 1. Plan proizvodnje

No *Broj*	**Sample code** *Oznaka uzorka*	**Glue type** *Vrsta ljepila*	**Reinforcement type** Vrsta ojačanja	**Reinforcement place** *Položaj ojačanja*	
				Bottom outer surface *Donja vanjska površina*	**1st glue line from the bottom** / *Prva linija lijepljenog spoja od donje površine*
1	F-Control	FF	---	---	---
2	FC-1	FF	Glass Fiber	X	---
3	FC-2	FF	Glass Fiber	---	X
4	FC-3	FF	Glass Fiber	X	X
5	FB-1	FF	Basalt	X	---
6	FB-2	FF	Basalt	---	X
7	FB-3	FF	Basalt	X	X
8	FJ-1	FF	Jute	X	---
9	FJ-2	FF	Jute	---	X
10	FJ-3	FF	Jute	X	X
11	FP-1	FF	Cotton	X	---
12	FP-2	FF	Cotton	---	X
13	FP-3	FF	Cotton	X	X
14	E-Control	E	---	---	---
15	EC-1	E	Glass Fiber	X	---
16	EC-2	E	Glass Fiber	---	X
17	EC-3	E	Glass Fiber	X	X
18	EB-1	E	Basalt	X	---
19	EB-2	E	Basalt	---	X
20	EB-3	E	Basalt	X	X
21	EJ-1	E	Jute	X	---
22	EJ-2	E	Jute	---	X
23	EJ-3	E	Jute	X	X
24	EP-1	E	Cotton	X	---
25	EP-2	E	Cotton	---	X
26	EP-3	E	Cotton	X	X
27	P-Control	PU	---	---	---
28	PC-1	PU	Glass Fiber	X	---
29	PC-2	PU	Glass Fiber	---	X
30	PC-3	PU	Glass Fiber	X	X
31	PB-1	PU	Basalt	X	---
32	PB-2	PU	Basalt	---	X
33	PB-3	PU	Basalt	X	X
34	PJ-1	PU	Jute	X	---
35	PJ-2	PU	Jute	---	X
36	PJ-3	PU	Jute	X	X
37	PP-1	PU	Cotton	X	---
38	PP-2	PU	Cotton	---	X
39	PP-3	PU	Cotton	X	X

USM) camera and measured with the MShot Image Analysis System program.

Oven-dry specific gravity, equilibrium moisture content, thickness swelling, and water absorption tests for ten samples each were determined according to EN 323, EN 322, and TS EN 317, respectively. Density profile values were measured on a DAX 5000 GreCon X-ray density-measuring device. The water absorption and thickness swelling test were performed at 2, 24-, 168-, 336- and 504-hour intervals.

Mechanical properties, bending strength, modulus of elasticity, and compressive strength parallel to the grain were measured according to EN 310 and TS 2595, respectively. The span/depth ratio was adjusted to 16 for bending test samples. Ten samples were prepared for each group. Figure 3 presents the bending strength and compressive strength test image.

The data were analyzed using SPSS 20 statistical program. Analysis of variance (univariate) was conducted to determine the effects of glue type, reinforce-


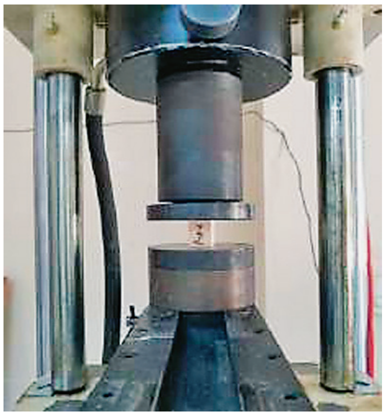

Figure 3 Bending strength and compressive strength test image
Slika 3. Prikaz ispitivanja čvrstoće na savijanje i čvrstoće na tlak

ment type, and reinforcement place on mechanical and physical properties. Besides, Duncan's Multiple Range Test (α=0.05) determined significant differences between groups.

3 RESULTS AND DISCUSSION
3. REZULTATI I RASPRAVA

3.1 Oven-dry density
3.1. Gustoća u apsolutno suhom stanju

Statistical analysis showed that glue type, reinforcement type, and reinforcement place significantly affected oven-dry density. Table 2 shows the homogeneity groups found as the result of the test for oven-dry density. According to the test results, the highest oven-dry density was found in the group produced with phenol-formaldehyde (0.547 g/cm^3), while the lowest oven-dry density was found for the group glued with polyurethane (0.511 g/cm^3).

When the effect of the reinforcement type was examined, the highest oven-dry density was found in the samples using glass fiber. In contrast, the lowest oven-dry density was determined in the samples without reinforcement. Other studies reported similar results stating that the board oven-dry density values increased with reinforcement (Bal, 2014; Kramar and Kral, 2019) because the reinforcing material density was higher than the veneer density. In addition, the amount of glue increases with the use of the reinforcing agent, which increases the oven-dry density (Bal *et al*., 2015).

Regarding the effect of reinforcement placement in the LVLs, the third group provided the highest oven-dry density (the one having two reinforcing sheets). In contrast, samples without reinforcement had the lowest oven-dry density. As expected, the first and second group provided similar oven-dry density since only one reinforcement material was present in both groups. The oven-dry density in the third group was higher than that in the first and second group due to the increased reinforcement and glue.

3.2 Equilibrium moisture content
3.2. Ravnotežni sadržaj vode

Glue type, reinforcement type, and reinforcement placement statistically significantly affected equilibri-

Table 2 Duncan test results for oven-dry density and equilibrium moisture content (α = 0.05)
Tablica 2. Rezultati Duncanova testa za gustoću uzoraka u apsolutno suhom stanju i ravnotežni sadržaj vode (α = 0,05)

Groups / *Grupe*		**Oven-dry density, g/cm^3** *Gustoća u apsolutno suhom stanju,* g/cm^3	**Equilibrium moisture content, %** *Ravnotežni sadržaj vode,* %
Glue type *vrsta ljepila*	Phenol formaldehyde	0.547 **a**	9.33 **a**
	Epoxy	0.538 **b**	7.04 **c**
	Polyurethane	0.511 **c**	7.46 **b**
Reinforcement type *vrsta ojačanja*	Control group	0.494 **d**	7.83 **c**
	Glass Fiber	0.544 **a**	7.84 **c**
	Basalt	0.535 **b**	7.85 **c**
	Jute	0.523 **c**	8.12 **a**
	Cotton	0.538 **b**	8.00 **b**
Reinforcement place *položaj ojačanja*	Control group	0.494 **c**	7.83 **c**
	1. Group	0.530 **b**	7.82 **c**
	2. Group	0.533 **b**	8.12 **a**
	3. Group	0.543 **a**	7.92 **b**

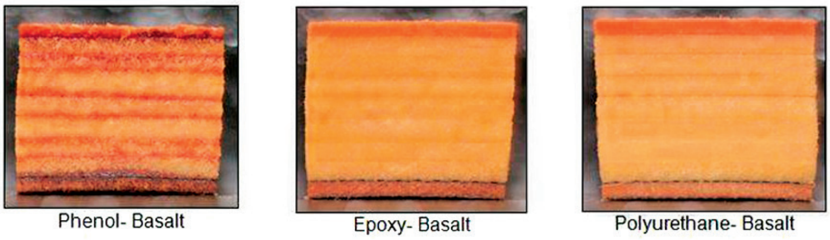

Figure 4 Images of samples after 504 hours
Slika 4. Slike uzoraka nakon 504 sata potapanja u vodi

um moisture content. Table 2 presents the homogeneity groups found as the result of the test for equilibrium moisture content. According to the test results, the highest equilibrium moisture content was found in the phenol-formaldehyde group (9.33 %), while the lowest equilibrium moisture content was found in the epoxy group (7.04 %). None of the groups reached 12 % equilibrium moisture.

Examining the effect of the reinforcement type showed that the samples with jute reinforcement had the highest equilibrium moisture content. In contrast, samples without reinforcement had the lowest equilibrium moisture content. The equilibrium moisture content of the control group and samples using glass fiber and basalt were similar. Since jute and cotton are cellulosic materials, they increase the amount of equilibrium moisture by taking moisture from the atmosphere.

In the case of reinforcement placement, the second group provided the highest equilibrium moisture content, while the first group provided the lowest.

3.3 Thickness swelling and water absorption
3.3. Debljinsko bubrenje i upijanje vode

Statistical analysis showed that glue type, reinforcement type and placement, as well as soaking time, significantly affected thickness swelling. Table 3 presents the homogeneity groups for thickness swelling tests. The test results showed that, while samples produced with phenol- formaldehyde glue had the highest thickness swelling, samples produced with epoxy, on the other hand, had the lowest thickness swelling. Since phenol-formaldehyde glue is water-based, it compels more in a hot press than epoxy and polyurethane, resulting in a more spring back in the water. In addition, the phenol-formaldehyde glue line weakened more over time in water than epoxy and polyurethane glues resulting in a thickness increase. During gluing, some epoxy penetrates the veneer (slightly impregnated) and hardens there. For this reason, the thickness swelling of the samples produced with epoxy glue was less than that of

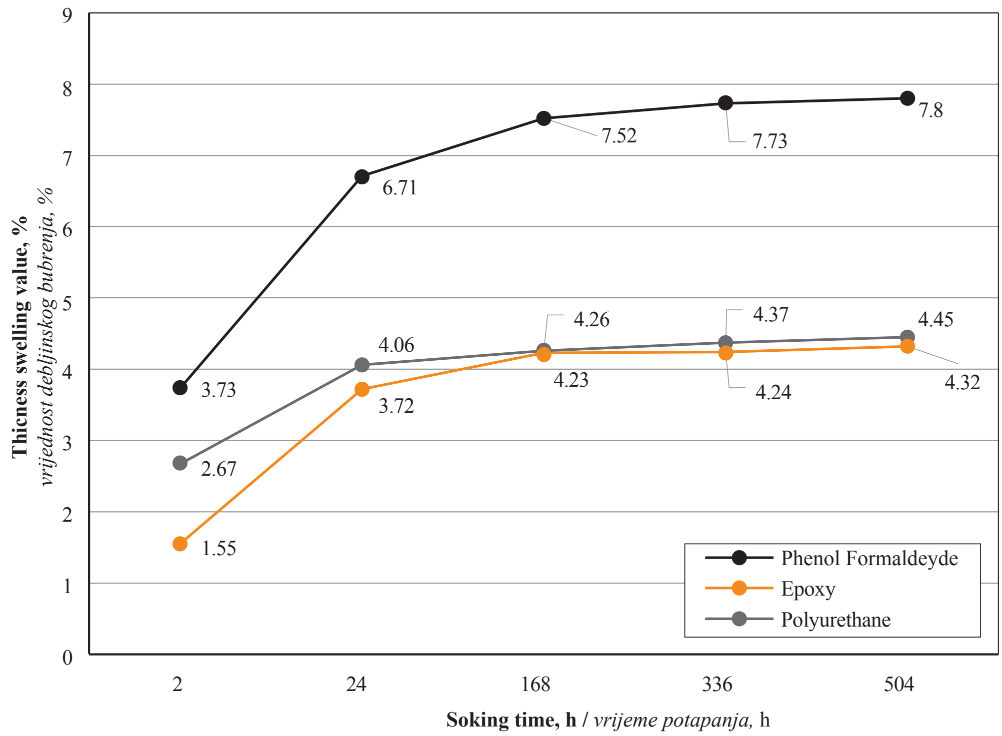

Figure 5 Interaction graph showing average thickness swelling of boards according to soaking time and glue type
Slika 5. Grafikon ovisnosti srednje vrijednosti debljinskog bubrenja ploča o vremenu potapanja i vrsti ljepila

Table 3 Duncan test results for thickness swelling and water absorption (α = 0.05)
Tablica 3. Rezultati Duncanova testa za debljinsko bubrenje i upijanje vode (α = 0,05)

Groups / *Grupe*		**Thickness swelling salue, %** *Vrijednost debljinskog bubrenja, %*	**Water absorption value, %** *Vrijednost upijanja vode, %*
Glue type *vrsta ljepila*	Phenol Formaldehyde	6.70 **a**	81.53 **a**
	Epoxy	3.61 **c**	66.96 **c**
	Polyurethane	3.96 **b**	76.88 **b**
Reinforcement type *vrsta ojačanja*	Control Group	3.91 **d**	88.82 **a**
	Glass Fiber	4.79 **b**	71.92 **e**
	Basalt	4.68 **c**	73.49 **d**
	Jute	5.19 **a**	75.94 **b**
	Cotton	4.66 **c**	74.58 **c**
Reinforcement place *položaj ojačanja*	Control Group	3.91 **d**	88.82 **a**
	1. Group	5.13 **a**	76.33 **b**
	2. Group	4.57 **c**	74.16 **c**
	3. Group	4.79 **b**	71.46 **d**
Soaking time, h *vrijeme potapanja,* h	2	2.65 **d**	22.25 **e**
	24	4.83 **c**	52.30 **d**
	168	5.34 **b**	88.42 **c**
	336	5.47 **a**	103.24 **b**
	504	5.50 **a**	109.40 **a**

polyurethane glued samples since polyurethane glue remains on the veneer surface and forms the foam.

The reinforcement worsened the thickness swelling of LVLs. The jute samples had the highest thickness swelling values, while the control samples had the lowest ones. In reinforced samples, the bottom of the samples expanded less than the non-reinforced upper sides. The reinforcing material reduced the increase in the width direction. While this caused concave bending on the reinforced surface during the test, it caused convex bending on the non- reinforced upper surface (Figure 4); this bending possibly caused an increase in thickness.

Considering the waiting time in the water, the thickness swelling increased with time. Thickness swelling increased significantly up to the 336th hour (Figure 5).

Statistical analysis showed that glue type, reinforcement type, reinforcement place, and soaking time

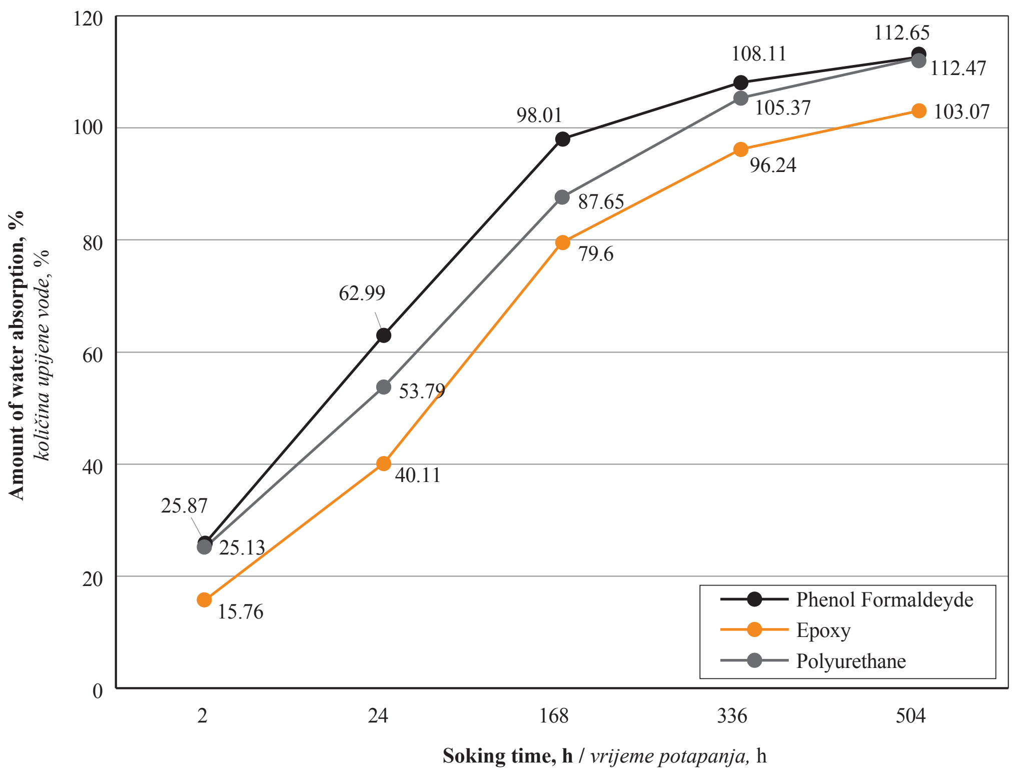

Figure 6 Interaction graph showing average water absorption of boards according to soaking time and glue type
Slika 6. Grafikon ovisnosti srednje vrijednosti upijanja vode ploča o vremenu potapanja i vrsti ljepila

significantly affected water absorption. Table 3 presents the homogeneity groups of the water absorption test result. Results showed that the group produced with phenol- formaldehyde had the highest water absorption, while the group glued with epoxy had the lowest. Similar results were reported in another study. Moradpour *et al*. (2018) reported that the boards produced with water-based UF glue absorb more water than those produced with non-water-based PMDI glue.

With the use of the reinforcement, the water absorption values of the samples decreased. The samples reinforced with glass fiber provided the lowest water absorption, while those reinforced with jute had the highest water absorption. The lower values for glass-fiber and basalt-fiber reinforced LVLs were due to their hydrophobic nature. Jute and cotton have hygroscopic natures, and their LVLs had higher water absorption values.

The reinforcement place had a significant effect. The control group had the highest water absorption value. In contrast, the third group provided the lowest water absorption values. With the increase in the number of reinforcements, water absorption decreased. Increasing the number of reinforcements also raised the amount of glue used in samples. Glue prevents water penetration into the sample, and this reduces the water absorption of the samples (Sulaiman *et al*., 2009; Wang and Chui, 2012a; Wang and Chui, 2012b).

Considering the soaking time in the water bath, water absorption values increase with the increase of the soaking time. A significant increase in water absorption value was observed until the 504th hour.

3.4 Bending strength and modulus of elasticity
3.4. Čvrstoća na savijanje i modul elastičnosti

Statistical analysis showed that glue type, reinforcement type, and reinforcement place significantly affected bending strength. Table 4 presents the homogeneity groups for bending strength test results. The results showed that the phenol-formaldehyde glued group provided the highest bending strength (102.49 MPa), while the polyurethane glued group had the lowest bending strength (83.01 MPa). Samples produced with phenol-formaldehyde and epoxy gave similar results. As phenol formaldehyde contains water, the evaporation of water in the hot press softens the veneers and causes them to compress more. This compression gives resistance to the board. Since epoxy and polyurethane glues are not water-based glues, water vapor does not occur in the hot press. The epoxy penetrates a little into the veneer compared to polyurethane, providing more compaction in the hot press. Therefore, the boards produced with polyurethane are thicker than those produced with phenol-formaldehyde and epoxy-glued LVLs, and their strength is low.

Table 5 presents the results of a simple analysis of variance test showing the effect of glue type on compaction rate. Statistical analysis showed that glue type had a significant effect on compression ratio. According to the statistical analysis results, the highest compression ratio was observed in the samples with phenol formaldehyde, while the lowest compression ratio was observed in the samples using polyurethane.

When looking at the reinforcement types, the best results were found in the samples using glass fiber (102.83 MPa), while the lowest was found in samples using cotton (91.24 MPa). Jute and cotton gave similar results. Since the strength values of glass fiber and basalt are higher than those of cotton and jute, the bending strength of the samples using glass fiber and basalt was higher. In addition, since the thickness of jute and cotton is thicker than that of glass fiber and basalt, it thickens the glue line and is thought to affect the bend-

Table 4 Duncan test results for bending strength, modulus of elasticity and compression strength parallel to grain (α = 0.05)
Tablica 4. Rezultati Duncanova testa za čvrstoću na savijanje, modul elastičnosti i čvrstoću na tlak paralelno s vlakancima (α = 0,05)

Groups / *Grupe*		**Bending strength value, MPa** *Vrijednost čvrstoće na savijanje,* MPa	**Modulus of elasticity value, MPa** *Vrijednost modula elastičnosti,* MPa	**Compression strength parallel to grain value, MPa** *Vrijednost čvrstoće na tlak paralelno s vlakancima,* MPa
Glue type *vrsta ljepila*	Phenol Formaldehyde	102.49 **a**	10934.49 **a**	59.15 **b**
	Epoxy	100.37 **a**	10484.38 **b**	61.22 **a**
	Polyurethane	83.01 **b**	9096.16 **c**	50.33 **c**
Reinforcement type *vrsta ojačanja*	Control Group	86.44 **d**	8659.43 **d**	50.71 **c**
	Glass Fiber	102.83 **a**	10835.52 **a**	59.68 **a**
	Basalt	98.62 **b**	10423.38 **b**	58.72 **a**
	Jute	91.42 **c**	10008.09 **c**	55.70 **b**
	Cotton	91.24 **c**	9923.80 **c**	55.57 **b**
Reinforcement place *položaj ojačanja*	Control Group	86.44 **c**	8659.43 **b**	50.71 **d**
	1. Group	101.89 **a**	10348.63 **a**	53.07 **c**
	2. Group	92.90 **b**	10225.61 **a**	58.72 **b**
	3. Group	93.29 **b**	10318.86 **a**	60.56 **a**

Table 5 Duncan test results for compaction rate
Tablica 5. Rezultati Duncanova testa za vrijednosti stupnja ugušćenja

Groups / *Grupe*	α=0.05		
	a	b	c
Glue type / *Vrsta ljepila*	%	%	%
Phenol Formaldehyde	17.74		
Epoxy		5.27	
Polyurethane			0.37

ing strength negatively. Figure 7 presents the images of glue lines using reinforcement. With the use of reinforcement material, the density of the bottom surface of the board increases, resulting in a raised bending strength (Figure 8).

Considering the effect of the reinforcement place, the best results were found in the first group, while the lowest bending strength was found in samples with no

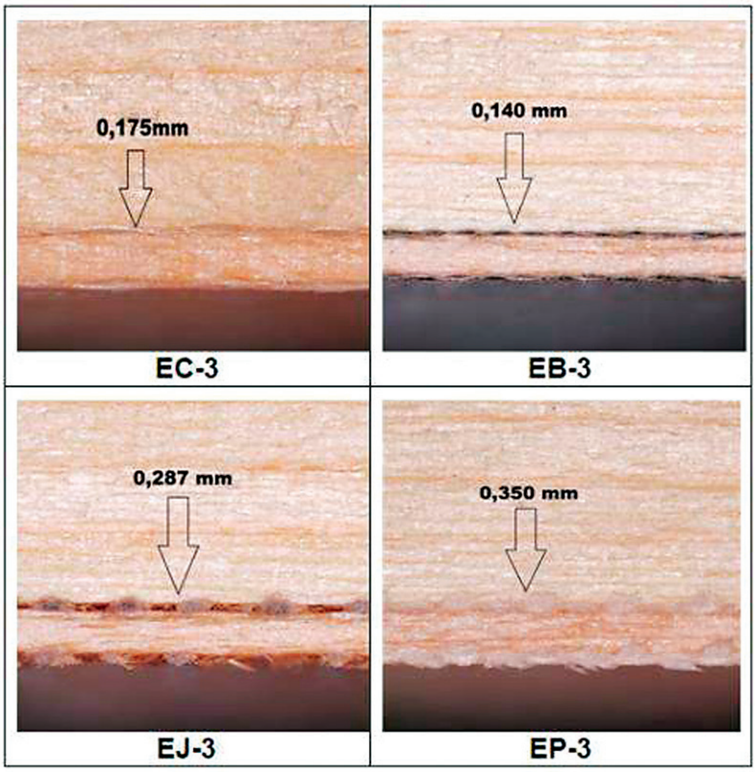

Figure 7 Image of glue line with reinforcement
Slika 7. Slika lijepljenog spoja s ojačanjem

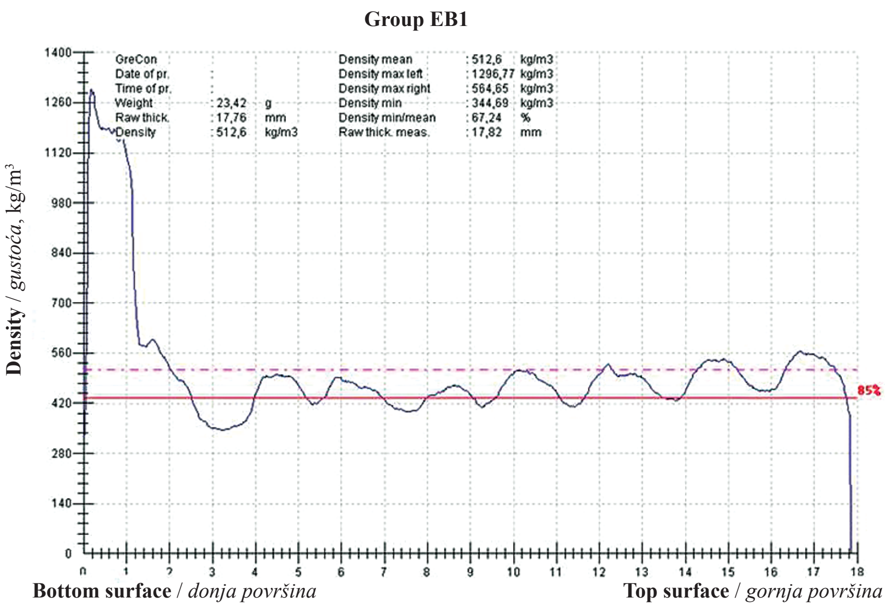

Figure 8 Density profile graph of EB1 sample
Slika 8. Grafikon profila gustoće uzorka EB1

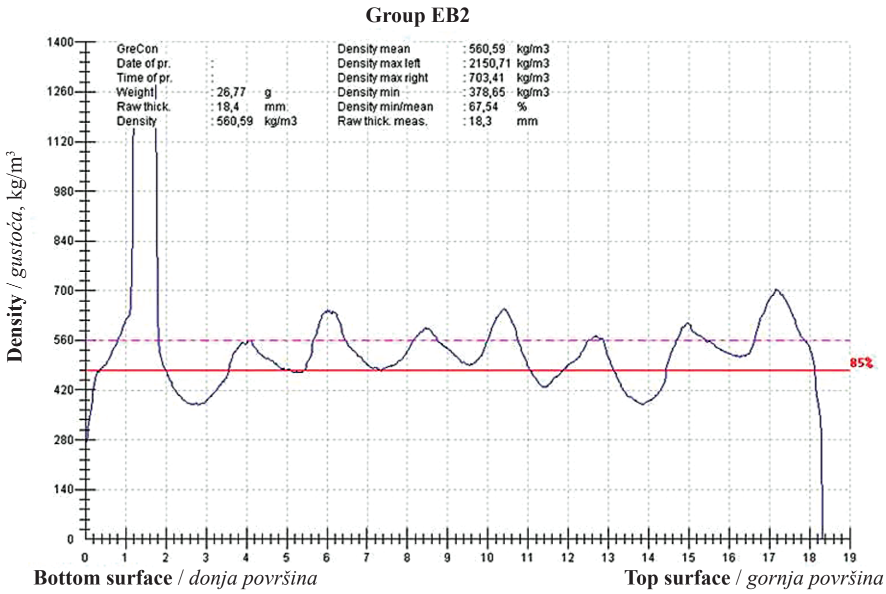

Figure 9 Density profile graph of EB2 sample
Slika 9. Grafikon profila gustoće uzorka EB2

reinforcement. The bending strength of samples in the second and third groups provided similar results. Bending strength increased with the use of reinforcement. Samples exposed to bending strength broke from the bottom surface where tensile stress occurs. Therefore, the bending strength of the first group was improved compared to the control group. In the second group, reinforced in the first glue line from the bottom of the boards, bending strength was lower than in the first group. The reinforcement material cannot prevent the deformation of the sub-veneer where cracking begins. Figure 9 presents the density profile graph. In the second group, the density of the first glue line from the bottom increased, while the density of the bottom layer where the fracture started remained low. In the third group, the bending strength increased more than in the second group. The deformation of the bottom layer, where the fracture occurs, was prevented by the reinforcement material. In a similar study, the reinforcement of the bottom surface of plywood gave better results than the ones reinforced from the upper surface (Kramar and Kral, 2019). In another study, strengthening the bottom surface with natural fibers increased the bending strength of the solid wood material (Borri *et al*., 2013).

The statistical analysis showed that the glue type and the reinforcement type significantly affected the modulus of elasticity, while the reinforcement place did not. Table 4 shows the homogeneity groups of the modulus of elasticity test result. According to the test results, the phenol-formaldehyde glued group provided the highest modulus of elasticity (10934.49 MPa), while polyurethane glued group provided the lowest modulus of elasticity (9096.16 MPa). The modulus of elasticity was low because the boards using polyurethane were less compressed in the hot press than those using phenol and epoxy and foaming in the glue line. Since phenol formaldehyde is water-based, the board is compressed more by the effect of water vapor in the hot press, improving the modulus of elasticity of the board.

Regarding the effect of reinforcement types, the best results were found in the samples using glass fiber (10835.52 MPa), while the lowest were found in the samples using cotton (9923.8013 MPa). Jute and cotton gave similar results. Since the modulus of elasticity of glass fiber and basalt itself is higher than that of cotton and jute, the modulus of elasticity of the samples using glass fiber and basalt was also higher. The reinforcement place also affected modulus of elasticity. The first, second, and third group provided similar results. However, the modulus of elasticity of the reinforced boards was significantly higher than that of the control group.

3.5 Compression strength parallel to grain
3.5. Čvrstoća na vlak paralelno s vlakancima

Statistical analysis showed that glue type, reinforcement type, and reinforcement place significantly affected compression strength parallel to the grain. Table 4 shows the homogeneity groups of the test result for compression strength parallel to the grain. According to the test results, the epoxy-glued group provided the highest compression strength parallel to grain (61.22 MPa); on the contrary, polyurethane glued group supplied the lowest compression strength parallel to grain (50.33 MPa). Since the density of the polyurethane boards (0.511 g/cm^3) was lower than that of the boards produced with phenol-formaldehyde (0.547 g/cm^3) and epoxy (0.538 g/cm^3), the compression strength parallel to grain determined for the groups was also low. In the compression strength parallel to the grain, separation occurred in the reinforcement line in

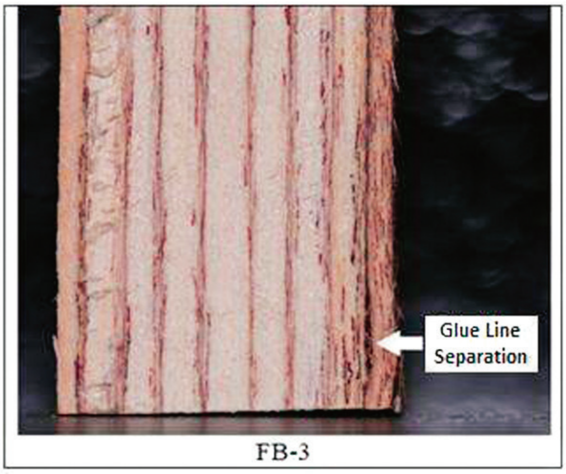

Figure 10 Glue line separation as a result of compression strength parallel to grain
Slika 10. Odljepljivanje sljubnice nakon ispitivanja čvrstoće na vlak

the phenol group samples. In contrast, no separation from the reinforcement in the epoxy-glued group was observed (Figure 10).

When considering the reinforcement types, the best results were found in the samples using glass fiber and basalt, while the lowest ones were found in samples using cotton and jute. Since the glass fiber and basalt thickness is less than that of cotton and jute, the glue line thickness of the samples using glass fiber and basalt was thinner and had higher densities resulting in an increased compression strength parallel to the grain.

Considering the effect of the reinforcement place, the third group provided the best results (60.56 MPa), while the unreinforced control group had the lowest compression strength parallel to the grain. With the increase in the number of reinforcements used, the density of the board increases, as well as the compression strength parallel to the grain. The density of the glue line using the reinforcement material increases, and as this density increases and approaches the middle point of the board, the compression strength parallel to the grain increases, too. For this reason, the compression strength parallel to the grain of the second group was higher than that of the first group.

4 CONCLUSIONS
4. ZAKLJUČAK

This study investigated the effects of three different glue types, four reinforcement types, and three reinforcement places on the physical and mechanical properties of LVL.

As a result of the study, the following conclusions were made:

Among them, phenol-formaldehyde (FF) glued LVLs had the highest density compared to other glues. Regardless of the type, reinforcement increased the density of the resulting samples.

The epoxy-glued samples had the lowest equilibrium moisture, while phenol- formaldehyde glued samples had the highest ones. In addition, samples having jute and cotton reinforcement had higher equilibrium moisture than the ones reinforced with glass fiber and basalt.

Epoxy-glued samples provided the lowest thickness swelling, while the reinforcement increased thickness swelling. The jute reinforcement resulted in the highest increase in thickness swelling.

Epoxy-glued samples had the lowest water absorption, while phenol- formaldehyde-glued samples had the highest ones. With the use of reinforcement, the amount of water absorption decreased.

The samples reinforced with glass fiber and glued with phenol-formaldehyde provided the highest bending strength. The samples produced with phenol-formaldehyde and epoxy provided statistically similar bending strength properties. Also, reinforcement increased the bending strength of the boards. The reinforcement at the tension surface of the sample provided the highest bending strength.

For the modulus of elasticity, samples glued with FF provided the highest value, while those glued with polyurethane had the lowest value. The modulus of elasticity of the samples increased with reinforcement.

The epoxy-glued samples provided the highest compression strength parallel to the grain when using glass fiber and basalt. The compression strength parallel to the grain increased with the number of reinforcements.

Acknowledgements – Zahvala

This study was supported by the Scientific Research Projects Coordination Unit of Kahramanmaras Sutcu Imam University.

5 REFERENCES
5. LITERATURA

1. Auriga, R.; Gumowska, A.; Szymanowski, K.; Wronka, A.; Robles, E.; Ocipka, P.; Kowaluk, G., 2020: Performance properties of plywood composites reinforced with carbon fibers. Composite Structures, 248: 112533. https://doi.org/10.1016/j.compstruct.2020.112533
2. Bal, B. C., 2014: Some physical and mechanical properties of reinforced laminated veneer lumber. Construction and Building Materials, 68: 120-126. https://doi.org/10.1016/j.conbuildmat.2014.06.042
3. Bal, B. C.; Bektaş, İ.; Mengeloğlu, F.; Karakuş, K.; Demir, H. Ö., 2015: Some technological properties of poplar plywood panels reinforced with glass fiber fabric. Construction and Building Materials, 101: 952-957. https://doi.org/10.1016/j.conbuildmat.2015.10.152
4. Borri, A.; Corradi, M.; Speranzini, E., 2013: Reinforcement of wood with natural fibers. Composites. Part B:

Engineering, 53: 1-8. https://doi.org/10.1016/j.compositesb.2013.04.039
5. Bozkurt, Y.; Erdin, N., 1997: Ağaç Teknolojisi Ders Kitabı. I.Ü. Orman Fakültesi, Yayın no: 445, S: 1, Istanbul.
6. Çolak, S.; Çolakoğlu, G.; Aydın, I., 2007: Effects of logs steaming, veneer drying and aging on the mechanical properties of laminated veneer lumber (LVL). Building and Environment, 42 (1): 93-98. https://doi.org/10.1016/j.buildenv.2005.08.008
7. Jorda, J.; Kain, G.; Barbu, M.-C.; Haupt, M.; Krišťák, L., 2020: Investigation of 3D-moldability of flax fiber reinforced beech plywood. Polymers, 12: 2852. https://doi.org/10.3390/polym12122852
8. Kramar, S.; Kral, P., 2019: Reinforcing effect of a thin basalt fiber-reinforced polymer plywood coating. BioResources, 14 (1): 2062-2078.
9. Laufenberg, T. L.; Rowlands, R. E.; Krueger, G. P., 1984: Economic feasibility of synthetic fiber reinforced laminated veneer lumber (LVL). Forest Products Journal, 34: 15-22.
10. Liu, Y.; Guan, M.; Chen, X.; Zhang, Y.; Zhou, M., 2019: Flexural properties evaluation of carbon-fiber fabric reinforced poplar/eucalyptus composite plywood formwork. Composite Structures, 224: 111073. https://doi.org/10.1016/j.compstruct.2019.111073
11. Moezzipour, B.; Ahmadi, M., 2017: Physical and mechanical properties of reinforced ply wood with natural fibers. Journal of the Indian Academy of Wood Science, 14: 70-73. http://dx.doi.org/10.1007/s13196-017-0189-7
12. Moradpour, P.; Pirayesh, H.; Gerami, M.; Jouybari, I. R., 2018: Laminated strand lumber (LSL) reinforced by GFRP; Mechanical and physical properties. Construction and Building Materials, 158: 236-242. https://doi.org/10.1016/j.conbuildmat.2017.09.172
13. Sulaiman, O.; Salim, N.; Hashim, R.; Yusof, L. H. M.; Razak, W.; Yunus, N. Y. M.; Hashim, W. S.; Azmy, M. H., 2009: Evaluation on the suitability of some adhesives for laminated veneer lumber from oil palm trunks. Material and Design, 30: 3572-3580. https://doi.org/10.1016/j.matdes.2009.02.027
14. Speranzini, E.; Tralascia, S., 2010: Engineered lumber: LVL and solid wood reinforced with natural fibres. In Proceedings of the WCTE 2010, World Conference on Timber Engineering, Trentino, Italy, 20 – 24 June, Volume 2, pp. 1685-1690.
15. Valdes, M.; Giaccu, G. F.; Meloni, D.; Concu, G., 2020: Reinforcement of maritime pine cross-laminated timber panels by means of natural flax fibers. Construction and Building Materials, 233: 117741. https://doi.org/10.1016/j.conbuildmat.2019.117741
16. Wang, B. J.; Chui, Y. H., 2012a: Performance evaluation of phenol formaldehyde resin impregnated veneers and laminated veneer lumber. Wood and Fiber Science, 44 (1): 5-13.
17. Wang, B. J.; Chui, Y. H., 2012b: Manufacturing of LVL using cost-effective resin impregnation and lay up technologies. Wood Science and Technology, 46 (6): 1043-1059. https://doi.org/10.1007/s00226-012-0465-z
18. ***EN 323:2005 Wood-Based Panels – Determination of Density. European Committee for Standardization, Brussels, Belgium.
19. ***EN 322:2005 Wood-Based Panels – Determination of Moisture Content. European Committee for Standardization, Brussels, Belgium.
20. ***EN 310:2005 Wood-Based Panels – Determination of Modulus of Elasticity in Bending and of Bending Strength. European Committee for Standardization, Brussels, Belgium.
21. ***TS EN 317:1999 Particleboards and fibreboards – Determination of swelling in thickness after immersion in water. TSE, Ankara.
22. ***TS 2595:1977 Wood – Determination of Ultimate Stress in Compression Parallel to Grain. TSE, Ankara.

Corresponding address:

İLKAY ATAR

Kahramanmaras Sutcu Imam University, Faculty of Forestry, Department of Forest Industry Engineering, Kahramanmaraş 46040, TURKEY, e-mail: ilkayatar53@gmail.com

Hossein Rajabloo, Vahid Vaziri*, Loya Jamalirad, Majid Mokaber-Esfahani[1]

The Effect of Citric Acid Treatment on Particleboard Properties Obtained from a Combination of Garden Tree Branches with Bagasse and Palm Leaves

Utjecaj tretmana limunskom kiselinom na svojstva iverice proizvedene od grana vrtnog drveća pomiješanih s ostatkom od prerade šećerne trske i palminim lišćem

ORIGINAL SCIENTIFIC PAPER
Izvorni znanstveni rad
Received – prispjelo: 18. 9. 2023.
Accepted – prihvaćeno: 15. 1. 2024.
UDK: 630*83; 674.812
https://doi.org/10.5552/drvind.2024.0154

ABSTRACT • *The aim of this research was to determine the effect of citric acid treatment on the particleboard properties obtained by mixing three types of lignocellulosic sources. The board was produced by mixing garden tree branches, bagasse and palm leaves in different mass portions (90:5:5, 70:15:15, 50:25:25). Urea-formaldehyde (UF) resin was used at two levels as 10 % surface layer and 8 % middle layer, and 8 % surface layer and 6 % middle layer based on the raw materials. Citric acid was used at three levels of 0, 10, and 20 % by weight. The physical and mechanical properties of particleboards are measured according to the European Standard EN. Fourier transform infrared spectroscopy was used to distinguish the effect of citric acid treatment on the particles. The results showed that, when the amount of citric acid increased, the water absorption of panels decreased, and the mechanical properties improved. As garden tree branch content in the particleboard increased, so did the total resistance. According to the results of this study, the particleboards containing 70 % garden tree branches, 0 % citric acid, and 8 % UF resin, as well as those of 50 % garden tree branches, 0 % citric acid, and 10 % UF resin can be used for type P1 boards (bending strength of 10 MPa and 0.24 MPa internal bonding). In comparison, the boards containing 90 % garden tree branches, 10 % citric acid and 10 % UF resin were proposed for type P2 boards (bending strength of 11 MPa, modulus of elasticity of 1600 MPa and internal bonding of 0.35 MPa).*

KEYWORDS: *citric acid treatment; bagasse; palm leaves; garden tree branches; particleboard*

SAŽETAK • *Cilj ovog istraživanja bio je utvrditi utjecaj tretmana limunskom kiselinom na svojstva iverice proizvedene miješanjem triju vrsta lignoceluloznog materijala. Ploča je proizvedena miješanjem grana vrtnog drveća,*

* Corresponding author
[1] Authors are M.Sc. graduated student, assistant professor, associate professor and assistant professor at Gonbad Kavous University, Gonbad Kavous, Iran. https://orcid.org/0009-0009-4606-8805; https://orcid.org/0000-0003-3119-5157; https://orcid.org/0000-0002-7767-4172; https://orcid.org/0000-0002-2128-719X

ostataka od prerade šećerne trske i palmina lišća u različitim masenim udjelima (90 : 5 : 5; 70 : 15 : 15; 50 : 25 : 25). Urea-formaldehidna (UF) smola dodavana je u različitim udjelima s obzirom na lignoceluloznu sirovinu: 10 % u površinski sloj i 8 % u srednji sloj te 8 % u površinski sloj i 6 % u srednji sloj. Primijenjena su tri težinska udjela limunske kiseline: 0, 10 i 20 %. Fizička i mehanička svojstva ploča iverica mjerena su na temelju europskog standarda. Za određivanje utjecaja tretmana limunskom kiselinom na čestice lignoceluloznog materijala primijenjena je Fourierova infracrvena spektroskopija. Rezultati su pokazali da se s povećanjem količine limunske kiseline smanjilo upijanje vode ploča i da su se poboljšala njezina mehanička svojstva. Kako se udio grana vrtnog drveća u iverici povećavao, tako se povećavala i ukupna otpornost ploče. Kao ploče tipa P1 (čvrstoća na savijanje od 10 MPa i čvrstoća na raslojavanje od 0,24 MPa) mogu se upotrebljavati iverice koje sadržavaju 70 % grana vrtnog drveća, 0 % limunske kiseline i 8 % UF smole te iverice koje imaju 50 % grana vrtnog drveća, 0 % limunske kiseline i 10 % UF smole. Za usporedbu, ploče koje sadržavaju 90 % grana vrtnog drveća, 10 % limunske kiseline i 10 % UF smole predlažu se kao ploče tipa P2 (čvrstoća na savijanje 11 MPa, modul elastičnosti 1600 MPa i čvrstoća na raslojavanje 0,35 MPa).

KLJUČNE RIJEČI: *tretman limunskom kiselinom; ostatak od prerade šećerne trske; palmino lišće; grane vrtnog drveća; iverica*

1 INTRODUCTION
1. UVOD

Demand for the utilization of wood products in the world and, subsequently in Iran, has increased significantly (Baharlouei *et al*., 2020). Due to the scarcity of forest resources in Iran and the ban on the import of bark logs, the use of other lignocellulosic sources, including agricultural and garden waste, is unavoidable (Vaziri *et al*., 2018; Avarand *et al*., 2018).

The release of toxic gases and the high price of resin led to the use of alternative materials (Mostafalo *et al*., 2019). Due to environmental concerns, the use of synthetic adhesives containing harmful chemicals is decreasing (Umemura *et al*., 2012). Therefore, in the future, emphasis will be placed on the use of natural adhesives (Umemura *et al*., 2013). In the literature survey, natural polymers from plants and animals are used as a natural resin and chemical activator of wooden surfaces (Pizzi, 2006). In the activation method, compounds such as surface lignin and hemicellulose are activated (Umemura *et al*., 2012).

Citric acid can be easily obtained by the fermentation of compounds containing glucose and sucrose (Tsao *et al*., 1999). Citric acid has been researched as a crosslinking agent for wood (Vukusic *et al*., 2006; Šefc *et al*., 2009; Huaxu *et al.,* 2021), plant fiber (Ghosh and Samanta, 1995), pulp and paper (Yang *et al*., 1996).

Umemura *et al*. (2013) used a solution of sucrose and citric acid as a natural resin for producing particleboard with a 25:75 % mixture. Considering the relationship between adhesion and proper bonding of wood particles, they found that these two materials can be used as natural adhesives for the manufacture of particleboard. The internal bonding, bending strength, and thickness swelling values of such boards were comparable to or higher than the type 18 requirements of the Japanese industrial standard for particleboard, JIS A 5908 (2003).

Ksumah *et al.* (2016) investigated the use of sweet sorghum bagasse and citric acid for particleboard manufacturing. The citric acid content was varied in the range of 0-30 wt%. The physical properties of boards improved with increasing citric acid content up to 20 wt%. Infrared (IR) spectra analysis suggests the presence of ester linkages where the carboxyl groups of citric acid had reacted with the hydroxyl groups of the sorghum bagasse to give the boards good physical properties.

Zhao *et al*. (2016) investigated the effect of citric acid on the tannin-sucrose resin and physical properties of the particleboard. The results showed that the particleboards containing 20 and 33.3 % citric acid resin at 200 °C satisfies the requirements of the type 18 JIS A 5908.

Widyorini *et al.* (2016) investigated the physical and mechanical properties of particleboard from bamboo using citric acid. The results showed that the dimensional stability and mechanical properties of the particleboards could be significantly improved by adding citric acid. The particleboards containing citric acid could meet the requirements of the type 18 JIS A 5908.

Kusumah *et al.* (2017) investigated the effects of the weight ratio of citric acid to sucrose on the physical and mechanical properties of particleboard. The results showed that the mechanical properties of particleboards bonded with adhesives in citric acid/sucrose weight ratios of 15/85 and 10/90 were better than those of particleboards in other ratios. As the sucrose content increases, the thickness swelling of the particleboard increases. According to the results of thermal analysis and measurements of the infrared spectra, reactions leading to ester linkages occurred between the citric acid, sucrose and sweet sorghum bagasse.

Widyorini *et al.* (2018) used elephant dung fibers as material for composite board and citric acid as a bonding agent. The results showed that elephant dung fibers can be used as a potential material for composite board. By adding citric acid, the quality of the composite board could be significantly improved.

Mostafalo *et al*. (2019) investigated the effect of citric acid treatment on particleboard properties. The results showed that resin content could be reduced due to the good performance of citric acid in improving strength. It can be concluded that particleboard containing 20 % urea-formaldehyde resin can be used for type P1 boards. The suitability of urea-formaldehyde resin of 10 % and citric acid of 20 % for type P2 boards was given.

Widyorini *et al.* (2019) focused on the effect of an extractive treatment and the application of citric acid on the particleboard properties made from *salacca* frond. The hot water extractive treatment was carried out by boiling the particles for 2 hours. The results showed that the addition of citric acid led to an improvement in the physical and mechanical properties of the particleboard. When using citric acid as an adhesive, the hot water treatment of *salacca* frond is not necessary.

Syamani *et al*. (2020) analyzed the utilization of sugarcane bagasse and citric acid for particleboards production. The infrared (IR) spectra analysis showed the formation of an ester linkage between the carboxyl groups of citric acid and the hydroxyl groups of the sugarcane particles, providing the boards with good physical and mechanical properties.

Due to the shortage of wood resources in Iran, particleboard production companies will face a significant challenge in the future, so companies are focusing on recycling using agricultural and garden waste and other lignocellulosic waste. This research studied the effect of citric acid pretreatment on the particleboard properties obtained from garden tree branches, bagasse and palm leaves. Finally, based on the result, with the aim of increasing the use of palm waste and bagasse as required by particleboard standards, it can be proposed as a solution for the industry.

2 MATERIALS AND METHODS
2. MATERIJALI I METODE

2.1 Raw material
2.1. Sirovina

The lignocellulosic raw material for this research was obtained as follows: garden tree branches (mixture of plum and peach) from Momaz Golestan Particleboard Company, bagasse from Khuzestan province and palm leaves from Kerman**.** These particles were sieved to the size passed through and retained by 20-40 mesh (fine particles with a thickness of 0.41-0.84 mm) and 10-20 mesh (coarse particles with a thickness of 0.841-1 mm). After being prepared, these particles were dried in an oven at a temperature of 80 degrees Celsius until the moisture content of 4 %.

2.2 Adhesive
2.2. Ljepilo

Citric acid**)** Anhydrous**(** was dissolved in distilled water to the concentration of 50 wt%. Prepared citric acid was then added during the production of particleboard at three levels of 0, 10, and 20 % by weight. The characteristics of citric acid are given in Table 1.

Urea-formaldehyde (UF) resin was used at two levels as a 10 % surface layer and 8 % middle layer, and 8 % surface layer and 6 % middle layer based on the dry weight of the particles. The characteristics of urea-formaldehyde resin are given in Table 2. Ammonium chloride as a hardener was also used at 2 % of the dry weight of the resin.

2.3 Manufacture of particleboard
2.3. Proizvodnja ploča iverica

The mixed proportion of garden tree branches, bagasse and palm leave was selected at three levels: (90 % : 5 % : 5 %), (70 % : 15 % : 15 %), and (50 %: 25 %: 25 %), respectively.

A citric acid solution was sprayed onto dried particles to achieve various citric acid contents, i.e., 10, 20 wt%. These particles were dried at 80 ˚C to a final moisture content of 4 % by weight. In order to produce three-layer particleboard, the ratio of coarse particles to fine particles was 60:40.

Table 1 Characteristics of citric acid
Tablica 1. Svojstva limunske kiseline

Density, g/cm³ *Gustoća,* g/cm³	**Melting point, °C** *Talište,* °C	**Molar mass, g/mol** *Molna masa,* g/mol	**pH**	**Purity, %** *Čistoća,* %
1.665	153	192.13	1.7	99

Table 2 Characteristics of urea-formaldehyde resin
Tablica 2. Svojstva urea-formaldehidne smole

Density, g/cm³ *Gustoća,* g/cm³	**Viscosity, cP** *Viskoznost,* cP	**Gel time, s** *Vrijeme želiranja,* s	**pH**	**Solids, %** *Sadržaj suhe tvari,* %
1.27	320	56	7	61

The particleboard was hot-pressed at 170 °C for 7 min at a pressing pressure of 30 kg/cm². Other factors, including board density of 0.7 g/cm³ and board thickness of 16 mm, were considered constant for all treatments. After each mixture was prepared, the resin in a blender was sprayed onto the particles. These particles were formed into mats using a forming box with the size of 450 mm × 450 mm (Figure 1 and 2). In total, 18 variants of boards were manufactured (Table 3).

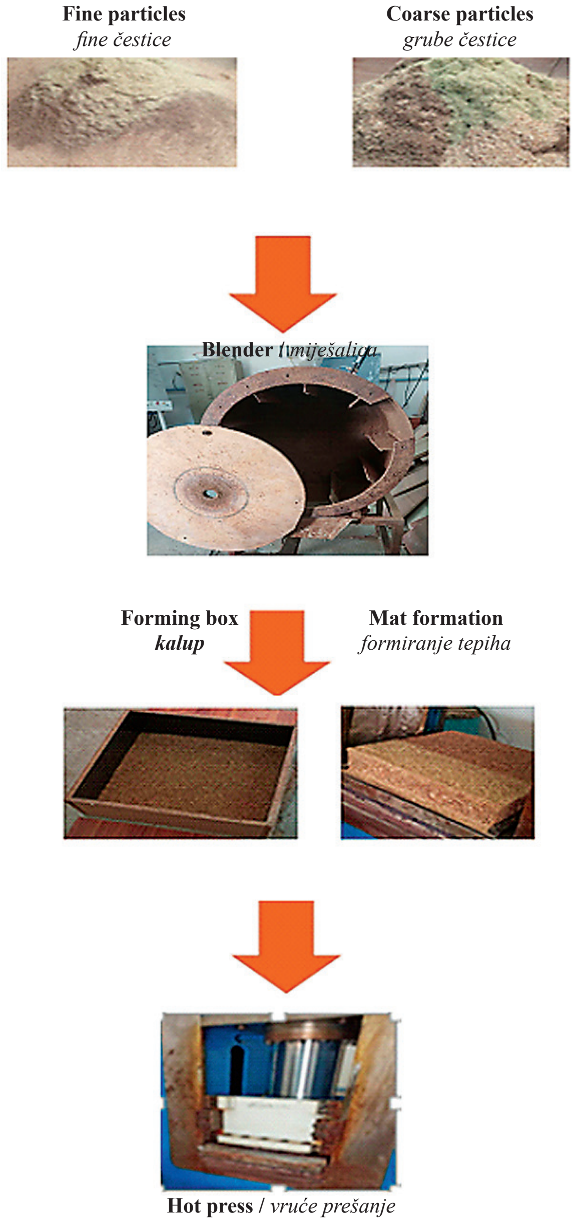

Figure 1 Production stages of particleboard
Slika 1. Faze proizvodnje ploče iverice

2.4 Evaluation of board properties
2.4. Ocjena svojstava ploča

The number of three specimens of every particleboard were tested to obtain a reliable average. After two weeks of conditioning at 20 °C and a relative humidity of approx. 65 %, the panels were cut according to the standard EN 326-1. After immersion in water for 24 hours, water absorption and thickness swelling were measured according to standard EN 317, bending strength and modulus of elasticity according to standard EN 310, and internal bonding according to standard EN 319. The results of this study were compared with those for type P1 board (bending strength of 10 MPa and internal bonding of 0.24 MPa) and type P2 board (bending strength of 11 MPa, modulus of elasticity of 1600 MPa and internal bonding of 0.35 MPa) according to EN 312 standards.

2.5 Fourier transform infrared spectroscopy (FT-IR)
2.5. Fourierova infracrvena spektroskopija (FT-IR)

A Fourier transform infrared spectrometer (model PUYCOM SP1100) was used to determine the effect of citric acid treatment on particles. The edge of the particleboard was scratched to obtain particles. These particles were ground into powder. An FT-IR spectrometer (PUYCOM, SP 1100) was used with the KBr disc method and was recorded by an average of 16 scans at a resolution of 4 cm^{-1} in the range 400 - 4000 cm^{-1}.

2.6 Data analysis
2.6. Analiza podataka

The results were analyzed by a factorial test in a completely randomized design. To compare the means, Duncan's test with a 95 % confidence level was used.

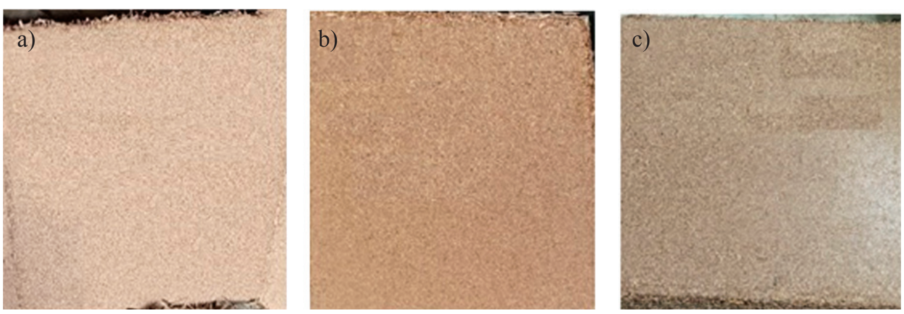

Figure 2 Pictures of particleboards: a) treatment G90A0R10, b) treatment G70A0R10, c) treatment G50A0R10
Slika 2. Slike ploča iverica: a) tretman G90A0R10, b) tretman G70A0R10, c) tretman G50A0R10

Table 3 Combination of test samples
Tablica 3. Kombinacije ispitnih uzoraka

Treatment code *Oznaka tretmana*	**Particles for producing particleboard, %** *Sirovina za proizvodnju ploče iverice, %*			**Adhesive, %** *Ljepilo, %*	
	Garden tree branches (G) *Grane vrtnog drveća* (G)	**Bagasse** *Ostatak od prerade šećerne trske*	**Palm leaves** *Palmino lišće*	**Citric acid (A)** *Limunska kiselina* (A)	**UF resin in surface layer (R)** *UF smola u površinskom sloju* (R)
G50A0R8	50	25	25	0	8
G70A0R8	70	15	15	0	8
G90A0R8	90	5	5	0	8
G50A0R10	50	25	25	0	10
G70A0R10	70	15	15	0	10
G90A0R10	90	5	5	0	10
G50A10R8	50	25	25	10	8
G70A10R8	70	15	15	10	8
G90A10R8	90	5	5	10	8
G50A10R10	50	25	25	10	10
G70A10R10	70	15	15	10	10
G90A10R10	90	5	5	10	10
G50A20R8	50	25	25	20	8
G70A20R8	70	15	15	20	8
G90A20R8	90	5	5	20	8
G50A20R10	50	25	25	20	10
G70A20R10	70	15	15	20	10
G90A20R10	90	5	5	20	10

3 RESULTS AND DISCUSSION
3. REZULTATI I RASPRAVA

3.1 FT-IR analysis
3.1. FT-IR analiza

The FT-IR spectra of citric acid, particleboard without citric acid used a control sample, particleboard with 10 % and particleboard with 20 % citric acid treatment were merged in S1, S2, S3, and S4 in Figure 3, respectively.

In FT-IR spectra of citric acid (S1), the stretching vibration of the acidic carbonyl group in citric acid can be seen in the absorption peaks of around 1740 cm^{-1} and 1640 cm^{-1}. In the spectrum of particleboards (S2, S3, and S4), the peak in the region of 3433 cm^{-1} corresponds to the stretching vibration of the abundant hydroxyl groups in the structure of lignocellulosic materials (garden tree branches, bagasse and palm leaves) derived from cellulose, hemicellulose and lignin.

In S2, S3, and S4, the peak in the region around 2930 cm^{-1} corresponds to stretching vibrations of aliphatic CH bonds in the lignocellulosic structures. The strong peaks at about 1045 cm^{-1} to 1050 cm^{-1} are related to the stretching vibrations of the aliphatic ether C-O-C bond. Also, the peak observed in the region of 1729 cm^{-1} indicates the stretching vibration associated with the ester carbonyl group, and its increase intensity in the S4 compared to S3 indicates an increase in the number of ester groups resulting from the esterification reaction between the carboxyl group of citric acid and the hydroxyl groups of lignocellulosic materials (Mostafalo *et al*., 2019; Widyorini *et al*., 2019). The absorption peak of the acid carbonyl group in S1 was shifted from 1740 cm^{-1} to 1729 cm^{-1} in S3 and S4. The ester bonds increase the adhesion in the particleboard structure.

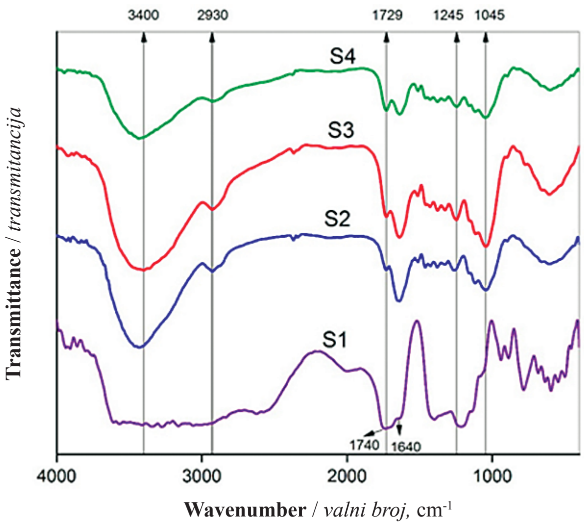

Figure 3 FT-IR spectra of citric acid (S1), particleboard without citric acid used a control sample (S2), particleboard with 10 % citric acid (S3), and particleboard with 20 % citric acid (S4)
Slika 3. FT-IR spektri limunske kiseline (S1), iverice bez limunske kiseline – kontrolni uzorak (S2), iverice s 10 % limunske kiseline (S3) i iverice s 20 % limunske kiseline (S4)

Table 4 Results of variance analysis
Tablica 4. Rezultati analize varijance

Parameter	Source of variance* *Izvor varijance**	Degrees of freedom *Stupnjevi slobode*	Mean square *Srednji kvadrat*	*F* value *F-vrijednost*	*P* Sig.
Bending strength *čvrstoća na savijanje*	Factor A	1	4.576	80.607	0.000
	Factor B	2	4.785	84.282	0.000
	Factor C	2	2.850	50.201	0.000
	B×C	4	0.282	4.967	0.003
	A×B	2	0.233	4.101	0.025
	A×C	2	0.174	3.071	0.049
	A×B×C	4	0.110	1.939	0.035
	Error	36	0.057		
	Corrected Total	53			
Modulus of elasticity *modul elastičnosti*	Factor A	1	43067.130	164.996	0.000
	Factor B	2	49040.796	187.882	0.000
	Factor C	2	75804.019	290.416	0.000
	B×C	4	1293.963	4.957	0.003
	A×B	2	1688.685	6.470	0.004
	A×C	2	192.463	0.737	0.035
	A×B×C	4	2018.519	7.733	0.000
	Error	36	261.019		
	Corrected Total	53			

*Factor A – resin; Factor B – mixture garden tree branches; Factor C – citric acid / *faktor A – smola; faktor B – smjesa grana vrtnog drveća; faktor C – limunska kiselina*

3.2 Bending strength and modulus of elasticity
3.2. Čvrstoća na savijanje i modul elastičnosti

The results of variance analysis showed that the independent and dependent effects of the variable factors had a significant effect on the bending strength and modulus of elasticity of the boards at a 95 % confidence level (Table 4).

The bending strength and modulus of elasticity improved with increasing UF resin and citric acid content (Figure 4 and 5). Since citric acid has a melting point of 153 °C, it melts during the pressing, improving fiber bonding and acting like a resin (Umemura *et al.*, 2013). As the proportion of garden tree branches increases, both the bending strength and modulus of elasticity of the particleboards increase, so they have the highest resistance in a mixture of 90 % garden tree branches. The highest values of modulus of elasticity and bending strength were obtained from the mixture of 90 % garden tree branches, 20 % citric acid and 10 % UF resin (treatment G90A20R10). The lowest values of bending strength and modulus of elasticity were found in a mixture containing 50 % garden tree branches, 0 % citric acid and 8 % UF resin (treatment G50A0R8). For a better insight into the obtained results of bending strength and modulus of elasticity of particleboards made by mixing three types of lignocellulosic sources, it is important to highlight that, accord-

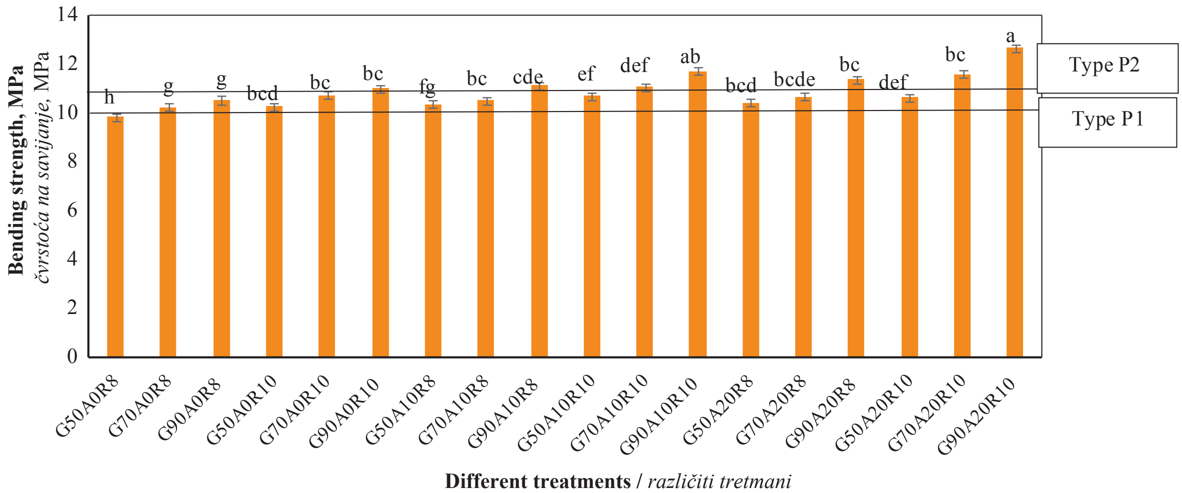

Figure 4 The effect of different treatments on bending strength of particleboards
Slika 4. Utjecaj različitih tretmana na čvrstoću na savijanje ploča iverica

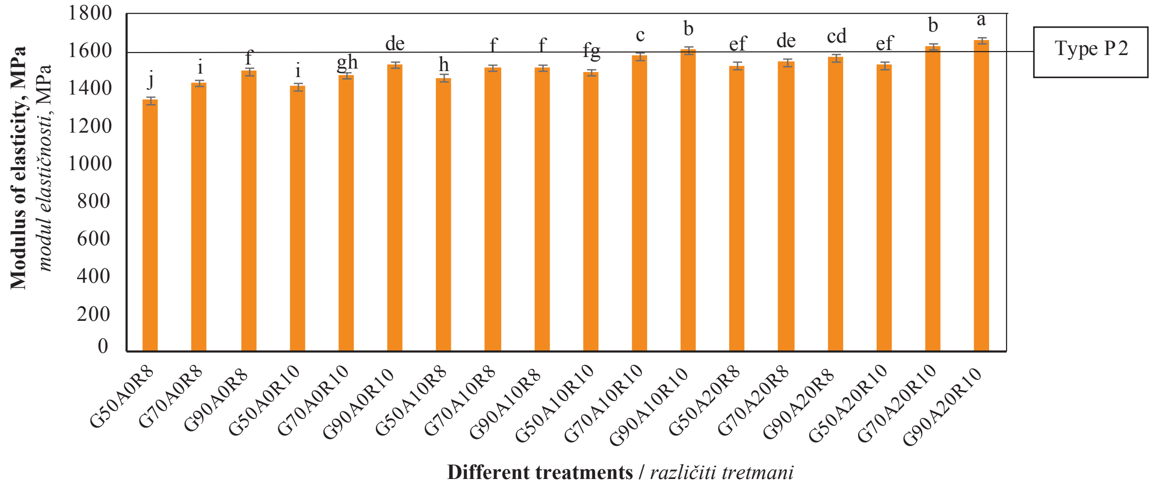

Figure 5 The effect of different treatments on modulus of elasticity of particleboards
Slika 5. Utjecaj različitih tretmana na modul elastičnosti ploča iverica

ing to EN 312 standards, the bending strength of boards with thickness ranging from 13 mm to 20 mm type P1 is 10 MPa, while that of type P2 is 11 MPa, and the modulus of elasticity is 1600 MPa. All particleboards, except the boards containing 50 % garden tree branches, 0 % citric acid and 8 % UF resin (treatment G50A0R8), met the requirements of EN 312 standards for type P1. The boards containing 90 % garden tree branches, 10 % citric acid and 10 % UF resin (treatment G90A10R10) and the boards containing 90 % garden tree branches, 20 % citric acid and 10 % UF resin (treatment G90A20R10) and the boards containing 70 % garden tree branches, 20 % citric acid and 10 % UF resin (treatment G70A20R10) met the requirements of EN 312 standards for type P2

3.3 Internal bonding
3.3. Čvrstoća na raslojavanje

The results of variance analysis showed that the independent and dependent effects of the variable factors had a significant effect on internal bonding at the 95 % confidence level (Table 5).

As the UF resin content increases from 8 to 10 %, the internal bonding increases from 0.36 MPa to 0.52 MPa. As the UF resin and citric acid content and the proportion of green tree branches increased, the internal bonding increased as well (Figure 6.). The highest internal bonding value was obtained with a mixture containing 90 % garden tree branches, 20 % citric acid and 10 % UF resin (treatment G90A20R10). According to the results of the FTIR spectrum, the intensity of the peak at approximately 1729 cm^{-1} increases with increasing citric acid content. This peak is attributed to C=O stretching by carboxyl groups and/or C=O ester groups, which improves the internal bonding of the boards (Ksumah *et al*., 2016). The results showed that the internal bonding of all the boards is higher than that of type P1 boards according to EN 312 standards (0.24 MPa for a thickness ranging from 13 mm to 20 mm). Also, internal bonding of all the boards, except for the boards containing 50 % and 70 % garden tree branches, 0 % citric acid and 8 % UF resin (treatment G50A0R8 and treatment G70A0R8) and the boards containing 50 % garden tree branches, 10 % and 20 % citric acid and 8 % UF resin (treatment G50A10R8 and treatment G50A20R8), is higher than that of type P2 boards according to EN 312 standards (0.35 MPa for a thickness ranging from 13 mm to 20 mm).

Table 5 Results of variance analysis
Tablica 5. Rezultati analize varijance

Parameter	**Source of variance*** *Izvor varijance**	**Degrees of freedom** *Stupnjevi slobode*	**Mean square** *Srednji kvadrat*	***F* value** *F-vrijednost*	***P* Sig.**
Internal bonding *čvrstoća na raslojavanje*	Factor A	1	0.365	1021.43	0.000
	Factor B	2	0.065	181.352	0.000
	Factor C	2	0.034	94.306	0.000
	B×C	4	0.001	1.275	0.298
	A×B	2	0.001	2.005	0.149
	A×C	2	0.001	1.508	0.235
	A×B×C	4	0.001	3.093	0.027
	Error	36	0.0003		
	Corrected Total	53			

*Factor A – resin; Factor B – mixture garden tree branches; Factor C – citric acid / *faktor A – smola; faktor B – smjesa grana vrtnog drveća; faktor C – limunska kiselina*

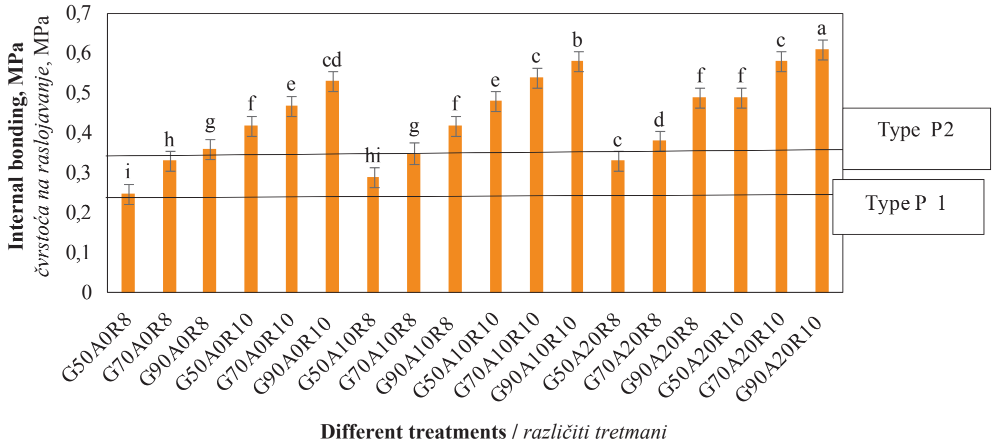

Figure 6 The effect of different treatments on internal bonding of particleboards
Slika 6. Utjecaj različitih tretmana na čvrstoću na raslojavanje ploča iverica

3.4 Water absorption and thickness swelling
3.4. Upijanje vode i debljinsko bubrenje

The results of variance analysis showed that the independent and dependent effects of the variable factors had a significant effect on water absorption and thickness swelling after 24 hours of immersion in water at a 95 % confidence level (Table 6).

With increasing UF resin and citric acid content and an increasing proportion of garden tree branches, water absorption and thickness swelling decreased. Boards containing 10 % UF resin and 20 % citric acid showed the lowest water absorption and thickness swelling (Figure 7.). As the content of citric acid and UF resin increases, the entanglement and bonding between the particles increase, and the number of voids decreases, resulting in less water absorption and less thickness swelling of the particleboards (Syamani *et al.*, 2020; Widyorini *et al.*, 2018).

4 CONCLUSIONS
4. ZAKLJUČAK

In the spectroscopic results, the peak shown in the 1729 cm^{-1} region is attributed to C=O stretching due to carboxyl groups and/or C=O ester groups, and its intensity is increased in 20 % citric acid compared to 10 % citric acid due to the increase in the number of ester groups caused by the reaction between the carboxyl group of citric acid and the hydroxyl groups of

Table 6 Results of variance analysis
Tablica 6. Rezultati analize varijance

Parameter	Source of variance* *Izvor varijance**	Degrees of freedom *Stupnjevi slobode*	Mean square *Srednji kvadrat*	*F* value *F-vrijednost*	*P* Sig.
Water absorption after 24 h *upijanje vode nakon 24* h	Factor A	1	141.200	1126.89	0.000
	Factor B	2	36.866	28.431	0.000
	Factor C	2	162.156	125.056	0.000
	B×C	4	5.892	4.544	0.004
	A×B	2	27.837	21.468	0.000
	A×C	2	31.808	24.531	0.000
	A×B×C	4	4.984	3.844	0.011
	Error	36	1.297		
	Corrected Total	53			
Thickness swelling after 24 h *debljinsko bubrenje nakon 24* h	Factor A	1	134.111	295.472	0.000
	Factor B	2	56.925	125.417	0.000
	Factor C	2	47.607	104.887	0.000
	B×C	4	0.504	1.111	0.047
	A×B	2	4.334	9.549	0.000
	A×C	2	6.401	14.103	0.000
	A×B×C	4	0.767	1.691	0.024
	Error	36	0.454		
	Corrected Total	53			

*Factor A – resin; Factor B – mixture garden tree branches; Factor C – citric acid / *faktor A – smola; faktor B – smjesa grana vrtnog drveća; faktor C – limunska kiselina*

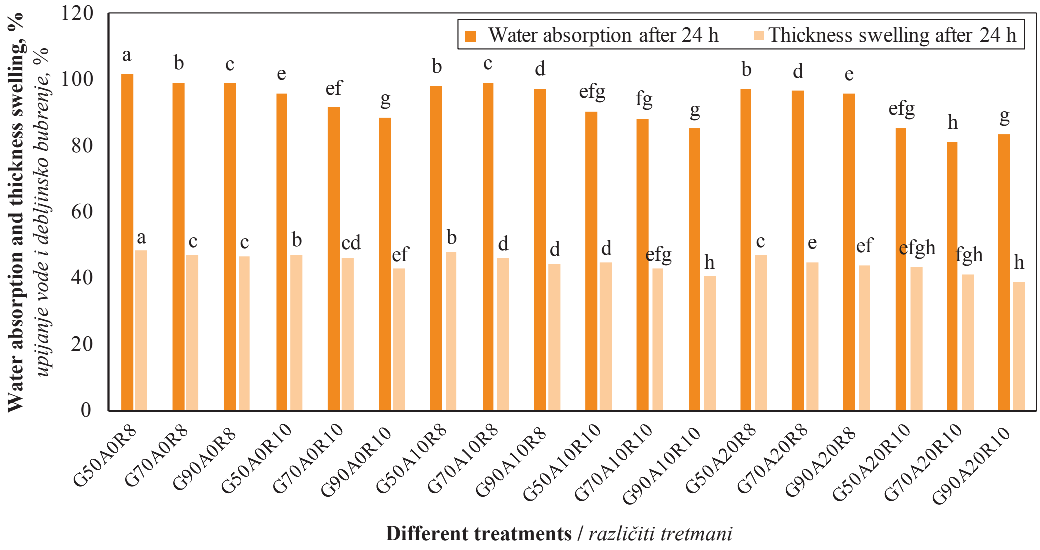

Figure 7 The effect of different treatments on water absorption and thickness swelling of particleboards after 24 hours of immersion in water
Slika 7. Utjecaj različitih tretmana na upijanje vode i debljinsko bubrenje ploča iverica nakon 24 sata potapanja u vodi

the particles. Thus, forming an ester linkage would provide good adhesion and impart excellent particleboard properties (Ksumah *et al*., 2017).

The results showed that all the boards, except for those containing 50 % garden tree branches, no citric acid, and UF 8 % resin (treatment G50A0R8), had a strength exceeding the EN˝312 standard for general use (Type P1). Considering the price of citric acid and the lack of wood resources, two types of boards for type P1 can be proposed to the factories, namely: 1) the boards containing 70 % garden tree branches, 0 % citric acid and 8 % UF resin (treatment G70A0R8) 2) the boards containing 50 % garden tree branches, 0 % citric acid and 10 % UF resin (treatment G50A0R10).

The boards containing 70 % and 90 % garden tree branches, 20 % citric acid and 10 % UF resin (treatment G70A20R10 and treatment G90A20R10), as well as the boards containing 90 % garden tree branches, 10 % citric acid and 10 % UF resin (treatment G90A10R10) have a higher resistance than specified by the EN312 standard for interior fittings (Type P2).

5 REFERENCES
5. LITERATURA

1. Avarand, M.; Jamalirad, L.; Aminian, H.; Vaziri, V., 2018: Physical and mechanical properties of particleboard made from mixing corn stalk, wheat straw and industrial wood particles. Journal of Wood and Forest Science and Technology, 25 (4): 103-115. https://doi.org/10.22069/JWFST.2018.14859.1740
2. Baharlouei, F.; Vaziri, V.; Faraji, F.; Aminian, H., 2020: The effect of alkali treatment and different amounts of resin on the physical and mechanical properties of particleboard made from bagasse. Forest and Wood Products, 73 (3): 343-351. https://doi.org/10.22059/JFWP.2020.296429.1070
3. Šefc, B.; Trajković, J.; Hasan, M.; Katović, D.; Bischof Vukušić, S.; Frančić, M., 2009: Dimensional stability of wood modified by citric acid using different catalysts. Drvna industrija, 60(1): 23-26.
4. Ghosh, P.; Das, D.; Samanta, A. K.,1995: Modification of jute with citric acid. Journal of Polymer Materials, 12: 297-305.
5. Huaxu, Z.; Hua, L. S.; Tahir, P. M.; Ashaari, Z.; Al-Edrus, S. S. O.; Ibrahim, N. A.; Mohamad, S. F., 2021: Physico-mechanical and biological durability of citric acid-bonded rubberwood particleboard. Polymers, 13 (1): 98-109. https://doi.org/10.3390/polym13010098
6. Kusumah, S.; Arinana, A.; Hadi, Y.; Guswenrivo, I.; Yoshimura, T.; Umemura, K.; Tanaka, S.; Kanayama, K., 2017: Utilization of sweet sorghum bagasse and citric acid in the manufacturing of particleboard III: Influence of adding sucrose on the properties of particleboard. BioResources, 12 (4): 7498-7514. https://doi.org/10.15376/biores.12.4.7498-7514.
7. Kusumah, S. S.; Umemura, K.; Yoshioka, K.; Miyafuji, H.; Kanayama, K., 2016: Utilization of sweet sorghum bagasse and citric acid for manufacturing of particleboard I: Effects of pre-drying treatment and citric acid content on the board properties. Industrial Crops and Products, 84: 34-42. https://doi.org/10.1016/J.INDCROP.2016.01.042
8. Mostafalo, A.; Vaziri, V.; Rostami Charati, F.; Faraji, F., 2019: Effect of the addition of citric acid on particleboard properties. Iranian Journal of Wood and Paper Industries, 10 (1): 89-99. https://doi.org/20.1001.1.20089066.1398.10.1.8.5
9. Pizzi, A., 2006: Recent developments in eco-efficient bio-based adhesives for wood bending: opportunities and issues. Journal of Adhesion Science and Technology, 20: 829-846. https://doi.org/10.1163/156856106777638635
10. Syamani, F.; Sudarmanto, A.; Subiyanto, B., 2020: High quality sugarcane bagasse-citric acid particleboards. IOP Conference Series: Earth and Environmental Science, 415: 012006. https://doi.org/10.1088/1755-1315/415/1/012006
11. Tsao, G.; Cao, N.; Du, J.; Gong, C., 1999: Production of multifunctional organic renewable resources. Advances

in Biochemical Engineering / Biotechnology, 65: 243-278. https://doi.org/10.1007/3-540-49194-5_10
12. Umemura, K.; Sugihara, O.; Kawai, S., 2013: Investigation of a new natural adhesive composed of citric acid and sucrose for particleboard. Effects of board density and pressing temperature. Journal of Wood Science, 59 (3): 203-208. https://doi.org/10.1007/s10086-014-1437-8
13. Umemura, K.; Ueda, T.; Munawar, S. S.; Kawai, S., 2012: Application of Citric acid as natural adhesive for wood. Journal of Applied Polymer Science, 123 (4): 1991-1996. https://doi.org/10.1002/app.3470
14. Vaziri, V.; Mesgarhaye Kashani, M. H., 2018: The effect of alkali treatment of bamboo on the physical and mechanical properties of particleboard made from bamboo-industrial wood particles. Iranian Journal of Wood and Paper Industries, 8 (4): 605-615. https://doi.org/20.1001.1.20089066.1400.12.1.5.6
15. Vukusic, S.; Katovic, D.; Schramm, C.; Trajkovic, J.; Sefc, B., 2006: Polycarboxylic acids as non-formaldehyde anti-swelling agents for wood. Holzforschung, 60 (4): 439-444. https://doi.org/10.1515/HF.2006.069
16. Widyorini, R.; Kusuma, D. G.; Widyanto, N.; Tibertius, P.; Sudihyo, J., 2018. Properties of citric acid bonded composite board from elephant dung fibers. Journal of the Korean Wood Science and Technology, 46 (2): 132-142. https://doi.org/10.5658/WOOD.2018.46.2.132
17. Widyorini, R.; Umemura, K.; Isnan, R.; Putra, D. R.; Awaludin, A.; Prayitno, T. A., 2016: Manufacture and properties of citric acid-bonded particleboards made from bamboo materials. European Journal of Wood and Wood Products, 74 (1): 57-65. https://doi.org/10.1007/s00107-015-0967-0
18. Widyorini, R.; Umemura, K.; Soraya, D. K.; Dewi, G. K.; Nugroho, W. D., 2019: Effect of citric acid content and extractives treatment on the manufacturing process and properties of citric acid-bonded *Salacca* frond particleboard. BioResources, 14 (2): 4171-4180. https://doi.org/10.15376/biores.14.2.4171-4180
19. Yang, C. Q.; Xu, Y.; Wang, D., 1996: FT-IR spectroscopy study of the polycarboxylic acids
used for paper wet strength improvement. Industrial & Engineering Chemistry Research, 35: 4037-4042. https://doi.org/10.1021/IE960207U
20. Zhao, Z.; Umemura, K.; Kanayama, K., 2016: Effects of the addition of citric acid on tannin-sucrose adhesive and physical properties of the particleboard. BioResources, 11 (1): 1319-1333. https://doi.org/10.15376/biores.11.1.1319-1333
21. ***EN 310:1993 Wood based panel. Determination of modulus of elasticity in bending and of bending strength. The European Committee for Standardization. Brussels, Belgium.
22. ***EN 312:2010: Particleboard – Specification. Requirements for general purpose boards for use in dry conditions. The European Committee for Standardization. Brussels, Belgium.
23. ***EN 317:1993: Particleboard and fiberboards. Determination of swelling in thickness after immersion in water. The European Committee for Standardization. Brussels, Belgium.
24. ***EN 319:1993 Determination of tensile strength perpendicular to the plane of the board. The European Committee for Standardization. Brussels, Belgium.
25. ***EN 326-1:1994 Wood-based panels sampling, cutting and inspection sampling and cutting of test pieces and expression of test results. The European Committee for Standardization. Brussels, Belgium.
26. ***JIS A 5908:2003 Particleboards (in Japanese). Japanese Standards Association, Tokyo, Japan, pp. 25.

Corresponding address:
VAHID VAZIRI
Gonbad Kavous University, Basirat Bolvar, Gonbad Kavous, Golestan, IRAN, e-mail: vahidvaziri@gmail.com

Yasemin Simsek Turker*[1]

Experimental Investigation of Rotational Behavior of Glulam Column-Beam Connection Reinforced with Carbon, Glass, Basalt and Aramid FRP Fabric

Eksperimentalno istraživanje rotacijskog ponašanja spoja između lameliranog stupa i grede ojačanoga polimernim tkaninama s vlaknima karbona, stakla, bazalta i aramida

ORIGINAL SCIENTIFIC PAPER
Izvorni znanstveni rad
Received – prispjelo: 20. 11. 2023.
Accepted – prihvaćeno: 31. 1. 2024.
UDK: 674.028; 674.06
https://doi.org/10.5552/drvind.2024.0162

ABSTRACT • *In the domain of modern timber structural systems, timber frame constructions distinguish themselves as preferred and commonly used building methods. Their appeal arises from their architectural adaptability and their distinctive attributes, which enable rapid assembly. In this type of structural system, the effectiveness of the connections between beams and columns plays a pivotal role in determining how forces are distributed, ensuring lateral stiffness, and upholding structural safety. Various methods have been developed to ensure column-beam connections in wooden structures. Column-beam connection points deteriorate and get damaged over time. These critical areas need to be strengthened over time. In this study, glulam columns (140 mm × 140 mm) and beams (140 mm × 280 mm), which are often used as load-bearing elements in wooden structures, were used. Columns and beams are connected to each other according to the wooden notching method. Column-beam connection areas are reinforced with carbon, glass, basalt and aramid fiber reinforced polymer fabrics. After the strengthening process, bending tests of the column-beam connection samples were carried out and the load carrying capacity, total amount of energy consumed, and maximum stiffness values were determined. Additionally, FRP damages occurring in the column-beam connection areas were observed during the experiments. The optimal outcomes for encasing column-beam connections have been identified with carbon-based fiber reinforced polymers. Glass-based fiber reinforced polymers yielded the least favorable results. Aramid-based fiber-reinforced polymers demonstrated similar outcomes to those wrapped with carbon-based counterparts. Consequently, it can be deduced that reinforcing column-beam connections with FRP fabrics, be they carbon, aramid, basalt, or glass-based, can markedly enhance their strength and durability, thereby extending their operational lifespan.*

KEYWORDS: *glulam, column-beam, connection, FRP fabric, reinforced*

* Corresponding author
[1] Author is researcher at Suleyman Demirel University, Faculty of Engineering, Department of Civil Engineering, Isparta, Turkey.

SAŽETAK • *U suvremenim konstrukcijama drvene se okvirne konstrukcije smatraju poželjnima i često su primjenjivane metode gradnje. Njihova prikladnost proizlazi iz njihove arhitektonske prilagodljivosti i prepoznatljivih svojstava koja omogućuju brzu montažu. U toj vrsti konstrukcijskog sustava učinkovitost spoja grede i stupa ima ključnu ulogu u određivanju načina raspodjele sila, osiguravanju bočne krutosti i održavanju strukturne sigurnosti. Razvijene su različite metode za osiguranje spojeva stupova i greda u drvenim konstrukcijama. Spojne točke stupova i greda s vremenom propadaju i oštećuju se, pa ih treba ojačati. U ovom su istraživanju korišteni lamelirani stupovi (140 mm × 140 mm) i lamelirane grede (140 mm × 280 mm) koje se često upotrebljavaju kao nosivi elementi u drvenim konstrukcijama. Stupovi i grede međusobno su povezani kutnim trokrakim spojem s pravokutnim urezima. Područja spoja grede i stupa ojačana su polimernim tkaninama ojačanim vlaknima karbona, stakla, bazalta i aramida. Nakon procesa ojačanja spoja provedena su ispitivanja na savijanje uzoraka spoja stupa i grede te su određene nosivost, ukupna količina utrošene energije i maksimalne vrijednosti krutosti. Osim toga, tijekom pokusa praćena su oštećenja polimernih tkanina ojačanih vlaknima koja su se dogodila u područjima spoja stupa i grede. Optimalni rezultati za ojačanje spojeva stupa i grede dobiveni su s polimernom tkaninom kojoj su dodana karbonska vlakna. Polimerna tkanina ojačana staklenim vlaknima dala je najnepovoljnije rezultate. Polimerne tkanine ojačane vlaknima na bazi aramida pokazale su slične rezultate kao i polimerne tkanine ojačane karbonskim vlaknima. Posljedično, može se zaključiti da ojačanje spojeva stupa i grede polimernim tkaninama kojima su dodana vlakna, bilo da je riječ o karbonu, aramidu, bazaltu ili staklu, može znatno povećati njihovu čvrstoću i izdržljivost, čime se produljuje njihov vijek trajanja.*

KLJUČNE RIJEČI: *lamelirano drvo; spoj stupa i grede; polimerne tkanine ojačane polimernim vlaknima; ojačanje*

1 INTRODUCTION
1. UVOD

Timber, as a widespread and natural resource, has been used for centuries in the building of housing and lightweight structures. The relatively recent development of laminated timber and other engineered wood products has further enabled timber to be used in buildings with a higher structural performance requirement, including long-span systems and mid- and high-rise building projects.

Over time, timber structures are vulnerable to biodegradation, including fungal, bacterial, and insect damage. These factors diminish their load-bearing capacity, necessitating frequent maintenance and restoration efforts (Li *et al*., 2017). Preserving ancient timber buildings requires a "heritage-respecting" approach, prioritizing their integrity and striving to restore them as faithfully as possible to their original state. This approach avoids extensive replacement of original building materials (Kilincarslan and Türker, 2020). Traditional restoration methods for timber structures, which impact their load-bearing properties and construction processes, are intricate and may result in additional structural harm. Modern technology allows for a more precise approach, addressing damaged sections individually and incorporating new materials for restoration in a scientifically sound manner (Borri *et al.*, 2013; Franke *et al.*, 2015; Gomez and Svecova, 2008; Hoseinpour *et al.*, 2018; Zhou *et al.*, 2015). Recent research and practical applications have demonstrated that Fiber Reinforced Polymer (FRP) has emerged as the leading technology for strengthening aging and deteriorating structures (Biscaia *et al.*, 2016; Kabir *et al.*, 2016; Vanerek *et al.*, 2014).

FRP composites have found extensive application in fortifying historical wooden edifices due to their lightweight nature, impressive strength, and resistance to corrosion (Athijayamani *et al.*, 2010; Ku *et al.*, 2011; Li *et al.*, 2014; Lopez-Anido *et al.*, 2005; Malkapuram *et al.*, 2009; Morales-Conde *et al.*, 2015; Valluzzi *et al.*, 2015). At present, there are two primary methods for reinforcing timber structures with FRP: (1) Near-Surface Mounted (NSM), involving the mechanical coupling of timber and composite plates, and (2) Externally Bonded Reinforcement (EBR), wherein composite plates are affixed to the outer surface of the timber (Rescalvo *et al.*, 2019). While NSM excels in terms of reinforcement strength (Isleyen *et al.*, 2021a), EBR technology boasts advantages such as simplified construction, reduced stress concentration, enhanced ductility, minimal aesthetic disruption, and widespread use in matrix reinforcement (İşleyen *et al.*, 2021b; Kilincarslan and Turker, 2021).

The exploration of glulam beams primarily revolves around enhancing wood resistance to bending and its overall strength. Presently, scholars worldwide have engaged in extensive investigations regarding the fortification of timber beams in two primary directions: the chemical alteration of wood or reinforcing substances and the physical enhancement of beams. This latter approach predominantly involves the incorporation of steel bars (Yang and Liu, 2006; Wei *et al.*, 2014), the affixation of steel plates (Yang, 2016), and the bonding of composite reinforcing materials (Zhou *et al.*, 2020; Gilbert *et al.*, 2014). Furthermore, research indicates that both methods effectively enhance the material properties of wood, with physical reinforcement notably exerting a more substantial influence on augmenting the load-bearing capacity of glulam beams, encompassing flexural strength and stiffness. Presently, there is considerable interest in the performance of FRP materials when combined with other substances (Xiong *et al.*, 2022). The use of FRP for reinforcing flexural members is widespread, primarily owing to its exceptional tensile strength (Lu *et al.*, 2021; Dong *et al.*, 2019).

Among the array of composite reinforcement materials, carbon fiber-reinforced polymer (CFRP) stands out as the most widely used. In recent years, researchers have embarked on a series of empirical investigations concerning the augmentation of glulam beams through CFRP, delving into the intricacies of reinforcement mechanisms and failure modes (Yang and Sun, 2009; He *et al.*, 2022; Vahedian *et al.*, 2019). These endeavors have illuminated the profound capacity of CFRP to significantly enhance the load-bearing prowess of glulam beams, resulting in a ductile failure mode for the reinforced counterparts (Issa and Kmeid, 2005; Ma *et al.*, 2005). Furthermore, the research demonstrates that the incorporation of two and three layers of CFRP composite sheets results in remarkable increases in flexural strength, registering at 41.82 % and 60.24 %, respectively, when compared to their unreinforced timber counterparts (Khelifa *et al.*, 2015). Notably, CFRP also imparts heightened stiffness and elastic modulus to the beams.

Xie *et al*. (2007) and Wang *et al*. (2010) provided the calculation equations for ultimate bearing capacity and ultimate bending moment. Timbolmas *et al*. introduced an analytical model for forecasting the bending behavior of composite glulam beams under tension and compression, aligning their predictions with experimental results and demonstrating a minimal mean variation of around 15 %. Daniel *et al*. (2022) employed a probability design model and reliability analysis to assess CFRP-reinforced beams, the outcomes of which were rigorously confirmed through highly precise experiments. Moreover, widely used reinforcement materials encompass basalt fiber-reinforced polymer (BFRP) (Xiong *et al*., 2022), glass fiber-reinforced polymer (GFRP) (Todorovic *et al*., 2022), and natural fiber-reinforced polymer (NFRP). Wang *et al*., (2022), Zuo *et al*., (2015) and Wdowia and Brol (2019) conducted reinforcement of glulam beams using BFRP and subsequently scrutinized their structural performance, encompassing bearing capacity and deflection. This approach was deemed proficient in enhancing the bending resistance of glulam beams, thus mitigating the adverse impacts stemming from wood defects. Furthermore, Hay *et al*. (2006) validated the efficacy of a diagonal scheme in augmenting the average ultimate load, flexural stiffness, and deformability of the beams. Additionally, this study underscored the superiority of diagonal GFRP sheets over vertical sheets for shear-strengthening timber stringers.

Emerson (2004) undertook the reinforcement of deteriorated timber pier columns using glass fiber reinforced polymer (GFRP). His research demonstrated that the bearing capacity of GFRP-reinforced timber columns surpassed that of bare timber columns by approximately 17 %. Chidiaq (2003) conducted axial compression experiments on timber columns fortified with CFRP, revealing that the load-bearing capacity of these enhanced timber columns witnessed an augmentation of 15–25 %. Mallinath (2005) delved into experimental investigations involving glulam columns reinforced with both GFRP and CFRP. The findings indicated that CFRP exhibited a more pronounced strengthening effect compared to GFRP. Furthermore, Taheri (2005) embarked on a CFRP reinforcement study focusing on square glulam columns. His work demonstrated that the load-bearing capacity of the reinforced glulam columns experienced a substantial increase, ranging from approximately 60 % to 70 %.

Vetter *et al*. (2021) carried out an analytical investigation into how wood material properties impact the flexural behavior of FRP-reinforced glulam. This study encompassed an exploration of three distinct cross-sectional dimensions, two reinforcement techniques (simple tension and U-shaped reinforcement up to mid-depth), six varying quantities of FRP layers (ranging from 0 to 7), and three different ratios of tension-to-compression moduli (2:1, 1:1, 0.5:1), totaling 99 simulations. The ratio of tensile-to-compressive wood strength emerged as a pivotal factor influencing moment resistance enhancements, particularly when wood in tension exhibited significant weakness compared to compression (0.5:1), resulting in a substantial 1.95-fold moment resistance increase. Conversely, in cases where wood in tension outperformed that in compression (2:1), the maximum moment resistance increase observed was 1.19. This finding aligns with prior literature, emphasizing that FRP contribution is most pronounced for specimens with weaker wood properties (Johns and Lacroix, 2000).

In this study, the glulam column-beam connection, which is combined with a wood notching connection, is wrapped with 4 different fiber reinforced polymers: carbon, glass, basalt and aramid. After winding, the rotational behavior of the cone-beam connections under cyclic loads was investigated. As a result, load carrying capacity, total energy consumption and maximum stiffness values were examined.

2 MATERIALS AND METHODS
2. MATERIJALI I METODE

In this study, layered laminated timber columns and beams produced from spruce wood were used. 140 mm × 140 mm (C1414) column and 140 mm ×

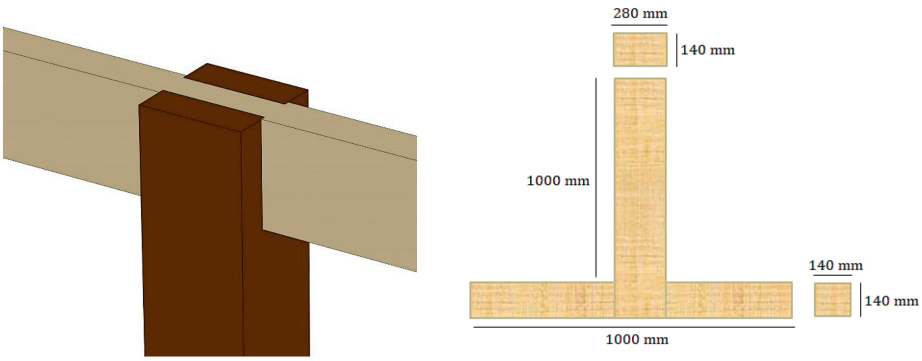

Figure 1 Wooden notched column-beam connection, A: Wooden notched connection example, B: Figural representation of dimensions of column-beam connection
Slika 1. Kutni trokraki spoj stupa i grede s pravokutnim urezima, A: primjer kutnog trokrakog spoja s pravokutnim urezima, B: shematski prikaz dimenzija spoja stupa i grede

280 (B1428) mm beam elements are connected to each other with a wooden notched connection. Columns and beams were supplied from Nasreddin Forest Products (Naswood) Antalya. By laminating spruce timbers with melamine formaldehyde glue and a balancing humidity of 11–12 %, glulam columns and beams are created. The columns and beams made of spruce glulam at the plant fall within the GL24h resistance class. Glulam beams have the features: 16.5 MPa tensile parallel, 0.5 MPa tensile rectangular, 24 MPa pressure parallel, 2.5 MPa shear and torsion, 11,600 MPa modulus of elasticity parallel, 390 MPa modulus of elasticity rectangular and 720 MPa shear modulus.

140 mm × 140 mm columns and 140 mm × 280 mm beams are connected to each other using wooden notched connections. The wood notch connection is given in Figure 1.

The FRP application was made with glass, carbon, aramid and basalt at the joints of the connected columns and beams. The properties of the column-beam connection samples to be tested are given in Table 1.

Figure 2 shows the image of the fiber reinforced polymer fabrics used in the study. The properties of the four fabrics are given in Table 2.

The strengthening process with fiber reinforced polymers was done in four stages. First, the application surfaces were cleaned so that the application could be carried out correctly and the FRPs could adhere. After cleaning the surfaces of wooden columns and beams, the primer was applied to the surfaces. After applying the primer, the surface was allowed to dry and then epoxy adhesive was applied to the surface. FRP fabrics (previously cut to the appropriate dimensions) were applied to the adhesive applied surfaces. In the final stage, epoxy adhesive was applied again on the FRP fabrics.

Carbon, glass, basalt and aramid-based fiber reinforced polymers were used in the study. The technical specifications of the fiber reinforced polymers used are available in UNAL TEKNIK catalogs (UNAL-

Table 1 Properties and codes of samples produced
Tablica 1. Svojstva i oznake pripremljenih uzoraka

No *Red. br.*	**Column size** *Dimenzije stupa,* mm	**Beam size** *Dimenzije grede,* mm	**Reinforcement fabric type** *Vrsta ojačanja tkanine*	**Reinforcement status** *Status ojačanja*	**Sample code** *Oznaka uzorka*
1	140x140	140x280	-	-	C1414B1428-UR
2	140x140	140x280	Glass	+	C1414B1428-G-R
3	140x140	140x280	Carbon	+	C1414B1428- C-R
4	140x140	140x280	Aramid	+	C1414B1428-A-R
5	140x140	140x280	Basalt	+	C1414B1428-B-R

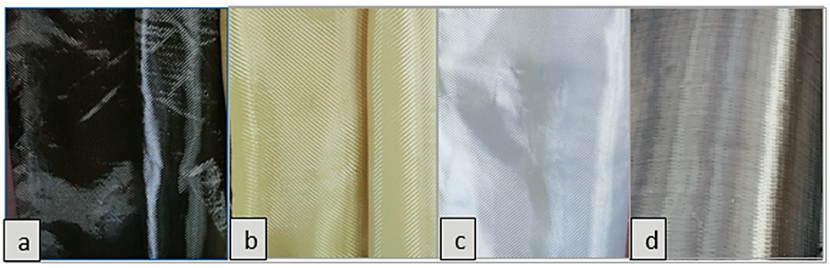

Figure 2 Fiber reinforced polymer fabrics: a) Basalt based FRP, b) Aramid based FRP, c) Glass based FRP, d) Carbon based FRP
Slika 2. Polimerne tkanine ojačane vlaknima: a) na bazi bazalta, b) na bazi aramida, c) na bazi stakla, d) na bazi karbona

Table 2 Properties of carbon, glass, aramid and basalt fabrics
Tablica 2. Svojstva karbonskih, staklenih, aramidnih i bazaltnih tkanina

Material properties *Svojstva materijala*	**Carbon** *Karbon*	**Aramid**	**Glass** *Staklo*	**Basalt** *Bazalt*
Weight / *gramaža,* g/m^2	300	300	300	200
Modulus of elasticity, GPa / *modul elastičnosti,* GPa	230	100	72	82
Tensile strength, N/mm^2 / *vlačna čvrstoća,* N/mm^2	4900	3300	3900	3200
Design section thickness, mm / *dizajnirana debljina presjeka,* mm	0.166	0.170	0.162	0.167

Figure 3 Strengthening stage with fiber reinforcement polymer fabrics
Slika 3. Faza ojačanja polimernim tkaninama s dodanim vlaknima

TEKNIK, 2023). Strengthening of column-beam connection areas was done in 5 stages. First, the rear part of the column was strengthened, and then the beam was wrapped. Then, the column and beam connection points were strengthened at a 45-degree angle. Finally, the upper and lower parts of the arm were reinforced in the connection area. The strengthening phase of column-beam connection areas is given in Figure 4.

The reinforcement steps given in Figure 4 were performed for four different fiber-reinforced polymers. The load-displacement test was carried out in a sufficiently strong frame created with steel bearing elements. The experimental setup is given in Figure 5.

During the experiments, the specimens underwent multiple cycles of controlled displacements applied at the beam end positions. The loading speed was set to 0.2 mm/s. Figure 6 illustrates the sequence of loading stages employed in every test, totaling 24 steps (with each step repeated three times).

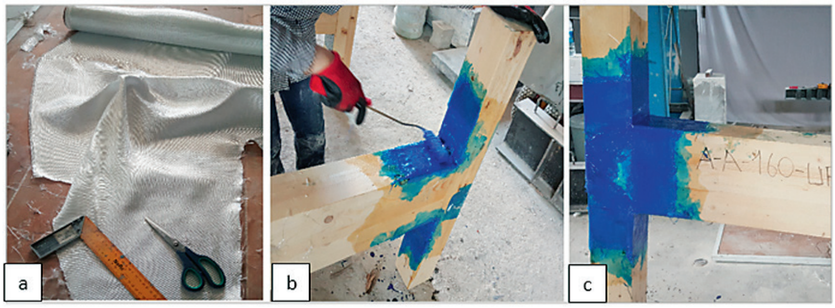

Figure 4 Strengthening phase: a) Sizing of FRP fabrics, b) Application of FRP fabrics, c) Final state of column-beam connection wrapped with FRP
Slika 4. Faze ojačanja: a) dimenzioniranje FRP tkanina, b) primjena FRP tkanina, c) konačno stanje spoja stupa i grede omotane FRP-om

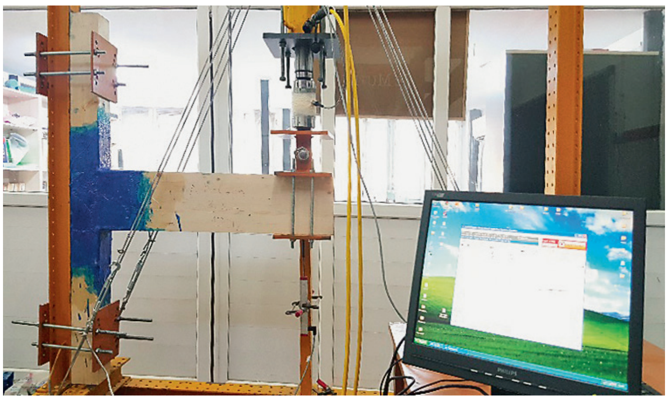

Figure 5 Experimental setup installed in the laboratory
Slika 5. Postavka eksperimenta u laboratoriju

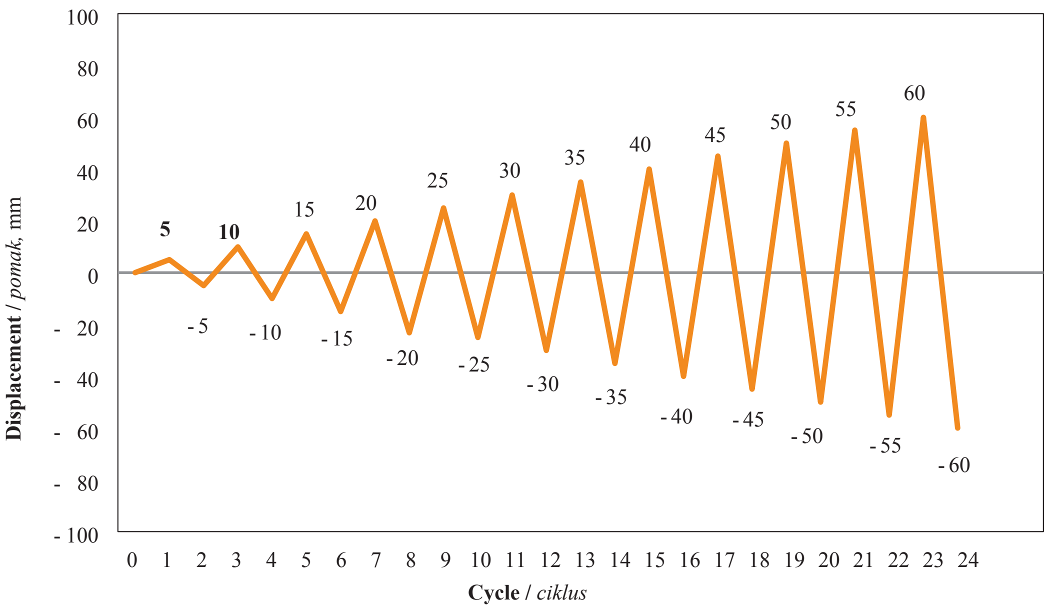

Figure 6 Basic loading steps for all experiments
Slika 6. Osnovni koraci opterećenja za sve eksperimente

The specimens experienced cyclic vertical displacements in both the upward and downward directions. Analyzing the load-displacement graphs provided insights into the structural responses of the materials investigated in these studies.

The assessment focused on the samples ability to dissipate energy and on how their stiffness evolved during the trial. Load-displacement graphs obtained at the end of each experiment were instrumental in the calculations. These graphs were initially segregated into cycles for each sample. The push and pull directions of each cycle were used to compute the stiffness values (k) of the samples. In these computations, the stiffness values were derived by determining the gradient of the line connecting the load points corresponding to the most significant displacements in the push and pull directions with the load positions where the load transitions sign. The connection stiffness Kj for each degree of loading displacement was computed as (Zhang *et al.*, 2020).

$$K_J = \frac{\sum_{i=1}^{n} F_J^i}{\sum_{i=1}^{n} D_j^i} \quad (1)$$

At the occurrence of the i^{th} cycle at the j^{th} level of loading displacement, the peak load is denoted as F_J^i and the corresponding displacement as D_j^i.

Through the calculation of the enclosed areas beneath the load-displacement curves for each cycle within the samples, the capacity of the samples for dissipating energy was assessed. The cumulative sum of these areas at the end of the experiment reflects the overall energy dissipation capability of the sample. Additionally, the hysteresis curve provides a means to ascertain the equivalent viscous damper ratio, a pivotal metric in quantifying energy dissipation capacity (Zhang *et al.*, 2020; Sasmal *et al.*, 2011).

$$E = \frac{S(ABC + CDA)}{S(OBE + ODF)}' \quad (2)$$

$$\zeta_{eq} = \frac{1}{2\Pi} \cdot \frac{S(ABC + CDA)}{S(OBE + ODF)}' \quad (3)$$

Let S (ABC + CDA) denote the hysteresis loop area, while S (OBE + ODF) represents the combined area of triangles OBE and ODF. In this context, E stands for the energy dissipation coefficient. The parameter ζeq, known as the equivalent viscous damper ratio, is determined by the ratio of the energy dissipated within the hysteretic loop to the strain energy, divided by the constant 2π.

The estimation of plastic deformation energy absorbed by the sample is derived from the energy dissipation capacity using the methods outlined in (Chopra, 1995). These computations unveiled the sample capacity for energy dissipation in each cycle, as well as the total energy dissipated by the conclusion of the experiment. Additionally, each cycle encompassed the assessment of the sample stiffness values in both push and pull directions.

3 RESULTS AND DISCUSSION
3. REZULTATI I RASPRAVA

3.1 Load-Displacement
3.1. Graf opterećenje – pomak

Figure 7 presents the load-displacement graph for sample code C1414B1428-UR, C1414B1428-G-R,

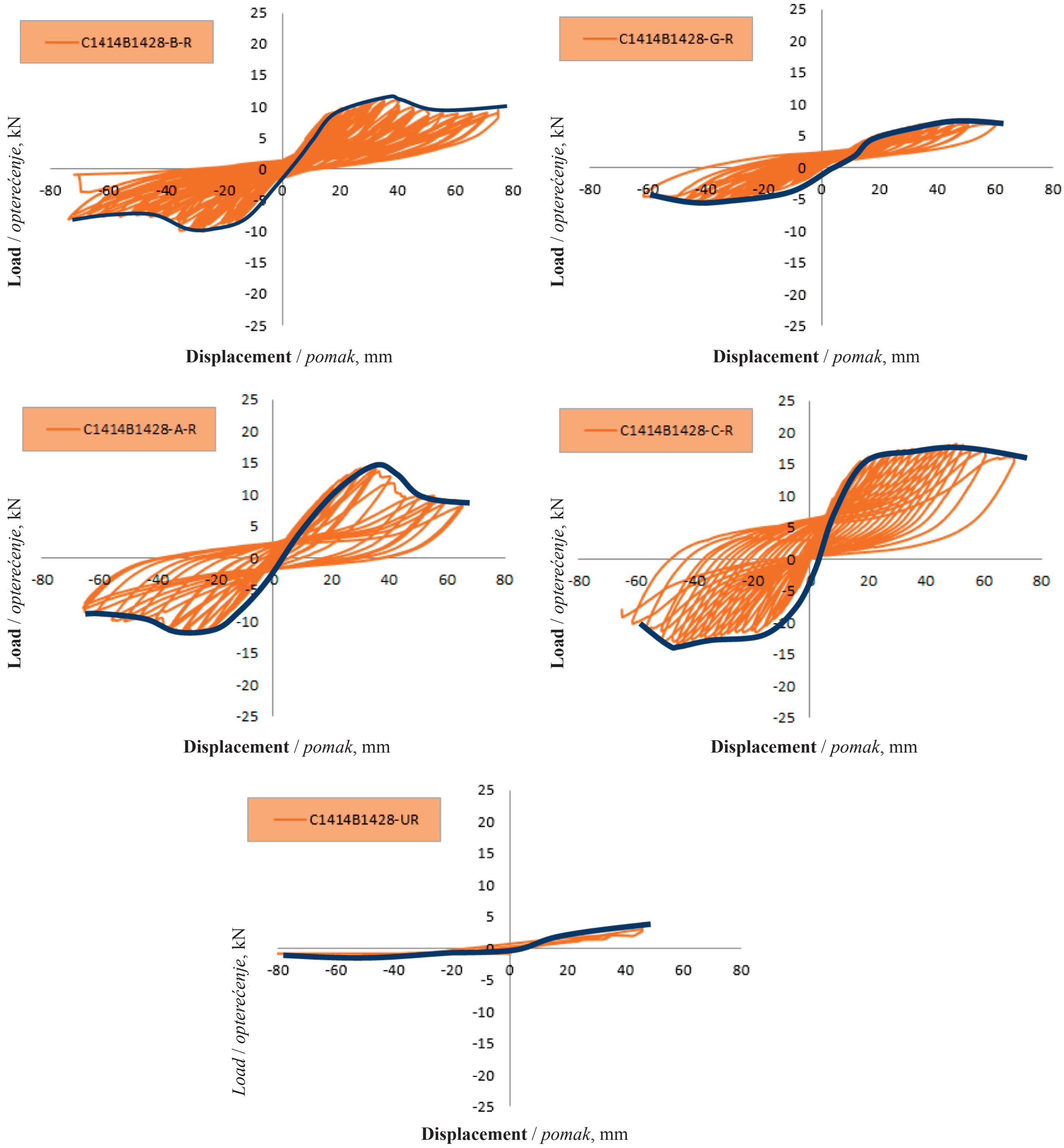

Figure 7 Load-displacement graph of S1212K1224-G-UR, S1212K1224-1-G-R, S1212K1224-2-G-R, and S1212K1224-3-G-R column-beam samples
Slika 7. Graf opterećenje – pomak za uzorke spoja stupa i grede S1212K1224-G-UR, S1212K1224-1-G-R, S1212K1224-2-G-R te S1212K1224-3-G-R

C1414B1428-C-R, C1414B1428-B-R, and C1414B1428-A-R.

The unreinforced sample labeled as C1414K1428-UR demonstrated a peak load-bearing capacity of 6.37 kN during the push (positive) phase and 8.79 kN during the pull (negative) phase. Analyzing the results of the reinforced samples, C1414K1428-C-R displayed load-bearing capacity of 17.64 kN in the push direction and 15.48 kN in the pull direction. For the C1414K1428-A-R sample, the load-bearing capacity was measured at 14.18 kN in the push direction and 13.27 kN in the pull direction. The C1414K1428-B-R sample exhibited load-bearing capacity of 12.10 kN in the push direction and 10.07 kN in the pull direction. For the C1414K1428-G-R sample, the load-bearing capacity was measured at 08.21 kN in the push direction and 06.72 kN in the pull direction. Furthermore, a comparison of strength reduction was conducted between the cycle where each sample reached its load-bearing capacity and the most recent cycle. When the load carrying capacity values were examined, it was determined that the highest load carrying capacity was obtained in the column-beam connection wrapped with carbon-based fiber reinforced polymers. It was determined that the load carrying capacity of the column-beam connection wrapped with carbon-based fiber-reinforced polymer was approximately 128.57 % higher than the column-beam connection wrapped with glass-based fiber-reinforced polymer.

3.2 Energy dissipation capacities
3.2. Kapaciteti rasipanja energije

The calculation of energy dissipation capacity in the specimens involved determining the enclosed areas under the load-displacement curves throughout each cycle. Primarily, a comprehensive comparison of energy dissipation capacity was performed across all the samples. Figure 8 shows the total energy dissipation consumed (*TEDC*) and the cycle energy dissipation capacity (*CEDC*) values of the column-beam connections reinforced 1, 2 and 3 times with carbon fiber reinforced polymer. Figure 8 shows the total energy consumption (*TEDC*) and cycle energy dissipation capacity (*CEDC*) values of column-beam connections reinforced with carbon, glass, basalt and aramid-based fiber-reinforced polymer.

It was determined that the highest energy absorption capacity value belongs to the C1414B1428-C-R sample reinforced with 2526 kN·mm, while the lowest value belongs to the C1414B1428-UR sample reinforced with 2111 kN·mm. Among the wrapped column-beam connections, the energy consumption capacity of the column-beam connections wrapped with glass fiber reinforced polymers had the lowest value. This highlights the notable effectiveness of the FRP retrofitting approach in this context.

Upon examination of Figure 9, it becomes evident that the stiffness values of the sample C1414B1428-C-R surpass those of the other samples in both directions, namely the push and pull (maximum stiffness value in the push direction: 984 kN/m, maximum stiffness value in the pull direction: 997 kN/m). Conversely, the samples with the sample code C1414B1428-UR exhibit the lowest stiffness values in both directions (maximum stiffness in the push direction: 610 kN/m, maximum stiffness in the pull direction: 611 kN/m). In wrapped column-beam connections, the stiffness value of the C1414B1428-C-R sample connection is approximately 38 % higher than the C1414B1428-G-R sample connection, 24 % higher than the C1414B1428-B-R sample connection, and 18 % higher than the C1414B1428-A-R sample connection. This result is

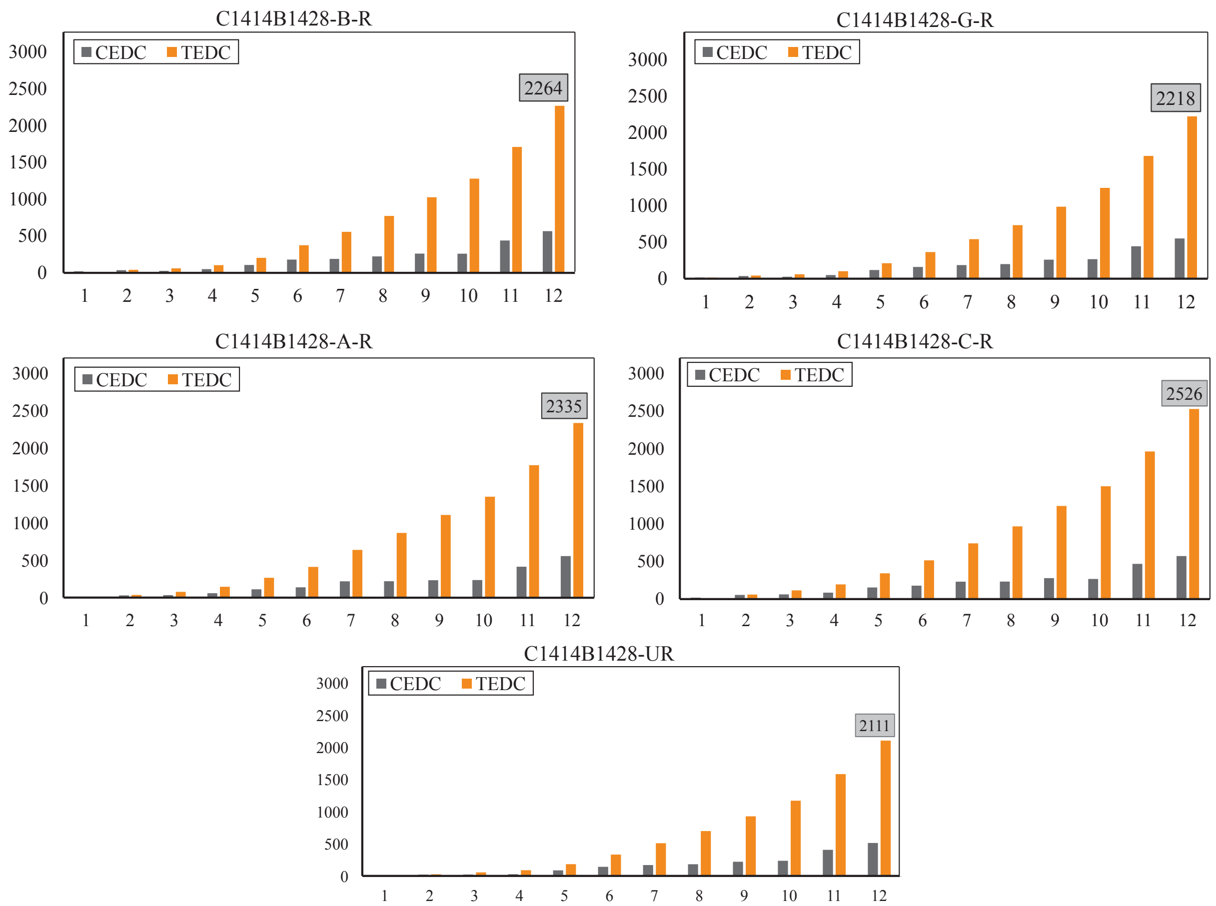

Figure 8 Energy consumption capacities of column-beam connections reinforced with carbon, glass, basalt and aramid
Slika 8. Kapaciteti potrošnje energije spojeva stupa i grede ojačanih karbonom, staklom, bazaltom i aramidom

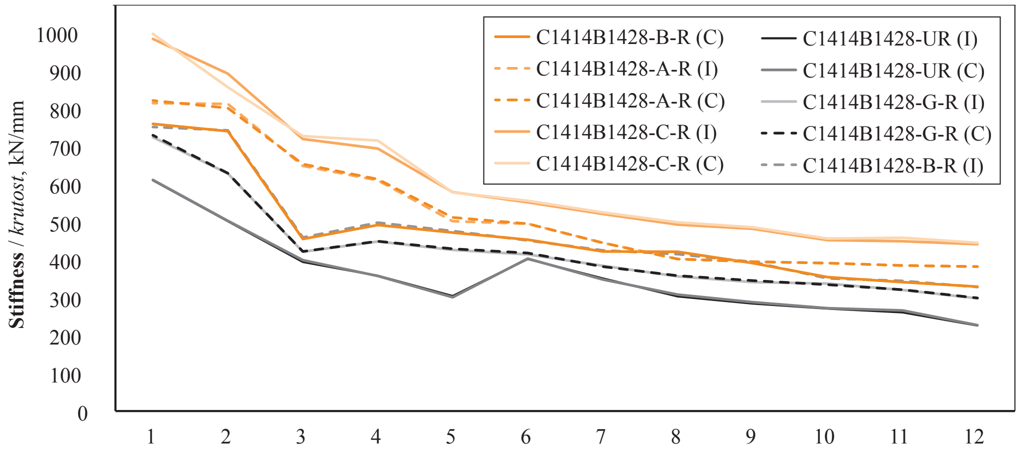

Figure 9 Change in stiffness in push (I) and pull (C) direction of samples reinforced with carbon, aramid, basalt, glass fiber polimers
Slika 9. Promjena krutosti u smjeru guranja (I) i povlačenja (C) uzoraka ojačanih ugljičnim, aramidnim, bazaltnim i staklenim vlaknima

consistent with the investigation carried out by Mangır (2018) and Kılıncarslan and Simsek Turker (2021), who examined the rotational performance of concrete column-beam assemblies. In their research, Mangır (2018) and Kılıncarslan and Simsek Turker (2021), observed that the rigidity measurements of the samples reinforced with FRP surpassed those of the unreinforced sample. In all samples, the initial rigidity progressively diminished in both orientations over the course of the experiment owing to the formation of cracks and ruptures in the FRP material.

3.3 FRP Damages in joint zones during the experiment
3.3. Oštećenja polimernih tkanina ojačanih vlaknima u zonama spoja tijekom eksperimenta

In this study, wrapping was carried out in the column-beam regions with four types of fiber-reinforced polymer fabrics. As a result of the wrapping, experiments were carried out on the column-beam connection samples. During the experiments, images of fractures and explosions occurring in carbon, aramid, basalt and glass fiber reinforced polymers were recorded. A few of the images obtained during the study are given in Figure 10.

4 CONCLUSIONS
4. ZAKLJUČAK

In this study, the glulam column-beam connection, which is combined with a wood notching connection, is wrapped with four different fiber reinforced polymers: carbon, glass, basalt and aramid. After winding, the rotational behavior of the cone-beam connections under cyclic loads was investigated. As a result, the values of the load carrying capacity, total energy consumption and maximum stiffness were examined.

When the load carrying capacity values were examined, it was determined that the highest load carrying capacity was obtained in the column-beam connection wrapped with carbon-based fiber reinforced polymers. It was determined that the load carrying capacity of the column-beam connection wrapped with carbon-based fiber-reinforced polymer was approxi-

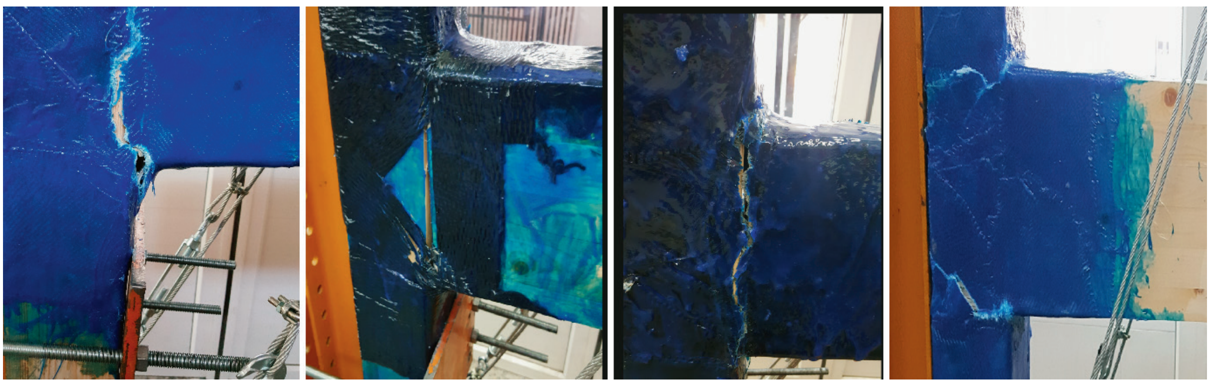

a) b) c) d)
Figure 10 FRP damages in joint zones during the experiment: a) Aramid, b) Carbon, c) Basalt, d) Glass FRP
Slika 10. Oštećenja polimernih tkanina ojačanih vlaknima u zonama spoja tijekom eksperimenta: a) aramid, b) karbon, c) bazalt, d) staklo

mately 128.57 % higher than the column-beam connection wrapped with glass-based fiber-reinforced polymer.

It was determined that the highest energy absorption capacity belongs to the C1414B1428-C-R sample reinforced with 2526 kN.mm, while the lowest value belongs to the sample C1414B1428-UR reinforced with 2111 kN.mm. Among the wrapped column-beam connections, the energy consumption capacity of the column-beam connections wrapped with glass fiber reinforced polymers had the lowest value. This highlights the notable effectiveness of the FRP retrofitting approach in this context. In wrapped column-beam connections, the stiffness value of the C1414B1428-C-R sample connection is approximately 38 % higher than the C1414B1428-G-R sample connection, 24 % higher than the C1414B1428-B-R sample connection, and 18 % higher than the C1414B1428-A-R sample connection.

In summary, it has been verified that the reinforced samples exhibit higher stiffness values compared to the unreinforced ones. Furthermore, the incorporation of column-beam combinations in all samples has resulted in elevated load-carrying capacities, enhanced levels of energy dissipation, and improved stiffness. It has been determined that the best results in wrapping column-beam connections are obtained with carbon-based fiber reinforced polymers. It has also been determined that the lowest values were obtained with glass-based fiber reinforced polymers. It has been determined that column-beam connections wrapped with aramid-based fiber-reinforced polymers give similar results to connections wrapped with carbon-based fiber-reinforced polymers. As a result, it can be concluded that the strength and durability of column-beam connections reinforced with carbon, aramid, basalt and glass-based FRP fabrics can be significantly increased and thus their service life can be extended.

5 REFERENCES
5. LITERATURA

1. Athijayamani, A.; Thiruchitrambalam, M.; Manikandan, V.; Pazhanivel, B., 2010: Mechanical properties of natural fibers reinforced polyester hybrid composite. International Journal of Plastics Technology, 14 (1):104-116. https://doi.org/10.1007/ s12588-009-0016-0
2. Biscaia, H. C.; Chastre, C.; Borba, I. S.; Silva, C.; Cruz, D., 2016: Experimental evaluation of bonding between CFRP laminates and different structural materials. Journal of Composites for Construction, 20 (3). https://doi.org/10.1061/(ASCE)CC.1943-5614.0000631
3. Borri, A.; Corradi, M.; Speranzini, E., 2013: Reinforcement of wood with natural fibers. Composites. Part B: Engineering, 53:1-8. https://doi.org/10.1016/j.compositesb.2013.04.039
4. Chidiaq, R., 2003: Axial compression of rounded wood poles reinforced with carbon fiber. MSc Special Project, Department of Civil Engineering, Rutgers, State University of New Jersey, Piscataway, N.J.
5. Chopra, A. K., 1995: Dynamics of structures: theory and applications to earthquake engineering. Prentice Hall, Englewood Cliffs, New Jersey.
6. Daniel, H.; Habashneh, M.; Rad, M. M., 2022: Reliability-based numerical analysis of glulam beams reinforced by CFRP plate. Scientific Reports, 12 (1): 13587.
7. Dong, Z. Q.; Wu, G.; Zhao, X. L.; Zhu, H.; Shao, X. X., 2019: Behaviors of hybrid beams composed of seawater sea-sand concrete (SWSSC) and a prefabricated UHPC shell reinforced with FRP bars. Construction and Building Materials, 213: 32-42. https://doi.org/10.1016/j.conbuildmat.2019.04.059
8. Emerson, R. N., 2004: In situ repair technique for decayed timber piles. Strutures Congress, 1:1-9.
9. Franke, S.; Franke, B.; Harte, A. M., 2015: Failure modes and reinforcement techniques for timber beams – State of the art. Construction and Building Materials, 97: 2-13. https://doi.org/10.1016/j.conbuildmat.2015.06.021
10. Gilbert, B. P.; Underhill, I. D.; Bailleres, H.; El Hanandeh, A.; McGavin, R. L., 2014: Veneer Based Composite hollow utility poles manufactured from hardwood plantation thinned trees. Construction and Building Materials, 66: 458-466. https://doi.org/10.1016/j. conbuildmat.2014.05.093
11. Gomez, S.; Svecova, D., 2008: Behavior of split timber stringers reinforced with external GFRP sheets. Journal of Composites for Construction, 12 (2): 202-211. https://doi.org/10.1061/(ASCE)1090-0268(2008)12:2(202)
12. Hay, S.; Thiessen, K.; Svecova, D.; Bakht, B., 2006: Effectiveness of GFRP sheets for shear strengthening of timber. Journal of Composites for Construction, 10 (6): 483-491. https://doi.org/ 10.1061/(ASCE)1090-0268(2006)10:6(483)
13. He, M. J.; Wang, Y. X.; Li, Z.; Zhou, L. A.; Tong, Y. C.; Sun, X. F., 2022: An experimental and analytical study on the bending performance of CFRP-reinforced glulam beams. Frontiers in Materials, 8: 802249. https://doi.org/10.3389/fmats.2021.802249
14. Hoseinpour, H.; Valluzzi, M. R.; Garbin, E.; Panizza, M., 2018: Analytical investigation of timber beams strengthened with composite materials. Construction and Building Materials, 191: 1242-1251. https://doi.org/10.1016/j.conbuildmat.2018.10.014
15. Isleyen, U. K.; Ghoroubi, R.; Mercimek, O.; Anil, O.; Erdem, R. T., 2021a: Behavior of glulam timber beam strengthened with carbon fiber reinforced polymer strip for flexural loading. Journal of Reinforced Plastics and Composites, 40 (17-18): 665-685. https://doi.org/10.1177/ 0731684421997924
16. İşleyen, Ü. K.; Ghoroubi, R.; Mercimek, Ö.; Anil, Ö.; Togay, A.; Erdem, R. T., 2021b: Effect of anchorage number and CFRP strips length on behavior of strengthened glulam timber beam for flexural loading. Advances in Structural Engineering, 24 (9): 1869-1882. https://doi.org/10.1177/1369433220988622
17. Issa, C. A.; Kmeid, Z., 2005: Advanced wood engineering: glulam beams. Construction and Building Materials, 19 (2): 99-106. https://doi.org/10.1016/j.conbuildmat.2004.05.013
18. Johns, K. C.; Lacroix, S., 2000: Composite reinforcement of timber in bending. Canadian Journal of Civil Engineering, 27: 899-906.
19. Kabir, M. I.; Shrestha, R.; Samali, B., 2016: Effects of applied environmental conditions on the pull-out

strengths of CFRP-concrete bond. Construction and Building Materials, 114: 817-830. https://doi.org/10.1016/j.conbuildmat.2016.03. 195
20. Khelifa, M.; Auchet, S.; Meausoone, P. J.; Celzard, A., 2015: Finite element analysis of flexural strengthening of timber beams with Carbon Fibre-Reinforced Polymers. Engineering Structures, 101: 364-375. https://doi.org/10.1016/j.engstruct.2015.07.046
21. Kilincarslan, E.; Türker, Y., 2020: Investigation of wooden beam behaviors reinforced with fiber reinforced polymers. Organic Polymer Material Research, 2 (1): 7. https://doi.org/10.30564/opmr.v2i1.1783
22. Kilincarslan, S.; Turker, Y. S., 2021: Experimental investigation of the rotational behaviour of glulam column-beam joints reinforced with fiber reinforced polymer composites. Composite Structures, 262 (1): 113612. https://doi.org/10.1016/j. compstruct.2021.113612
23. Ku, H.; Wang, H.; Pattarachaiyakoop, N.; Trada, M., 2011: A review on the tensile properties of natural fiber reinforced polymer composites. Composites. Part B, 42 (4): 856-873. https://doi.org/10.1016/j.compositesb.2011.01.010
24. Li, J.; Zhang, X.; Li, J.; Li, R.; Qian, M.; Song, P., 2017: An experimental study of the damage degrees to ancient building timber caused by lightning strikes. Journal of Electrostatics, 90: 23-30. https://doi.org/10.1016/j.elstat.2017.08.009
25. Li, Y.; Tsai, M.; Wei, T.; Wang, W., 2014: A study on wood beams strengthened by FRP composite materials. Construction and Building Materials, 62: 118-125. https://doi.org/10.1016/j.conbuildmat.2014.03.036
26. Lopez-Anido, R. A.; Muszynski, L.; Gardner, D. J.; Goodell, B.; Herzog, B., 2005: Performance-based material evaluation of reinforced glued laminated timber (Glulam) beams. Journal of Testing and Evaluation, 33: 6.
27. Lu, Z.; Li, J.; Xie, J.; Huang, P.; Xue, L., 2021: Durability of flexurally strengthened RC beams with prestressed CFRP sheet under wet-dry cycling in a chloride-containing environment. Composite Structures, 255: 112869. https://doi.org/10.1016/j.compstruct.2020.112869
28. Ma, J. X.; Jiang, X. M.; Hu, P.; Hu, M., 2005: Experimental study on bending behaviour of timber beams reinforced with CFRP sheets. Industrial Construction, 35 (8): 35-39.
29. Malkapuram, R.; Kumar, V.; Negi, Y. S., 2009: Recent development in natural fiber reinforced Polypropylene composites. Journal of Reinforced Plastics and Composites, 28 (10): 1169-1189. https://doi.org/10.1177/0731684407087759
30. Mallinath, N., 2005: Experimental and computational investigation of FRP reinforced GLULAM columns including associated software development. Cananda: Dalhousie University.
31. Mangır, A., 2018: Experimental investigation on the seismic performance of beam-column joints in low-strength reinforced concrete structures. PhD Thesis, Istanbul University, Institute of Graduate Studies in Science and Engineering, İstanbul, Turkey.
32. Morales-Conde, M. J.; Rodriguez-Linan, C.; Rubio-De Hita, P., 2015: Bending and shear reinforcements for timber beams using GFRP plates. Construction and Building Materials, 96: 461-472. https://doi.org/10.1016/j.conbuildmat.2015.07.079
33. Rescalvo, F. J.; Suarez, E.; Abarkane, C.; Cruz-Valdivieso, A.; Gallego, A., 2019: Experimental validation of a CFRP laminated/fabric hybrid layout for retrofitting and repairing timber beams. Mechanics of Advanced Materials and Structures, 26 (22):1902-1909. https://doi.org/10.1080/15376494.2018.1455940
34. Sasmal, S.; Novák, B.; Ramanjaneyulu, K., 2011: Numerical analysis of fiber composite-steel plate upgraded beam-column sub-assemblages under cyclic loading. Composite Structures, 93 (2): 599-610. https://doi.org/10.1016/j.compstruct.2010.08.019
35. Taheri, F.; Nagaraj, M.; Cheraghi, N., 2005: FRP-Reinforced Glulaminated Columns. FRP International, 2 (3): 10-12.
36. Todorovic, M.; Glisovic, I.; Stevanovic, B., 2022: Experimental investigation of end-notched glulam beams reinforced with GFRP bars. European Journal of Wood and Wood Products, 80 (5): 10711085. https://doi.org/10.1007/s00107-022-01822-6
37. Vahedian, A.; Shrestha, R.; Crews, K., 2019: Experimental and analytical investigation on CFRP strengthened glulam laminated timber beams: full-scale experiments. Composites. Part B: Engineering, 164: 377-389. https://doi.org/10.1016/j. compositesb.2018.12.007
38. Valluzzi, M. R.; Nardon, F.; Garbin, E.; Panizza, M., 2015: Multi-scale characterization of moisture and thermal cycle effects on composite-to-timber strengthening. Construction and Building Materials, 102: 102. https://doi.org/10.1016/j.conbuild mat.2015.07.008
39. Vanerek, J.; Benesova, A.; Rovnanik, P.; Drochytka, R., 2014: Evaluation of FRP/wood adhesively bonded epoxy joints on environmental exposures. Journal of Adhesion Science and Technology, 28 (14-15):1405-1417. https://doi.org/10.1080/01694243. 2012.698096
40. Vetter, Y.; Stakheiko, M.; Chen, H.; Siciliano, S.; Lacroix, D., 2021: Analytical Investigation of Wood Material Properties on the Flexural Behaviour of FRP Reinforced Glulam. In: Proceedings of CSCE 2021 Annual Conference, pp. 10.
41. Wang, Q. F.; Li, F.; Chen, H. J.; Huang, Y. H.; Yang, Y. X., 2010: Experimental study on flexural behaviour of timber beams reinforced with BFRP sheets. Industrial Construction, 40 (4): 126-130.
42. Wang, Y. Z.; Ma, Y. P.; Wang, L. Q.; Li, F. T., 2022: Flexural behaviour of fast-growing poplar glulam beams reinforced by carbon fibre. Journal of Civil and Environmental Engineering, 44 (6): 124-135.
43. Wdowiak, A.; Brol, J., 2019: Effectiveness of reinforcing bent non-uniform pre-stressed glulam beams with Basalt Fibre Reinforced Polymers rods. Materials, 12: 3141. https://doi.org/10.3390/ma12193141
44. Wei, Y.; Wang, X. W.; Li, G. F., 2014: Mechanical properties test of bamboo scimber flexural specimens of reinforced with bars. Acta Materiae Compositae Sinica, 31 (4): 1030-1036.
45. Xie, Q. F.; Zhao, H. T.; Xue, J. Y.; Wu, Z. H., 2007: Experimental study on flexural performance of wood beams strengthened with CFRP sheets. Industrial Construction, 37 (7): 104-107.
46. Xiong, Z.; Lin, L H.; Qiao, S. H.; Li, LJ.; Li, Y. L.; He, S.; Li, Z.; Liu, F.; Yulong Chen, Y., 2022: Axial performance of seawater sea-sand concrete columns reinforced with basalt fibre-reinforced polymer bars under concentric compressive load. Journal of Building Engineering, 47: 103828. https://doi.org/10.1016/j.jobe.2021.103828
47. Xiong, Z.; Mai, G. H.; Chen, P. X.; Zeng, H. M.; Li, LJ.; Liu, F.; You, W. T., 2022: Investigation on fatigue bond behaviour between GFRP bars and seawater sea-sand

concrete. China Journal of Highway and Transport, 35 (2): 259-268.
48. Yang, H. F.; Liu, W. Q., 2006: Analysis study of flexural deformation of FRP reinforced glulam beams. Journal of Nanjing University of Technology, 6 (3): 1-5 + 14.
49. Yang, X. H., 2016: Research on the flexural behavior and design method for steel plate strengthened glulam beam. Harbin: Northeast Forestry University.
50. Yang, X. J.; Sun, Y. F., 2009: Study on flexural properties of glulam with reinforced carbon fibre. Forestry and Grassland Machinery, 10: 17-19 + 22.
51. Zhang, J.; Hu, X.; Sun, Q.; Zhang, Y.; Zhu, W.; Li, L., 2020: Experimental study on seismic performance of glulam-concrete composite beam-to-column joints. Composite Structures, 236: 111864. https://doi.org/10.1016/j.compstruct.2020.111864
52. Zhou, A.; Tam, L.-H.; Yu, Z.; Lau, D., 2015: Effect of moisture on the mechanical properties of CFRP-wood composite: An experimental and atomistic investigation. Composites. Part B: Engineering, 71: 63-73. https://doi.org/10.1016/j. compositesb.2014.10.051
53. Zhou, C. D.; Yang, L. G.; Shiha, A., 2020: Experimental study on flexural behaviour of timber beams strengthened in both tension and compression zone. China Civil Engineering Journal, 53 (11): 55-63. https://doi.org/10.15951/j.tmgcxb.2020.11.006
54. Zuo, H. L.; Bu, D. W.; Guo, N.; He, D. P., 2015: Effect of basalt fibre composite on flexural behaviour of gluam beams. Journal of Northeast Agricultural University, 43 (04): 91-95.
55. ***UNALTEKNIK, 2023: (online), http://unalteknikas.com.tr/ (Accessed Oct. 10, 2023).

Corresponding address:

YASEMIN SIMSEK TURKER

Suleyman Demirel University, Faculty of Engineering, Department of Civil Engineering, Isparta, TURKEY,
e-mail: yaseminturker@sdu.edu.tr

Upute autorima

Opće odredbe

Časopis *Drvna industrija* objavljuje znanstvene radove (izvorne znanstvene radove, pregledne radove, prethodna priopćenja), stručne radove, izlaganja sa savjetovanja, stručne obavijesti, bibliografske radove, preglede te ostale priloge s područja biologije, kemije, fizike i tehnologije drva, pulpe i papira te drvnih proizvoda, uključujući i proizvodnu, upravljačku i tržišnu problematiku u drvnoj industriji.

Predaja rukopisa podrazumijeva uvjet da rad nije već predan negdje drugdje radi objavljivanja ili da nije već objavljen (osim sažetka, dijelova objavljenih predavanja ili magistarskih radova odnosno disertacija, što mora biti navedeno u napomeni) te da su objavljivanje odobrili svi suautori (ako rad ima više autora) i ovlaštene osobe ustanove u kojoj je istraživanje provedeno. Cjelokupni sadržaj Drvne industrije dostupan je za skidanje s interneta, tiskanje, daljnju distribuciju, čitanje i ponovno korištenje bez ograničenja sve dok se naznače autor(i) i originalni izvor prema Creative Commons Attribution 4.0 International License (CC BY). Autor(i) zadržavaju izdavačka prava bez ograničenja.

Znanstveni i stručni radovi objavljuju se na engleskom jeziku, uz sažetak na hrvatskome. Također, naslov, podnaslovi i svi važni rezultati trebaju biti napisani dvojezično. Uredništvo osigurava inozemnim autorima prijevod na hrvatski. Ostali se članci uglavnom objavljuju na hrvatskome. Znanstveni i stručni radovi podliježu temeljitoj recenziji najmanje dvaju recenzenata. Izbor recenzenata i odluku o klasifikaciji i prihvaćanju članka (prema preporukama recenzenata) donosi Urednički odbor.

Svi prilozi podvrgavaju se jezičnoj obradi. Urednici će od autora zahtijevati da tekst prilagode preporukama recenzenata i lektora, te zadržavaju i pravo da predlože skraćivanje ili poboljšanje teksta. Autori su potpuno odgovorni za svoje priloge. Podrazumijeva se da je autor pribavio dozvolu za objavljivanje dijelova teksta što su već negdje objavljeni te da objavljivanje članka ne ugrožava prava pojedinca ili pravne osobe. Radovi moraju izvještavati o istinitim znanstvenim ili tehničkim postignućima. Autori su odgovorni za terminološku i metrološku usklađenost svojih priloga. Radovi se šalju elektronički putem poveznice http://journal.sdewes.org/drvind

Upute

Predani radovi smiju sadržavati najviše 15 jednostrano pisanih A4 listova s dvostrukim proredom (30 redaka na stranici), uključujući i tablice, slike te popis literature, dodatke i ostale priloge. Dulje je članke preporučljivo podijeliti na dva ili više nastavaka. Tekst treba biti u *doc formatu*, u potpunosti napisan fontom *Times New Roman* (tekst, grafikoni i slike), normalnim stilom, bez dodatnog uređenja teksta.

Prva stranica poslanog rada treba sadržavati puni naslov, ime(na) i prezime(na) autora, podatke o zaposlenju autora (ustanova, grad i država) te sažetak s ključnim riječima (duljina sažetka približno 1/2 stranice A4).

Posljednja stranica treba sadržavati titule, zanimanje, zvanje i adresu (svakog) autora, s naznakom osobe s kojom će Uredništvo biti u vezi.

Znanstveni i stručni radovi moraju biti sažeti i precizni. Osnovna poglavlja trebaju biti označena odgovarajućim podnaslovima. Napomene se ispisuju na dnu pripadajuće stranice, a obrojčavaju se susljedno. One koje se odnose na naslov označuju se zvjezdicom, a ostale uzdignutim arapskim brojkama. Napomene koje se odnose na tablice pišu se ispod tablica, a označavaju se uzdignutim malim pisanim slovima, abecednim redom.

Latinska imena trebaju biti pisana kosim slovima (italicom), a ako je cijeli tekst pisan kosim slovima, latinska imena trebaju biti podcrtana.

U uvodu treba definirati problem i, koliko je moguće, predočiti granice postojećih spoznaja, tako da se čitateljima koji se ne bave područjem o kojemu je riječ omogući razumijevanje ciljeva rada.

Materijal i metode trebaju biti što preciznije opisane da omoguće drugim znanstvenicima ponavljanje pokusa. Glavni eksperimentalni podaci trebaju biti dvojezično navedeni.

Rezultati trebaju obuhvatiti samo materijal koji se izravno odnosi na predmet. Obvezatna je primjena metričkog sustava. Preporučuje se upotreba SI jedinica. Rjeđe rabljene fizikalne vrijednosti, simboli i jedinice trebaju biti objašnjeni pri njihovu prvom spominjanju u tekstu. Za pisanje formula valja se koristiti Equation Editorom (programom za pisanje formula u MS Wordu). Jedinice se pišu normalnim (uspravnim) slovima, a fizikalni simboli i faktori kosima (italicom). Formule se susljedno obrojčavaju arapskim brojkama u zagradama, npr. (1) na kraju retka.

Broj slika mora biti ograničen samo na one koje su prijeko potrebne za objašnjenje teksta. Isti podaci ne smiju biti navedeni i u tablici i na slici. Slike i tablice trebaju biti zasebno obrojčane, arapskim brojkama, a u tekstu se na njih upućuje jasnim naznakama ("tablica 1" ili "slika 1"). Naslovi, zaglavlja, legende i sav ostali tekst u slikama i tablicama treba biti napisan hrvatskim i engleskim jezikom.

Slike je potrebno rasporediti na odgovarajuća mjesta u tekstu, trebaju biti izrađene u rezoluciji 600 dpi, crno-bijele (objavljivanje slika u koloru moguće je na zahtjev autora), formata jpg ili tiff, potpune i jasno razumljive bez pozivanja na tekst priloga.

Svi grafikoni i tablice izrađuju se kao crno-bijeli prilozi (osim na zahtjev). Tablice i grafikoni trebaju biti na svojim mjestima u tekstu te originalnog formata u kojemu su izrađeni radi naknadnog ubacivanja hrvatskog prijevoda. Ako ne postoji mogućnost za to, potrebno je poslati originalne dokumente u formatu u kojemu su napravljeni (*excel* ili *statistica* format).

Naslovi slika i crteža ne pišu se velikim tiskanim slovima. Crteži i grafikoni trebaju odgovarati stilu časopisa (fontovima i izgledu). Slova i brojke moraju biti dovoljno veliki da budu lako čitljivi nakon smanjenja širine slike ili tablice. Fotomikrografije moraju imati naznaku uvećanja, poželjno u mikrometrima. Uvećanje može biti dodatno naznačeno na kraju naslova slike, npr. "uvećanje 7500 : l".

Diskusija i zaključak mogu, ako autori žele, biti spojeni u jedan odjeljak. U tom tekstu treba objasniti rezultate s obzirom na problem postavljen u uvodu i u odnosu prema odgovarajućim zapažanjima autora ili drugih istraživača. Valja izbjegavati ponavljanje podataka već iznesenih u odjeljku *Rezultati*. Mogu se razmotriti naznake za daljnja istraživanja ili primjenu. Ako su rezultati i diskusija spojeni u isti odjeljak, zaključke je nužno napisati izdvojeno. Zahvale se navode na kraju rukopisa. Odgovarajuću literaturu treba citirati u tekstu, i to prema harvardskom sustavu (*ime – godina*), npr. (Bađun, 1965). Nadalje, bibliografija mora biti navedena na kraju teksta, i to abecednim redom prezimena autora, s naslovima i potpunim navodima bibliografskih referenci. Popis literature mora biti selektivan, a svaka referenca na kraju mora imati naveden DOI broj, ako ga posjeduje (http://www.doi.org) (provjeriti na http://www.crossref.org).

Primjeri navođenja literature

Članci u časopisima: Prezime autora, inicijal(i) osobnog imena, godina: Naslov. Naziv časopisa, godište (ev. broj): stranice (od – do). Doi broj.

Primjer

Kärki, T., 2001: Variation of wood density and shrinkage in European aspen (*Populus tremula*). Holz als Roh- und Werkstoff, 59: 79-84. http://dx.doi.org/10.1007/s001070050479.

Knjige: Prezime autora, inicijal(i) osobnog imena, godina: Naslov. (ev. izdavač/editor): izdanje (ev. svezak). Mjesto izdanja, izdavač (ev. stranice od – do).

Primjeri

Krpan, J., 1970: Tehnologija furnira i ploča. Drugo izdanje. Zagreb, Tehnička knjiga.

Wilson, J. W.; Wellwood, R. W., 1965: Intra-increment chemical properties of certain western Canadian coniferous species. U: W. A. Cote, Jr. (Ed.): Cellular Ultrastructure of Woody Plants. Syracuse, N.Y., Syracuse Univ. Press, pp. 551- 559.

Ostale publikacije (brošure, studije itd.)

Müller, D., 1977: Beitrag zür Klassifizierung asiatischer Baumarten. Mitteilung der Bundesforschungsanstalt für Forstund Holzvvirt schaft Hamburg, Nr. 98. Hamburg: M. Wiederbusch.

Web stranice

***1997: "Guide to Punctuation" (online), University of Sussex, www.informatics.sussex.ac.uk/department/docs/punctuation/node 00.html. First published 1997 (pristupljeno 27. siječnja 2010).

Autoru se prije konačnog tiska šalje pdf rada. Rad je potrebno pažljivo pročitati, ispraviti te vratiti Uredništvu s listom ispravaka. Autori znanstvenih i stručnih radova besplatno dobivaju po jedan primjerak časopisa. Autoru svakog priloga također se dostavlja besplatan primjerak časopisa.

Dodatne informacije o načinu pisanja znanstvenih radova mogu se naći na web adresi:
www.ease.org.uk/publications/author-guidelines

Instructions for authors

General terms

The "Drvna industrija" ("Wood Industry") journal publishes scientific papers (original scientific papers, review papers, previous notes), professional papers, conference papers, professional information, bibliographical and survey articles and other contributions related to biology, chemistry, physics and technology of wood, pulp and paper and wood products, including production, management and marketing issues in the wood industry.

Submission of a paper implies that the work has not been submitted for publication elsewhere or published before (except in the form of an abstract or as part of a published lecture, review or thesis, in which case it must be stated in a footnote); that the publication is approved by all co-authors (if any) and by the authorities of the institution where the research has been carried out. The complete content of the journal *Drvna industrija* (Wood Industry) is available on the Internet permitting any users to download, print, further distribute, read and reuse it with no limits provided that the author(s) and the original source are identified in accordance with the Creative Commons Attribution 4.0 International License (CC BY). The authors retain their copyrights.

The scientific and professional papers shall be published in English with summary in Croatian. The titles, headings and all the relevant results shall be also presented bilingually. The Editor's Office shall provide the translation into Croatian for foreign authors. Other articles are generally published in Croatian. The scientific and professional papers will be subject to a thorough review by at least two selected referees. The Editorial Board shall make the choice of reviewers, as well as the decision about the classification of the paper and its acceptance (based on reviewers' recommendations).

All contributions are subject to proofreading. The editors will require authors to modify the text in the light of the recommendations made by reviewers and language advisers, and they reserve the right to suggest abbreviations and text improvements. Authors are fully responsible for the contents of their contributions. It shall be assumed that the author has obtained the permission for the reproduction of portions of text published elsewhere, and that the publication of the paper in question does not infringe upon any individual or corporate rights. Papers shall report on true scientific or technical achievement. Authors are responsible for the terminological and metrological consistency of their contributions. The contributions are to be submitted by the link http://journal.sdewes.org/drvind

Details

Papers submitted shall consist of no more than 15 single-sided DIN A-4 sheets of 30 double-spaced lines, including tables, figures and references, appendices and other supplements. Longer papers should be divided into two or more continuing series. The text should be written in doc format, fully written using Times New Roman font (text, graphs and figures), in normal style without additional text editing.

The first page of the paper submitted should contain full title, name(s) of author(s) with professional affiliation (institution, city and state), abstract with keywords (approx. 1/2 sheet DIN A4).

The last page should provide the full titles, posts and address(es) of each author with indication of the contact person for the Editor's Office.

Scientific and professional papers shall be precise and concise. The main chapters should be characterized by appropriate headings. Footnotes shall be placed at the bottom of the same page and consecutively numbered. Those relating to the title should be marked by an asterix, others by superscript Arabic numerals. Footnotes relating to the tables shall be printed under the table and marked by small letters in alphabetical order.

Latin names shall be printed in italics and underlined.

Introduction should define the problem and if possible the framework of existing knowledge, to ensure that readers not working in that particular field are able to understand author's intentions.

Materials and methods should be as precise as possible to enable other scientists to repeat the experiment. The main experimental data should be presented bilingually.

The results should involve only material pertinent to the subject. The metric system shall be used. SI units are recommended. Rarely used physical values, symbols and units should be explained at their first appearance in the text. Formulas should be written by using Equation Editor (program for writing formulas in MS Word). Units shall be written in normal (upright) letters, physical symbols and factors in italics. Formulas shall be consecutively numbered with Arabic numerals in parenthesis (e.g. (1)) at the end of the line.

The number of figures shall be limited to those absolutely necessary for clarification of the text. The same information must not be presented in both a table and a figure. Figures and tables should be numbered separately with Arabic numerals, and should be referred to in the text with clear remarks ("Table 1" or "Figure 1"). Titles, headings, legends and all the other text in figures and tables should be written in both Croatian and English.

Figures should be inserted into the text. They should be of 600 dpi resolution, black and white (color photographs only on request), in jpg or tiff format, completely clear and understandable without reference to the text of the contribution.

All graphs and tables shall be black and white (unless requested otherwise). Tables and graphs should be inserted into the text in their original format in order to insert them subsequently into the Croatian version. If this is not possible, original document should be sent in the format in which it was made (excel or statistica format).

The captions to figures and drawings shall not be written in block letters. Line drawings and graphs should conform to the style of the journal (font size and appearance). Letters and numbers shall be sufficiently large to be readily legible after reduction of the width of a figure or table. Photomicrographs should have a mark indicating magnification, preferably in micrometers. Magnification can be additionally indicated at the end of the figure title, e.g. "Mag. 7500:1".

Discussion and conclusion may, if desired by authors, be combined into one chapter. This text should interpret the results relating to the problem outlined in the introduction and to related observations by the author(s) or other researchers. Repeating the data already presented in the "Results" chapter should be avoided. Implications for further studies or application may be discussed. A conclusion shall be expressed separately if results and discussion are combined in the same chapter. Acknowledgements are presented at the end of the paper. Relevant literature shall be cited in the text according to the Harvard system ("name – year"), e.g. (Bađun, 1965). In addition, the bibliography shall be listed at the end of the text in alphabetical order of the author's names, together with the title and full quotation of the bibliographical reference. The list of references shall be selective, and each reference shall have its DOI number (http://www.doi.org) (check at http://www.crossref.org).:

Example of references

Journal articles: Author's second name, initial(s) of the first name, year: Title. Journal name, volume (ev. issue): pages (from - to). DOI number.

Example:
Kärki, T., 2001: Variation of wood density and shrinkage in European aspen (*Populus tremula*). Holz als Roh- und Werkstoff, 59: 79-84. http://dx.doi.org/10.1007/s001070050479.

Books:
Author's second name, initial(s) of the first name, year: Title. (ev. Publisher/editor): edition, (ev. volume). Place of publishing, publisher (ev. pages from - to).

Examples:
Krpan, J. 1970: Tehnologija furnira i ploča. Drugo izdanje. Zagreb: Tehnička knjiga.
Wilson, J.W.; Wellwood, R.W. 1965: Intra-increment chemical properties of certain western Canadian coniferous species. U: W. A. Cote, Jr. (Ed.): Cellular Ultrastructure of Woody Plants. Syracuse, N.Y., Syracuse Univ. Press, pp. 551-559.

Other publications (brochures, studies, etc.):
Müller, D. 1977: Beitrag zur Klassifizierung asiatischer Baumarten. Mitteilung der Bundesforschungsanslalt für Forst- und Holzwirtschaft Hamburg, Nr. 98. Hamburg: M. Wiederbusch.

Websites:
***1997: "Guide to Punctuation" (online), University of Sussex, www.informatics.sussex.ac.uk/department/docs/punctuation/node00.html. First published 1997 (Accessed Jan. 27, 2010).

The paper will be sent to the author in pdf format before printing. The paper should be carefully corrected and sent back to the Editor's Office with the list of corrections made. Each contributor will receive 1 copy of the journal.

Further information on the way of writing scientific papers can be found on the following website:

www.ease.org.uk/publications/author-guidelines

HRVATSKA KOMORA
INŽENJERA ŠUMARSTVA
I DRVNE TEHNOLOGIJE

HRVATSKA KOMORA INŽENJERA ŠUMARSTVA I DRVNE TEHNOLOGIJE

Osnovana je na temelju Zakona o Hrvatskoj komori inženjera šumarstva i drvne tehnologije.

Komora je samostalna i neovisna strukovna organizacija koja obavlja povjerene joj javne ovlasti, čuva ugled, čast i prava svojih članova, skrbi da ovlašteni inženjeri obavljaju svoje poslove savjesno i u skladu sa zakonom, promiče, zastupa i usklađuje njihove interese pred državnim i drugim tijelima u zemlji i inozemstvu.

Članovi komore:

inženjeri šumarstva i drvne tehnologije koji obavljaju stručne poslove iz područja šumarstva, lovstva i drvne tehnologije.

Stručni poslovi:

projektiranje, izrada, procjena, izvođenje i nadzor radova iz područja uzgajanja, uređivanja, iskorištavanja i otvaranja šuma, lovstva, zaštite šuma, hortikulture, rasadničarske proizvodnje, savjetovanja, ispitivanja kvalitete proizvoda, sudskoga vještačenja, izrade i revizije stručnih studija i planova, kontrola projekata i stručne dokumentacije, izgradnja uređaja, izbor opreme, objekata, procesa i sustava, stručno osposobljavanje i licenciranje radova u šumarstvu, lovstvu i preradi drva.

Zadaci Komore:

- promicanje razvoja struke i skrb o stručnom usavršavanju članova,
- poticanje donošenja propisa kojima se utvrđuju javne ovlasti Komore,
- reagiranje struke na pripremu propisa iz područja šumarstva, lovstva i drvne tehnologije,
- suradnja s nadležnim institucijama i zastupanje struke u odnosu prema njima,
- organizacija stručnoga usavršavanja,
- zastupanje interesa svojih članova,
- izdavanje pečata i iskaznice ovlaštenim inženjerima,
- briga i nadzor poštivanja kodeksa strukovne etike,
- osiguravanje članova Komore za štetu koja bi mogla nastati investitorima i trećim osobama i sl.

Članovima Komore izdaje se rješenje, pečat i iskaznica ovlaštenoga inženjera.
Za uspješno obavljanje zadataka te za postizanje ciljeva ravnopravnoga i jednakovrijednoga zastupanja struka udruženih u Komoru, članovi Komore organizirani su u razrede:

- Razred inženjera šumarstva
- Razred inženjera drvne tehnologije

HRVATSKA KOMORA INŽENJERA ŠUMARSTVA I DRVNE TEHNOLOGIJE
Prilaz Gjure Deželića 63
10000 ZAGREB

telefon:
++ 385 1 376-5501
e-mail:
info@hkisdt.hr

www.hkisdt.hr


povežite se s prirodom
drvodjelac
Drvodjelac d.o.o.
Petra Preradovića 14, Ivanec, Hrvatska
+385 (0)42 781 922 | www.drvodjelac.hr